

Modelling of energy forestry: growth, water relations and economics

K. L. Perttu and P. J. Kowalik (Editors)

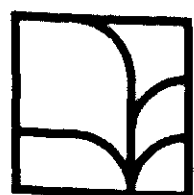


Simulation Monographs 30

Simulation Monographs is a series on
computer simulation in agriculture and
its supporting sciences

Modelling of energy forestry: growth, water relations and economics

K. L. Perttu and P. J. Kowalik (Editors)



Pudoc Wageningen 1989

CIP-data Koninklijke Bibliotheek, Den Haag

Simulation

ISBN 90-220-0947-5

NUGI 835

**© Centre for Agricultural Publishing and Documentation (Pudoc), Wageningen,
the Netherlands**

**No part of this publication, apart from bibliographic data and brief quotations embodied
in critical reviews, may be reported, re-recorded or published in any form including print,
photocopy, microfilm, electronic or electromagnetic record without written permission
from the publisher: Pudoc, P.O. Box 4, 6700 AA Wageningen, the Netherlands.**

Printed in the Netherlands

Contents

Preface	vii
Contributors	viii
INTRODUCTION	
1 Climatic, edaphic and management requirements for energy forestry	3
2 Approaches to modelling growth and water for forestry	13
GROWTH PROCESSES IN WILLOW STANDS	
3 Introduction to modelling of plant growth	19
4 Photosynthetic light response of single leaves and small plants	25
5 Simulated growth of willow stands related to variations in weather and foliar nitrogen content	33
6 Allocation of biomass during growth of willow	65
7 Willow stand growth and seasonal nitrogen turnover	77
WATER RELATIONS IN WILLOW STANDS	
8 Introduction to modelling of plant water conditions	89
9 Simulation of diurnal transpiration from willow stands	97
10 Willow stand evaporation: Simulation of diurnal distribution using synoptic weather data	121
11 Simulated water balance of a willow stand on clay soil	147
ENERGY FORESTRY: ITS ECONOMICS AND PROSPECTS	
12 Economic potential of intensively cultivated energy forests in Sweden	165
13 Short-rotation forestry: an alternative energy resource?	181
APPENDIX	
14 Computer use in modelling energy forestry in Sweden	189
Index	197

Preface

This is the first comprehensive volume containing documentation on modelling of production, water relations and the economics of intensively cultivated short rotation energy forests. It contains thirteen separate chapters and an appendix, some of which also include listings of the computer programs. The purpose of this volume is to present comprehensive theoretical models, as well as to create a tool for the readers to apply their knowledge on short rotation energy forestry. The contributors of each chapter are individually identified, although the modelling approach as a whole is the result of a continuous exchange of information and opinions between the authors, editors and referees, who are responsible for the peer review of all the contributions to this book.

The separate chapters are sorted into four parts, to enable the reader to obtain a better overview of the content of the whole volume. The first part, *Introduction*, gives the background to energy forestry in general, and a discussion on the simulation models in particular. The second and third parts start with syntheses concerning modelling of growth and water relations, respectively. The second part, *Growth processes in willow stands*, continues with chapters on biomass growth processes, assimilate allocation and nitrogen turnover. The model presented in this part is a description of willow growth simulation with annual results from a three year cutting cycle. In the third part, *Water relations in willow stands*, three different models are presented on water relations in willow, which is one of the main species for Swedish energy forestry. The fourth part, *Energy forestry: its economics and prospects*, comprises an economic calculation for energy forestry on agricultural land in Sweden as well as the prospects for wood biomass as a regenerable, alternative energy resource. The appendix contains a description of the simulation packages, and a sample model for demonstration is given to facilitate the understanding of the modelling efforts.

The models presented in the different chapters contain the source codes, written in such a way that readers with knowledge of programming can easily use them in their own computers. The reason for this is the belief that these models can be applied to other species and environments after the necessary modification of certain variables and parameters.

Kurth L. Perttu
Piotr J. Kowalik

Contributors

Ågren, G.I., Swedish University of Agricultural Sciences, Department of Ecology and Environmental Research, Section of Systems Ecology, Box 7072, S-750 07 Uppsala, Sweden

Eckersten, H., Swedish University of Agricultural Sciences, Department of Ecology and Environmental Research, Section of Energy Forestry, Box 7072, S-750 07 Uppsala, Sweden

Ericsson, T., Swedish University of Agricultural Sciences, Department of Ecology and Environmental Research, Section of Forest Ecophysiology, Box 7072, S-750 07 Uppsala, Sweden

Halldin, S., University of Uppsala, Section of Hydrology, Västra Ågatan 24, S-752 20 Uppsala, Sweden

Jansson, P-E., Swedish University of Agricultural Sciences, Department of Soil Sciences, Box 7014, S-750 07 Uppsala, Sweden

Kowalik, P.J., Technical University of Gdansk, Faculty of Hydrotechnics, Majakowskiego 11, 80-952 Gdansk Wrzeszcz 6, Poland

Ledin, S., Swedish University of Agricultural Sciences, Department of Ecology and Environmental Research, Section of Energy Forestry, Box 7072, S-750 07 Uppsala, Sweden

Lindroth, A., Swedish University of Agricultural Sciences, Department of Ecology and Environmental Research, Section of Energy Forestry, Box 7072, S-750 07 Uppsala, Sweden

Lönnér, G., Swedish University of Agricultural Sciences, Department of Forest-Industry-Market Studies, Box 7013, S-750 07 Uppsala, Sweden

McDonald, A.J.S., Swedish University of Agricultural Sciences, Department of Ecology and Environmental Research, Section of Forest Ecophysiology, Box 7072, S-750 07 Uppsala, Sweden

Nilsson, L-O., Swedish University of Agricultural Sciences, Department of Ecology and Environmental Research, Section of Systems Ecology, Box 7072, S-750 07 Uppsala, Sweden

Parikka, M., Swedish University of Agricultural Sciences, Department of Forest-Industry-Market Studies, Box 7013, S-750 07 Uppsala, Sweden

Persson, G., Swedish University of Agricultural Sciences, Department of Soil Sciences, Box 7014, S-750 07 Uppsala, Sweden

Perttu, K.L., Swedish University of Agricultural Sciences, Department of Ecology and Environmental Research, Section of Energy Forestry, Box 7072, S-750 07 Uppsala, Sweden

INTRODUCTION

1 Climatic, edaphic and management requirements for energy forestry

Stig Ledin and Kurth L. Perttu

1.1 Background

Research on energy forestry started in Sweden in the mid-1970s, after the first 'oil crisis' (Sirén et al., 1984), when the need to decrease the country's dependence on imported fossil fuel, became apparent. Soon after, serious discussions also started about closing down Swedish nuclear power plants. The second 'oil crisis' in 1979 strengthened the conviction that oil consumption should be cut, especially for heating. Later, another factor entered the discussion, namely the possibility of using energy forest as an alternative land use to reduce the surplus of agricultural crops. There are similar possibilities in most western European countries and in North America. According to Gilliuss (1985), the biomass part of total energy consumption is 1% in developed countries, 39% in developing countries and 12% for the whole world. Hall & De Groot (1987) give corresponding figures of 1%, 43%, and 14%, respectively. These figures can easily be increased in many countries by improving the biomass production; for example, by using nitrogen-fixing species.

At least 400 000 hectares of agricultural land are available for fast-growing, broadleaf forests in Sweden. In addition, abandoned agricultural land, amounting to some 100 000 hectares, and suitable peatland, amounting to 700 000 hectares, can be considered. The exploitation of peatland will become economically attractive when cultivation methods and plant material have been further improved.

To boost production, which is the ultimate goal of energy forestry, basic research is being done in the fields of biogeophysics, ecology, genetics, soil science, and management measures. A series of different climatic, hydrological, ecological, and edaphic factors and processes influences plant growth and stand production (Figure 1).

The cultivation of an energy forest starts with the selection of site and plant material, followed by establishment, step by step (Table 1). The measures can differ with the purpose, the species, and the country concerned, but the examples given in the table stress the most important general factors. The established crop goes into the production phase with intensive management, which initially comprises careful weed control followed by fertilization programmes. If necessary, irrigation is applied when conditions allow.

The fast-growing short-rotation species can be coppiced at intervals of 3-5 years (excluding the period of establishment). Harvests can be repeated until the stumps have lost their vitality, probably after 20-40 years, depending on species. Between coppicing, the most important management factor is applica-

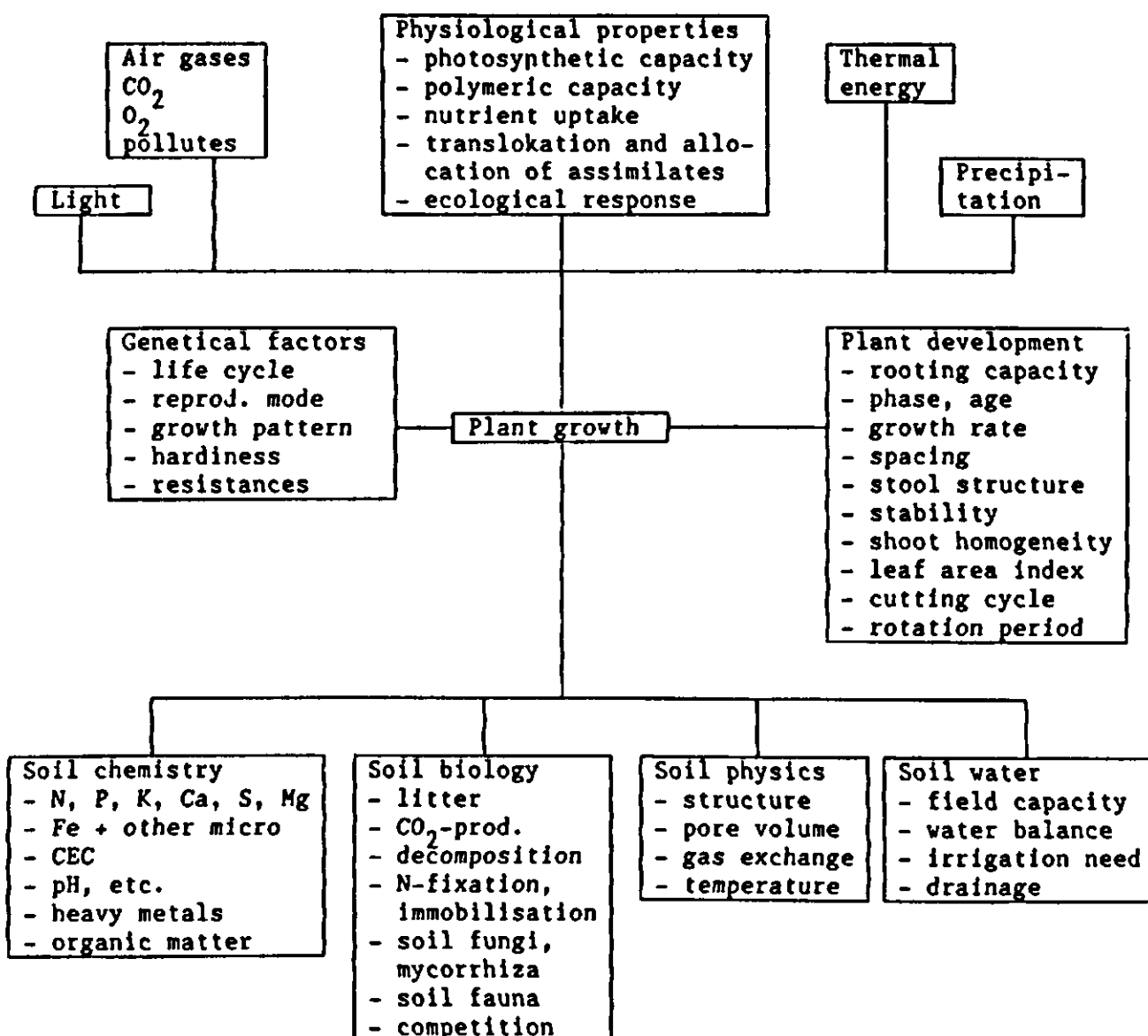


Figure 1. Ecological variables, factors and processes affecting plant growth. (After Sirén, 1983)..

tion of fertilizers (and water). The natural ability of soils to supply the crop with nutrients and water varies considerably. In Sweden, the humid climate renders irrigation unnecessary in many places, but there are no soils on which fertilization could be completely excluded if the aim is a high yield of biomass. Whenever possible, energy forests should be planted on soils with good water supply. Otherwise, the influence of water shortage can lower production considerably (by 50% or more).

The production of energy forests strongly depends on the climate of the area concerned. At higher latitudes, the air temperature is generally the main limiting factor. In other parts of the world, precipitation is the key climatic factor. When constructing growth models such facts must be borne in mind. Similar considerations apply to the edaphic factors. In the following pages, the main climatic, edaphic and management requirements for energy forestry in Sweden are discussed in greater detail.

1.2 Climatic premises for energy forestry in Sweden

Sweden is located in the northern taiga area between latitudes 55° 30' N and 69° N. The air temperature, consistent with a climate that is partly semi-maritime and partly semi-continental (Ångström, 1974), is the most limiting climatic factor for forest production (Perttu, 1980). The temperature sum,

defined as the sum of degrees exceeding a certain threshold value (in this case, the daily mean temperature of +5 °C) and which also limits the start and end of the growing season, lies between 1100 and 1700 day-degrees (Odin et al., 1983). The threshold value of +5 °C has been empirically found to be valid in Scandinavia. In other parts of the world where air temperature is a strongly limiting factor, the threshold value may be different: the correct figure must then be found out from production experiments. In Sweden, the temperature sum (T_{SUM}) can be represented by the following equation (Perttu, 1983):

$$T_{\text{sum}} = 4835 - 57.6 L - 0.9 H \quad \text{Equation 1}$$

where L is the latitude (degrees) and H is the elevation (metres) above sea-level. It is important to point out that this expression is valid only under average conditions and not at individual sites, where the microclimate is greatly influenced by local topography, nearby forests, etc. (cf. Geiger, 1971).

The most important climatic elements for energy forest production are the photosynthetically active part of solar radiation (light), air temperature and humidity, wind speed, and precipitation. The latter factor has an indirect influence (via the amount of plant-available water in soil) and a direct influence on the leaf temperature, when intercepted water evaporates. The relations between these elements and growth and water, respectively, are discussed in subsequent chapters.

The climate is favourable for intensive energy forestry in most of southern Sweden and along the coast of Gulf of Bothnia, where the length of the growing season varies between 160 and 230 days (Perttu, 1980). In northern Sweden, intensive energy forestry is limited mainly by the low temperatures and thus by the relatively short growing period. Spring and autumn frosts also occur on sites where energy forestry is possible (Christersson et al., 1984). These problems can mostly be overcome by selecting hardy species, by active management, and by locating plantations away from particularly frost-exposed localities (Perttu, 1981; Sirén et al., 1987).

Precipitation is generally sufficient for plant husbandry in most parts of Sweden, except the southeastern coastal area, where drought frequently occurs in early summer. In such areas, irrigation (preferably combined with fertilization) is often the only solution, since such measures boost energy forest production to levels where it can compete in economic terms both with traditional agriculture and with other energy sources.

1.3 Edaphic conditions required for energy forestry in Sweden

The basic edaphic properties of importance for the species used in energy forestry are the same as for other cultivated crops. The soil should be well able to supply the plants with water and nutrients while simultaneously allowing diffusion of oxygen into and carbon dioxide out of the rhizosphere to enable root respiration. Many energy forestry species, however, are more capable than

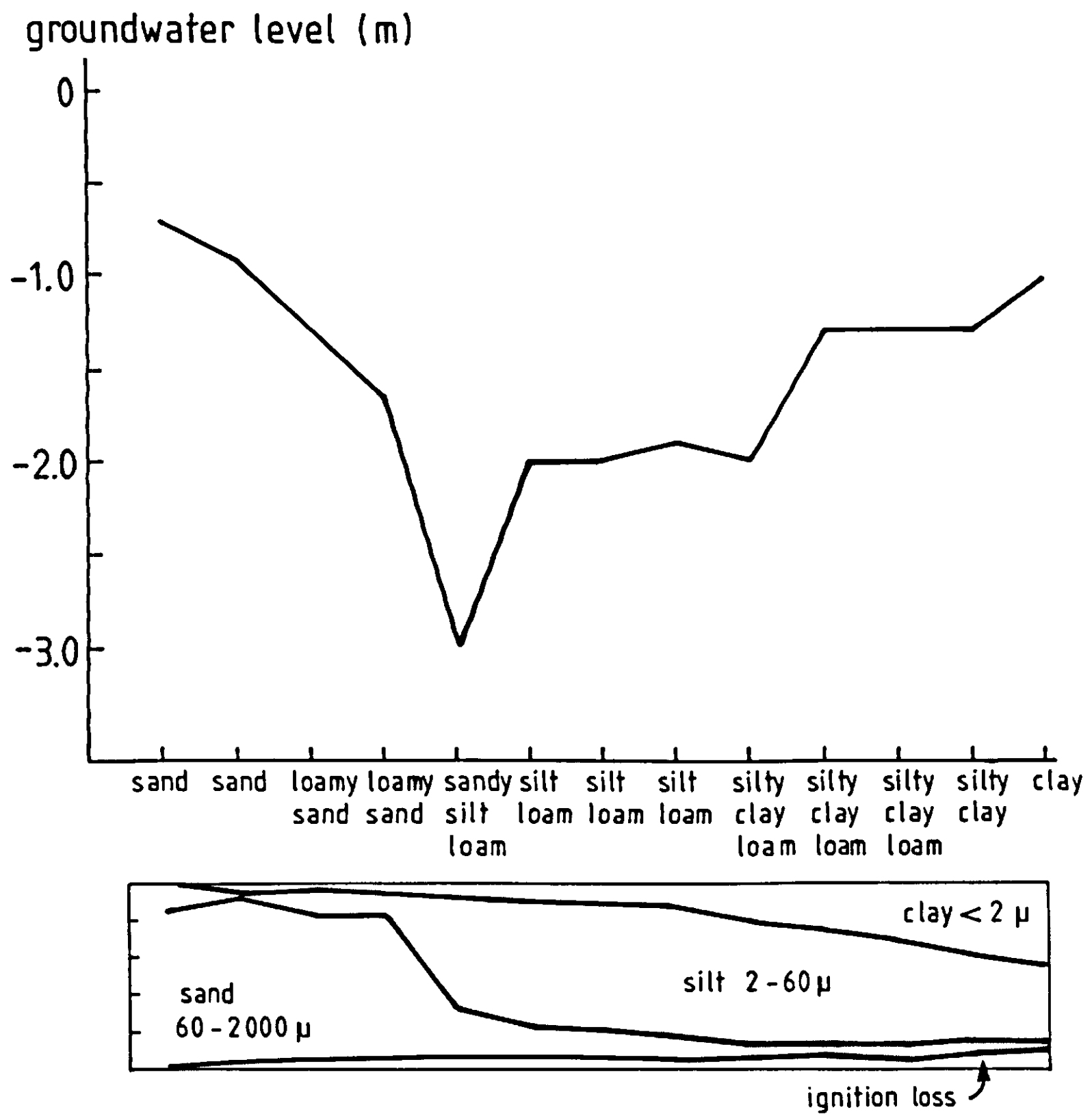


Figure 2. The groundwater level required to give a supply of at least 200 mm retained water and capillary-rise water in soil. (After Olsson & Samils, 1984).

conventional agricultural crops of taking advantage of an intermittently or constantly high groundwater level. Olsson & Samils (1984) have presented data on the highest groundwater level required to give a supply of at least 200 mm retained water and capillary rise water in different soils (Figure 2).

Energy forestry is suitable for agricultural land, where it gives large yields on fertile soils. But other criteria must also be taken into account; for instance, properties involving management techniques as well as plant material. Since short-rotation, fast-growing species should be harvested during winter, it is possible to use wetter soils that are flooded during spring and autumn. When frozen, these soils, can withstand heavy loads from tractors and harvesting machines. Such soils are not, however, suitable for agricultural crops that need to be sown every spring and harvested every autumn. In all cases, management must be adapted to the specific conditions revealed by soil survey. At the very least, soil type, thickness of soil horizons, nutrient status, and plant-available water must be known.

1.4 Selection of plant material

The plant material for energy forestry has to be carefully selected. This can be done in several ways, for instance, in Sweden selection campaigns have been conducted through a weekly agricultural magazine (Land). Readers were asked to send in the tallest shoots they could find of various *Salix* clones. Another source of plant material has been the selections made abroad. The third way, and the most important in the future, is via the breeding programmes currently in progress in many countries.

According to Sirén et al. (1987), the attributes of importance for selection are:

- dry matter production per units of time and area
- resistance to pest and pathogens
- frost hardiness
- adaptation and tolerance to different environmental conditions
- morphological characteristics
- wood quality in a wide sense.

Naturally, plant material with the overall top properties is selected for cultivation in a certain area. With time, research work will lead to new and better plants. However, already established cultivations will always contain material from earlier stages during the whole rotation period. This implies that plant material will gradually improve during the coming decade.

1.5 Management of established stands

As already pointed out, fertilization is a factor of great importance in management. It was also stressed that weeds must be eradicated before fertilization starts (Table 1). In the first year after establishment, before the canopy has closed, mechanical weed control with a row rotavator or, on stony soils, equipment similar to that used in sugar beet crops, could be used.

When choosing the fertilization routine one should consider the specific soil being used. If it has the property of a well-structured clay with good and deep root penetration, a wide variety of pore sizes and good nutrient adsorption properties, it is possible to achieve a high biomass yield if most nutrients are added at the beginning of the growing season. If, on the other hand, the soil has most pores of equal size with poor root penetration and poor ability of the soil material to adsorb nutrients, it is impossible to obtain good crop growth if the fertilizers are added in one application early in the spring. Instead, attempts should be made to adjust fertilization to the current uptake and growth potential of the plants. Naturally, this also holds for soils of the type just mentioned, with a wide variety of pore sizes, etc. However, in practice the fertilization regime is also governed by technical considerations. The requirement for several additions of fertilizers during the growing season forces the farmer to invest in a new management system, e.g. sprinkler or trickle irrigation combined with fertilization.

Table 1. The most important measures needed for establishing energy forests in Sweden. (After Sirén et al., 1987).

<i>Measures to be taken</i>	<i>Time of the year</i>
Soil characterization	The summer before planting
Soil improvement including clearing and drainage	
Eradication of perennial and annual weeds with glyphosate, $4\text{-}6\text{ l ha}^{-1}$. Ploughing not earlier than 3 weeks after spraying	August-September the year before planting
Further soil improvement by liming (if $\text{pH} < 5$) and fertilization with macro- and micronutrients based on soil analyses. Deep rotovation or ploughing	September-October the year before planting
Plant-bed preparation, i.e. harrowing or rotovation	When the soil is sufficiently dry in the spring
Planting	Immediately after plant bed preparation
Weed control with soil herbicides to prevent herbs developing from seeds	Immediately after planting
Fertilization with nitrogen, 60 kg ha^{-1}	In July, when the weeds are definitely out-competed by the young trees
Irrigation to supply the crop with 20-30 mm water per week (including precipitation) during the main part of the growing season	If necessary and possible

In the first production year in practical energy forestry in Sweden, the amount of added nitrogen (N) is in the range of $90\text{-}120\text{ kg ha}^{-1}$. In the second production year and in subsequent years during the build-up phase, the addition of N is in the range of $120\text{-}150\text{ kg ha}^{-1}$. Later, the amounts of N can be lowered to $60\text{-}80\text{ kg ha}^{-1}\text{ yr}^{-1}$. The additions of phosphorus (P) and potassium (K) are dependent on the soil status (as is the case for N on organic soils). The

amounts are usually in the range of 20-50 kg ha⁻¹ yr⁻¹ for P and 80-100 kg ha⁻¹ yr⁻¹ for K.

1.6 Damage in energy forest plantations

Willow energy forests are damaged by browsing animals (moose, deer, hare, rabbit, vole), snow and wind breaks, drought, summer frosts, insects, fungi, bacteria, viruses, etc. Each of these threats could be reduced by management measures and the selection of plant material. The fight against such threats is continuous and will go on as long as the cultivation proceeds. The plantation manager must be constantly alert when it comes to taking precautions and measures during the growing season. The condition of plantations will vary from practically free of damage to severely hit by several of the factors listed above.

1.7 Harvesting and utilization of energy wood

Energy forests can be harvested manually or by special machines. Promising prototypes of harvesting machines have been developed in Northern Ireland, the United States and Sweden.

The Swedish machine developed for harvesting willow, can be attached to a standard farm tractor. Two circular saws cut the willow stems about 10 cm above the soil surface, one row at a time. The stems are automatically transported backwards on to a platform where they are gathered into a vertical bundle weighing as much as 2.5 t. The platform can be tilted and the bundle tipped off at, for instance, the end of the field close to a tractor road. The machine is adapted for harvesting material with stems ranging from 3 to 6 m in height and from 1 to 6 cm in diameter. Its capacity is currently 0.8-1 ha in eight hours, but this is expected to increase to about 1.5 ha when the equipment has been improved in the light of winter harvest experiences. The length of the harvesting season is typically about 100 days, and the machine can be run on a two shift basis.

The biomass is intended to be used for different purposes, such as fuel for heating and raw material for the forest and chemical industries. Willow biomass has been used in many different ways: the whole shoots are used to make structures to prevent erosion, in the furniture industry, as a raw material for packing-boxes (mainly for butter and cheese), for wooden shoes (clogs), baskets, toys, etc. The leaves have been harvested green for livestock fodder and the bark is still used in tannery processes (Sirén et al., 1987).

The heating value of *Salix* wood with bark is 19-20 MJ kg⁻¹ (Flower Ellis & Sennerby-Forsse, 1984), which is somewhat lower than that of traditional fuelwood. The use of willow as fuelwood is, however, very interesting thanks to its rapid growth, which is 12-15 t ha⁻¹ yr⁻¹ of dry matter stemwood, corresponding to 5-6 t of oil equivalents. The water content of willow wood at

harvest is usually 45-55%, a value which in many cases is somewhat too high for immediate combustion. However, a couple of weeks of storage even during winter, will lower this value to a more acceptable level. If stored in bundles during the summer period, the water content will drop to about 20% (Stridsberg & Thörnqvist, 1984). The ash content of willow wood is around 1.7%. The final product will enter the market mainly as fuelchips used in the district heating plants that are very common in Sweden. It will, therefore, compete qualitatively and economically with residues from traditional forestry.

1.8 References

Ångström, A., 1974. Sveriges klimat. [Climate of Sweden]. General-stabens Litografiska Anstalts Förlag, Stockholm, 188 pp.

Christersson, L., von Fircks, H. & Perttu, K., 1984. Sommarfroster. [Frosts during the growing season]. Swedish University of Agricultural Sciences, Section of Energy Forestry, Uppsala. Report 37, 24 pp.

Flower-Ellis, J.G.K. & Sennerby-Forsse, L., 1984. Growth analysis and wood properties of *Salix* grown under intensive culture. Book of Abstracts p. 46. BioEnergy 84 World Conference, 18-21 June, 1984, Göteborg, Sweden. Vasastadens Bokbinderi AB, Göteborg.

Geiger, R., 1971. The climate near the ground. Harvard University Press. Cambridge, Massachusetts, 611 pp.

Gilliusson, R., 1985. Wood energy: Global needs. In: G. Sirén & C.P. Mitchell (Eds): Forest energy and fuelwood crisis. Report 41:2-15. Proceedings of IUFRO Project Group P1.09.00 meeting, 8-9 June, 1984, Uppsala, Sweden. Swedish University of Agricultural Sciences, Section of Energy Forestry, Uppsala.

Hall, D.O. & De Groot, P.J., 1987. Introduction: The biomass framework. In: D.O. Hall & R.P. Overend (Eds): Biomass, regenerable energy. John Wiley & Sons, Chichester, New York, Brisbane, Toronto, Singapore, pp. 3-24.

Odin, H., Eriksson, B. & Perttu, K., 1983. Temperaturklimatkartor för svenska skogsbruk. [Temperature climate maps for Swedish forestry]. Report 45, 57 pp. Swedish University of Agricultural Sciences, Department of Forest Soils, Uppsala.

Olsson, M.T. & Samils, B., 1984. Site characterization at energy forestry production. Report 48, 83 pp. Swedish University of Agricultural Sciences, Department of Forest Soils, Uppsala.

Perttu, K., 1980. Abiotic premises for growing energy forests. In: K. Perttu (Ed.): Proceedings from a symposium arranged by the International Energy Agency (IEA) planning group on Growth and Production, September 24, 1979, Bogesund, Stockholm. Report 8:25-34. Swedish University of Agricultural Sciences, Section of Energy Forestry, Uppsala.

Perttu, K., 1981. II. Radiation cooling and frost risk. In: G. Ericsson (Ed.): Climatic zones regarding the cultivation of *Picea abies* L. in Sweden. Research Notes 36, 25 pp. Swedish University of Agricultural Sciences, Department of Forest Genetics, Uppsala.

Perttu, K., 1983. Temperature restraints on energy forestry in Sweden. *International Journal of Biometeorology*, Volume 27(3):189-196.

Sirén, G., 1983. *Energiskogsodling*. [Cultivation of energy forests]. No. 1983:11, 255 pp. Nämnden för energiproduktionsforskning, Stockholm.

Sirén, G., Perttu, K., Sennerby-Forsse, L., Christersson, L., Ledin, S. & Granhall, U., 1984. *Energy Forestry – Information on research and experiments at the Swedish University of Agricultural Sciences. Section of Energy Forestry*, Uppsala. 16 pp.

Sirén, G., Sennerby-Forsse, L. & Ledin, S., 1987. Energy plantations – short rotation forestry in Sweden. In: D.O. Hall & R.P. Overend (Eds): *Biomass, regenerable energy*. John Wiley & Sons, Chichester, New York, Brisbane, Toronto, Singapore, pp. 119-143.

Stridsberg, S. & Thörnqvist, T., 1984. *Egenskaper och förbränningsbetingelser för energiskogsflis, inklusive lagringsförsök med energiskog*. [Properties of willow chips and combustion conditions, including whole tree storage experiments]. No. 2760771, 80 pp. Nämnden för energiproduktionsforskning, Stockholm.

2 Approaches to modelling growth and water for forestry

Kurth L. Perttu and Piotr J. Kowalik

2.1 Introduction

Mathematical modelling has become a logical complement to more conventional research activities, and the usefulness of such an approach in forest research has been clearly demonstrated in Sweden (e.g. Ågren & Axelsson, 1980; Ingestad et al., 1981; Linder, 1981; Eckersten et al., 1983) and in other countries (e.g. Hari et al., 1981; Sievänen, 1983; Kimmis & Scoullar, 1984; Mohren et al., 1984; Landsberg, 1986; Mohren, 1987). There are various reasons for modelling. Every modeller has a specific reason for developing a model, and many idiosyncratic models have subsequently never been used by other researchers. The development of models has become a goal in itself (Passioura, 1973) and the aim to develop usable models, for example, as predictive tools, is sometimes lost sight of. In many cases, models can be of help in organizing thoughts and exchange of information, act as a way of guiding research, e.g. to pinpoint areas where research is most needed, set priorities for future research, and be a new tool for describing a system. Other possible applications are to identify gaps in knowledge and data, in reviewing and synthesizing knowledge of a field, for comparing opinions and hypotheses, and to investigate possible future development. Simulation is also used in education, to teach and provide detailed understanding of the system concerned, and to create new knowledge for developing theories and generating hypotheses to facilitate the experimental testing of results. The growing use of simulation models has strengthened the possibilities of predicting future conditions of a system and of utilizing research results to solve management problems.

2.2 Simulation models and energy forestry

As indicated in the previous section, simulation models are important tools in many types of research, especially in the field of biogeophysics. The purpose of this book is to present the models recently developed and currently used in the rapidly expanding, research on and practice of short-rotation energy forestry (at present only *Salix*) in Sweden. The book is, divided into four parts and comprises thirteen chapters and an appendix. Most of the models presented deal with growth processes and water relations in *Salix* stands. A model for calculating the economics of energy forestry is also presented. As a background, the requirements for growing energy forests are underlined, and the merits of this type of short-rotation forestry as an alternative energy source are discussed. Five of the chapters contain the source code in FORTRAN of the simulation

models presented (Table 2). Each model can be adapted to various computers, depending on which simulation packages are available for the computer concerned. Examples of utilization of the computer facilities within the Swedish energy forestry research programme are demonstrated in the appendix.

In Sweden, various mathematical simulation models have been used to determine the growth pattern and production of short-rotation energy forests and the water conditions in the soil-plant-atmosphere system. The growth model currently in use (see Chapter 5) relates forest production to weather, because the potential growth depends on the physiological characteristics (e.g. foliar nitrogen content) of the plant species, in combination with weather conditions (mainly temperature and solar radiation). For a given site, growth may be lower because of incomplete canopy closure, shortage of water and nutrients (to a large degree determined by the site), and the occurrence of growth-disturbing factors such as pests, diseases, competition from other species (weeds) and large-scale damage to the plants, e.g. by wind, frost or air pollution. Such disturbances, which reduce the production considerably but appear irregularly, are not incorporated in the present version of the growth model. The models simulating the water conditions in the energy forest ecosystems contain a series of output variables that directly affect the growth relations (cf. Chapter 8). These models are complementary in that they have

Table 2. List of chapters with indications (*) whether source codes are included or not.

Author(s)	Chapter No.	Keywords
Ledin & Perttu	1	Requirements
Perttu & Kowalik	2	Modelling approach
Ågren, Kowalik & Perttu	3	Introduction, growth
McDonald	4	Photosynthesis
Eckersten, Lindroth & Nilsson	5*	Willow growth model
Eckersten & Ericsson	6	Biomass allocation
Ågren	7 ¹	Nitrogen turnover
Kowalik & Perttu	8	Introduction, water
Kowalik & Eckersten	9*	Transpiration
Halldin	10*	Evaporation
Persson & Jansson	11 ²	Water balance
Lönnér & Parikka	12*	Economy
Perttu	13	Alternative resource
Halldin	14*	Computer use

¹ From the equations presented, a simulation model can easily be implemented.

² This model is now available on IBM compatible PCs (for further information, contact the authors, see address in Preface).

different time resolutions and emphasize various compartments of the soil-plant-atmosphere system.

The first simulations of energy forest growth used relatively simple models, which incorporated only the basic growth processes, such as carbon dioxide assimilation and respiration, and the relation between such processes and different environmental conditions. Subsequently, more detailed information was introduced in the calculations by incorporating aspects such as the influence of nitrogen and water. The simple models were necessary for analysis of growth and yield in a broad sense and for contributing to a better understanding of primary production in this type of forest. However, many processes are very complex, and the models often also have become complex. Overall model behaviour should be tested against field data. By integrating the main aspects of forest growth, the models also allow the main factors that determine total stand growth to be ascertained. They, therefore, indicate ways of improving yield, of predicting the consequences of, for example, future weather changes, of calculating of economic yield, and of identifying research priorities (cf. e.g. Mohren, 1987).

Values used to determine the physiological parameters in the models are either based on literature data, on physiological processes, on laboratory measurement of characteristic physiological aspects, or estimated on the basis of general knowledge of the processes concerned. Parameters that characterize site conditions have been sampled in many different field experiments. These data have then been used to evaluate individual models, e.g. concerning the productivity and hydrology of the stand.

The major topic of this book is simulation, i.e. the design, construction and application of mathematical models of a dynamic character, and the study of their behaviour. Conscientious attempts have been made to gather experimental data to give the models correct parameters and to verify the results. All data required to run a model are specified, including the initial values needed to start the calculations. The programs are written and explained in such a way that the user can continue to build on them and apply them to similar problems.

The simulation models in this volume are in many aspects corroborated by measured data obtained from field experiments. They are explanatory in nature and intended to be used for evaluating energy forestry research and practices in various environmental conditions. The intention and belief is that the results of these modelling efforts will be used in other countries where corresponding work is planned or in progress.

2.4 References

Ågren, G.I. & Axelsson, B., 1980. PT – a tree growth model. In: T. Persson (Ed.): Structure and function of northern coniferous forests – an ecosystem study. Ecological Bulletin (Stockholm), 32:525-536.

Eckersten, H., Kowalik, P.J., Nilsson, L.-O. & Perttu K.L., 1983. Simulation of total willow production. Report 32, 45 pp. Swedish University of Agricultural Sciences, Section of Energy Forestry, Uppsala.

Hari, P., Mäkelä, A. & Sievänen, R., 1981. Systems concept in theoretical plant ecology. Systems Theory Laboratory Report B60, 33 pp. Helsinki University of Technology.

Ingestad, T., Aronsson, A. & Ågren, G.I., 1981. Nutrient flux density model of mineral nutrition in conifer ecosystems. In: S. Linder (Ed.): Understanding and modelling tree growth. *Studia Forestalia Suecica*, 160:61-71.

Kimmis, J.P. & Scoullar, K.A., 1984. The role of modelling in tree nutrition research and site nutrient management. In: G.D. Bowen & E.K.S. Nambiar (Eds): *Nutrition of plantation forests*. Academic Press, London, pp. 463-487.

Landsberg, J.J., 1986. *Physiological ecology of forest production*. Academic Press, London, 198 pp.

Linder, S. (Ed.), 1981. Understanding and predicting tree growth. *Studia Forestalia Suecica*, Nr 160, 87 pp.

Mohren, G.M.J., 1987. Simulation of forest growth, applied to Douglas fir stands in The Netherlands. Thesis. 184 pp.

Mohren, G.M.J., van Gerven, C.P. & Spitters, C.J.T., 1984. Simulation of primary production in even-aged stands of Douglas fir. *Forest Ecology and Management* 9:27-49.

Passioura, J.B., 1973. Sense and nonsense in crop simulation. *The Journal of the Australian Institute of Agricultural Science* 39:181-183.

Sievänen, R., 1983. Growth model for mini-rotation plantations. *Communicationes Instituti Forestalis Fenniae* No. 117, Helsinki, 41 pp.

GROWTH PROCESSES IN WILLOW STANDS

3 Introduction to modelling of plant growth

Göran I. Ågren, Piotr J. Kowalik & Kurth L. Perttu

3.1 Background

The usefulness of a modelling approach in forest research has been demonstrated by many authors (see Chapter 2). The ideal simulation model used to study forest growth should be derived from knowledge of the underlying physiological, physical and chemical processes, and how the actual weather and management measures influence them. In a recent evaluation, Mohren suggested that the ecophysiological aspects of primary production in plant canopies are related to the processes of:

absorption of photosynthetically active radiation by the foliage; uptake of carbon dioxide by assimilation through the stomata; loss of water vapour to the atmosphere through the open stomata, compensated for by root uptake of soil moisture, and subsequent transport to the foliage; maintenance of the living biological structure, thereby consuming assimilation products; distribution of the assimilates available for growth over the plant organs, and conversion of assimilation products into structural dry matter, together with incorporation of nutrients in the organic matter, and nutrient uptake by roots (Mohren, 1987, p. 11).

Mohren's (1987) enumeration of processes indicates at least three basic aspects on which one can focus when modelling plant growth. The oldest, and most commonly used way of formulating a plant growth model is to use photosynthetic rate as a base. The influence of other factors is then either ignored (e.g. assuming optimal nutrition) or introduced as modifying the photosynthetic rate. To a large extent these formulations emanate from the pioneering work of de Wit (1965) and could be named the 'Wageningen school'. The recognition that most natural ecosystems are nutrient-limited, particularly as regards nitrogen, has inspired others to focus on nitrogen. In this case, photosynthesis is not represented explicitly, but the accumulation of carbon (dry matter) is subordinate to the uptake of nutrients. The insistence on plant nutrition as a driving force in plant models has been particularly strongly emphasized by a group of scientists in Uppsala and may warrant the name 'Uppsala school', although other models, for example, FORCYTE (Kimmins, 1986), also rely heavily on nutrients. Chapters 4, 5 and 6 present examples of the Wageningen school, whereas the Uppsala approach is exemplified in Chapter 7.

The third aspect basic to modelling plant growth is water as a growth regulator. Although the modelling of water and plant relations is common,

the emphasis tends to be on the effect of plants on the water circulation through the ecosystem.

3.2 Discussion

The existence of different schools of modelling plant growth should not be understood as a conflict between different approaches but as complementary ways of looking at the world. It is normally impossible to see all sides of a complicated object simultaneously. However, even if the object is sufficiently transparent to, in principle, permit a full view of it, the resulting image is still so confusing that it is impossible to interpret it. Then, a common way to proceed is to look at one side, and only when this side makes sense to turn the object to display another side. In this piecemeal manner a picture of the object is created. However, sooner or later it will be necessary to look at two or more sides simultaneously and see how they connect, otherwise one will probably end up with a set of disjunct sides. Understanding how the sides connect is not a question of computational power (e.g. a computer able to handle ever more equations) but one of intelligent analysis of the prime features of each side to see how they join up. One such analysis of the relation between the Wageningen and the Uppsala schools is provided by Eckersten (1985b).

Another fundamental distinction in plant growth modelling is between levels of organization. Given the clear emphasis on the stand as the basic unit in this volume, this question only occasionally arises here. Passing from leaf photosynthesis (Chapter 4) to stand level (Chapters 5 and 6) is the most prominent example. Associated with levels of organization are time scales (Allen & Starr, 1982). The uniformity in the level of organization is also reflected in the time scales used here. In Chapter 4, McDonald, working at the highest resolution (the leaf and the small plant), is compelled to use the short time scale (hour). With a lower level of resolution (the stand), the time scale is changed to the day, but because of the importance of the within-year dynamics in deciduous stands, it is not possible to extend it up to the year, as can be done with coniferous forests (e.g. Ingestad et al., 1981). For example, weather is characterized using meteorological data from local weather stations in the form of totals of daily global radiation, daily minimum and maximum temperatures, etc. Also, the structural aspects of forest stands are dealt with only as far as is necessary to quantify the relation between environmental factors and stand growth, e.g. canopy structure and light interception.

Furthermore, there is feedback between the rates and the state variables, defined by de Wit (1982) as self-regulation, because plants control their own function and interact through the physical environment. When carrying more leaves, plants intercept more radiation and the shading effect is then a feedback factor that changes the structure of the stand and the stand functions (Hari et al., 1981). The root system occupies more and more of the soil volume and the plants begin to compete with each other, resulting in the abovementioned self-

regulation. For better understanding of growth models, two basic relations should be introduced. The first one is a cause-effect equation relating simultaneously operating factors to rates of plant growth in field conditions (Visser & Kowalik, 1974; Kowalik, 1984). An example of this relation is the so-called light response curve, giving the rate of assimilation of a leaf as a function of light intensity. The second basic relation is an equation for the accumulation of biomass of different parts of the plant as well as of the total plant body during the growing season. The growth can be approximated by summing the rates of growth, but the allocation of assimilates should be considered together with the feedback response. A particular carbon allocation pattern for a willow has to be calibrated, employing a particular descriptive distribution key.

At the most detailed level, photosynthetic rates at the leaf level of willow have been studied (McDonald, 1980; McDonald et al., 1981; Chapter 4 in this volume). The photosynthetic response to light is characterized by the leaf's maximum assimilation rate at light saturation, its slope at low light intensities, and also by the maintenance respiration of the tissue. In Chapter 4, McDonald estimates parameters of the response curve from data pertaining to leaves collected from the field as well, to whole-shoots of small plants grown in climate chambers to show some of the variables that may affect the shape of the photosynthetic light response curve. For example, small willow-shoots with good nutrient status may have higher light-saturated values for photosynthetic rate than shoots belonging to plants with a poor nutrient supply.

In Chapter 5 Eckersten et al. address the optimal production situation for the whole stand, using the light response curve of a small plant and assuming that water and nutrients are amply supplied and there are no pests and diseases. Primary production is then determined only by the amount of photosynthetically active radiation absorbed by the foliage moderated by the air temperature, but with a loss caused by respiration of 20% of gross assimilation. The allocation of biomass production to roots is a constant, 15% of the daily growth, whereas allocation to leaves is a function of the time during the growing period. The overall behaviour of the model seems to follow field measurements reasonably, both in the field plots used for calibration and in the independent plots (Eckersten, 1985a; Nilsson, 1985).

The simulation model described in Chapter 5 is applicable even in situations where empirical data on stand growth and yield are scarce. It can be used where the growing conditions are evolving rapidly, such as in short-rotation forestry, i.e. young stands on recently afforested sites. To obtain an idea of the possible variations in production, a 15-year period (1964-1978) at 13 different locations was examined. The mean annual stem production for 1-year-old shoots ranged between 6.5 and 9.8 t dry matter ha^{-1} , depending on site. Two- and three-year-old shoots reached levels of 9.0-13.1 and 10.2-14.6 t, respectively. The between-year variations were within $\pm 25\%$ for sites located in the inland areas and $\pm 15\%$ in the coastal regions. The simulations indicate what levels the farmers can expect in annual production because of variations in climate, even with all

other growth-limiting factors under control.

In Chapter 5 Eckersten et al. use empirically derived allocation functions, which require large amounts of data. But in Chapter 6 Eckersten & Ericsson relate the allocation pattern of dry matter between roots, stems and leaves to the plant nitrogen status, the size of the above-ground biomass and the time, respectively. They conclude that nitrogen affects canopy photosynthesis mainly through the shoot to root biomass partitioning. The shoot to root ratio decreases from 5.7 at 100% of potential production to about 1.5, when shortage of water or nutrients results in lower production. Mohren (1987) reported a decrease of similar magnitude for Douglas fir forest (from 4.0 at the potential production level to 2.5 when only 50% of potential production was possible because of lack of water and nutrients).

The abovementioned models deal with plant processes only. In Chapter 7 Ågren takes plant nitrogen as the pivotal element, and connects the external supply of nitrogen to foliar biomass production, accumulation of total biomass, and turnover of nitrogen for a willow stand. His approach can be used to project the long-term consequences of fertilization for stand production and for the balance between nitrogen uptake and mineralization in a rapidly growing stand of *Salix*. An annual application of N of about 120 kg ha⁻¹, corresponding to the annual harvest of the stem biomass, has to be added as fertilizer. Fertilization must be synchronized with growth in optimally growing *Salix* stands to avoid losses of nitrogen. The simulations show that if nitrogen mineralization is delayed until 15 days after the *Salix* has begun to take up nitrogen, the cumulative nitrogen uptake during the growing season can exceed the amount of nitrogen that has been delivered from mineralization by as much as 270 kg ha⁻¹; this figure is 140 kg ha⁻¹ when the uptake of nitrogen and mineralization start and end simultaneously. More empirical data on the subject of nutrient cycling in willow are given by Ericsson (1984) with additional recommendations on fertilizing strategy for willow plantations.

3.3 Conclusions

In the future, the models will have to be refined so they can handle the plant's carbon allocation patterns more precisely, with respect to nutrient and water stresses. The incorporation of the soil's capacity of buffering against environmentally-induced fluctuations in water and nutrient supply while at the same time not allowing losses of these to surrounding ecosystems is another challenge. An approach in which total stand growth is studied from underlying physiological processes should indicate the possibilities for increasing growth by proper management measures. These types of models are currently being developed by a group of biogeophysical researchers in Uppsala (Sweden).

3.4 References

Allen, T.F.H. & Starr, T.B. 1982. *Hierarchy; perspectives for ecological complexity*. The University of Chicago Press, Chicago. 310 pp.

Eckersten, H., 1985a. Willow growth as a function of climate, water and nitrogen. Dissertation. Report 25, 38 pp. Swedish University of Agricultural Sciences, Department of Ecology and Environmental Research, Uppsala.

Eckersten, H. 1985b. Comparison of two energy forest growth models based on photosynthesis and nitrogen productivity. *Agricultural and Forest Meteorology* 34:301-314.

Ericsson, T., 1984. Nutrient cycling in willow. Report 1984:5, 32 pp. IEA/FE PG 'B' - ENFOR, Canadian Forest Service.

Hari, P., Mäkelä, A. & Sievänen, R., 1981. Systems concept in theoretical plant ecology. *Systems Theory Laboratory Report B60*, 33 pp. Helsinki University of Technology.

Ingestad, T., Aronsson, A. & Ågren, G.I., 1981. Nutrient flux density model of mineral nutrition in conifer ecosystems. In: S. Linder (Ed.): *Understanding and predicting tree growth*. *Studia Forestalia Suecica* 160:61-71.

Kimmins, J.P. 1986. *Forest ecology*. Macmillan, New York.

Kowalik, P.J., 1984. Mathematical modelling of energy forest growth: an outline. In: K.L. Perttu (Ed.): *Ecology and management of forest biomass production systems*. Report 15:429-459. Swedish University of Agricultural Sciences, Department of Ecology and Environmental Research, Uppsala.

McDonald, J., 1980. Gas exchange research within the energy forestry project. In: K. Perttu (Ed.): *Proceedings from a symposium arranged by the International Energy Agency (IEA) planning group on growth and production, September 24, 1979, Bogesund, Stockholm*. Report 8:35-43. Swedish University of Agricultural Sciences, Department of Ecology and Environmental Research, Uppsala.

McDonald, J., Lohammar, T. & Linder, S., 1981. Effects of leaf nitrogen content on CO₂ exchange in a number of *Salix* clones. Report 16, 29 pp. Swedish University of Agricultural Sciences, Section of Energy Forestry, Uppsala.

Mohren, G.M.J., 1987. *Simulation of forest growth, applied to Douglas fir stands in The Netherlands*. Thesis. Pudoc, Wageningen, 184 pp.

Nilsson, L.-O., 1985. Growth and yield of willow stands in relation to climate and nutrition. Dissertation. Report 21, 38 pp. Swedish University of Agricultural Sciences, Department of Ecology and Environmental Research, Uppsala.

Visser, W.C. & Kowalik, P.J., 1974. Mathematical representation of the effect of simultaneously operating growth factors. Proc. 7th Intern. Colloquium Plant Analysis and Fertilizer Problems, Hanover 1974, pp. 473-503.

Wit, C.T. de, 1965. Photosynthesis of leaf canopies. *Agric. Res. Rep.* 663, 57 pp. Pudoc, Wageningen.

Wit, C.T. de, 1982. Simulation of living systems. In: F.W.T. Penning de Vries & H.H. van Laar (Eds.): *Simulation of plant growth and crop production*. pp. 3-8. *Simulation Monographs*, Pudoc, Wageningen.

4 Photosynthetic light response of single leaves and small plants

A. James S. McDonald

4.1 Introduction

The photosynthetic light response of single leaves depends on many internal and external factors (see reviews by Hesketh et al., 1983; Ludlow, 1983). Here, the discussion is confined to developmental stage and prevailing photon flux densities in the canopy. In a willow stand these two variables are unlikely to be independent. For example, as leaves become older, they may become progressively shaded. Alternatively, some leaves may complete their ontogeny and eventually die in fully exposed or very shaded environments but, even here, there will be seasonal variation in prevailing photon flux density.

4.2 Material and methods

In order to determine the extent to which light response in single leaves of a willow canopy is likely to vary, a limited study, incorporating extremes of developmental stage and photon flux density, was carried out. Three main current-year shoots were selected from a 1 year old *Salix viminalis* stand growing at Ultuna (latitude 59° 52' N), Sweden. The stand had received drip irrigation and high levels of fertilizer throughout the growing season. Three types of shoot were chosen in the latter part of the growing season: those whose leaves had all developed and remained in an exposed light environment; those whose leaves had all developed in exposed light but had become progressively shaded; those whose leaves had all developed and remained in a shaded climate.

One shoot was harvested on each of three consecutive days and transferred to a gas-exchange laboratory. The shoots were re-cut under water and the leaves sprayed at regular intervals with a mist sprinkler. For each shoot, single leaves were selected at 20, 40, 60, 80 and 100% distance from the shoot tip. The leaves were harvested consecutively with attached stem sections. Single leaves were enclosed in a measurement cuvette with the cut end of the stem kept under water. Net photosynthesis was measured when steady-state values had been reached at photon flux densities of approximately 0, 100, 200 and 1000 $\mu\text{mol m}^{-2} \text{s}^{-1}$. Other conditions in the cuvette were: air temperature = 20 °C and relative humidity = 75% with continuous mixing of air. It was assumed that by keeping the attached stem segment in water and by having a low vapour pressure deficit in the cuvette, leaf water potentials would be high and approximately equal in all leaves. Carbon dioxide (CO_2) exchange was measured by an open gas analysis system (IRGA type ADC mk III).

In a preliminary study, net CO_2 exchange was measured on intact field leaves

with a CO_2 porometer (IRGA type ADC, LCA 2). The measurements were made on sun leaves at saturating photon flux densities; air temperature = 20 °C and relative humidity > 70%. The measurements were made in the early morning on the assumption that leaf water potentials would be high in the well-irrigated stand. Shoots were then transferred to the laboratory and CO_2 exchange was measured on the same leaves, as described above.

4.3 Results and discussion

In the preliminary study (results not shown here) there was no significant difference between the light-saturated values as measured on intact field leaves and cut laboratory leaves. It was therefore concluded that the effect of leaf cutting on photosynthesis was minimal.

At most relative positions on the shoot, the sun leaves had higher light-saturated rates, P_{\max} , than the progressively or completely shaded leaves (Figure 3a). The light-saturated rates for sun leaves are amongst the highest reported for tree species (Sestak et al., 1971). These *Salix* data are consistent with the acclimation of sun and shade leaves in ecotypes from exposed habitats (Björkman & Holmgren, 1963; Björkman et al., 1972; Ludlow, 1983). The sun leaves with maximum light-saturated rates tended to be some distance behind the shoot tip, with the lowest values occurring in leaves near the tip or base of the shoot. The reason for this is not clear. It may be attributable to a time-dependence in the development of photosynthetic capacity (Leech & Baker, 1983) with a subsequent senescent phase (Thomas & Stoddart, 1980). Alternatively, it may reflect a seasonally changing growth (light) climate. To separate these variables would require a type of study similar to that reported by Field & Mooney (1983). Although the progressively shaded leaves had originally developed in light-exposed sites, they showed decreasing light-saturated rates with increasing distance from the shoot tip. The lowest of these leaves had similar light-saturated rates to the consistently low values of the completely shaded leaves.

In the top half of the shoots, the initial slope of the light response curve, α , did not vary much between leaves from different shoots (Figure 3b). This is consistent with the expected constancy in initial slope in sun and shade leaves (Björkman & Holmgren, 1963; Björkman et al., 1972; Ludlow, 1983).

The higher dark respiration rate, R_D , found in sun leaves (Figure 3c) is consistent with other data (Björkman et al., 1972; Ludlow, 1983), in which light-saturated and dark respiration rates have been positively correlated.

The advantages and disadvantages of different mathematical descriptions of photosynthetic light response have been discussed by Thornley (1976). Photosynthetic light response curves of single leaves normally have a well defined 'knee' (Figure 4) and can be approximated by a Blackman limiting response (Blackman, 1905; Thornley, 1976). The Blackman limiting responses are shown for sample sun and shade leaves belonging to the above field experiment (Figure

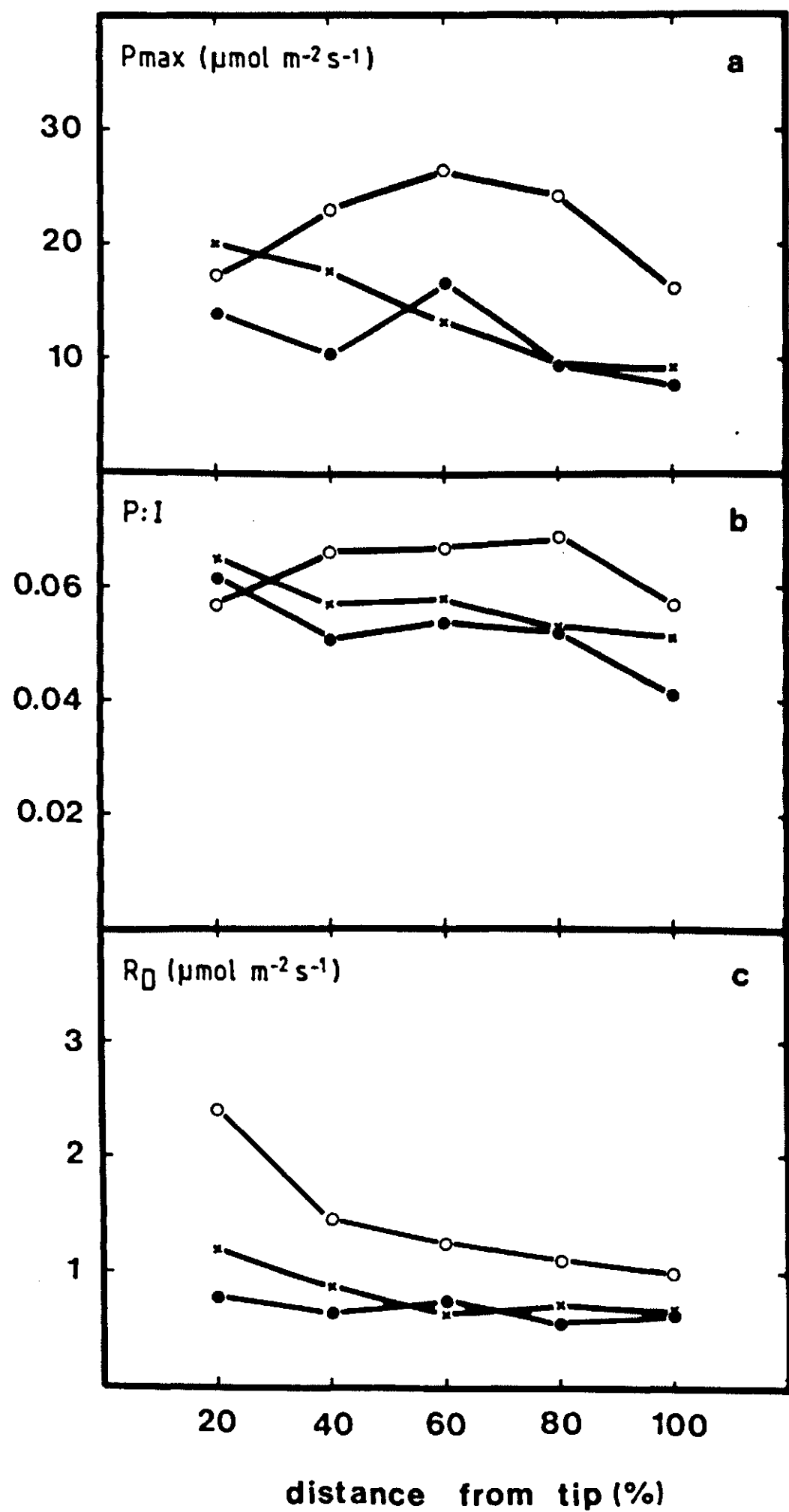


Figure 3. The dependence of (a) light-saturated photosynthetic rate, P_{\max} (CO_2 , $\mu\text{mol m}^{-2} \text{s}^{-1}$), (b) initial slope of the light response curve $P:I$ (CO_2 , $\mu\text{mol m}^{-2} \text{s}^{-1}/\text{quanta}$, $\mu\text{mol m}^{-2} \text{s}^{-1}$), (c) dark respiration rate, R_D (CO_2 , $\mu\text{mol m}^{-2} \text{s}^{-1}$) on leaf position (% shoot length behind growing tip). The symbols refer to: (O) sun leaves, (X) progressively shaded leaves, (●) shade leaves. Measurements were made towards the end of the growing season on leaves of *Salix viminalis* (see text).

5). Whole-plant (small shoot) responses (cf. Figure 6), on the other hand, tend to have a less well defined knee (McDonald, 1980). The photosynthetic light responses of small willow shoots (*S. aquatica* Smith.), grown at different

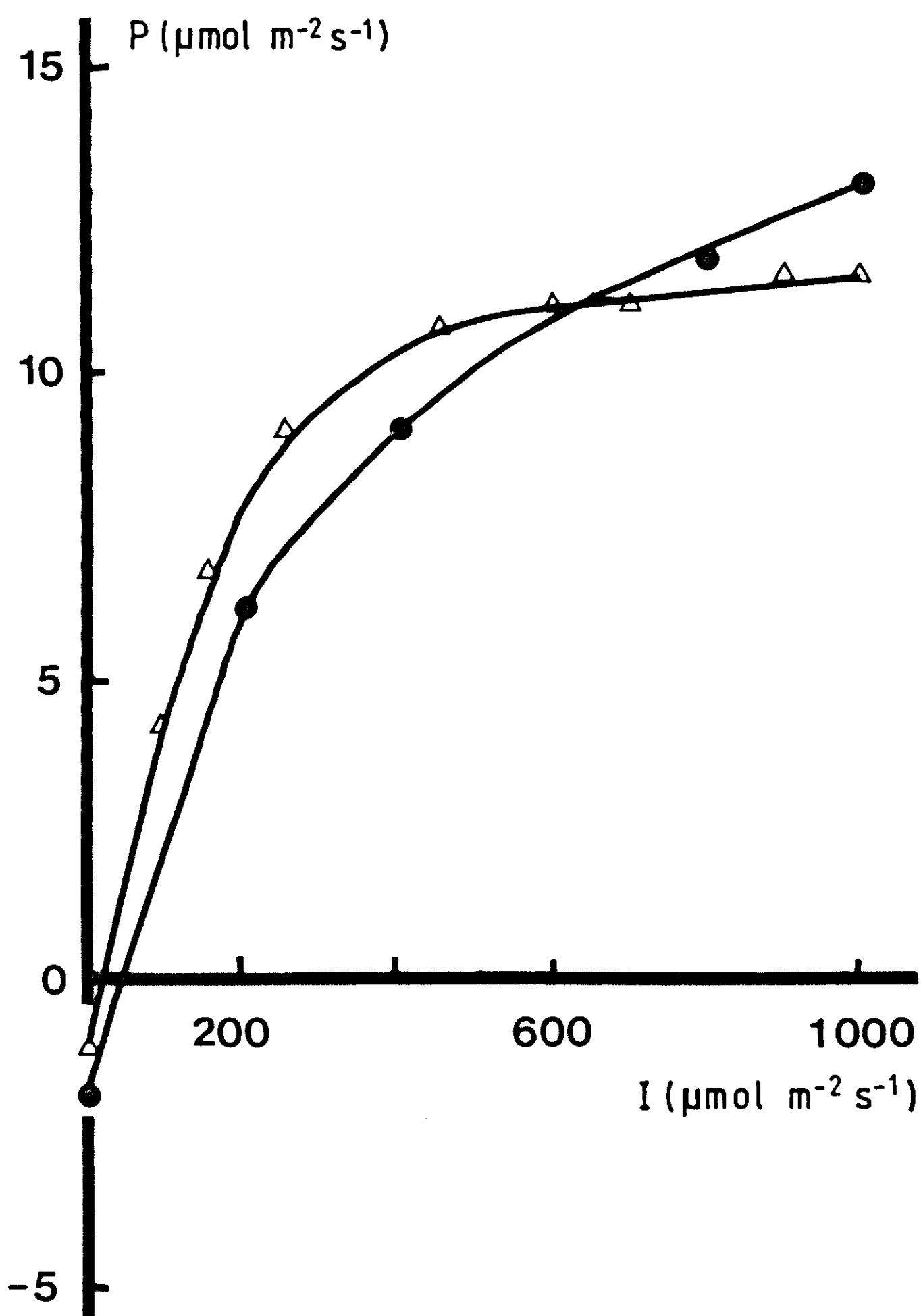


Figure 4. Net photosynthetic rates, P (CO_2 , $\mu\text{mol m}^{-2} \text{s}^{-1}$) in a single leaf (Δ) and in a whole shoot (\bullet) of *Salix aquatica* Smith. The single leaf and the whole shoot were grown in approximately the same environment: photo-period = 18 h, photon flux density, I , = $200 \mu\text{mol m}^{-2} \text{s}^{-1}$, air temperature = 20°C and relative humidity = 70%. The plants had sub-optimal nutrition.

photon flux densities and at optimal nutrition, are shown in Figure 6. The curves were evaluated at different photon flux densities after parameter estimation in the rectangular hyperbola

$$P = \alpha \cdot I \cdot P_{\max} / (\alpha \cdot I + P_{\max}) \quad \text{Equation 2}$$

where P is the photosynthetic rate per leaf area (CO_2 , $\mu\text{mol m}^{-2} \text{s}^{-1}$), α is the initial slope of the light response curve ($P:I$), I is the photon flux density

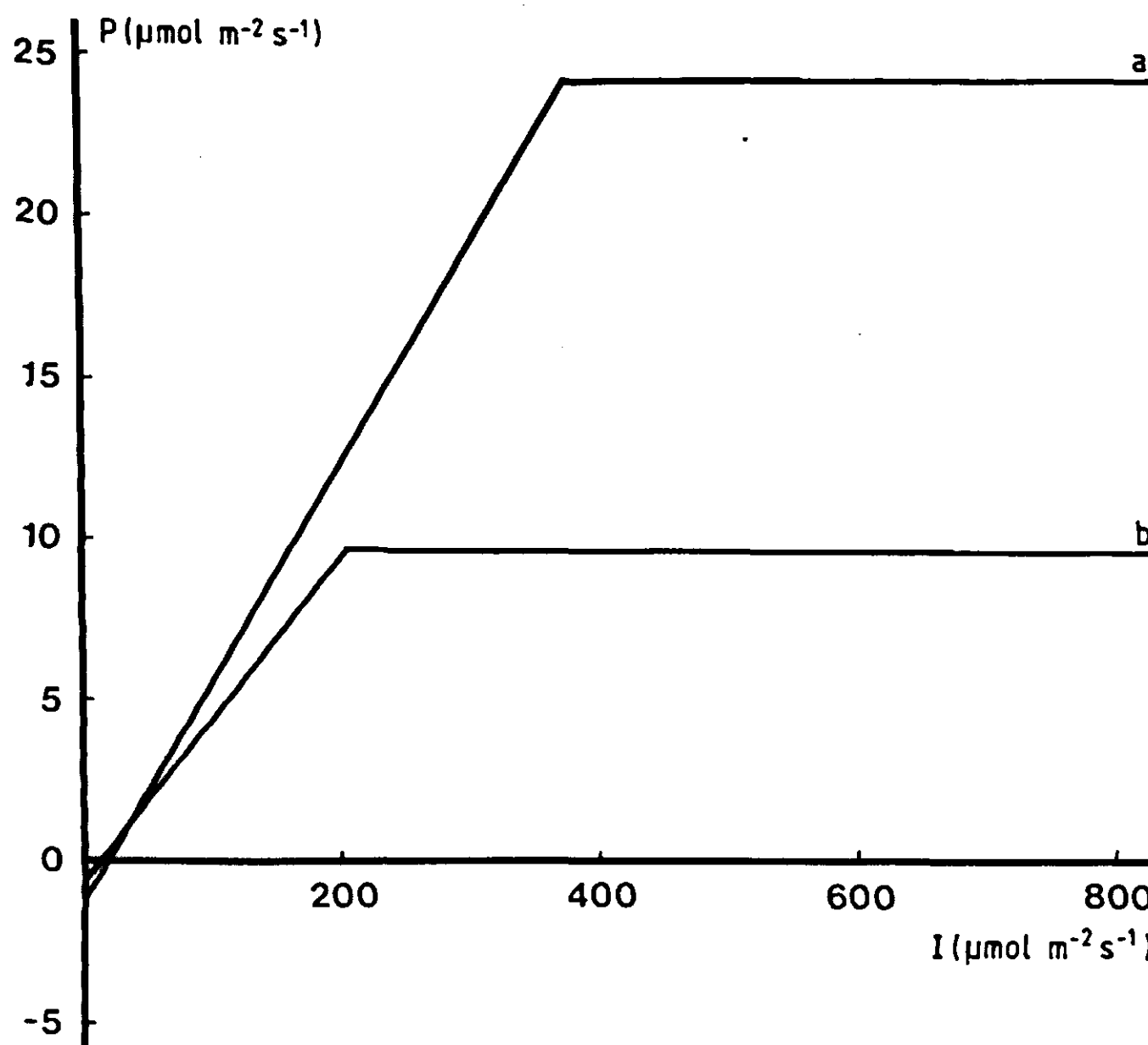


Figure 5. Blackman limiting responses for the dependence of photosynthetic rate, P (CO_2 , $\mu\text{mol m}^{-2} \text{s}^{-1}$) on photon flux density, I , (quanta, $\mu\text{mol m}^{-2} \text{s}^{-1}$). The curves are drawn from data for (a) a sun leaf and (b) a shade leaf both from a field experiment with *Salix viminalis* (see text). Both leaves were at a distance of 80% length behind the growing tip.

(quanta, $\mu\text{mol m}^{-2} \text{s}^{-1}$), and P_{\max} is the light-saturated rate of photosynthesis (CO_2 , $\mu\text{mol m}^{-2} \text{s}^{-1}$). Parameter values are summarized in Table 3.

The data of Figures 5 and 6 are consistent in showing that:

- the light compensation point is higher in sun leaves than in shade leaves
- at very low photon flux densities photosynthetic rate is higher in shade leaves than in sun leaves
- the photon flux density at which saturation first occurs is higher in sun leaves than in shade leaves.

These types of observation have previously been interpreted in terms of adjustment to the photosynthetic apparatus such that available light energy is utilized most efficiently at the prevailing light climate (e.g. Björkman & Holmgren, 1963). The factors involved have been summarized by Boardman (1977). Although there typically are differences between sun and shade leaves in both numbers and size of chloroplasts and in chlorophyll content per chloroplast, the decisive factor in accounting for higher light-saturated rates in sun leaves has to do with greater leaf thickness and the greater volume of photosynthetic tissue per leaf area (Hesketh et al., 1983). Normally there are greater amounts of both carboxylating enzyme and chlorophyll per leaf area in sun

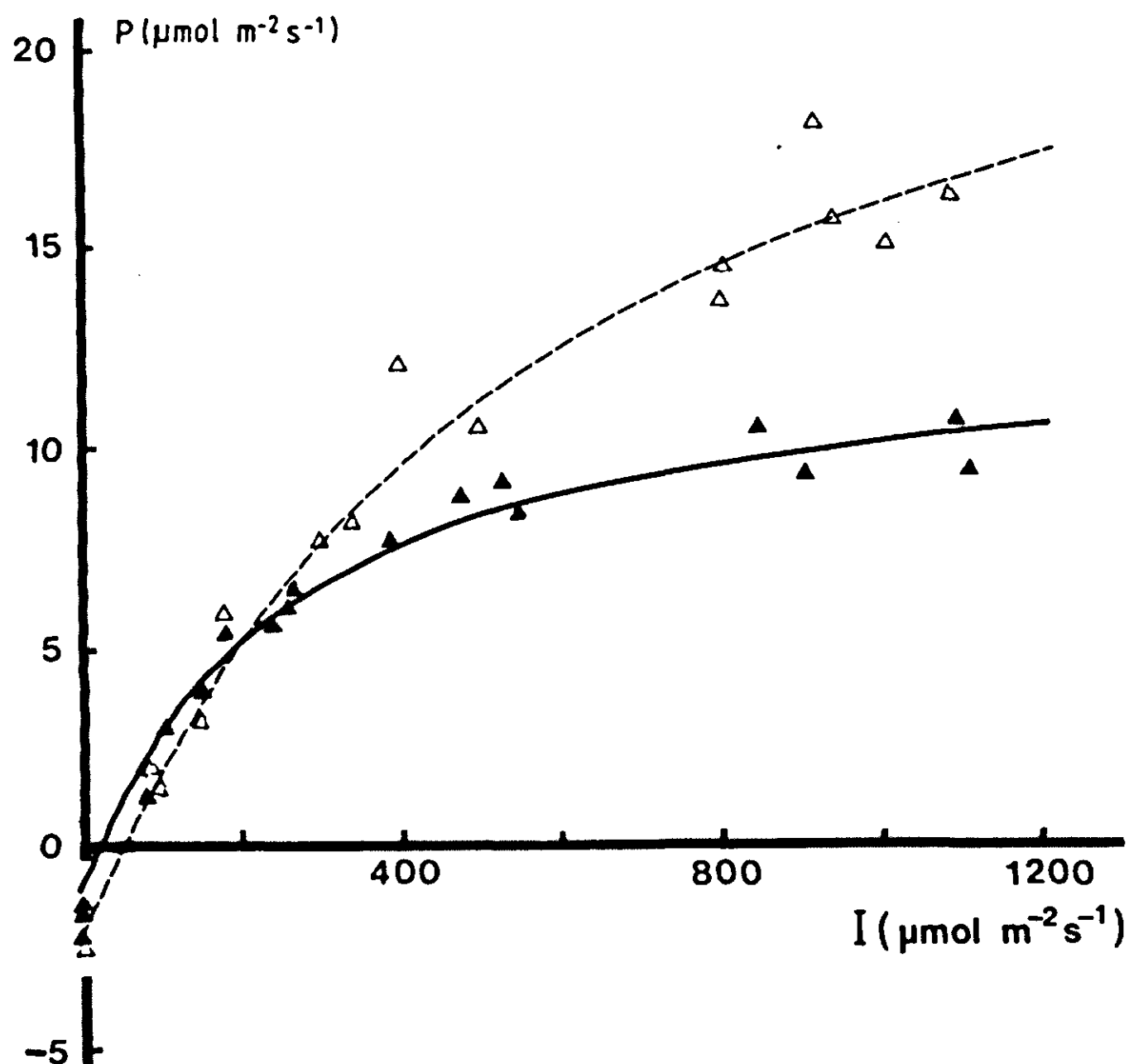


Figure 6. Net photosynthetic rates, P , in whole shoots of small *Salix aquatica* Smith. plants grown at $310 \mu\text{mol m}^{-2} \text{s}^{-1}$ (Δ) and at $50 \mu\text{mol m}^{-2} \text{s}^{-1}$ (\blacktriangle). The growth environment was: photoperiod = 20 h, air temperature = 20°C and relative humidity = 75%. The plants were grown at optimal nutrition (cf. Waring et al., 1985).

leaves. On the other hand, the proportionately higher investment in synthesis and maintenance of light-harvesting structure, rather than in carboxylating enzyme and carbon reductive processes, results in reduced respiration loss in shade leaves. This, in turn, confers the advantages of higher photosynthetic rates at low photon flux densities and a low light compensation point, appropriate to shaded environments.

Table 3. Parameter values estimated from data in Figures 6 and 7.

Growth environment	Parameters	
I quanta, $\mu\text{mol m}^{-2} \text{s}^{-1}$	α CO_2 : quanta	P_{\max} $\text{CO}_2 \mu\text{mol m}^{-2} \text{s}^{-1}$
300 (optimal nutrition)	0.044	25.6
50 (optimal nutrition)	0.050	12.9
300 (nutrient stress)	0.056	17.5

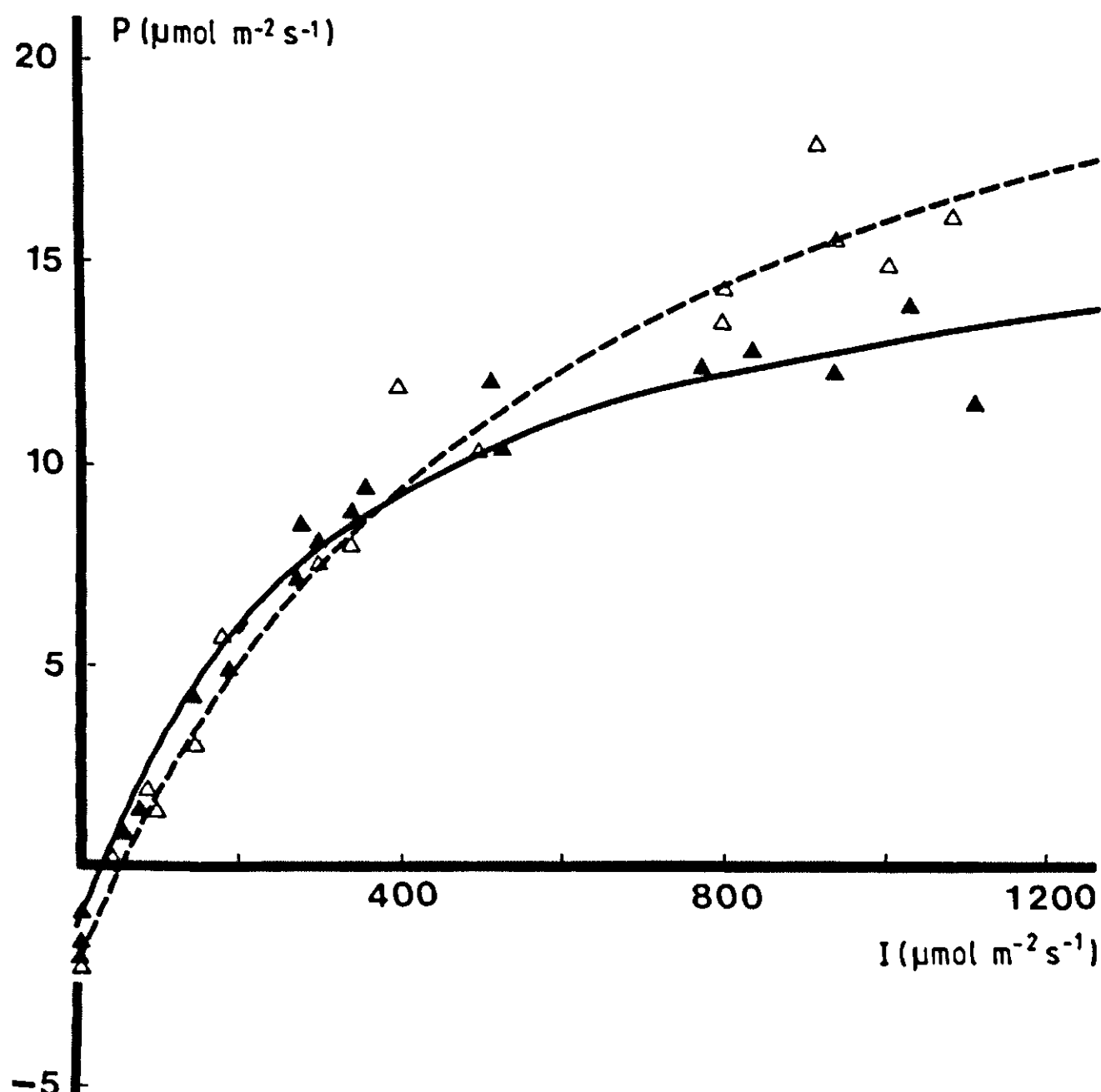


Figure 7. Net photosynthetic rates, P , in whole shoots of small *Salix aquatica* Smith. plants grown at optimal nutrient availability (Δ) and sub-optimal nutrient availability (\blacktriangle). The growth environment was: photoperiod = 20 h, photon flux density, I , = 310 $\mu\text{mol m}^{-2} \text{s}^{-1}$, air temperature = 20 $^{\circ}\text{C}$ and relative humidity = 75% (cf. Waring et al., 1985).

Other variables may affect the shape of the photosynthetic light response curve. For example, small willow shoots with better nutrition may have higher light-saturated values of photosynthetic rate than shoots belonging to plants with poor nutrition (Figure 7). The data of Figure 7 suggest that the rate of dark respiration may be slightly higher, and photosynthetic rate at low photon flux density may be lower, in leaves belonging to plants with better nutrition.

4.4 List of symbols

I	= photon flux density, quanta, ($\mu\text{mol m}^{-2} \text{s}^{-1}$)
P	= photosynthetic rate per leaf area, CO_2 , ($\mu\text{mol m}^{-2} \text{s}^{-1}$)
P_{\max}	= photosynthetic rate at light saturation, CO_2 , ($\mu\text{mol m}^{-2} \text{s}^{-1}$)
R_D	= dark respiration rate per leaf area, CO_2 , ($\mu\text{mol m}^{-2} \text{s}^{-1}$)
α	= initial slope of light response curve $P:I$
CO_2 :	quanta, (dimensionless)

4.5 References

Björkman, O. & Holmgren, P., 1963. Adaptability of the photosynthetic apparatus to light intensity in ecotypes from exposed and shaded habitats. *Physiologia Plantarum* 16:889-914.

Björkman, O., Boardman, M.K., Anderson, J.M., Thorne, S.W., Goodchild, D.J. & Pyliotis, N.A., 1972. Effect of light intensity during growth of *Atriplex patula* on the capacity of photosynthetic reactions, chloroplast components and structure. *Carnegie Institute of Washington Year Book* 71:115-135.

Blackman, F.F., 1905. Optima and limiting factors. *Annals of Botany* 19:281-295.

Boardman, N.K., 1977. Comparative photosynthesis of sun and shade plants. *Annual Review of Plant Physiology* 28:355-377.

Field, C. & Mooney, H.A., 1983. Leaf age and seasonal effects on light, water and nitrogen use efficiency in a Californian shrub. *Oecologia (Berlin)* 56:348-355.

Hesketh, J.D., Larson, E.M., Gordon, A.J. & Peters, D.B., 1983. Internal factors influencing photosynthesis and respiration. In: J.E. Dale & F.L. Milthorpe (Eds): *The growth and functioning of leaves*. Cambridge University Press, pp. 381-411.

Leech, R.M. & Baker, N.R., 1983. The development of photosynthetic capacity in leaves. In: J.E. Dale & F.L. Milthorpe (Eds): *The growth and functioning of leaves*. Cambridge University Press, pp. 271-307.

Ludlow, M.M., 1983. External factors influencing photosynthesis and respiration. In: J.E. Dale & F.L. Milthorpe (Eds): *The growth and functioning of leaves*. Cambridge University Press, pp. 347-379.

McDonald, A.J.S., 1980. Gas exchange within the Energy Forestry Project. In: K. Perttu (Ed.): *Proceedings from a symposium arranged by the International Energy Agency (IEA) planning group on Growth and Production*. September 24, 1979, Bogesund, Stockholm. Report 8:35-43. Swedish University of Agricultural Sciences, Section of Energy Forestry, Uppsala.

Sestak, Z., Jarvis, P.G. & Catsky, J., 1971. Criteria for the selection of suitable methods. In: Z. Sestak, J. Catsky & P.G. Jarvis (Eds): *Plant photosynthetic production; Manual of Methods*. Dr. W. Junk N.V. Publishers, The Hague, pp. 1-48.

Thomas, H. & Stoddart, J.L., 1980. Leaf senescence. *Annual Review of Plant Physiology* 31:83-111.

Thornley, J.H.M., 1976. *Mathematical models in plant physiology*. Academic Press, London, New York, San Francisco, 318 pp.

Waring, R.H., McDonald, A.J.S., Larsson, S., Ericsson, A., Wirén, A., Arwidsson, E., Ericsson, T. & Lohammar, T., 1985. Differences in chemical composition of plants grown at constant relative growth rates with stable mineral nutrition. *Oecologia (Berlin)* 66:157-160.

5 Simulated growth of willow stands related to variations in weather and foliar nitrogen content

Henrik Eckersten, Anders Lindroth and Lars-Owe Nilsson

5.1 Introduction

In the model of willow growth currently used at Uppsala in research on energy forestry growth is simulated by means of the photosynthetic processes in the foliage. The relations between light and photosynthesis for the species concerned were determined in the laboratory according to methods described in the previous chapter. The stand is treated as horizontally uniform and the vegetative growth is assumed to be uninfluenced by flowering, frost damage, insect attacks or other similar disturbances. The main input data to the model are the incoming solar radiation, the mean daily air temperature above the stand and the nitrogen content of the foliage. Water and nutrients (except nitrogen) are assumed not to limit growth.

The model was originally presented by Eckersten et al. in 1983. Over the years there have been successive improvements (see e.g. Eckersten, 1986b) to the model. The version presented here is the most recent and includes, for example, features for multiple-year simulations.

5.2 The growth model

5.2.1 *Initiation of growth*

A schematic picture of the growth model, which has a time step of one day, is given in Figure 8. Growth starts on the day of sprouting in the spring. This day, t_o , is estimated by summing mean daily air temperatures above 5 °C during the current spring. Neither the threshold value nor the starting day (here taken as 1 March in accordance with the observed lack of cambial activity before this date: Sennerby-Forsse, 1986) of the summation are well defined (Utaaker, 1963). For clone 082 in the southern part of Sweden, t_o was chosen to be equal to the day when this sum exceeded 40 day-degrees (G. Sirén, personal communication, 1986). On day t_o , the initial foliage biomass, $C_l(t_o)$, is assumed to develop during one day from assimilates stored in the plants originating from the growth of previous years. This is a strong simplification of the real process, which probably extends over several weeks, depending on the age of the root system and how often the stand has been cut, etc. (cf. Pontailler et al., 1984). Here, a pool of assimilates, C_a , available for sprouting is introduced. At time t_o , C_a is made available and 85% of the assimilates in C_a are utilized to form the initial leaves and 15% to form the initial stem biomass. C_a is then refilled again at the end of the growing season by assuming that a fraction, b_{av} , of the

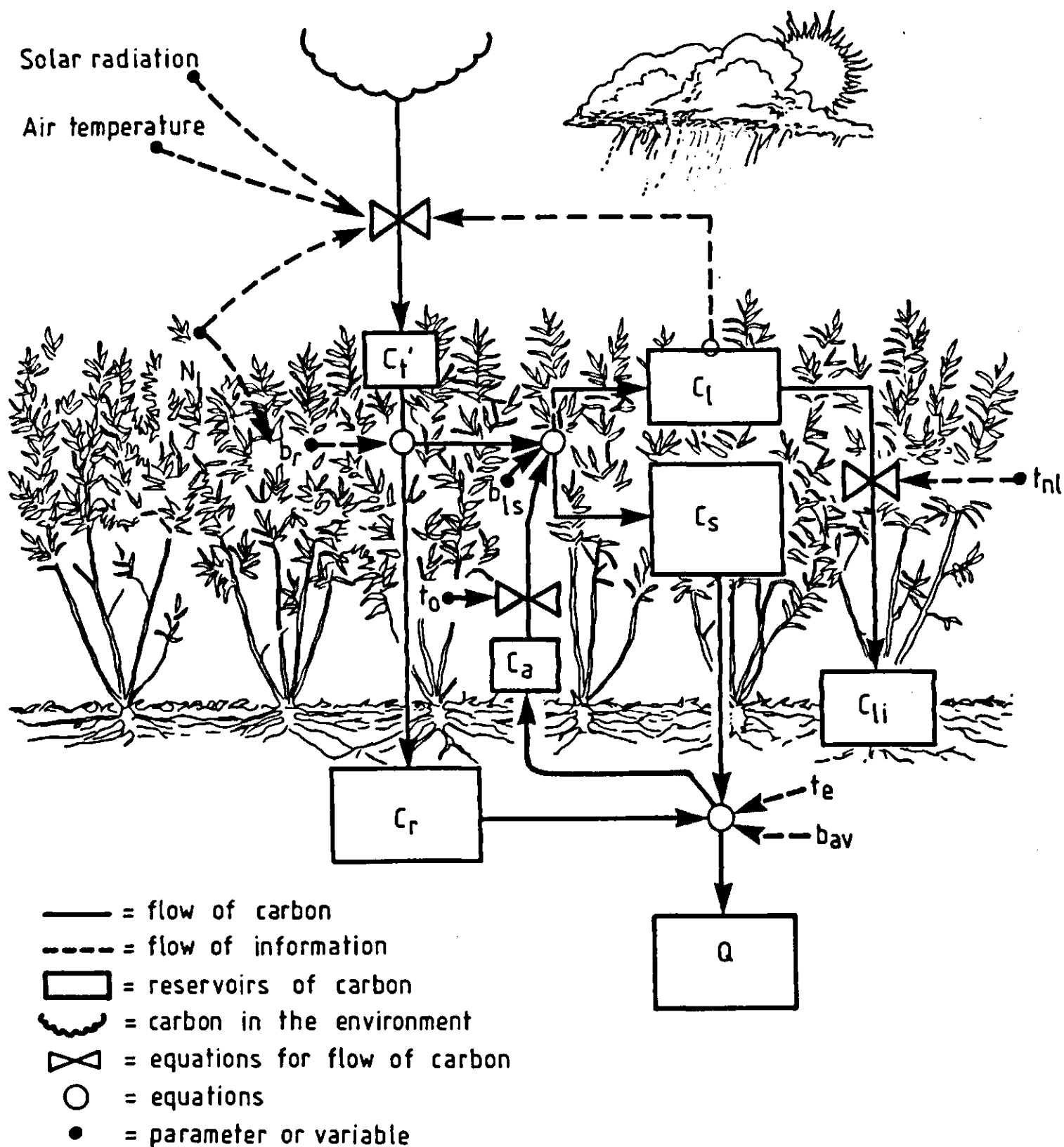


Figure 8. The flow of carbon in the willow growth model. b_{av} , b_{ls} and b_r are allometric coefficients. C_l , C_{li} , C_s and C_r are accumulated biomass during the growing season of leaves, leaf litter, stems and roots, respectively. C_a is a pool of assimilates for sprouting in spring and C'_t is daily total growth. N_l is the amount of nitrogen in the leaves. t_a , t_e and t_o are times for start of litterfall, end and start of the growing season, respectively. Q is biomass originating from previous years.

annual increment of stem and root biomass is delivered to this pool as

$$C_a = b_{av}(C_s + C_r) \quad \text{Equation 3}$$

where C_s and C_r are the accumulated growth of the current year of stems and roots, respectively.

Eckersten & Nilsson (1983), who simulated growth for both first- and second-year shoots with satisfactory results, presented estimated values of $C_s + C_r$ for the first-year growth and C_a for the start of the second-year growth. The value of b_{av} is determined using these data. For first-year shoots C_a is not taken from Equation 3. Instead, it is determined semi-empirically from the measurements

of C_l early in the spring at Studsvik during 1981. The value of C_a was allowed to vary until agreement between simulated C_l and this early measured value of C_l was achieved. This estimate of C_a is then also used for first-year shoots at other locations in southern and central Sweden and during the different years.

5.2.2 Growth

Daily total growth is obtained from the following equation (cf. de Wit, 1965)

$$\frac{d(C_t)}{dt} = P_d T_f (1 - r_g) \quad \text{Equation 4}$$

where C_t is the total biomass of leaves, stems and roots, t is the day number (from January), P_d is the daily potential gross photosynthesis, and r_g is the fraction of the daily gross photosynthesis that is lost by growth respiration, and that is here assumed to be constant (de Wit, 1965; Sievänen, 1983). T_f is a temperature-dependent growth function that is zero when T , the daily mean of the ambient air temperature, is below T_o , increases linearly to 1 as T increases to T_l , and then remains constant (cf. de Wit, 1965; Monteith, 1977; Larcher, 1980). For the Swedish climate it is not necessary to consider any decrease in T_f caused by high temperatures, since they rarely occur (Eckersten et al., 1987).

5.2.3 Canopy photosynthesis

The basic concept of the photosynthesis model was given by de Wit (1965) who developed it for sugarbeet. The photosynthesis, P , of the foliage is a function of the incident light per unit horizontal area, I , (photosynthetic active radiation, PAR, 400-700 nm) according to the well-known Michaelis-Menten equation

$$P = P_m I / (I + I_p) \quad \text{Equation 5}$$

where P_m is the maximum photosynthetic rate per unit foliage weight and I_p is a parameter, whose value equals the radiation intensity for $P = P_m/2$. According to laboratory measurements by McDonald et al. (1981), P_m depends on the foliar nitrogen concentration, n_l , and from their data, P_m was estimated as

$$P_m = c_{p1} + c_{p2} n_l \quad \text{Equation 6}$$

where c_{p1} and c_{p2} are coefficients. The symbol 'c' with different indices denotes the equation coefficient throughout the rest of this chapter. The values of these coefficients are listed at the end of the chapter.

The light extinction is assumed to follow Beer's law, according to

$$I = I_o \exp(-k A_i) \quad \text{Equation 7}$$

where I_o is PAR above the stand, A_i is the one-sided leaf area index accumulated from the canopy top and k is the light extinction coefficient (for PAR). Accord-

ing to measurements by Eckersten (1984) the light extinction coefficient depends on the leaf area, because

$$k = c_{k1} - c_{k2}A_i - c_{k3}A_i^2 \quad \text{Equation 8}$$

To estimate canopy photosynthesis, the canopy is divided into layers of unity leaf area indices from canopy top and downwards where k is assumed to be constant within each layer, while b_a (areal leaf weight), P_m and I_p are assumed to be constant over all layers. Thus, integrating Equation 5 over these layers and summing P for the whole canopy, the daily potential gross photosynthesis of the canopy for clear sky conditions, P_{dc} , (when temperature does not limit growth) is estimated as

$$P_{dc} = \int_0^{24} (b_a P_m \sum_{j=1}^{A_{li}} 1/k_j \ln((I_j(h) + I_p)/(I_j(h)\exp(-k_j) + I_p))) dh \quad \text{Equation 9}$$

where I_j is PAR at the upper surface of layer j , A_{li} is the canopy leaf area index and h is the time (hour) of the day. It is practical here to convert P_{dc} from units of g m^{-2} to kg ha^{-1} .

The potential gross photosynthesis for a completely overcast day, P_{do} , is calculated similarly to P_{dc} but using I_o in Equation 7 equal to 30% of that for the clear sky conditions (Eckersten, 1986a). The diurnal potential gross photosynthesis, P_d , is then estimated as (de Wit, 1965)

$$P_d = P_{do} + M(P_{dc} - P_{do}) \quad \text{Equation 10}$$

In the original procedure proposed by de Wit (1965) the scaling factor, M , was equal to the relative duration of bright sunshine, D . However, by comparing P_d estimated by using measured values of I_o (Equation 7) with P_d estimated by using the relative duration of sunshine (Equation 10), Eckersten (1986a) showed that the scaling factor is not a linear function of D , but instead:

$$M = -c_{M1} + c_{M2}D - c_{M3}D^2 \quad \text{Equation 11}$$

The calculations according to Equation 5 are usually performed using a time step of 1 hour.

5.2.4 Allocation of assimilates

The amount of assimilates allocated to roots is taken as a fraction, b_r , of the total daily growth

$$d(C_r)/dt = b_r d(C_t)/dt \quad \text{Equation 12}$$

The value of b_r is given as a function of the nitrogen concentration in the leaves and has a minimum value, b_{ro} , at the optimum foliar nitrogen concen-

tration, n_{lo} (cf. Ingestad & Ågren, 1984; Ågren, 1985), and increases as n_l decreases (cf. Ericsson 1981a,b; Waring et al., 1985; Eckersten, 1986b) as

$$b_r = 1 + b_{ro} - (1 - ((n_{lo} - n_l)/n_{lo})^2)^{0.5} \quad \text{Equation 13}$$

The remaining part of the daily total growth is allocated to above-ground compartments; the leaves and leaf litter are allocated a proportion, which is obtained by the derivation over time of the equation

$$(C_l + C_{li}) = b_{ls} (C_l + C_{li} + C_s) \quad \text{Equation 14}$$

where C_l is the accumulated growth of foliage and C_{li} is the accumulated leaf fall of the current year. The accumulated stem litter is assumed to be negligible. The leaf to shoot ratio, b_{ls} , is determined empirically by

$$b_{ls} = (b_{lso} - b_{lse}) \exp(-c_b(t - t_o)) + b_{lse} \quad \text{Equation 15}$$

where b_{lso} equals b_{ls} at time t_o . The value of b_{lso} is below unity implying that the initiation of foliage biomass at time t_o is also accompanied by an initiation of the stem biomass. At the end of the growing season, b_{ls} decreases towards b_{lse} and b_{ls} is only assumed to be climate-dependent through t_o .

Part of the leaf biomass is allocated to leaf litter according to an empirical time-dependent equation

$$C_{li}' = 0 \quad \tau < \tau_a \quad \text{Equation 16}$$

$$C_{li}' = C_l c_m (\tau - \tau_a)^2 \quad \tau > \tau_a \quad \text{Equation 17}$$

where τ is a normalized daynumber. τ is zero at the beginning and unity at the end of the average growing season (see below) at the site concerned. Index a refers to the day when leaf abscission is assumed to start. The average dates for start and end of growth at the different sites are taken from Perttu et al. (1978) who define the growing season as the period of consecutive days with daily mean air temperature above +5 °C.

The daily change in C_l is then the difference between the daily changes in $C_l + C_{li}$ (Equation 14) and in C_{li} (Equations 16 and 17). The stem growth is the remaining part of the above-ground growth.

5.2.5 Input data

The PAR for a completely clear sky, I_{oc} , was estimated using a simplified equation (cf. Kondratjev, 1969)

$$I_{oc} = c_{l1} S \sin^2(\beta) / (\sin(\beta) + c_{l2}) \quad \text{Equation 18}$$

where S is the 'solar constant', β the sun's elevation, c_{l1} and c_{l2} empirical coefficients. The solar constant was estimated using the equation given by Dogniaux (1977)

$$S = c_{s1} + c_{s2}\cos(\omega t) + c_{s3}\cos(2\omega t) - c_{s4}\cos(3\omega t) + c_{s5}\sin(\omega t) + c_{s6}\sin(2\omega t) + c_{s7}\sin(3\omega t) \quad \text{Equation 19}$$

where $\omega = 2\pi/366$. The sun's elevation, β , is estimated as

$$\beta = \sin(Y)\sin(\delta) + \cos(Y)\cos(\delta)\cos((h + 12)(15\pi/180)) \quad \text{Equation 20}$$

where Y is the latitude (north) and δ the sun's declination. δ is given by

$$\delta = c_{d1} - c_{d2}\cos(\omega t) - c_{d3}\cos(2\omega t) - c_{d4}\cos(3\omega t) + c_{d5}\sin(\omega t) + c_{d6}\sin(2\omega t) + c_{d7}\sin(3\omega t) \quad \text{Equation 21}$$

To apply the model to different locations in Sweden (see below) the relative duration of sunshine, D , had to be derived from the fraction of cloudiness during daytime, O_v . The relation between the relative duration of bright sunshine and fraction of cloudiness during daytime was estimated by Eckersten et al. (1987) as

$$D = c_{D1} - c_{D2}O_v; D \leq 1.0 \quad \text{Equation 22}$$

Hence, input data to the growth model are 24 h mean air temperature, mean daytime fraction of cloudiness (estimated from observations every third hour at the network stations of the Swedish Meteorological and Hydrological Institute), foliar nitrogen concentration (see below), start and end of the average growing season and latitude.

5.3 Test of the growth model

5.3.1 Verification of the model

The estimated growth of first year shoots was compared with the actual growth of an annually harvested stand of clone 082 (*S. viminalis*) at the Studsvik experimental site in 1981 on a marine silt soil (cf. Sirén, 1983). The stand was planted in 1978 at a density of 9 plants m^{-2} and was irrigated weekly using a sprinkler system. It was nitrogen fertilized with about 120 kg $\text{ha}^{-1}\text{year}^{-1}$ using liquid fertilizers (Wallco). Growth data consist of values for C_s , C_l , C_{li} and A_{li} , measured at 1-2 week intervals from early June until early October (Nilsson & Ericsson, 1986). The same data were also used to estimate the coefficients of the b_{ls} function (Equation 15) and to determine b_a as a linear function of time. The light extinction coefficient, k , was determined from measurements of light interception of this special stand (Eckersten, 1984). Since the nitrogen concentration of the foliage, n_l , was measured at 1-2 week intervals, these values were also used as input to the model. The short-term variations of the growth were simulated with reasonable accuracy (Figure 9), using the parameter values given in the list at the end of this chapter. The scatter, however, was larger for the stem biomass than for the leaf biomass. The seasonal growth development was also simulated with good results (Figure 10), except for the end of the growing

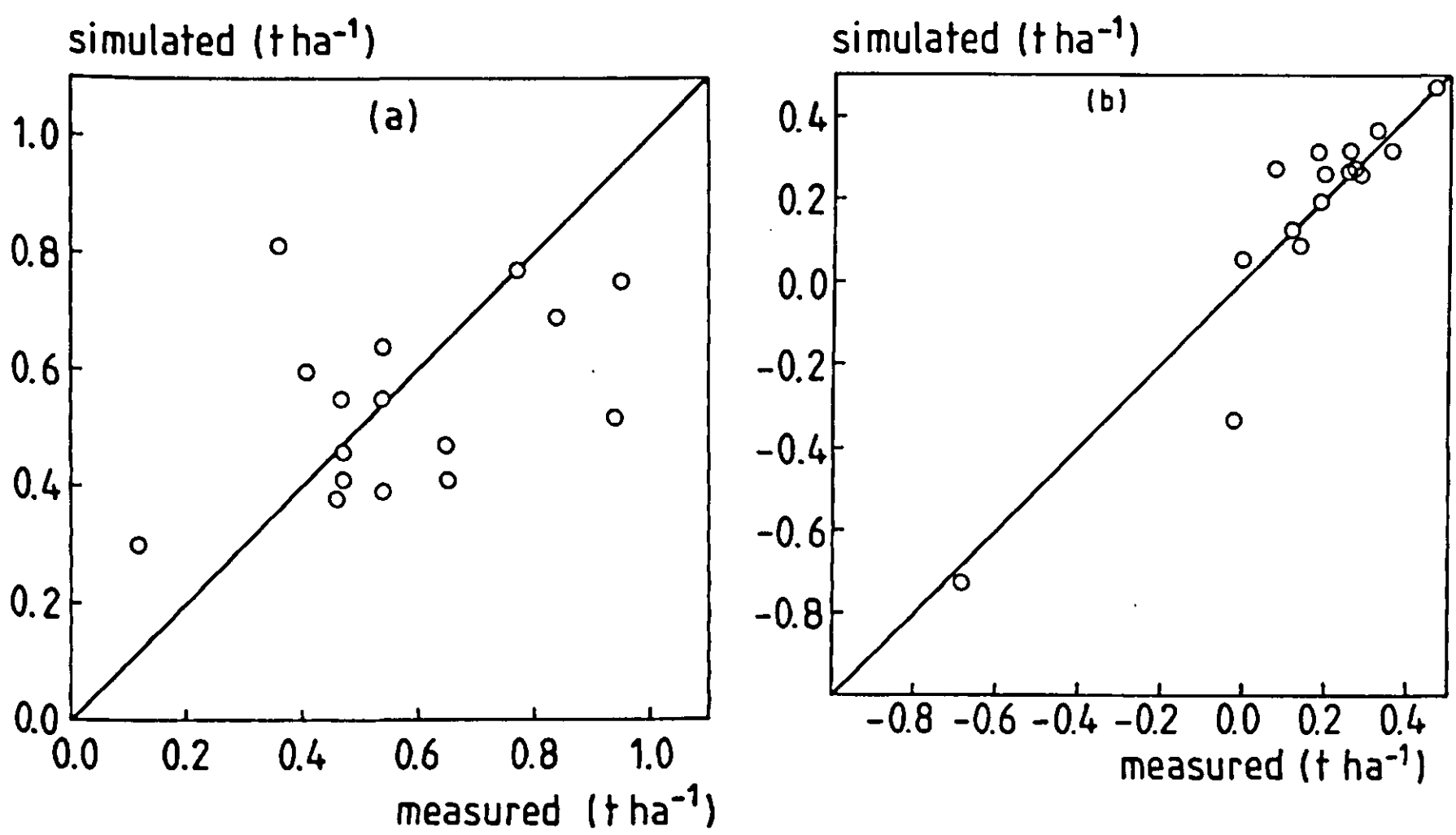


Figure 9. Simulated and measured weekly changes of (a) the stem dry weight and (b) the canopy leaf dry weight.

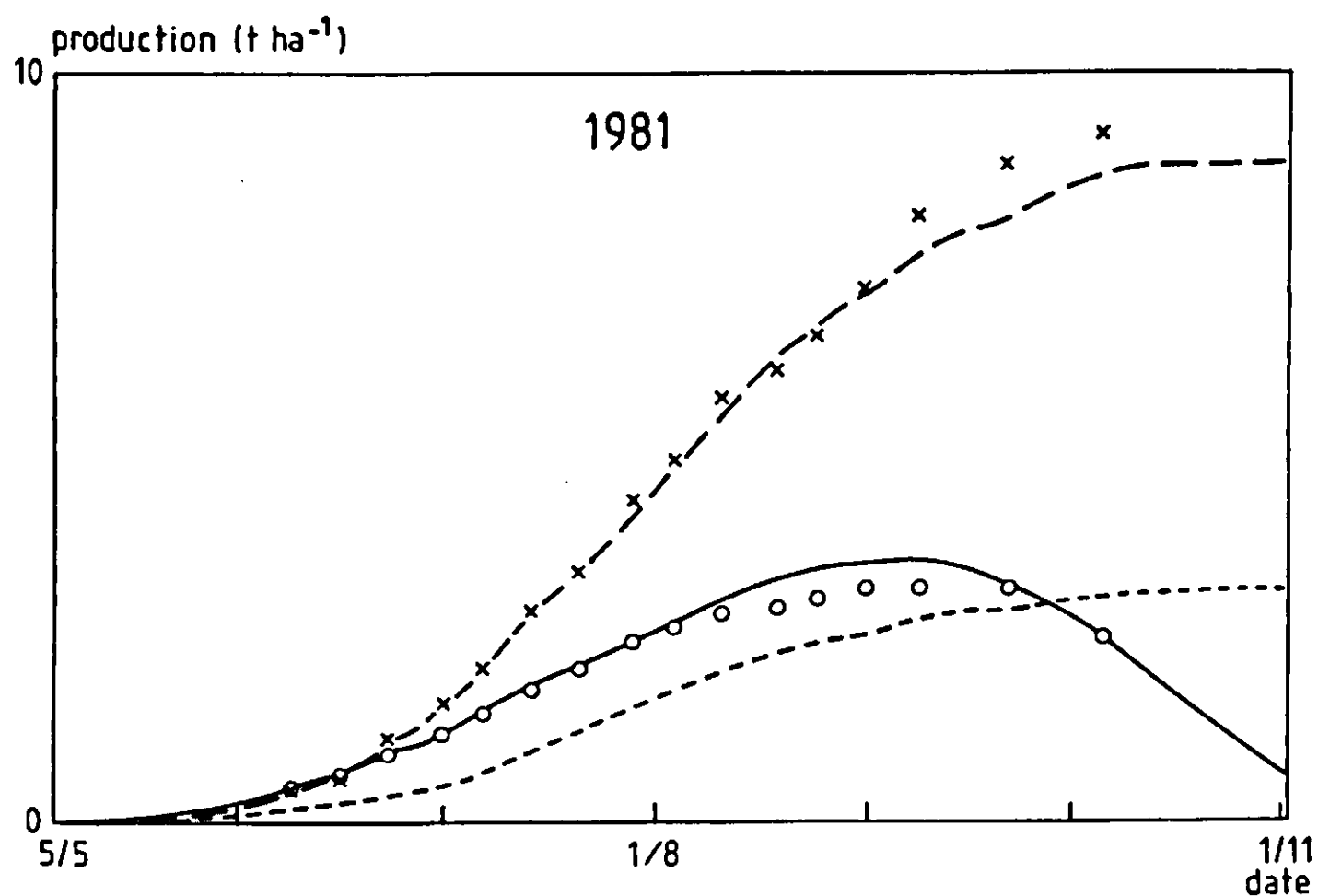


Figure 10. Accumulated biomass for *Salix viminalis*, clone 082, at Studsvik in 1981. Lines represent simulated values, and symbols (x) and (o) measured values. (—) and (o) represent leaf biomass, C_l , (---) and (x) represent stem biomass, C_s , and (---) represents root biomass, C_r . (Measured values after Nilsson & Ericsson, 1986)

season, when significant deviations occurred. An earlier version of this model was also tested against data obtained by measuring first- and second-year shoots from two stands of *Salix viminalis*, clone 683 (Eckersten & Nilsson, 1983), with good results.

5.3.2 Sensitivity of the model

The sensitivity of the model was analysed for first-year growth by changing the values of the parameters one at a time (Table 4). The relative change in seasonal maximum values of accumulated stem and leaf biomass was used as a measure of sensitivity. The model was found to be most sensitive to the parameters P_m and k but also to the driving variable n_l , which is probably more uncertain since it varies about $\pm 50\%$ depending on fertilization regime, etc. (see below). However, the high sensitivity to variations in n_l is apparent in the sense that n_l also affects the areal leaf weight, b_a , which is known to decrease with increasing n_l (Linder et al., 1981; cf. Chapter 6 in this volume) and b_a was not changed when the sensitivity to variations in n_l was examined. The value of the upper limit of the temperature function also has a relatively large influence on the production values. This is perhaps crucial, because the dependence of

Table 4. The relative change in the maximum values of accumulated stem and leaf biomass during the growing season for first-year shoots when parameter values are changed. (Note that n_l and t_o are not parameters).

Para- meter	Change of parameter	Relative change (%)		Comments
		C_s	C_l	
P_m	+10%	11.4	11.3	maximum photosynthetic rate
I_p	-10%	7.2	7.0	coefficient of light response curve
k	-10%	10.3	10.0	light extinction coefficient
r_g	-10%	3.8	3.7	growth respiration coefficient
T_o	-1 °C	2.5	1.6	lower temperature coefficient
T_l	-1 °C	6.4	5.6	upper temperature coefficient
b_a	+10%	8.3	8.1	areal leaf weight
b_{ls}	+10%	-2.1	12.8	leaf to shoot ratio
c_m	-10%	0.1	0.6	coefficient of leaf litterfall
τ_a	+10%	0.3	5.2	start day (normalized) for litterfall
b_r	-10%	5.0	5.0	root allocation coefficient
t_o	+10 days	-7.2	-1.3	first day of growing season
$C_l(t_o)$	+10%	1.3	1.5	initial leaf biomass
n_l	+10%	14.4	13.1	foliage nitrogen concentration

growth on temperature is poorly understood and the temperature is the climatic driving variable that shows the largest geographical variation in Sweden. Pelkonen (1984), for instance, reported values for T_o and T_l considerably lower than the values used here for a clone of *S. viminalis* grown under relatively cold climatic conditions (see further Eckersten et al., 1987). The areal leaf weight, b_a , is another parameter having relatively large effects on growth (see Equation 9). The value of the parameter varies during the season, implying that it has to be well determined to avoid significant systematic errors in the model, as shown by Eckersten and Ericsson in Chapter 6 in this volume.

5.4 Application of the model

5.4.1 Climatic variations

To estimate the potential production of energy forest at various locations and under different weather situations, the model was run using input data from 13 locations in southern Sweden (Figure 11) covering a period of 15 years (1964-1978) (in the case of a two-year cutting cycle, only 14 years were used). The parameters were those obtained from the Studsvik site, except for b_a which was taken as a constant mean value equal to 48 g m^{-2} . The simulations for second- and third-year growth were made in the same way as for the first-year growth, except that b_a was increased by 20% between Year 1 and Year 2 (taken from Eckersten & Nilsson, 1983) and, arbitrarily, by 5% between Year 2 and Year 3. The model was used to estimate the mean annual production of stem biomass for 1, 2, and 3-year cutting cycles using the set of parameter values listed at the end of this chapter. A cutting cycle is defined as the time between consecutive harvests of the stand: each cutting cycle starts with the same value of C_a .

Of the sites studied, Helsingborg was the warmest and Hagshult the coldest during the growing season (Table 5). Malmö received the most light and Hagshult the least. During the different years and at the different locations the date for start of the growing season varied between 7 April (Västervik) and 24 May (Visby and Uppsala). The length of the average growing season (Perttu et al., 1978) varied between 208 days (Uppsala) and 252 days (Helsingborg).

The mean stem production ranged between $6.5 \text{ t ha}^{-1} \text{ yr}^{-1}$ at Hagshult and $9.8 \text{ t ha}^{-1} \text{ yr}^{-1}$ at Helsingborg (Table 6) for the 1-year cutting cycle. It increased considerably for the longer cutting cycles; for the 3-year cutting cycle the values ranged between 10.2 and $14.6 \text{ t ha}^{-1} \text{ yr}^{-1}$. For the 1-year cutting cycle, the variation was within +27% and -14% for sites located in the inland areas, whereas those on the coast generally showed variations within $\pm 15\%$ (except for Visby, which has a variation similar to those of the inland sites). The standard deviations ranged between 7 and 14%. The variations in maximum and minimum values decreased gradually for the longer cutting cycles, but for the standard deviation there was no difference between 2- and 3-year cutting cycles.

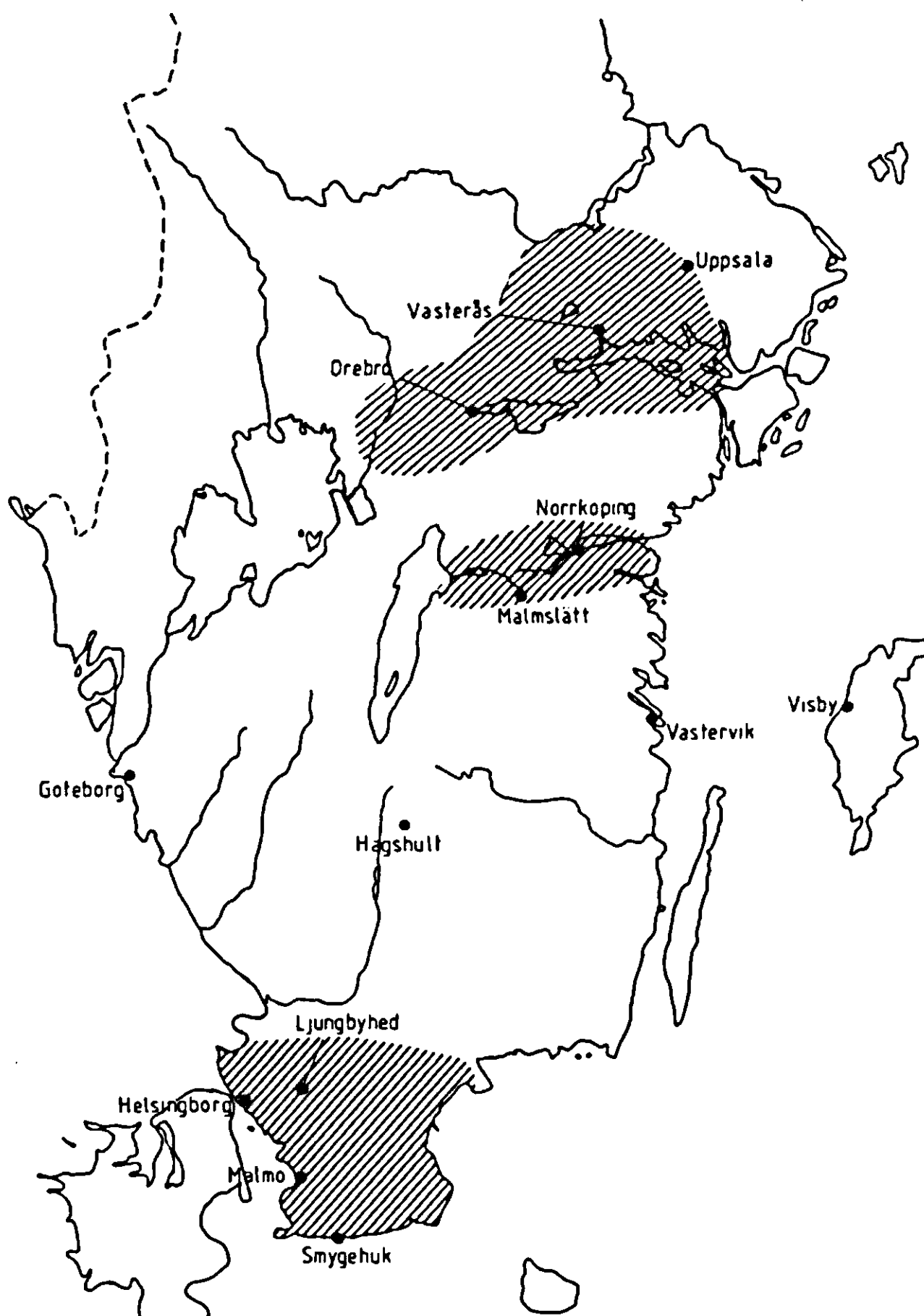


Figure 11. Map showing locations in southern Sweden used for simulation of willow growth during the period 1964-78. Hatched areas define the three regions that are compared. (After Eckersten et al., 1987).

Concerning the west to east gradient in south Sweden, the mean stem production for the 3-year cutting cycle was highest at Göteborg, being $13.3 \text{ t ha}^{-1} \text{ yr}$ and lowest at Hagshult, being 10.2 t ha^{-1} (Table 6). Hagshult also had the largest between-year variations of all sites studied. The difference between the west and the east coasts, represented by Göteborg and Västervik, respectively, was about 7%, although the variations were larger on the east coast. Visby had the same mean production as Västervik, but the between-year variation was larger at Visby.

Table 5. Annual mean values (1964-78) of air temperature sums for temperatures above 5 °C and estimated sums of PAR. <> is the relative standard deviation, expressed in %.

Location	Temperature sum, > 5°C (day-degrees)	Photosynthetic active radiation (Em-2)
Smygehuk	1520 <6>	5100 <7>
Malmö	1710 <6>	5120 <5>
Helsingborg	1750 <5>	5060 <8>
Ljungbyhed	1540 <6>	4800 <5>
Malmslätt	1450 <7>	4570 <8>
Norrköping	1490 <7>	4730 <8>
Örebro	1500 <7>	4770 <7>
Västerås	1480 <7>	4540 <7>
Uppsala	1390 <8>	4430 <8>
Göteborg	1570 <5>	4730 <7>
Hagshult	1260 <8>	4390 <8>
Västervik	1530 <7>	4710 <8>
Visby	1470 <7>	4770 <8>

5.4.2 *Variations in foliar nitrogen concentration*

It is well known that the mean value of the foliar nitrogen concentration in willow plantations usually decreases during the season, especially in non-fertilized stands (see Figure 12a). In the study of the model's performance described above, the foliar nitrogen concentration was held constant, a situation which can probably only be maintained for well-fertilized stands. To examine the influence of a development in nitrogen concentration that is supposed to be valid for a type of non-fertilized stand, on the production during different years, we here introduce the nitrogen concentration as a function of C_l (cf. Hansen & Aslyng, 1984)

$$n_l = c_{n1} - c_{n2} \ln(C_l); n_l \leq n_{l0} \quad \text{Equation 23}$$

The implication of this equation is that n_l decreases when C_l increases. However, according to Equation 13, this implies that C_r increases in relative terms, which in reality should then cause an increase in the uptake of nitrogen and thus counteract this decrease in n_l . This effect is not, however, explicitly considered by this approach, but when the coefficients of Equation 23 are determined from field measurements (Figure 12a), the influence of root growth on n_l is implicit in the equation.

To test the effect of introducing this type of n_l dependence, simulations were

Table 6. Mean annual stem biomass production and statistics for the different cutting cycles. The simulations always started on the first year of the period 1964-1978. The maximum and minimum values are given as deviations from the mean value. The numbers 1, 2 and 3 in the column headings refer to 1-, 2- and 3-year cutting cycles, respectively. The dotted lines separate the locations into the regions Skåne, Östergötland, Mälardalen and the west to east gradient, respectively (cf. Figure 11).

Location	Mean ($t\ ha^{-1}$)			SD (%)			Maximum (%)			Minimum (%)		
	1	2	3	1	2	3	1	2	3	1	2	3
Smygehuk	8.9	12.0	13.5	9	6	6	15	5	7	19	12	9
Malmö	9.7	13.0	14.4	8	4	3	12	4	3	16	7	4
Helsingborg	9.8	13.1	14.6	9	5	6	13	7	7	16	5	7
Ljungbyhed	8.6	11.6	12.9	10	5	5	14	6	6	23	10	7
<hr/>												
Malmslätt	8.1	10.9	12.2	12	7	6	18	10	9	27	14	7
Norrköping	8.6	11.6	12.9	11	6	6	17	9	9	20	12	7
<hr/>												
Örebro	8.7	11.7	13.1	10	4	5	17	5	6	22	9	6
Västerås	8.2	11.0	12.4	10	6	5	18	6	5	22	13	8
Uppsala	7.5	10.3	11.5	12	7	7	17	8	7	24	13	7
<hr/>												
Göteborg	8.9	11.9	13.3	8	6	5	16	6	4	13	9	9
Hagshult	6.5	9.0	10.2	14	8	7	25	14	11	25	12	7
Västervik	8.3	11.3	12.6	10	5	5	18	8	6	16	5	6
Visby	8.4	11.3	12.7	11	6	6	24	9	8	23	9	6

made using three years (1964-66) of data from Göteborg. Firstly, a constant n_l equal to 3.5% (i.e. identical to the simulations of Table 6a) was used and secondly n_l according to Equation 23 with coefficients estimated for clone 082 (Figure 12a). Using the constant value, C_s increased by 67% between Year 1 and Year 2 and by 12% between Year 2 and Year 3 (Figure 12b). Using n_l determined by Equation 23, which thus corresponds to the conditions of a fertile soil of the type found at Studsvik without fertilization, the first-year production was about the same as when using a constant n_l but the growth development during the season was different (Figure 12b). However, the increase in C_s between Year 1 and Year 2 was only 27% here and between Year 2 and Year 3 it was only 3%. Using the coefficients (Equation 23) determined for clone 683 (Figure 12a) instead, the first year growth was 9% lower than when using a constant n_l and the increase in C_s between Year 1 and Year 2 was 34%, whereas that between Year 2 and Year 3 was 5%.

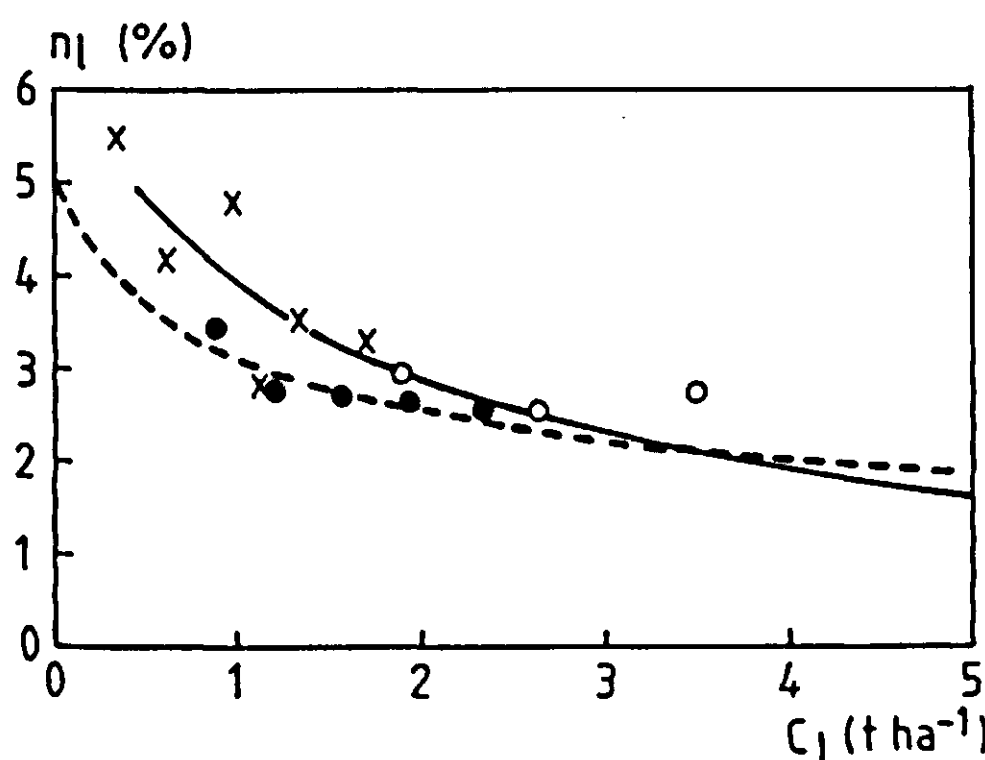


Figure 12a. Foliar nitrogen concentration, n_l , as function of leaf biomass, C_l , for plots of *Salix viminalis* at Studsvik in 1981 before application of fertilizers during the current year (i.e. mid-July). First-year shoots of clone 082: measured (x) and calculated (—) using the function $n_l = 3.88 - 1.41 \cdot \ln(C_l)$ with $r^2 = 0.64$. First-year shoots of clone 683: measured (●) and calculated (---) using the function $n_l = 3.11 - 0.79 \cdot \ln(C_l)$ with $r^2 = 0.79$. Second-year shoots of clone 683: measured (○) values. (Measured values after Nilsson & Ericsson, 1986).

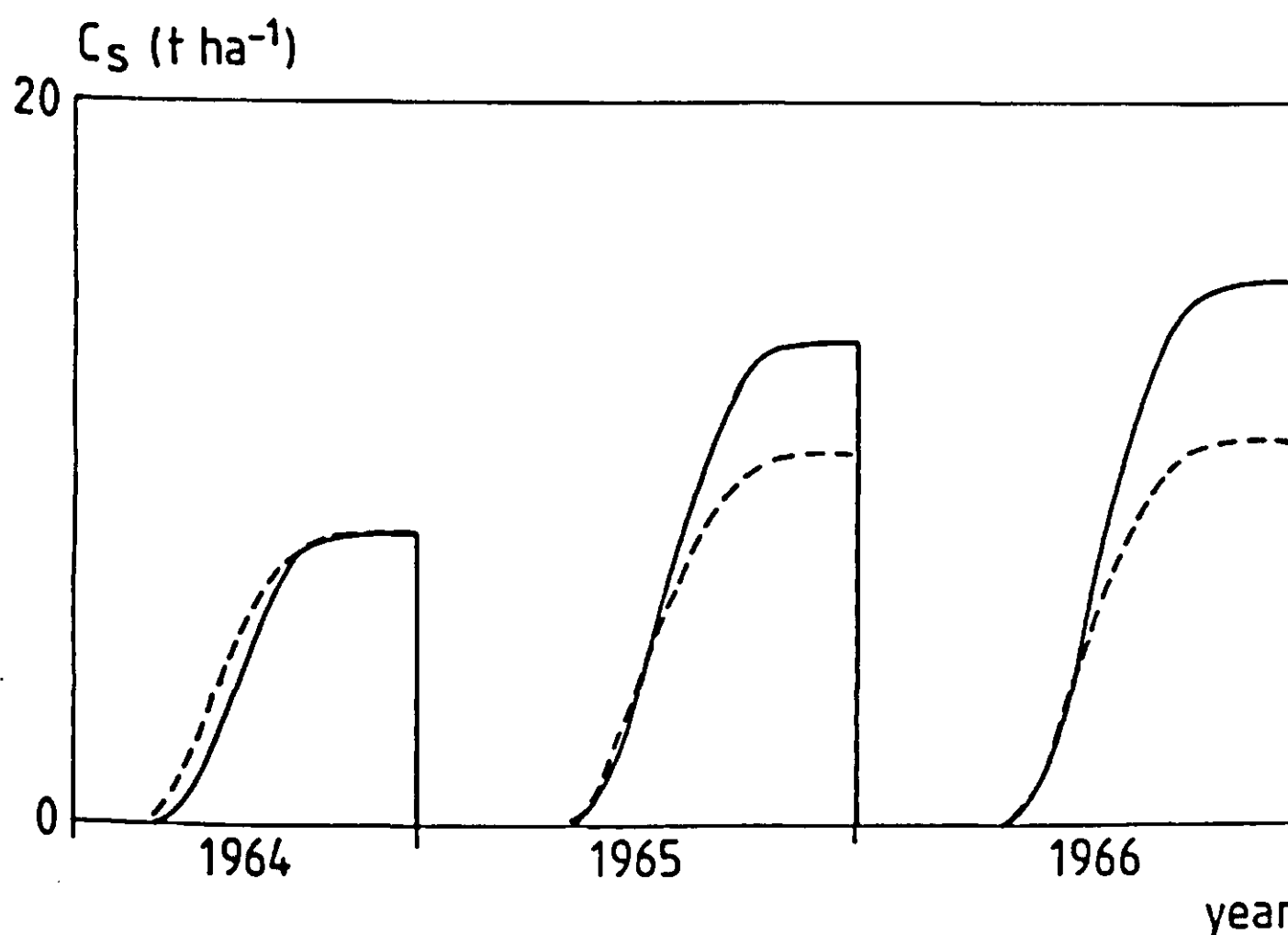


Figure 12b. Simulated annually accumulated stem production, C_s , for three consecutive years without harvest at Göteborg using $n_l = 3.5\%$ (—) and $n_l = 3.88 - 1.41 \cdot \ln(C_l)$ (---). (Cf. Table 6).

5.5 Discussion

The test of the model (Figures 9 and 10) shows that there are some systematic discrepancies between the model output and the measurements, especially at the end of the season. However, except for a few points, these discrepancies have the same order of accuracy as the biomass measurements. Nevertheless, it is interesting to discuss some factors that might be responsible for these discrepancies. One such factor is the plant water status. It has not yet been shown whether the growth of *Salix viminalis* can be maintained during a whole season under all climatic (Swedish) conditions, without restrictions arising with respect to the water factor. The stand used to test the model might occasionally have been subjected to a growth-reducing water stress despite an intensive irrigation (Eckersten, 1986a). Consequently, some of the measured values in Figure 9 might be irrelevant for the test of the model.

Another factor that might have caused the discrepancies is that the model does not consider any systematic variation of the nitrogen concentration within the canopy. From measurements at Studsvik on 2 September 1982, in a nitrogen-fertilized (about $120 \text{ kg ha}^{-1} \text{ yr}^{-1}$) stand of *S. viminalis*, clone 666, on the same type of soil as described above, it was found that n_l decreased with increasing accumulated leaf area index, A_i (Figure 13). Such a profile will affect the estimation of the canopy photosynthesis (see Equation 6) because the

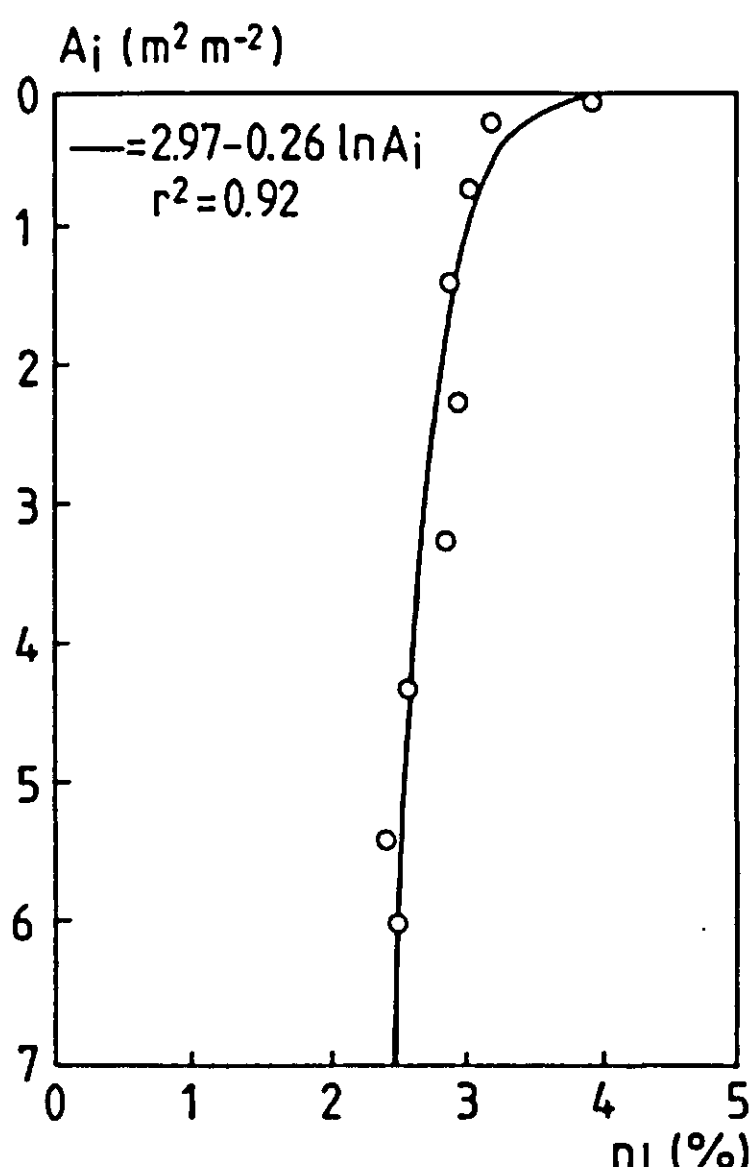


Figure 13. Foliar nitrogen concentration, n_l , as a function of leaf area index accumulated from the canopy top, A_i . (—) represents $n_l = 2.97 - 0.26 \cdot \ln(A_i)$ and (o) measured values for *S. viminalis* clone 666 at Studsvik 2 September 1982.

maximum photosynthetic rate, P_m , is a function of n_l . The effect on the simulated growth of using n_l as a function of A_i (see Figure 13) compared with using a constant n_l (equal to 2.8%, which was the mean foliar nitrogen concentration of this profile) was examined, using the three years of data from Göteborg mentioned earlier. Using n_l as a function of A_i , determined from the data of Figure 13, the simulated C_s was 17, 8 and 5% higher for the first-, second- and third-year growth, respectively. This indicates that the influence on the simulated growth of variations in n_l within the canopy deserves further investigation.

Concerning the underestimation of the stem growth at the end of the growing season (Figure 10), the most probable explanation is an overestimation of the amount of fallen leaves (Equation 17), because the model ignores the retranslocation of assimilates from leaves to stems which occurs at this time.

The considerable variation in simulated willow production between the various locations reflects the great variability in temperature and radiation climate between relatively closely located sites. Helsingborg, for instance, had about 50% higher predicted production than Hagshult. The higher variability in annual production of inland sites compared with coastal sites or near such sites (except for Visby) is explained by the sea's buffering influence on air temperature regime. The temporal variations in production at single sites, with maximum productions ranging from 31% to 65% above the minimum for the 1-year cutting cycle and from 7% to 19% for the 3-year cutting cycle over a time-span of 15 years, indicate that even if the farmer can control all other growth-limiting factors he must expect the annual production to vary considerably from year to year. An increase in the cutting cycle seems to decrease this variation considerably.

Not surprisingly, the model predicted the highest production in Skåne. However, the simulated productions of the Östergötland and Mälardalen regions were sufficiently high under the given environmental conditions to make energy forestry an interesting alternative energy source in these regions. Hagshult represents an extreme location in the inland of southern Sweden as regards the climate, which is here characterized by very low night temperatures (Ångström, 1974; Perttu, 1981). The predicted production at this location probably represents a relatively small area of the highlands of southern Sweden.

In Figure 12b the data show, as expected, that a considerably higher production is achieved if the foliar nitrogen concentration, n_l , is kept at a constant and high level. The effect was most pronounced for the second and third years of production where the non-fertilized situation caused reductions in the range of 25-30% compared with the situation when n_l is maintained at a moderately high and constant level. Compared with an optimal level (n_l equal to 5%) the reduction was considerable, even for first-year shoots (35%) and, of course, was even higher for second- and third-year shoots (45-50%). It should be noted, however, that these differences are somewhat too high (by 5-10%, cf. Table 4 and Chapter 6 in this volume), since the model ignores any influence of n_l on b_a . The effect of climatic variations on the production in the non-fertilized

Table 7. Mean values and standard deviations for all locations of mean annual stem production (dry weight) and its statistics (see Table 6) for a constant foliar nitrogen concentration, n_l , (data from Table 6) and for $n_l = 3.88 - 1.41 \ln(C_l)$, respectively. The numbers 1, 2 and 3 in the column headings refer to the different cutting cycles.

	C_s (t ha ⁻¹ yr ⁻¹)			SD (%)			Maximum (%)			Minimum (%)		
	1	2	3	1	2	3	1	2	3	1	2	3
Mean ($n_l=3.5$)	8.5	11.4	12.8	10	6	6	17	7	7	20	10	7
SD (%)	10	9	9	17	20	19	22	36	32	21	30	19
Mean ($n_l=f(C_l)$)	8.3	9.5	10.0	7	4	4	11	5	5	12	5	4
SD (%)	7	6	6	20	22	16	24	35	26	23	26	32

situation is, as expected, smaller than the values given in Table 6. The mean values for all locations of the mean annual stem production and of its statistics for n_l equal to 3.5% (i.e. data from Table 6) and for $n_l = 3.88 - 1.41 \ln(C_l)$, respectively, are given in Table 7.

In the future, this model will be refined further, concerning the plants' behaviour in terms of growth rates and carbon allocation patterns with respect to water and nutrient stresses (see Chapter 6, in this volume). Such a model will show whether limitations of water during warm sunny days will reduce growth, thus tending to diminish the variation in production between different years caused by variations in radiation and temperature.

5.6 List of symbols and parameter values

The parameter values presented below are those used in the simulations for *Salix viminalis*, clone 082, in Tables 6 and 7 and in Figures 9 and 12b.

A = leaf area index accumulated from canopy top, (dimensionless)
 A_{li} = leaf area index for whole canopy, (dimensionless)
 b_a = leaf weight, $40 + 0.088(t-t_o)$ in Figure 9; 48 in Tables 6 and 7 and in Figure 12b, (g m⁻²); Eckersten & Nilsson (1983)
 b_{av} = fraction of $C_r + C_s$ delivered to C_a , 0.03, (dimensionless); estimated from Eckersten & Nilsson (1983)
 b_{ls} = leaf to shoot biomass ratio, (dimensionless)
 b_{lso} = b_{ls} at time t_o , 0.85, (dimensionless); L-O Nilsson (unpublished data)

b_{ls}	= b_{ls} as time approaches infinity, 0.3, (dimensionless); estimated from Nilsson & Ericsson (1986)
b_r	= fraction of daily total growth delivered to roots, (dimensionless)
b_{ro}	= b_r minimum, 0.15, (dimensionless); cf. Ericsson (1981b)
C_a	= amount of assimilates (dry matter) available for flushing, (kg ha^{-1})
c_b	= decreasing rate of b_{ls} , 0.025, (d^{-1}); estimated from Nilsson & Ericsson (1986)
$c_{dj}, j=1-7$	= coefficients relating δ to t , 0.33281, 22.984, 0.3499, 0.1398, 3.7872, 0.03205, 0.07187, (rad); Dogniaux (1977)
c_{D1}, c_{D2}	= coefficients relating D to O_v , 1.167, 1.15, (dimensionless); Eckersten et al. (1987)
c_{l1}	= parameter relating I (400-700nm) to global radiation (300-3000nm) for clear sky conditions, 2.3, ($\mu\text{E J}^{-1}$); Eckersten et al. (1983)
c_{l2}	= parameter related to atmospheric turbidity, 0.31, (dimensionless); Eckersten (1986a)
c_{k1}, c_{k2}, c_{k3}	= coefficients relating k to A_i , 1.105, 0.007338, 0.02376, (dimensionless); Eckersten (1984)
C_l, C_s, C_r, C_t	= current year's accumulated growth (dry matter) of leaves, stems, roots and total, respectively, (kg ha^{-1})
$C_l(t_0)$	= initial foliage biomass (dry matter), 19, (kg ha^{-1}); Eckersten (1986b)
C_{li}	= accumulated leaf fall (dry matter) during the current year, (kg ha^{-1})
c_m	= coefficient corresponding to the relative rate of litterfall, 0.003, (day^{-1}); estimated from Nilsson & Ericsson (1986)
c_{M1}, c_{M2}, c_{M3}	= coefficients relating M to D , 0.007, 1.68, 0.657, (dimensionless); Eckersten (1986a)
c_{n1}, c_{n2}	= coefficients relating n_l to C_l ; see Figure 12a
c_{p1}, c_{p2}	= coefficients relating P_m to n_l , 0.018, 0.6, (h^{-1}); estimated from McDonald et al. (1981)
$c_{sj}; j=1-7$	= coefficients relating S to t , (1353, 45.326, 0.88018, 0.00461, 1.8037, 0.09746, 0.18412, (W m^{-2})); Dogniaux (1977)
C_t'	= daily total growth (dry matter), ($\text{kg ha}^{-1} \text{d}^{-1}$)
D	= relative duration of sunshine, (dimensionless)
d	= daynumber, (dimensionless); cf. t below
h	= hour of the day, (h)
I	= incident light intensity (400-700nm) on a horizontal surface, ($\mu\text{E m}^{-2} \text{s}^{-1}$)
I_j, I_o, I_{oc}	= I at top of an internal canopy layer, at canopy top, and at canopy top under clear sky conditions, respectively, ($\mu\text{E m}^{-2} \text{s}^{-1}$)

I_p	= parameter relating P to I , 380, ($\mu\text{E m}^{-2} \text{s}^{-1}$); estimated from McDonald et al. (1981)
k	= light extinction coefficient related to leaf area, (dimensionless)
k_j	= k for an internal canopy layer, (dimensionless)
M	= function relating P_d to P_{do} , P_{dc} and D , respectively, (dimensionless)
n_l	= foliar nitrogen concentration, (%)
n_{lo}	= optimal foliar nitrogen concentration, 5, (%); cf. Ericsson (1981b) and Waring et al. (1985)
N_l	= foliar nitrogen content, (kg ha^{-1})
O_v	= fraction of cloudiness during daytime, (dimensionless)
P	= rate of gross photosynthetic assimilation, CH_2O , per unit leaf dry weight, (h^{-1})
P_d , P_{dc} , P_{do}	= daily totals of assimilates, CH_2O , for the current day, for the clear current day, and for the overcast current day, respectively, ($\text{kg ha}^{-1} \text{d}^{-1}$)
P_m	= rate of maximum photosynthetic assimilation, CH_2O , per unit leaf dry weight, (h^{-1})
Q	= stem and root biomass (dry matter) originating from the previous year, (kg ha^{-1})
r_g	= fraction of daily gross photosynthesis lost by growth respiration, 0.25, (dimensionless); Sievänen (1983)
S	= solar radiation (300-3000nm) above the atmosphere received on a surface normal to the sun rays, (W m^{-2})
t	= time in days numbered from 1 January, (d)
t_a , t_e , t_o	= t at the start of the leaf abscission, at the end of the growing season, and at the start of the growing season, respectively, (d)
T	= air temperature ($^{\circ}\text{C}$)
T_o , T_l	= lowest and highest value of T in T_f , 5, 15 ($^{\circ}\text{C}$); cf. Utaaker (1963), de Wit (1965), and Eckersten et al. (1983)
T_f	= function relating growth to T , (dimensionless)
Y	= latitude, (rad)
β	= sun's elevation, (rad)
δ	= sun's declination (rad)
τ	= time normalized with respect to average growing season, (dimensionless)
τ_a	= τ at start of leaf abscission, 0.5, (dimensionless); estimated from Perttu et al. (1978) and Nilsson & Ericsson (1986)

5.7 Source code for the willow growth model

The source code of the willow growth model is written in FORTRAN 77 and makes use of the SIMP simulation support programs (cf. Appendix). It was developed at the Section of Energy Forestry, Swedish University of Agricultural Sciences, Uppsala. This version was created in September 1987. The comments in the source code refer to the equations, comments, discussions, etc. presented above in this paper.

```
SUBROUTINE TRANS
COMMI LAST PRP UPDATE 870831 10:02 PRIOR TO RUN No 308
      INTEGER*2 IGO,NCOMP
      COMMON/UVAL/ TIME,TIMER,IGO
      DIMENSION P( 49)
      EQUIVALENCE (P,PC10 )
      COMMON/UVAL/ PC10   ,PC11   ,PC12   ,PCA10  ,PCL10 ,PI     ,PLATR
      COMMON/UVAL/ PLATS  ,PN10   ,PN11   ,PN20   ,PN21   ,PP10  ,PP11
      COMMON/UVAL/ PR10   ,PR20   ,PR30   ,PR50   ,PR60   ,PR61  ,PR62
      COMMON/UVAL/ PR70   ,PR71   ,PST10  ,PST20  ,PST40  ,PT11  ,PT12
      COMMON/UVAL/ PT13   ,PT14   ,PT20   ,PT21   ,PT22   ,ZB10  ,ZB11
      COMMON/UVAL/ ZB12   ,ZBAV   ,ZBR10  ,ZBR20  ,ZD11   ,ZD12  ,ZDLAI
      COMMON/UVAL/ ZML10  ,ZML11 ,ZML12 ,ZRL10  ,ZTH10 ,ZTH11 ,ZTH12
      COMMON/UVAL/ PDUMMY(121)
      COMMON/UVAL/ NCOMP
      DIMENSION X(10)
      EQUIVALENCE (X(1),X01)
      COMMON/UVAL/ X01,X02,X03,X04,X05,X06,X07,X08,X09,X10
      DIMENSION T( 10)
      EQUIVALENCE (T,T0001)
      COMMON/UVAL/ T0001,T0002,T0003,T0004,T0005,T0006,T0007,T0008,T0009
      COMMON/UVAL/ T0010
      COMMON/UVAL/ G(226)
      COMMON/UVAL/ D(10)

CENDI
      REAL MP, IDAYNO, NCLEAF, NAI, LFSHAL
C
C ***** *****
C ***** MNEMONIC AND SIMP EQUIVALENCES *****
C ***** *****
C
C      For state variables
```

EQUIVALENCE

1 (CTOT ,X01), (CLEAF ,X02), (CSTEM,X03),(CROOT ,X04),(ALI ,X05)
2,(YR ,X08), (BLSPL ,X09), (CLITT ,X10)

C

C For auxiliary variables

C

EQUIVALENCE

1 (TACC ,G(3)),(TSTART,G(5)),(CABV ,G(6)),(ALEAFW,G(7))
2,(ASSDAY,G(10)),(SRAD ,G(11)),(ELEV ,G(12)),(DAYL ,G(13))
3,(DECL ,G(14)),(SRADC ,G(20)),(PARC ,G(21)),(PARO ,G(22))
4,(PARCAI,G(23)),(PAROAI,G(24)),(DREL ,G(25)),(MP ,G(26))
5,(EXTK ,G(30)),(TFUNC ,G(40)),(PMAX ,G(50)),(ASSDC ,G(52))
6,(ASSDO ,G(53)),(DAYNR ,G(60)),(DNORM ,G(61)),(TIMRAD,G(62))
7,(IDAYNO,G(63)),(HH ,G(65)),(LEAPNO,G(68)),(NCLEAF,G(71))
8,(NAI ,G(72)),(DAI ,G(80)),(DAYLEN,G(81)),(CTDAY ,G(100))
9,(CLDAY ,G(101)),(CSDAY ,G(102)),(CRDAY ,G(103)),(ALIDAY,G(104))

C

EQUIVALENCE

1 (BLS ,G(108)),(CLIDAY,G(109)),(DNORML,G(162)),(ROOTAL,G(173))
2,(LFSHAL,G(195)),(CLTOTD,G(201)),(SWL ,G(202))

C

C For driving variables

C EQUIVALENCE

1 (SCON ,D(1)),(TEMP ,D(2))

C

C **** EXPLANATION OF SYMBOLS ****

C ****

C State variables

C

ALI Canopy one-sided plan leaf area index (-)
BLSPL Function for leaf to shoot ratio, bls (-)
CLEAF Accumulated leaf biomass (kg ha⁻¹)
CLITT Accumulated amount of fallen leaves (kg ha⁻¹)
CSTEM Accumulated stem biomass (kg ha⁻¹)
CTOT Total accumulated biomass (kg ha⁻¹)
YR Years since start of simulation (year)

C

C Input variables

C

SCON Sun conditions; Either the duration of bright sunshine (h)
(PST20=0) or the relative cloudiness during daytime (-)
(PST20=1).

C	TEMP	Mean 24h air temperature at screen height (deg. C)
Auxiliary variables		
C	ALEAFW	Areal leaf weight (g m^{-2})
C	ALIDAY	Rate of change of leaf area index (day^{-1})
C	ASSDAY	The daily potential gross photosynthesis ($\text{kg ha}^{-1} \text{ day}^{-1}$)
C	ASSDC	The daily potential gross photosynthesis for the clear sky conditions ($\text{kg ha}^{-1} \text{ day}^{-1}$)
C	ASSDO	The daily potential gross photosynthesis for the overcast sky conditions ($\text{kg ha}^{-1} \text{ day}^{-1}$)
C	BLS	Rate of change of the leaf to shoot allocation function (day^{-1})
C	CABV	Accumulated above ground biomass (kg ha^{-1})
C	CLDAY	Rate of change of leaf biomass ($\text{kg ha}^{-1} \text{ day}^{-1}$)
C	CLIDAY	Rate of change of leaf fall ($\text{kg ha}^{-1} \text{ day}^{-1}$)
C	CLTOTD	Rate of change of total leaf biomass ($\text{kg ha}^{-1} \text{ day}^{-1}$)
C	CRDAY	Rate of change of root biomass ($\text{kg ha}^{-1} \text{ day}^{-1}$)
C	CSDAY	Rate of change of stem biomass ($\text{kg ha}^{-1} \text{ day}^{-1}$)
C	CTDAY	Rate of change of total biomass ($\text{kg ha}^{-1} \text{ day}^{-1}$)
C	DAI	Area of leaves ($\text{m}^2 \text{ m}^{-2}$) per leaf layer. The area can be chosen through parameter ZDLAI
C	DAYL	The astronomical daylength (h)
C	DAYLEN	Auxiliary variable related to DAYL
C	DAYNR	Cyclic daynumber equal to 0.0 at 00:00 January 1
C	DECL	Sun's declination (rad)
C	DNORM	Normalized daynumber equal to zero at the beginning of the average growing season and unity at the end
C	DNORML	The squared value of the number of normalized days (DNORM) from the day when leaf abscission begins to the current date
C	DREL	Relative duration of bright sunshine during daytime (-)
C	ELEV	The sine of the sun's elevation (-)
C	EXTK	Extinction coeff. for photosynthetic active radiation (-)
C	HH	Hour of the day (h)
C	IDAYNO	Cyclic integer daynumber
C	LEAPNO	Flag for leap year
C	LFSHAL	Function for leaf to shoot ratio, bls, for the day following the current day (-)
C	MP	The scaling factor for fractioning of clear and overcast diurnal gross photosynthesis respectively (-)
C	NAI	The nitrogen concentration when used as a function of leaf area index accumulated from canopy top (%)
C	NCLEAF	The nitrogen concentration when used as a function of the leaf biomass (%)

C	PARC	Photosynthetic active radiation (PAR) above canopy for clear sky conditions ($\text{microE s}^{-1} \text{m}^{-2}$)
C	PARCAI	PAR for clear sky conditions at various leaf levels within the canopy ($\text{microE s}^{-1} \text{m}^{-2}$)
C	PARO	PAR above canopy for an overcast sky ($\text{microE s}^{-1} \text{m}^{-2}$)
C	PAROAI	PAR for overcast conditions at various leaf levels within the canopy ($\text{microE s}^{-1} \text{m}^{-2}$)
C	PMAX	The maximum photosynthesis rate ($\text{mg CH}_2\text{O m}^{-2} \text{h}^{-1}$)
C	ROOTAL	The root allocation as a function of nitrogen concentration
C	SRAD	The solar 'constant' (W m^{-2})
C	SRADC	The same as PARC
C	SWL	Flag for start/end of growing season
C	TACC	Accumulated air temperature (day-deg.)
C	TIMRAD	The hour of the day +12, in radians (rad)
C	TFUNC	The growth temperature function (-)
C	TSTART	The day (-number) of flushing in the spring
C	Y...	Variables beginning with the letter 'Y' are used internally in different steps of the calulations
C	For parameters (defined by the PRP program of the SIMP package)	
C	PC10-12	The coefficients a,b,c of the light extinction coefficient equation $k(Ai)=a+b*Ai+c*Ai^{**2}$. Observe - if $k(Ai)$ is wanted (i.e., $dAi>Ai$) then PC11 and PC12 should be $2*b$ and $4*c$, respectively
C	PCA10	Ratio between leaf biomass and above ground biomass at day TSTART (-)
C	PCL10	Initial leaf biomass at day TSTART (kg ha^{-1})
C	PI	Coefficient of the photosynthesis light response curve ($\text{microE m}^{-2} \text{s}^{-1}$)
C	PLATR	Latitude of the radiation/cloudiness measurement station (deg.)
C	PLATS	Latitude of the location of growth simulation (deg.)
C	PP10-11	Coefficients a and b of the function for maximum photosynthesis rate; $Pm^*=a+b*nl$ ($\text{mgCO}_2 \text{g}^{-1} \text{h}^{-1}$)
C	PN10-11	Coefficients a and b of the nitrogen concentration function dependent in leaf biomass; $nl(Cl)=a+b*ln(Cl)$ (%)
C	PN20-21	Coefficients a and b of the nitrogen concentration function dependent on accumulated leaf area ; $nl(Ai)=a+b*ln(Ai)$ (%)
C	PR10,20	Coefficients a and b of the incoming light conversion function; $loc=b*S*sinh2/(sinh+a)$ (b: $\text{microE}(400-700\text{nm})$ J-1(300-3000nm))
C	PR30	Coefficient c of clear to overcast radiation conversion function; $loo=c*loc$
C	PR50	Mean fraction of suntrack (units of time) not obscured by the

C horizon at the location of radiation/cloudiness measurements
 C PR60-62 Coefficients a, b and c of the function fractioning between
 C clear and overcast diurnal gross photosynthesis respectively;
 C $M=a+b*D+c*D^{**2}$
 C PR70-71 Coefficients a and b of the equation transforming between
 C relative duration of sunshine and relative cloudiness during
 C daytime; $D=a+b*Ov$
 C PT11-14 Temperatures (T0, T1, T2, T3 ($^{\circ}$ C)) defining the growth
 C temperature function
 C PT20 Threshold temperature (T4) for accumulated temperature ($^{\circ}$ C)
 C PT21 Limit for start of growth (day-deg.)
 C PT22 Day (-number) for start of accumulation of temperature (TACC)
 C ZBAV Fraction of annual increment of shoot and root biomass
 C delivered to pool of assimilates available for sprouting in
 C the spring
 C ZBR10 Minimum value (fraction) of the root allocation function; bro
 C ZBR20 Optimum nitrogen concentration; nlo (%)
 C ZB10-12 Coefficients a, b and c of the leaf to shoot allocation
 C function; $bls=(a-b)*exp(-c*(t-to))+b$
 C ZD11 Start (daynumber) of the average growing season
 C ZD12 End (daynumber) of the average growing season
 C ZDLAI Size of internal canopy leaf layers, dAi, ($m^2 m^{-2}$)
 C ZML10-12 Coefficients a, b and tna of leaf fall function;
 C $Cli=(a+b*((tn-tna)^{**2}))*Cl$
 C ZRL10 Fraction of daily gross photosynthesis lost by respiration;
 C rg
 C ZTH10 Areal leaf weight; ba (g/m^2)
 C ZTH11 Ratio between areal leaf weight for 1-year-old shoots
 C and current shoots minus one
 C ZTH12 Ratio between areal leaf weight for 2-year-old shoots
 C and 1-year-old shoots minus 1
 C PST10 Number of years from start year to next leap year. If start
 C year equals the leap year the value should be = 4.
 C PST20 Flag for type of light input data. 0 = duration of bright
 C sunshine and 1 = relative cloudiness
 C PST40 Cutting cycle (number of years)

+++++ EVERY DAY +++++++

C

CALL ECDCDA(TIME,D)	!Read input data
CTDAY=0	!Ct'
CLDAY=0	!Cl'
CSDAY=0	!Cs'

```

CRDAY=0          !Cr'
ALIDAY=0         !Ali'
BLS=0            !bls'
CLIDAY=0         !Cli'
YZ60=AMAX1(CLEAF,1.0) !nl(Cl)=(a+b*ln(Cl)) min nlo
NCLEAF=PN10+PN11* ALOG(YZ60/1000)
NCLEAF=AMIN1(NCLEAF,ZBR20)
YP26=(YR+PST10)/4          !Time
YP27=INT(YP26)
IF (YP26.EQ.YP27) LEAPNO=1.0 !if leapyear sw=1
YZ11=365+LEAPNO
IDAYNO=TIME-YZ11*YR
IF (IDAYNO.LT.PT22) GOTO 1000 !if t<tD...
YP25=TEMP-PT20          !Tacc=Tacc+((Ta-T4)max0)
TACC=TACC+AMAX1(YP25,0.0)
IF (TACC.GE.PT21) GOTO 2    !if Tacc>=T5...
TSTART=IDAYNO          !to=t
GOTO 1000

C
C++++++ During growing season ++++++
C
C++++++ Every day ++++++
C
2    ASSDC=0          !Pdc
ASSDO=0          !Pdo
HH=0            !hour

C
C++++++ Every hour ++++++
C    LOOP1 start+++++
C
5    HH=HH+1          !hour
DAYNR=IDAYNO+HH/24      !t
TIMRAD=((DAYNR-INT(DAYNR))*24+12)*3.14/12 !hour*=hour+12
DNORM=(DAYNR-ZD11)/(ZD12-ZD11) !tn

C
IF (TEMP.GT.PT13) GOTO 20
IF (PT12.LE.PT11) GOTO 22
TFUNC=(TEMP-PT11)/(PT12-PT11) !Tf=(Ta-To)/(T1-To) if
                                To<Ta<T1
GOTO 22
20   TFUNC=1-(TEMP-PT13)/(PT14-PT13) !Tf=1-(Ta-T2)/(T3-T2) if
                                Ta>T2
22   IF (TEMP.LE.PT11.OR.TEMP.GE.PT14) TFUNC=0.0 !Tf=0 if Ta<To or Ta>T3
      IF (TEMP.GE.PT12.AND.TEMP.LE.PT13) TFUNC=1.0 !Tf=1 if T1<Ta<T2

```

```

C
    YP22=2*3.14/366                                !DEC=f(t)
    DECL=0.33281-22.984*COS(DAYNR*YP22)-0.3499*COS(DAYNR*2*YP22)
    DECL=DECL-0.1398*COS(DAYNR*3*YP22)+3.7872*SIN(DAYNR*YP22)
    DECL=DECL+0.03205*SIN(DAYNR*2*YP22)+0.07187*SIN(DAYNR*3*YP22)
    DECL=DECL*3.14/180
    SRAD=1353+45.326*COS(DAYNR*YP22)+0.88018*COS(DAYNR*2*YP22)
                                                !S=f(t)
    SRAD=SRAD-0.00461*COS(DAYNR*3*YP22)+1.8037*SIN(DAYNR*YP22)
    SRAD=SRAD+0.09746*SIN(DAYNR*2*YP22)+0.18412*SIN(DAYNR*3*YP22)
C
C
    !sinh=sin(LATs)*sin(DEC)+cos(LATs)*cos(DEC)*cos(hour*)
C
    YP23=PLATS*3.14/180
    ELEV=SIN(YP23)*SIN(DECL)+COS(YP23)*COS(DECL)*COS(TIMRAD)
C
    SRADC=PR20*SRAD*(ELEV**2)/(PR10+ELEV)  !loc=b*So*sinh2/(sinh+a)
    IF (ELEV.LE.0) SRADC=0
    IF (SRADC.EQ.0) GOTO 10
    PARC=SRADC                                !I(Ai)=loc
    PARO=PR30*SRADC                            !Ioo=c*loc
C
    YZ50=0                                     !ba=a*(1+b*(shootage>=1)+c*(shootage=2))
    YZ51=0
    YZ52=YR/PST40
    YZ52=YZ52-INT(YZ52)
    IF (YZ52.GT.0) YZ50=1
    IF (YZ52.GE.0.66) YZ51=1
    ALEAFW=(1+YZ50*ZTH11+YZ51*ZTH12)*ZTH10
C
    C++++++ Canopy internal layers ++++++
C
    YP12=0
C
    C
    LOOP2 start+++++ /+++++ ++++++ ++++++ ++++++ ++++++ ++++++
C
    7
    B=ALI-YP12
    DAI=AMIN1(ZDLAI,B)                      !dAi
    IF (DAI.EQ.0) GOTO 10                    !if dAi=0...
    YP13=YP12+DAI/2                          !Aj=Ai+dAi/2
C
    NAI=NCLEAF                                !nl(Aj)=nl(Cl)
    IF (PN21.EQ.0) GOTO 8                    !if d(nl)/dAi=0...

```



```

60     DREL=PR70+PR71*SCON           !SCON=Ov; D=a+b*Ov
70     DREL=AMIN1(DREL,1.0)         !0<=D<=1
     DREL=AMAX1(DREL,0.0)
     MP=PR60+PR61*DREL+PR62*DREL**2   !M=a+b*D+c*D**2
C
C     !Pd=Pdo+M*(Pdc-Pdo); (g m-2 --> tonnes ha-1)
C
C     ASSDAY=(ASSDO+MP*(ASSDC-ASSDO))/100
C
C     !bls(+) = a-b*exp(-c*(t(+) - to))+b
C
     LFSHAL=(ZB10-ZB11)*EXP(-ZB12*(DAYNR-TSTART))+ZB11
     BLS=LFSHAL-BLSPL           !bls'
C
C     !br=1+bro-(1-x**2)**0.5; x=(nlo-nl(Cl))/nlo
C
     ROOTAL=1+ZBR10-(1-((ZBR20-NCLEAF)/ZBR20)**2)**0.5
     ROOTAL=AMAX1(ROOTAL,ZBR10)      !br=brn max bro
C
     CTDAY=ASSDAY*TFUNC           !Ct=Pd*Tf
C
C     !(Cl+Cli)'=bls*Ct*(1-br)+(Cl+Cli+Cs)*bls'
C
     CLTOTD=BLSPL*CTDAY*(1-ROOTAL)+(CLEAF+CLITT+CSTEM)*BLS
C
     DNORML=(DNORM-ZML12)**2
     IF (DNORM.LT.ZML12) DNORML=0      !Cl'=0 if tn<tna
     CLIDAY=(ZML10+ZML11*DNORML)*CLEAF !Cl'=(a+b*((tn-tna)**2))*Cl
C
     CLDAY=CLTOTD-CLIDAY           !Cl'=(Cl+Cl)-Cl'
C
C     !Cs'=(1/bls-1)*(Cl+Cl)-Cl+Cs/bls*bls'
C
     CSDAY=(1/BLSPL-1)*CLTOTD-(CLEAF+CLITT+CSTEM)/BLSPL*BLS
     CRDAY=ROOTAL*CTDAY           !Cr'=br*Ct'
     ALIDAY=(CLEAF+CLDAY)/10/ALEAFW-ALI !Ali'=Cl/ba-Ali
     CABV=CABV+ZBAV*(CRDAY+CSDAY)   !Ca=Ca+bav*(Cr'+Cs')
C
999    IF (IDAYNO.LE.YZ11) GOTO 1000      !if t<=te...
C
C++++++ End of growing season ++++++
C
C++++++ Initiation of next years growth ++++++

```

```

YR=YR+1                                !year=year+1
YZ40=PCA10*CABV                         !Cl(to) if no harvest
YZ41=(1-PCA10)*CABV                     !Cs(to) if no harvest
YZ42=YR/PST40
YZ43=INT(YZ42)
IF (YZ43.EQ.YZ42) YZ40=PCL10          !Cl(to) if harvest
YZ44=PCL10*(1-PCA10)/PCA10
IF (YZ43.EQ.YZ42) YZ41=YZ44          !Cs(to) if harvest
CLEAF=YZ40                               !Cl(to)
CSTEM=YZ41                               !Cs(to)
CROOT=0                                  !Cr(to)
CTOT=CLEAF+CSTEM                         !Ct(to)
ALI=CLEAF/ZTH10/10                       !Ali(to)
BLSPL=ZB10                               !bls(to)
CLITT=0                                  !Cli(to)
TACC=0                                   !Tacc
CABV=0                                   !Ca(to)
LEAPNO=0                                 !leap year
SWL=0                                    !swl
GOTO 1010

```

C

C++++++ After every day +++++++

C

```

1000   CTOT=CTOT+CTDAY
       CROOT=CROOT+CRDAY
       CLEAF=CLEAF+CLDAY
       IF (CLEAF.LT.0.0) SWL=1.0 !if Cl<0 sw=1 --> stop of
           growing season
       CSTEM=CSTEM+CSDAY
       ALI=ALI+ALIDAY
       BLSPL=BLSPL+BLS
       CLITT=CLITT+CLIDAY
1010   RETURN
       ENTRY INITIL
       CALL ECDCIN
       END

```

----- Parameter values used for Göteborg -----

PC10	= 1.11	PP11	= 8.80	PT11	= 5.00	ZD11	= 98.0
PC11	=-7.338E-03	PR10	= 0.310	PT12	= 15.0	ZD12	= 333.
PC12	=-2.376E-02	PR20	= 2.30	PT13	= 50.0	ZDLAI	= 1.00
PCA10	= 0.850	PR30	= 0.300	PT14	= 60.0	ZML10	= 0.000E+00
PCL10	= 19.0	PR50	= 1.00	PT20	= 5.00	ZML11	= 0.300
PI	= 380.	PR60	=-7.000E-03	PT21	= 40.0	ZML12	= 0.500
PLATR	= 58.8	PR61	= 1.68	PT22	= 60.0	ZRL10	= 0.250
PLATS	= 57.8	PR62	=-0.657	ZB10	= 0.850	ZTH10	= 48.0
PN10	= 3.50	PR70	= 1.17	ZB11	= 0.300	ZTH11	= 0.200
PN11	= 0.000E+00	PR71	= -1.15	ZB12	= 2.500E-02	ZTH12	= 5.000E-02
PN20	= 0.000E+00	PST10	= 4.00	ZBAV	= 3.000E-02		
PN21	= 0.000E+00	PST20	= 1.00	ZBR10	= 0.150		
PP10	= 26.0	PST40	= 3.00	ZBR20	= 5.00		

----- Initial compartment values -----

X01 = 22.4	X04 = 0.000E+00	X07 = 2.500E+03	X10 = 0.000E+00
X02 = 19.0	X05 = 5.000E-02	X08 = 0.000E+00	
X03 = 3.40	X06 = 0.000E+00	X09 = 0.850	

5.8 Acknowledgements

The present study was conducted within the Swedish Energy Forestry Project funded by the Swedish Energy Administration. The authors are given in alphabetical order.

5.9 References

Ågren, G. I., 1985. Theory for growth of plants derived from the nitrogen productivity concept. *Physiologia Plantarum* 64:17-28.

Ångström, A., 1974. *Sveriges klimat* [Swedish climate]. Generalstabens Litografiska Anstalts Förlag, Stockholm, 188 pp.

Dogniaux, R., 1977. Computer procedure for accurate calculation of radiation data related to solar energy utilization. *Proceedings of the UNESCO/WMO Symposium on Solar Energy*, 30 Aug. – 3 Sept. 1976, Geneva. World Meteorological Organization, WMO-No. 477:191-197.

Eckersten, H., 1984. Light penetration and photosynthesis in a willow stand. In: K.L. Perttu (Ed.): *Ecology and management of forest biomass production systems*. Report 15:29-45. Swedish University of Agricultural Sciences, Department of Ecology and Environmental Research, Uppsala.

Eckersten, H., 1986a. Simulated willow growth and transpiration: the effect of high and low resolution weather data. *Agricultural and Forest Meteorology* 38:289-306.

Eckersten, H., 1986b. Willow growth as a function of climate, water and nitrogen. Dissertation, Report 25, 124 pp. Swedish University of Agricultural Sciences, Department of Ecology and Environmental Research, Uppsala.

Eckersten, H., Kowalik, P., Nilsson, L.O. & Perttu, K., 1983. Simulation of total willow production. Report 32, 45 pp. Swedish University of Agricultural Sciences, Section of Energy Forestry, Uppsala.

Eckersten, H., Lindroth, A. & Nilsson, L.O., 1987. Willow production related to climatic variations in southern Sweden. *Scandinavian Journal of Forest Research* 2:99-110.

Eckersten, H. & Nilsson, L.O., 1983. Radiation and temperature influences on deciduous forest production. In: D. Auclair (Ed.): *Mesures des biomasses et des accroissements forestiers. Les Colloques de l'INRA*, No. 19. Paris. ISSN 0293-1915. pp. 153-165.

Ericsson, T., 1981a. Effects of varied nitrogen stress on growth and nutrition in three *Salix* clones. *Physiologia Plantarum* 51:423-429.

Ericsson, T., 1981b. Growth and nutrition of three *Salix* clones in low conductivity solutions. *Physiologia Plantarum* 52:239-244.

Hansen, S. & Aslyng, H.C., 1984. Nitrogen balance in crop production. Simulation model NITCROS. Royal Veterinary and Agricultural University, Hydrotechnical Laboratory, Copenhagen.

Ingestad, T. & Ågren, G.I., 1984. Fertilization for long-term maximum production. In: K.L. Perttu (Ed.): *Ecology and management of forest biomass production systems*. Report 15:155-165. Swedish University of Agricultural Sciences, Department of Ecology and Environmental Research, Uppsala.

Kondratjev, K. Y. A., 1969. *Radiation in the atmosphere*. Academic Press, New York, London. 900 pp.

Larcher, W., 1980. *Physiological plant ecology*. Springer-Verlag, Berlin, Heidelberg, New York. 303 pp. (Second edition).

Linder, S., McDonald, J. & Lohammar, T., 1981. *Effekten av kvävetillstånd och odlingsljus på fotosyntes och andning hos björkplantor* [Effect of nitrogen status and irradiance during cultivation on photosynthesis and respiration in birch seedlings]. Report 12, 19 pp. Swedish University of Agricultural Sciences, Section of Energy Forestry, Uppsala.

McDonald, J., Lohammar, T. & Linder, S., 1981. Effects of leaf nitrogen content on CO₂ exchange in a number of *Salix* clones. Report 16, 29 pp. Swedish University of Agricultural Sciences, Section of Energy Forestry, Uppsala.

Monteith, J.L., 1977. *Climate and the efficiency of crop production in Britain*. Royal Society, London. B. 281:277-294.

Nilsson, L.O. & Ericsson, T., 1986. Influence of shoot age on growth and nutrient uptake patterns in a willow plantation. *Canadian Journal of Forest Research* 16:185-190.

Pelkonen, P., 1984. Carbon dioxide exchange in willow clones. In: K.L. Perttu (Ed.): Ecology and management of forest biomass systems. Report 15:187-196. Swedish University of Agricultural Sciences, Department of Ecology and Environmental Research, Uppsala.

Perttu, K., 1981. II. Radiation cooling and frost risk. In: G. Eriksson (Ed.): Climatic zones regarding the cultivation of *Picea abies* L. in Sweden. Research Notes 36, 25 pp. Swedish University of Agricultural Sciences, Department of Forest Genetics, Uppsala.

Perttu, K., Odin, H. & Engsjö, T., 1978. Vegetationsperioder, temperatursummor och växtenheter som medelvärden med standardavvikelse för perioden 1961-1976 [Vegetation periods, temperature sums, and growth units as mean values with standard deviations during 1961-1976]. Research Notes 101, 296 pp. Swedish University of Agricultural Sciences, Department of Reforestation, Umeå.

Pontailler, J.Y., Leroux, M. & Saugier, B., 1984. Evolution d'un taillis de chataigniers apres coupe: photosynthese et croissance des rejets [The evolution of coppice of chestnut trees after cutting: photosynthesis and growth of rejects]. Acta Oecologica Plantarum, Vol. 5 (19), No. 1, pp. 89-99.

Sennerby-Forsse, L., 1986. Seasonal variation in ultrastructure of cambium in young stems of willow (*Salix viminalis*) in relation to phenology. Physiologia Plantarum 67:529-537.

Sievänen, R., 1983. Growth model for mini-rotation plantations. Communicationes Instituti Forestalis Fenniae, 117:1-41. Helsinki.

Sirén, G., 1983. Energiskogsodling [Cultivation of energy forests]. NE 1983:11, Nämnden för energiproduktionsforskning, Stockholm. 255 pp.

Utaaker, K., 1963. The local climate of Nes, Hedmark. Universitetet i Bergen Skrifter Nr 28, 143 pp. Norwegian Universities Press, Bergen-Oslo.

Waring, R.H., McDonald, A.J.S., Larsson, S., Ericsson, T., Wiren, A., Arwidsson, E., Ericsson, A. & Lohammar, T., 1985. Effects of light and nutrient stress on growth and some chemistries in *Salix dasyclados*. Oecologia (Berlin), 66:157-160.

Wit, C.T. de, 1965. Photosynthesis of leaf canopies. Agricultural Research Report, Pudoc, Wageningen, 663:1-57.

6 Allocation of biomass during growth of willow

Henrik Eckersten and Tom Ericsson

6.1 Introduction

Considerable efforts have been expended in the search for crop varieties or ecotypes with high photosynthetic rates per unit of leaf area (Muramoto et al., 1965; Irvine, 1967; Duncan & Hesketh, 1968; Hanson, 1971 and Delaney & Dobrenz, 1974). These investigations have been based on the assumption that high photosynthetic rates per unit area should correlate well with growth. Generally, however, it has been found that growth does not correlate particularly well with photosynthesis per unit leaf area. The rate of leaf area expansion seems to have a greater influence on the dry matter production than the specific net assimilation rate does. This statement is supported by the linear dependence between total biomass production during a growing season and the accumulated absorbed radiation as given by Monteith (1977) and Monteith & Elston (1983) for agricultural crops and by Linder (1985) for forests. The data from which these dependences are calculated pertain to treatments with a wide range of water and nutrient availabilities. It seems that factors affecting the rate of leaf area development are of primary importance for the photosynthetic rate and thus also for biomass production.

Many factors, besides the genotype, influence the rate of leaf area expansion. The availability of water and nutrients are the main abiotic factors accounting for differences in crop production; fortunately these factors can often be controlled by man under field conditions. A strong influence of nutrient availability on the partitioning of the photosynthate between root and shoot has been demonstrated for a large number of tree species, including willows (see Ingestad & Lund, 1979; Ingestad, 1980; Ericsson, 1981a,b; Jia & Ingestad, 1984 and Ingestad & Kähr, 1985). The pattern of the photoassimilate distribution between above- and below-ground parts associated with water availability is, however, less well understood and literature reports in this field are sometimes contradictory (Bradford & Hsiao, 1982; Raynal et al., 1985).

This chapter presents the allocation parameters that Eckersten et al. used in the previous chapter in the simulation of willow growth (cf. also Eckersten et al. 1983; Eckersten 1986). In the Uppsala simulation model the plant is divided into three main pools of biomass: roots, stems and leaves. The roots and leaves are used for the uptake of nutrients and carbon respectively, while the main energy is stored in the stems, which are also the harvested part of the forest. There is also a pool of movable assimilates within the plant, which increasingly influences growth as the plant becomes older. The effect of this pool is easily recognized after harvesting stands of different ages, but it is not treated here.

The partitioning expressions have mostly been given as functions of time, but here they are also given as functions of other factors such as nitrogen status and biomass.

The photosynthetic rate in the simulation model is proportional to the leaf dry weight, and is then a function of the leaf nitrogen status. However, an alternative is to give the photosynthetic rate as a function of unit leaf area. The latter function is only weakly dependent on the nitrogen status according to Waring et al. (1985). In this chapter both methods have been applied, starting with the former.

6.2 Root - shoot partitioning

A certain fraction of the daily net photosynthesis per unit of ground surface, C'_t , is delivered to roots. When the plant nutrient status is low, this fraction, b'_r , is high, because the plant, in relative terms, needs more roots and the energy

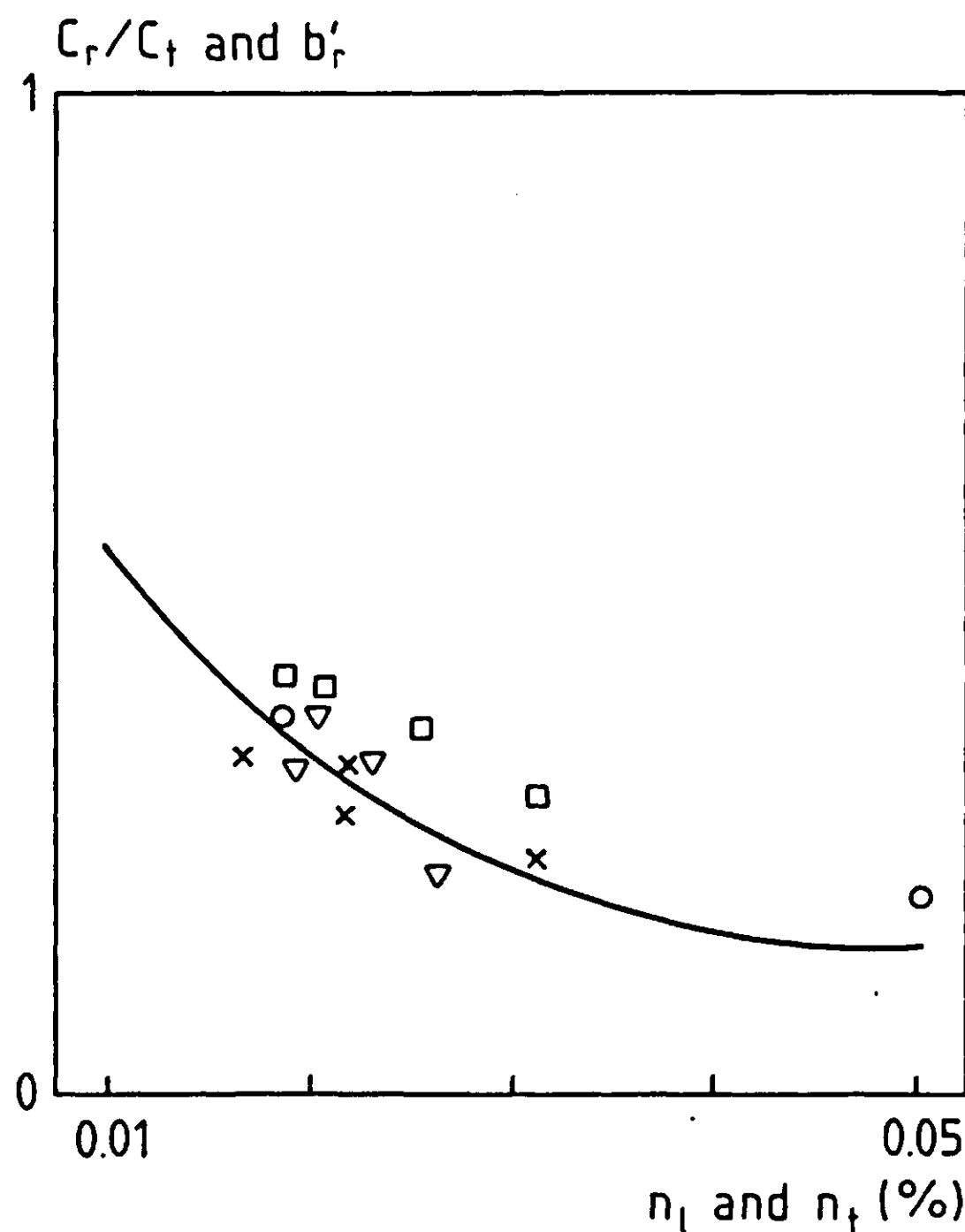


Figure 14. The ratio between accumulated values of root biomass, C_r , and total biomass, C_t , as reported by Ericsson (1981b) on *Salix viminalis* = x, *Salix aquatica* = □, and *Salix fragilis* = ▽, and by Waring et al. (1985) on *Salix dasyclados* = o. The line represents daily net photosynthesis delivered to roots, b'_r , (see Equation 24) and n_l and n_t stand for nitrogen concentrations in the leaves and in the whole plant, respectively. (After Eckersten, 1986).

cost for the active uptake of nutrients is higher than when nutrient status is high. In the model, the plant nutrient status is represented by the foliar nitrogen concentration, n_l . For *Salix* grown under different nutrition conditions in a laboratory environment the roots fraction was a function of n_l (Ericsson, 1981a,b and Waring et al., 1985). The relationship is similar for many *Salix* species and, following these values (see Figure 14), b'_r is given according to

$$b'_r = 1 + b'_{ro} - (1 - ((n_{lo} - n_l)/n_{lo})^2)^{0.5} \quad \text{Equation 24}$$

where n_{lo} is the value of n_l corresponding to the lowest relative allocation of assimilates to roots, b'_{ro} . Since the plants used in the experiments illustrated in Figure 14 did not become older than a few months, no death of roots occurred and thus the figures measured also include the production of fine roots. The root respiration is not included in the figure; therefore, the curve in Figure 14 underestimates the real value of b'_r by this amount.

The influence, in quantitative terms, of the plant water status on the root-shoot partitioning is not fully understood. Qualitatively, the response should be similar to that for the plant nutrient status, except that there should be no energy costs for the passive uptake of water (cf. Ray, 1972).

6.3 Leaf - stem partitioning

The assimilates allocated to the above-ground part are partitioned between leaves and stems. Because the photosynthesis is proportional to the dry weight of the leaf, it is necessary to know the total leaf biomass in order to calculate the total canopy photosynthesis. The partitioning of biomass between leaves and stems depends both on environmental and internal variables. The fraction of accumulated leaf biomass of the accumulated shoot biomass is expressed as

$$b_{ls} = (C_l + C_{li})/(C_l + C_{li} + C_s) \quad \text{Equation 25}$$

where C_l , C_{li} and C_s are the accumulated leaf, leaf fall and shoot biomass of the current year, respectively. b_{ls} is, preliminarily, taken as a function of time.

Measurements were made on four different *Salix viminalis* stands, cultivated for the purpose of obtaining a high yield. These stands are: (i) clone 082, 9 plants/m², first-season shoots, fourth-season roots, growing on old farmland on marine silt soils at Studsvik 58.8 °N and 17.4 °E, alt. 5m, (ii) clone 683, 16 plants/m², first-season shoots, fourth-season roots, same site as (i), (iii) the same as for (ii) but with second-season shoots, (iv) clone 082, 4 plants/m², first-season shoots, third-season roots, gyttja clay at Köping 59.8 °N and 16.0 °E, alt. 10 m (Eckersten et al., 1983). From these measurements, b_{ls} has been found to approximately follow the equation

$$b_{ls} = (c_o - c_l) \exp(-c_2(t - t_o)) + c_l \quad \text{Equation 26}$$

where c_o equals b_{ls} on the first day of the growing season. As time approaches infinity (or, in reality at the end of the growing season), b_{ls} decreases to c_l

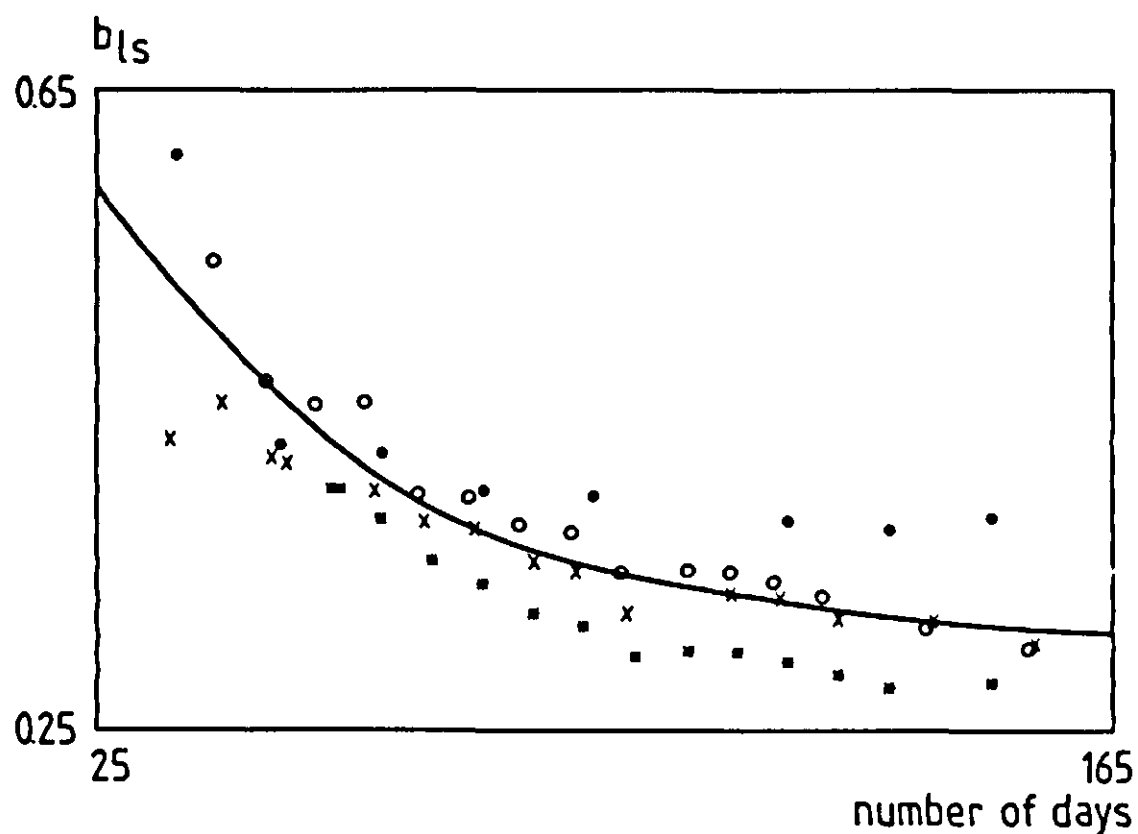


Figure 15a: The fraction of leaves of the shoot biomass, b_{ls} , plotted against number of days since the start of the growing period (5 May). The dots represent measurements for *Salix viminalis*; x = clone 082 at Studsvik, o = clone 683 first-season shoots, \bullet = clone 683 second-season shoots, and $*$ = clone 082 at Köping. The line represents Equation 26 for c_0 , c_1 and c_2 equal to 0.85, 0.30 and 0.025, respectively. (After data from Nilsson & Ericsson, 1986 and Eckersten et al., 1983).

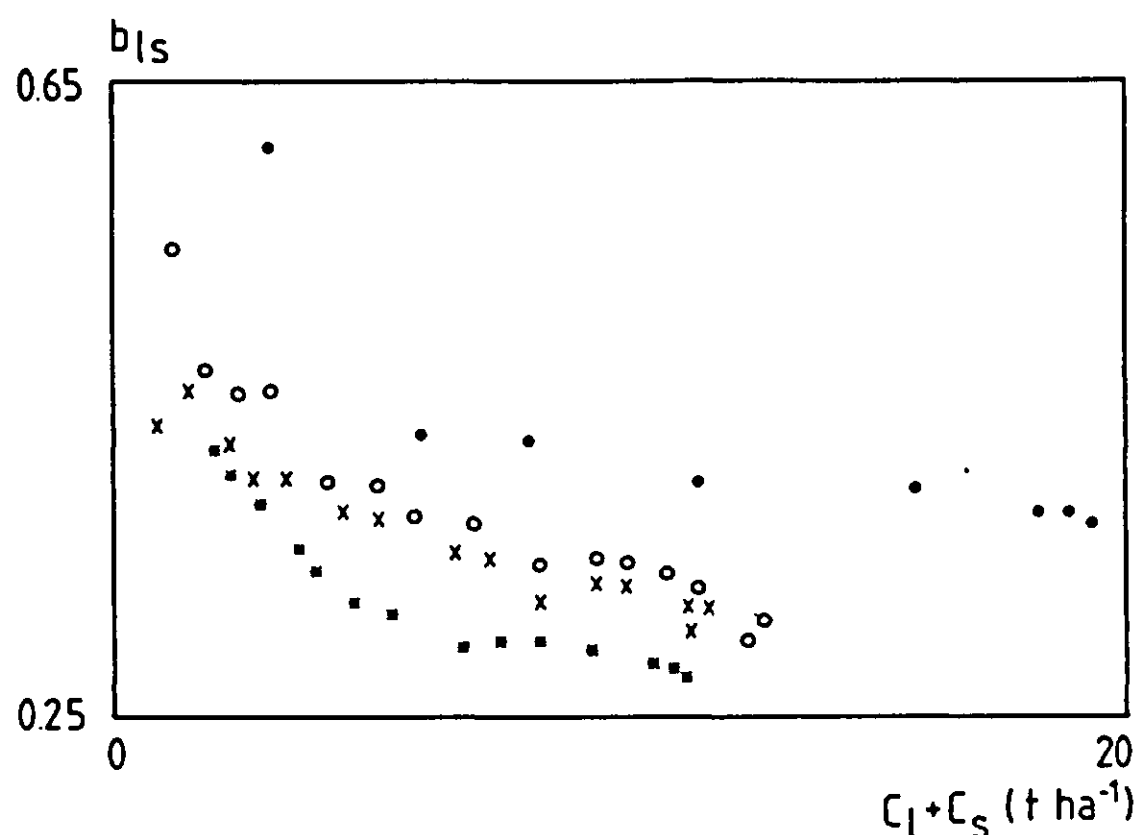


Figure 15b: The fraction of leaves of the shoot biomass, b_{ls} , plotted against shoot biomass, $C_l + C_s$. The dots represent measurements for *Salix viminalis*; x = clone 082 at Studsvik, o = clone 683 first-season shoots, \bullet = clone 683 second-season shoots, and $*$ = clone 082 at Köping. (After data from Nilsson & Ericsson, 1986).

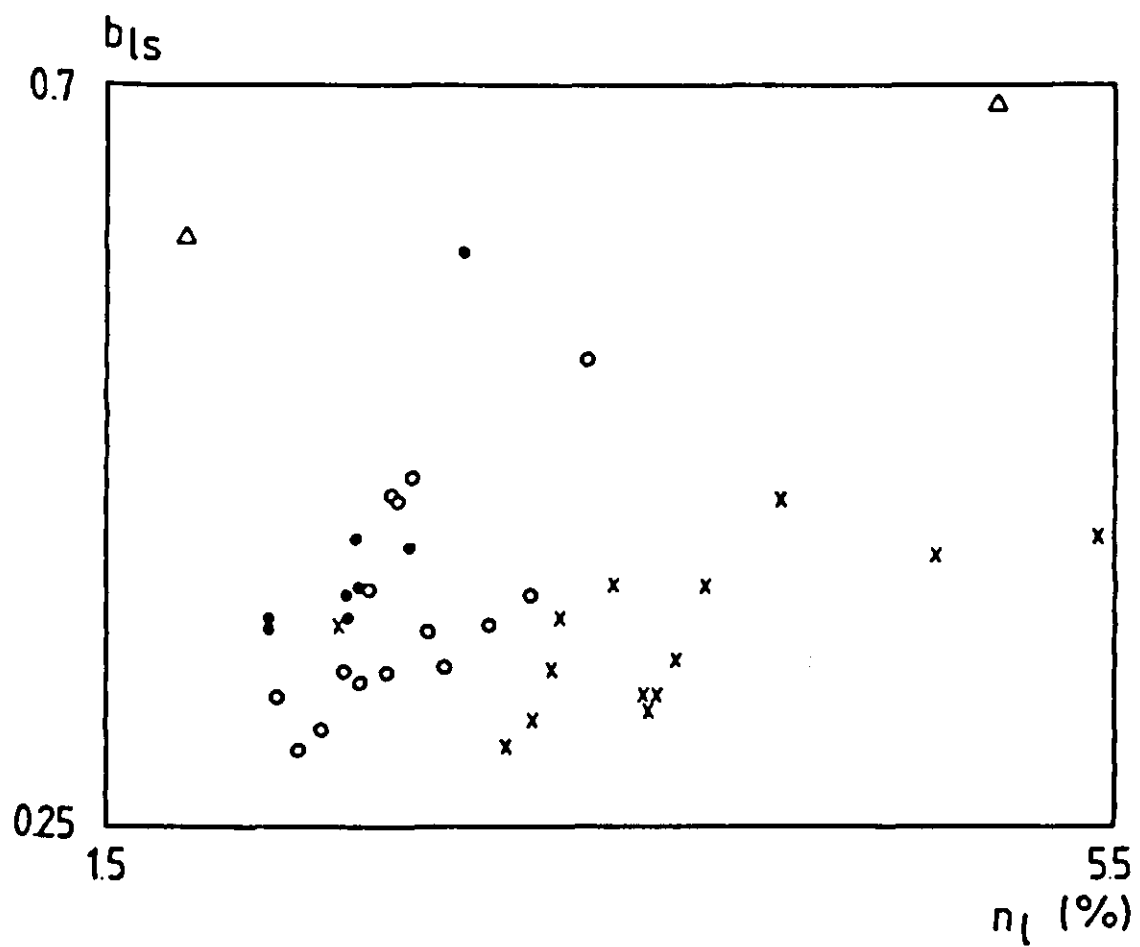


Figure 15c: The fraction of leaves of the shoot biomass, b_{ls} , plotted against foliar nitrogen concentration, n_l . The dots represent measurements for *Salix viminalis*; x = clone 082 at Studsvik, o = clone 683 first-season shoots, and \bullet = clone 683 second-season shoots. Δ = *Salix dasyclados* (Waring et al., 1985). (After data from Nilsson & Ericsson, 1986).

(Figure 15a). Figure 15a shows a remarkable similarity for first-season shoots at Studsvik, whereas the second-season shoots have a higher value for b_{ls} and the less dense stand at Köping has a lower fraction of leaves (i.e. a lower value for b_{ls}). When relating b_{ls} to the shoot biomass ($C_l + C_s$) instead of time, the disparity between shoots of different age and between sites increased (Figure 15b). The fraction of leaves might increase with increasing foliar nitrogen concentration, n_l , which might be explained by the leaf canopy being the first part of the plant to increase its biomass as the total photosynthesis increases. In Figure 15c, b_{ls} is plotted against n_l for the four stands. When the values for small plants of *S. dasyclados* growing in laboratory environment at different nutritional conditions (Waring et al., 1985; Figure 15c) are introduced it becomes clear that b_{ls} is not a function of n_l alone.

6.4 Areal leaf weight

The potential photosynthesis, defined as photosynthesis not being limited by water or temperature conditions, is a function of the light absorbed by the leaves. The response to light, which varies with the foliar nitrogen concentration, is expressed per unit of leaf weight. The absorption of light is, however, a function of the leaf area and consequently the photosynthesis per unit of ground surface, P , is proportional to the areal leaf dry weight, b_a ($= 100 \cdot C_l / L_{ai}$, where L_{ai} is the canopy leaf area index), according to (Eckersten, 1986)

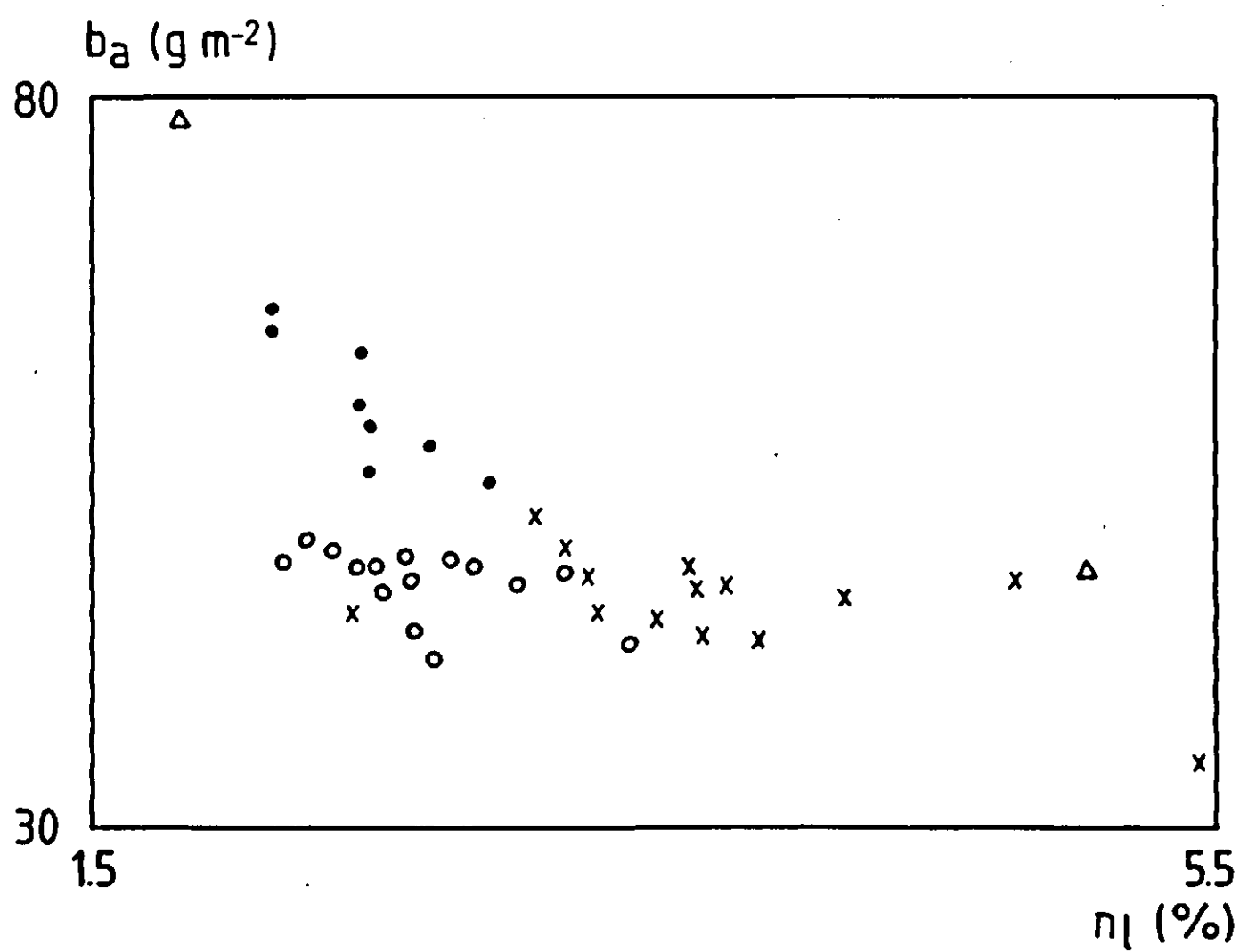


Figure 16a: Areal leaf dry weight, b_a , plotted against foliar nitrogen concentration, n_l : $x = Salix viminalis$ clone 082 at Studsvik, $o = Salix viminalis$ clone 683 first-season shoots, $\bullet = Salix viminalis$ clone 683 second-season shoots, $\Delta = Salix dasyclados$. (After data from Nilsson & Ericsson, 1986, Eckersten et al., 1983, and Waring et al., 1985).

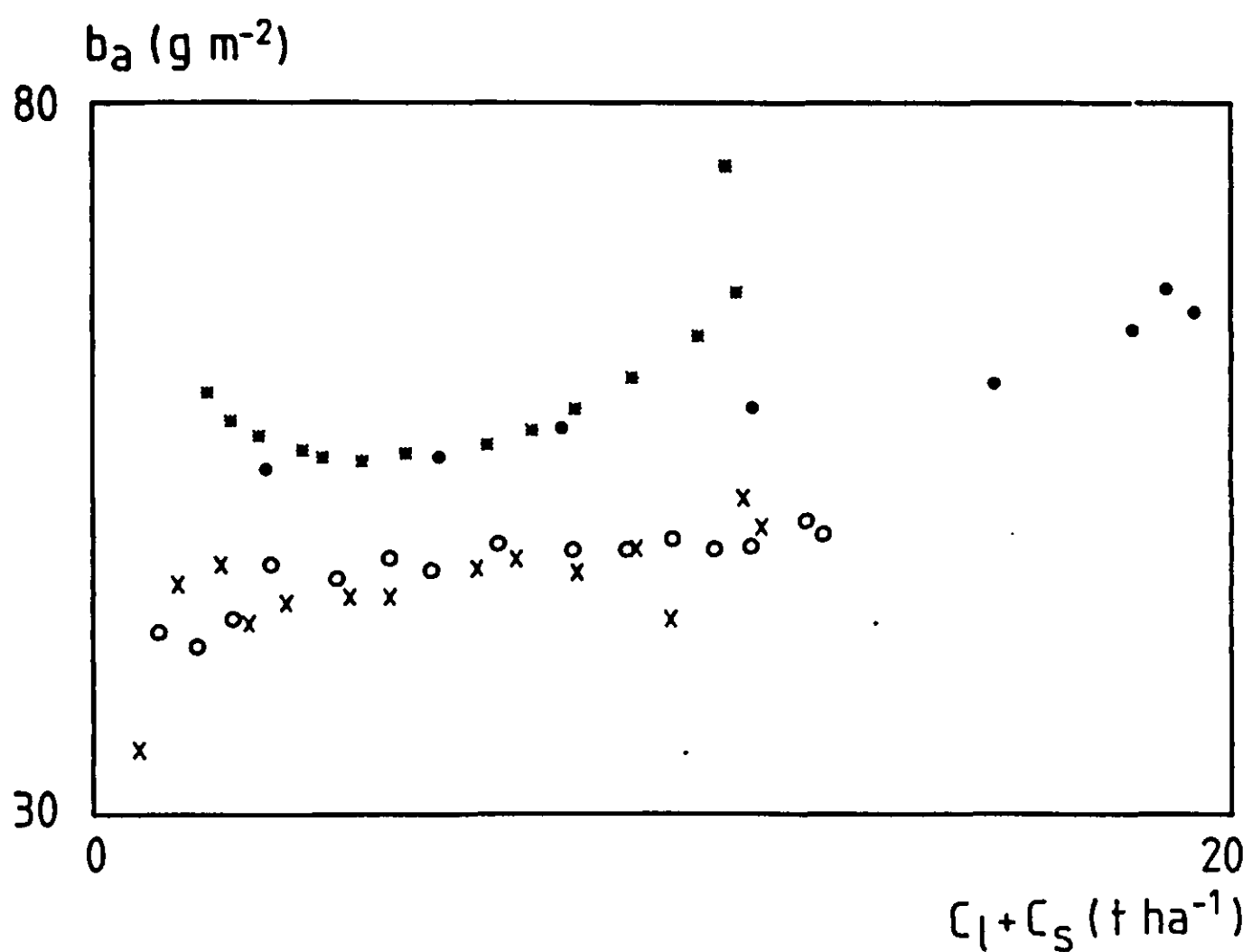


Figure 16b: Areal leaf dry weight, b_a , plotted against shoot biomass, $C_l + C_s$: $x = Salix viminalis$ clone 082 at Studsvik, $o = Salix viminalis$ clone 683 first-season shoots, $\bullet = Salix viminalis$ clone 683 second-season shoots, $*$ = *Salix viminalis* clone 082 at Köping, $\Delta = Salix dasyclados$. (After data from Nilsson & Ericsson, 1986, Eckersten et al., 1983, and Waring et al., 1985).

$$P = \int_0^{L_{ai}} b_a \frac{P_m I}{I + p_l} dL_i \quad \text{Equation 27}$$

where P_m is the maximum photosynthetic rate expressed per unit of leaf dry matter and p_l is a parameter that equals the ratio between P_m and the light use efficiency at low light intensities. I is the light absorbed by the leaves and L_i is the leaf area index accumulated from canopy top.

P_m is known to increase with the foliar nitrogen concentration, n_l . However, laboratory experiments show that b_a decreases with increasing n_l and hence compensates, at least partly, for the increase in P_m . In other words, the increasing photosynthetic rate per unit of dry weight when increasing the nitrogen concentration is accompanied by the leaves becoming thinner.

When plotting b_a against n_l for the four *Salix* stands presented previously it is obvious that not only n_l affects b_a (Figure 16a). In Figure 16b, b_a is plotted against the shoot biomass, which does not represent the development of b_a better than n_l does. Values measured in laboratory on *S. dasyclados* are also given in Figure 16a.

6.5 Modified allometric functions

In the preceding section, it was shown that the foliar nitrogen concentration, n_l , influences the photosynthesis (per unit of ground surface, Equation 27) both through an increasing photosynthesis per unit of leaf dry weight and through a decreasing areal leaf weight, b_a . This means that n_l influences the photosynthesis per unit of leaf area less than the photosynthesis per unit of leaf dry weight. Denoting the maximum photosynthesis per unit of leaf area with P_m' the potential photosynthesis per unit of ground surface is (cf. Equation 27)

$$P' = \int_0^{L_{ai}} \frac{P_m' I}{I + p_l} dL_i \quad \text{Equation 28}$$

Assuming that P_m' is independent of n_l , P' is a function of n_l only because L_{ai} is a function of n_l . Equations 27 and 28 correspond theoretically with two different strategies of the plant as regards carbon uptake. Using Equation 27 the increase in photosynthesis per unit ground surface is strongly controlled by the development of the leaf thickness, whereas using Equation 28 it is stimulated only by an increasing leaf area.

Using Equation 28 (instead of Equation 27) in the shoot growth simulations in Chapter 5 makes it unnecessary to determine the leaf biomass, C_l , explicitly. Hence the determinations of b_{ls} (Equations 25 and 26) and b_a are replaced by

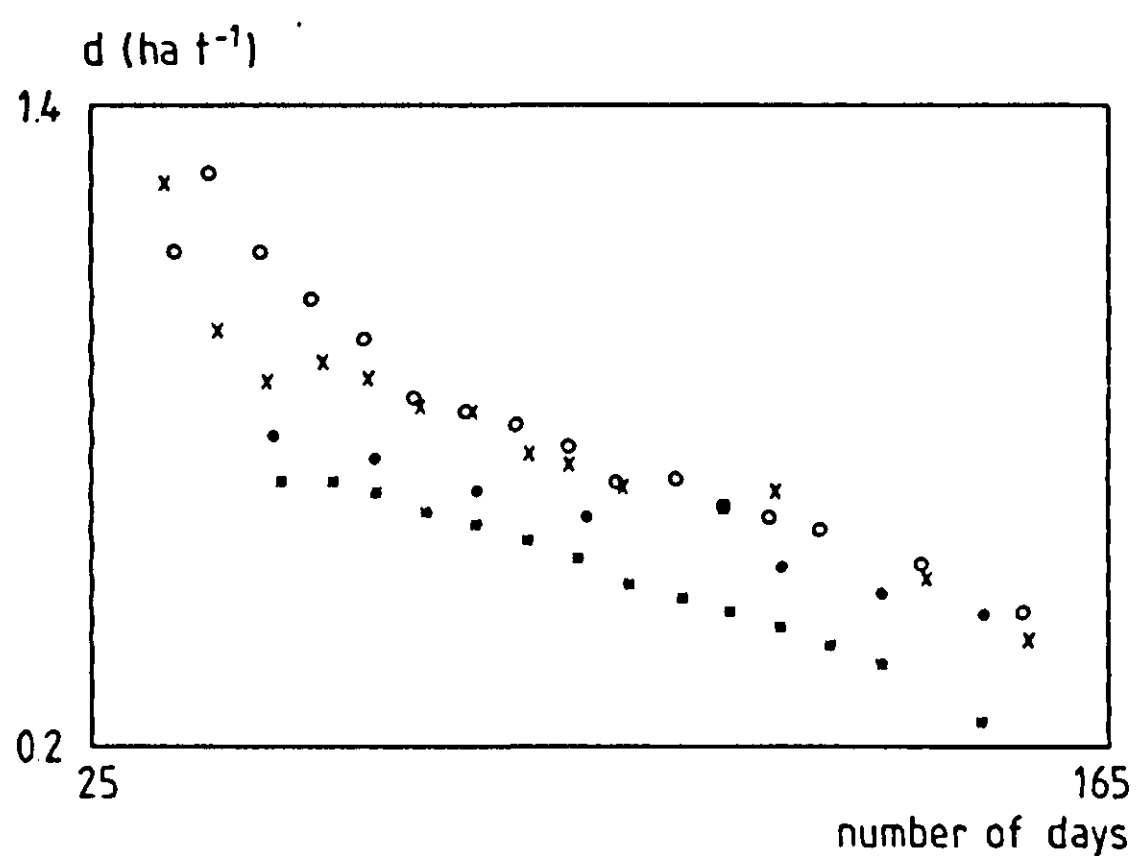


Figure 17a: The ratio between leaf area and shoot biomass, d , plotted against number of days since the start of the growing period (5 May). Dots represent measurements for *Salix viminalis*: x = clone 082 at Studsvik, o = clone 683 first season shoots, \bullet = clone 683 second-season shoots, and $*$ = clone 082 at Köping. (After data from Nilsson & Ericsson, 1986; Eckersten et al., 1983).

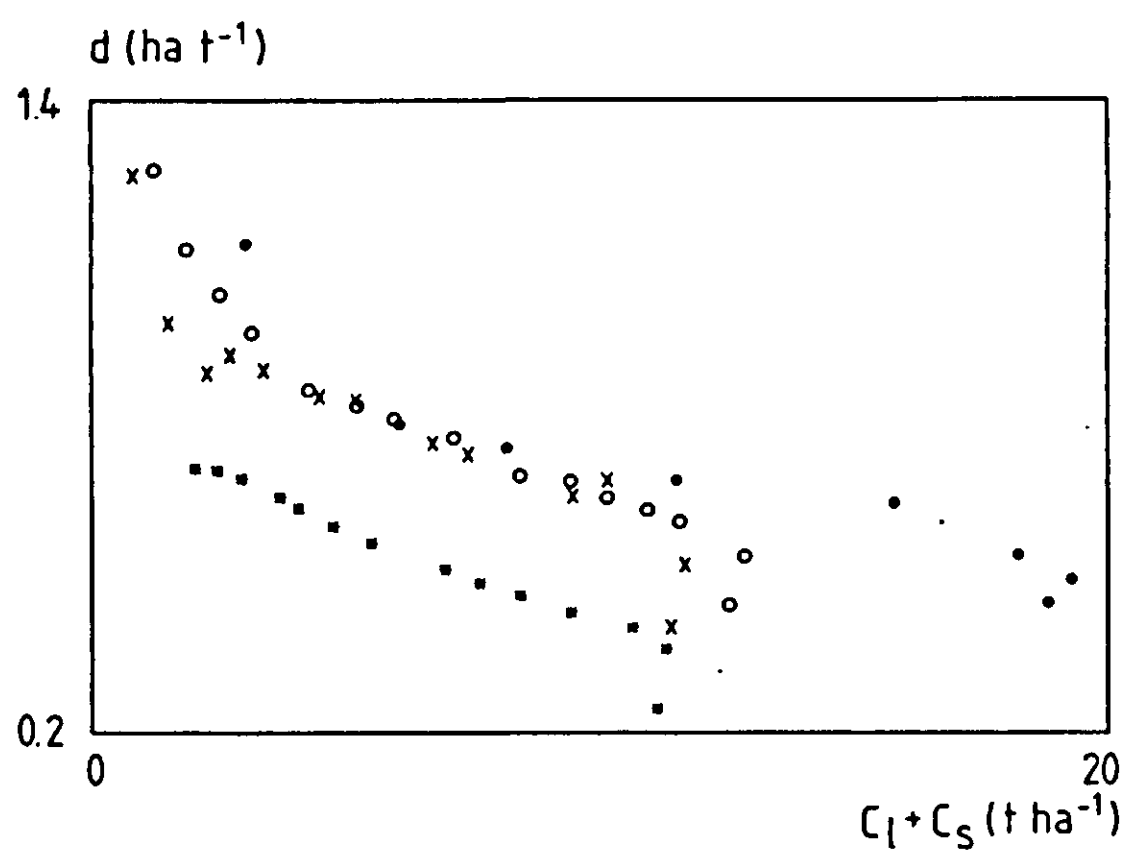


Figure 17b: The ratio between leaf area and shoot biomass, d , plotted against shoot biomass, $C_l + C_s$. Dots represent measurements for *Salix viminalis*: x = clone 082 at Studsvik, o = clone 683 first-season shoots, \bullet = clone 683 second-season shoots, and $*$ = clone 082 at Köping. (After data from Nilsson & Ericsson, 1986 and Eckersten et al., 1983).

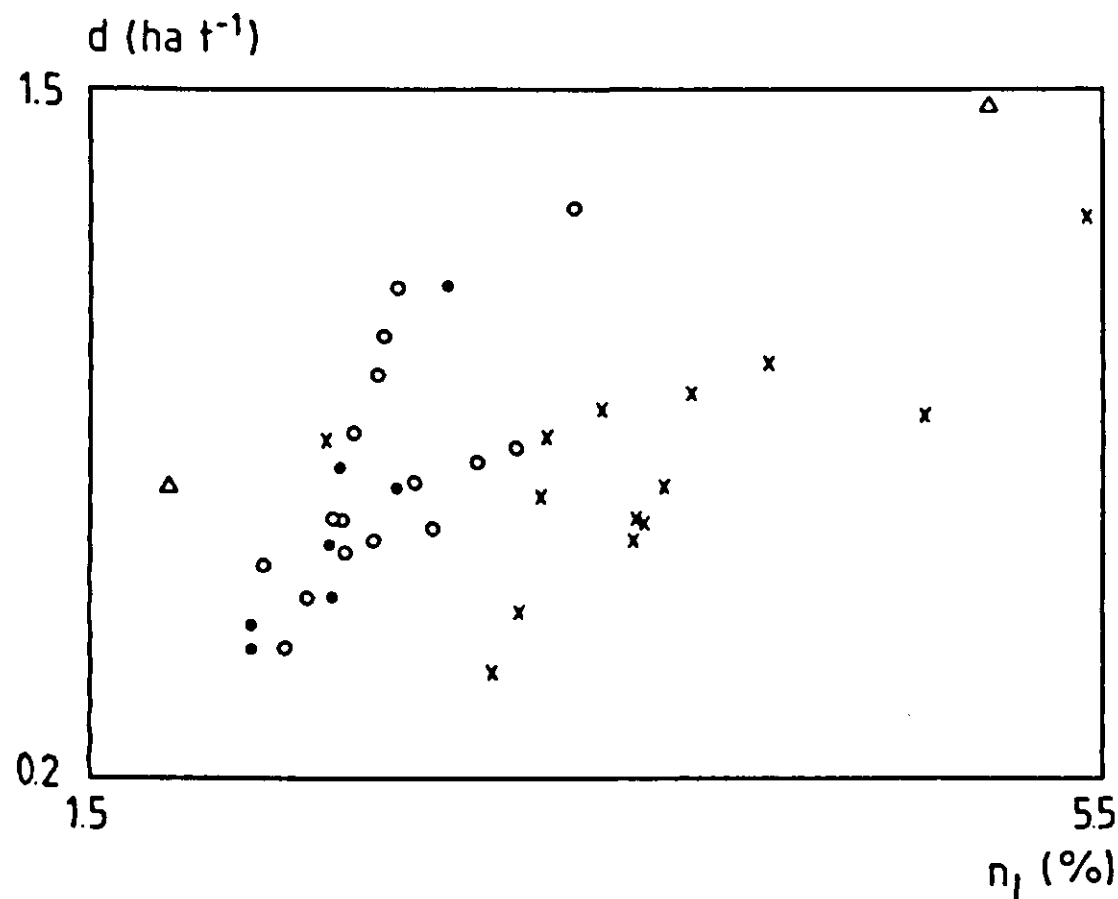


Figure 17c: The ratio between leaf area and shoot biomass, d , plotted against foliar nitrogen concentration, n_l . Dots represent measurements for *Salix viminalis*: x = clone 082 at Studsvik, o = clone 683 first-season shoots, \bullet = clone 683 second-season shoots. Δ = *Salix dasyclados* (Waring et al., 1985). (After data from Nilsson & Ericsson, 1986 and Eckersten et al., 1983).

the leaf area index estimated as a function of shoot biomass. The allometric function d is introduced as (Eckersten et al., 1983)

$$d = L_{ai}/(C_l + C_s) \quad \text{Equation 29}$$

d should depend on n_l (Figure 17c) but it seems to correlate better with the shoot biomass (Figure 17b). The disagreement between first- and second-season shoots for b_{ls} (Figure 15b) seems to have disappeared for d . (The low values of d for high values of shoot biomass in Figure 17b correspond to the shedding of leaves during autumn). However, d shows different relationships to shoot biomass for the different sites (Studsvik and Köping) which in their turn differ from each other, mainly in planting density and soil type. d and b_{ls} show similar relations to time (Figures 15a and 17a).

6.6 Discussion and conclusions

The photosynthesis was assumed to be proportional to the leaf dry weight and the light absorption to be proportional to the leaf area (Equation 27) or both were assumed to be proportional to the leaf area (Equation 28). Both these methods represent a simplified estimate of canopy photosynthesis. In reality, photosynthesis and light absorption are related to both leaf dry weight and leaf area, but there is scope for further research in investigating how they are related in quantitative terms. If photosynthesis is entered as a function of leaf area instead of as a function of leaf dry weight it is necessary to estimate the areal leaf dry weight, b_a , only in order to obtain the stem biomass production

explicitly. It then follows that b_a gives no feedback on the production, as it does when Equation 27 is used, and thus the growth simulation is less sensitive to errors in b_a . Since there is, so far, no general function for b_a (the correlation between b_a and leaf nitrogen status, or shoot biomass, differed between clones (Figures 16a and b)) it is a great advantage for the simulation technique that b_a does not influence the growth dynamics.

The poor correlation between plant nitrogen status and the leaf biomass fraction of the shoot biomass (Figure 15c), as well as the areal leaf weight (Figure 16a) and the fact that the photosynthetic rate per unit of leaf area seems to be fairly independent of the foliar nitrogen concentration (Waring et al., 1985), suggests that photosynthesis should be a function of unit leaf area (Equation 28). The development of L_{ai} is then calculated by differentiation over time of the function d , which describes the ratio between leaf area index and shoot biomass (Equation 29). d seems to be a rather general function of shoot biomass (Figure 17b). The stand at Köping differs from the other three. Disregarding the values of Köping, d is estimated, by regression, from Figure 17b to be

$$d = c_3 - c_4 (\ln(C_l + C_s)) \quad \text{Equation 30}$$

where c_3 and c_4 are coefficients equal to 1.208 and 0.232, respectively (the coefficient of determination is 0.90 and the number of values 30 (the two last occasions in each time series were cancelled because of leaf shedding). This equation should then replace Equation 29 when determining L_{ai} for the calculations of the canopy photosynthesis (Equation 28).

As a consequence of Equations 28 and 30 and the assumption that photosynthesis per unit leaf area is independent of leaf nitrogen status, the canopy photosynthesis (given a certain canopy) and the partitioning of biomass within the shoot are independent of the leaf nitrogen status. The leaf nitrogen status affects growth only through the partitioning of assimilates between roots and shoot. However, further research should be done to ascertain whether the photosynthesis per unit of leaf area is independent of n_l (cf. Goudriaan & van Keulen, 1979; Waring et al. 1985).

6.7 List of symbols

b_a	= areal leaf dry weight, $100 \cdot C_l / L_{ai}$, (g m^{-2})
b_{ls}	= fraction accumulated leaf biomass of the shoot biomass, (dimensionless)
b'_r	= daily fraction of net photosynthesis delivered to roots, (dimensionless)
b'_{ro}	= minimum value of b'_r , (dimensionless)
c_0, c_1	= coefficients for estimating b_{ls} , (dimensionless)
c_2	= coefficient for estimating b_{ls} , (day^{-1})
c_3, c_4	= coefficients for estimating d , (ha t^{-1})

C_l, C_{li}	= accumulated oven-dry biomass of leaf and leaf fall, respectively, (t ha^{-1})
C_s	= accumulated oven-dry stem biomass during current year, (t)
C'	= daily total oven-dry biomass growth per unit ground surface, (t $ha^{-1} day^{-1}$)
d	= specific leaf area of shoot, $L_{ai}/(C_l + C_s)$, ($ha t^{-1}$)
I	= incident light on a horizontal surface, ($\mu E m^{-2} s^{-1}$)
L_{ai}, L_i	= leaf area index for whole canopy and accumulated from canopy top, respectively, ($m^2 m^{-2}$)
n_l	= foliar nitrogen concentration on dry matter basis, (%)
n_{lo}	= optimal foliar nitrogen concentration on dry matter basis, (%)
P, P'	= photosynthesis per unit of ground surface estimated using P_m and P'_m , respectively, ($g m^{-2} h^{-1}$)
p_l	= parameter equal to light that gives photosynthesis equal to half of its maximum value ($\mu E m^{-2} s^{-1}$)
P_m	= maximum photosynthetic rate per unit of leaf dry weight, (h^{-1})
P'_m	= maximum photosynthetic rate per unit of leaf area, ($g m^{-2} h^{-1}$)
t	= day numbered from January, (day)
t_0	= t at start of the growing season, (day)

6.8 References

Bradford, K.J. & Hsiao, T.C., 1982. Physiological responses to moderate water stress. In: O.L. Lange, P.S. Nobel, C.B. Osmond & H. Ziegler (Eds): Encyclopedia of plant physiology, New Series, Volume 12 B, pp. 264-324. Physiological Plant Ecology II. Springer-Verlag, Berlin.

Delaney, R.H. & Dobrenz, K., 1974. Yield of alfalfa as related to carbon exchange. *Agronomy Journal* 66:498-500.

Duncan, W.G. & Hesketh, J.D., 1968. Net photosynthetic rates, relative leaf growth rates and leaf numbers of 22 races of maize grown at eight temperatures. *Crop Science* 8:670-674.

Eckersten, H., 1986. Willow growth as a function of climate, water and nitrogen. Dissertation. Report 25, 38 pp. Swedish University of Agricultural Sciences, Department of Ecology & Environmental Research, Uppsala.

Eckersten, H., Kowalik, P., Nilsson, L.O. & Perttu, K., 1983. Simulation of total willow production. Report 32, 64 pp. Swedish University of Agricultural Sciences, Section of Energy Forestry, Uppsala.

Ericsson, T., 1981a. Effects of varied nitrogen stress on growth and nutrition in three *Salix* clones. *Physiologia Plantarum* 51:423-429.

Ericsson, T., 1981b. Growth and nutrition of three *Salix* clones in low conductivity solutions. *Physiologia Plantarum* 52:239-244.

Goudriaan, J. & van Keulen, H., 1979. The direct and indirect effects of nitrogen shortage on photosynthesis and transpiration in maize and sunflower. *Netherlands Journal of Agricultural Sciences* 27:227-234.

Hanson, W.D., 1971. Selection for differential productivity among juvenile maize plants: associated net photosynthetic rate and leaf area changes. *Crop Science* 11:334-339.

Ingestad, T., 1980. Growth, nutrition and nitrogen fixation in grey alder at varied rate of nitrogen addition. *Physiologia Plantarum* 50:353-364.

Ingestad, T. & Kähr, M., 1985. Nutrition and growth of coniferous seedlings at varied relative nitrogen addition rate. *Physiologia Plantarum* 65:109-116.

Ingestad, T. & Lund, A.-B., 1979. Nitrogen stress in birch seedlings. I. Growth technique and growth. *Physiologia Plantarum* 45:137-148.

Irvine, J.E., 1967. Photosynthesis in sugarcane varieties under field conditions. *Crop Science* 7:297-300.

Jia, H. & Ingestad, T., 1984. Nutrient requirements and stress response of *Populus simonii* and *Paulownia tomentosa*. *Physiologia Plantarum* 62:117-124.

Linder, S., 1985. Potential and actual production in Australian forest stands. In: J.J. Landsberg & W. Parsons (Eds): *Research for forest management*. pp. 11-35. CSIRO, Melbourne.

Monteith, J.L., 1977. Climate and the efficiency of crop production in Britain. *Philosophical Transactions of the Royal Society of London*, B281, 277-294.

Monteith, J.L. & Elston, J., 1983. Performance and productivity of foliage in the field. In: J.E. Dale & F.L. Milthorpe (Eds): *The growth and functioning of leaves*. Cambridge University Press, 499-518.

Muramoto, H.J., Hesketh, J. & El-Sharkawy, M., 1965. Relationships among rate of leaf area development, photosynthetic rate and rate of dry matter production among American cultivated cottons and other species. *Crop Science* 5:163-166.

Nilsson, L.O. & Ericsson, T., 1986. Influence of shoot age on growth and nutrient uptake patterns in a willow plantation. *Canadian Journal of Forest Research*, Volume 16:185-190.

Ray, P.M., 1972. *The living plant*. Saunders College Publishing, Philadelphia, 206 pp.

Raynal, D.J., Grime, J.P. & Boot, R., 1985. A new method for the experimental droughting of plants. *Annals of Botany* 55:893-897.

Waring, R.H., McDonald, A.J.S., Larsson, S., Ericsson, T., Wirén, A., Arwidsson, E., Ericsson, A. & Lohammar, T., 1985. Effects of light and nutrient stress on growth and some chemistries in *Salix dasyclados*. *Oecologia (Berlin)*, 66:157-160.

7 Willow stand growth and seasonal nitrogen turnover

Göran I. Ågren

7.1 Introduction

High yielding energy forest plantations (see Chapter 1) require nutrient supplies at rates that well exceed those normally used in agriculture or forestry. Ingestad & Ågren (1984) calculated that in a *Salix* stand with an annual stem wood production (all biomass data are expressed as oven-dry matter) of 20 000 kg ha⁻¹, an annual nitrogen uptake of 630 kg ha⁻¹ would be required. Most of this nitrogen comes from decomposition of old leaves (260 kg ha⁻¹) and old fine roots (250 kg ha⁻¹) and is thus recycled in the stand, whereas 120 kg ha⁻¹, corresponding to the removal in stem harvest, has to be added as fertilizer.

This chapter investigates the likely build-up of nitrogen stores in the soil and the required time schedule of fertilization in order to maintain optimal growth in a *Salix* stand. The description of the decomposition process follows the theory developed by Bosatta & Ågren (1985). However, in that theory a function linking decomposition rate with climate is left unspecified and, therefore, this chapter includes sensitivity tests of the relationships between climate and decomposition rate.

7.2 Theory

The theory contains two separate parts, one describing plant development with the associated demand for nitrogen and the other describing nitrogen mineralization and, hence, the supply to meet the demand from the plants. The plant growth is exactly the same as described by Ingestad & Ågren (1984), i.e. the plants are divided into leaves, L , stems, S , and roots, R . The leaves are assumed to be growing at optimal nitrogen concentration in the leaves, n_{opt} , throughout the growing season, which is assumed to extend from 1 June (day 1) to 15 September (day 105), after which the leaf biomass declines linearly until 15 October (day 135). The growth rate of the leaves is calculated using the nitrogen productivity concept (Ågren, 1983, 1985). Growth rates of stems and roots are assumed to be proportional to the leaf biomass. Hence

$$\frac{dL}{dt} = (an_{opt} - bL n_{opt})L \quad \text{Equation 31}$$

$$\frac{dS}{dt} = p_S L \quad \text{Equation 32}$$

$$\frac{dR}{dt} = p_R L$$

Equation 33

The growth model used here is an alternative to the one presented by Eckersten et al. in Chapter 5. It has the advantage of being much simpler. Also, since it is constructed for a discussion of the relation between growth and nitrogen turnover, it is logical to use a growth model that is driven by nitrogen uptake in the plants.

The uptake rate of nitrogen, U , is then

$$U = n_{opt} dL/dt + n_S dS/dt + n_R dR/dt \quad \text{Equation 34}$$

where n_R and n_S are the nitrogen concentrations in roots and stems, respectively.

To describe the net nitrogen mineralization of a given cohort of litter, $m(t)$, requires knowledge of both the loss of carbon from the litter and the net change in nitrogen in the litter. Bosatta & Ågren (1985) hypothesize that the rates of decomposition decrease with the age of the litter. However, it is not the age *per se* that controls rates, but the substrate quality, $q(t)$, which is a measure of the accessibility of the litter to micro-organisms, that is used to formulate the decomposition rates. The properties of the microbial community decomposing the substrate are given by the following parameters: f_C , f_N , $e(q)$, and $u(q,t)$ (see list of symbols).

The microbial growth rate depends both on substrate quality and on time. The temporal variation derives from changes in the environment, primarily climatic ones. The two sources of variation are thus independent and the microbial growth rate can be written

$$u(q,t) = u_1(q)u_2(t) \quad \text{Equation 35}$$

The equations describing the amount of carbon, C , amount of nitrogen, N , and the quality of a substrate starting with an initial nitrogen/carbon ratio of r_o and initial quality of q_o are then

$$\int_0^t u_2(t')dt' = \int_{q(t)}^{q_o} dq' / \{\epsilon f_C u_1(q')\} \quad \text{Equation 36}$$

$$C(t) = C_o \exp \left\{ - \int_{q(t)}^{q_o} dq' \frac{1-e(q')}{\epsilon \delta e(q')} \right\} \quad \text{Equation 37}$$

$$N(t) = C(t) \left[\frac{f_N}{f_C} + \left(\frac{r_o}{f_C} - \frac{f_N}{f_C} \right) \exp \left\{ -\frac{q_o - q(t)}{\varepsilon} \right\} \right] \quad \text{Equation 38}$$

where ε is a constant related to the scale chosen for q .

To complete the definition of the problem it is necessary to specify the three functions $e(q)$, $u_1(q)$, and $u_2(t)$. I follow Ågren & Bosatta (1987) in the choice of e and u_1 . Hence

$$e(q) = e_1 q \quad \text{Equation 39}$$

$$u_1(q) = u_o q^\beta \quad \text{Equation 40}$$

These functions ensure that all litter will eventually decompose and with $\beta > 1$ that the specific decomposition rate decreases monotonously. Finally, high production energy forest plantations require water supplies to be sufficient not to restrict growth, and soil moisture should therefore not be an important limitation for microbial activity either. The regulation of microbial activity during the year is, therefore, most likely to derive from soil temperature variations, which I approximate with a cosinefunction (cf. Ågren & Axelsson, 1980)

$$u_2(t) = \{1 + \cos(\omega t + \varphi)\}/2 \quad \text{Equation 41}$$

where the two parameters ω and φ are used to determine the length and start of the period of decomposition relative to the plant's growing season. Winters are assumed to be periods of no activity and in the present representation are contracted to the point where $u_2=0$.

These particular choices of models for the microbial behaviour, Equations 39-41, permit analytical solutions of Equations 36 and 37 giving

$$q(t) = q_o \{1 + \gamma (t + \sin(\omega t + \varphi)/\omega)/2\}^{1/(1-\beta)} \quad \text{Equation 42}$$

$$\gamma = \varepsilon f_C (\beta-1) u_o q_o^{\beta-1} \quad \text{Equation 43}$$

$$C(q) = C_o (q(t)/q_o)^{1/\varepsilon e_1} \exp\{(q_o - q(t))/\varepsilon\} \quad \text{Equation 44}$$

7.3 Results

The parameter values describing growth and nitrogen utilization by the forest are the same as those used previously by Ingestad & Ågren (1984) for *Salix*. Ågren & Bosatta (1987) estimated parameter values for decomposition of Scots pine needle litter which will be used as reference values for both decomposition of leaves and roots, although *Salix* can be expected to differ in these respects. The microbial carbon and nitrogen concentrations will be given the same values as previously used by Bosatta & Staaf (1982) and Bosatta & Ågren (1985) in

similar calculations, namely $f_C=0.5$ and $f_N=0.04$. The parameter values used are summarized in Tables 8 and 9.

The basic problem to be elucidated here is the extent to which supply of and demand for nitrogen are in phase with each other and which factors are most critical in order to keep them in phase. Factors possibly of importance are the parameters describing the interaction between litter and microorganisms (e_1 , β , q_o , and u_o) and the period of mineralization relative to growth. In order to simplify the analysis, a well-established stand (i.e. one in which the annual uptake to leaves and roots is precisely balanced by mineralization of litter of leaves and roots) will be considered. The problem of reaching such a state has already been analysed by Ingestad & Ågren (1984). In the present case this means that the mineralization is assumed to take place in litter formed at the steady state rate over the last 50-100 years (depending on parameter values).

As a reference system, parameter values corresponding to Scots pine needles have been chosen for the decomposition system (because this information is available) and it has been assumed that the mineralization period starts and ends at the same time as the vegetative growth. This system behaves as is illustrated by the dotted curves in Figure 18. At approximately day 110 the nitrogen deficit is maximum (around 190 kg ha^{-1}) and then decreases to 120

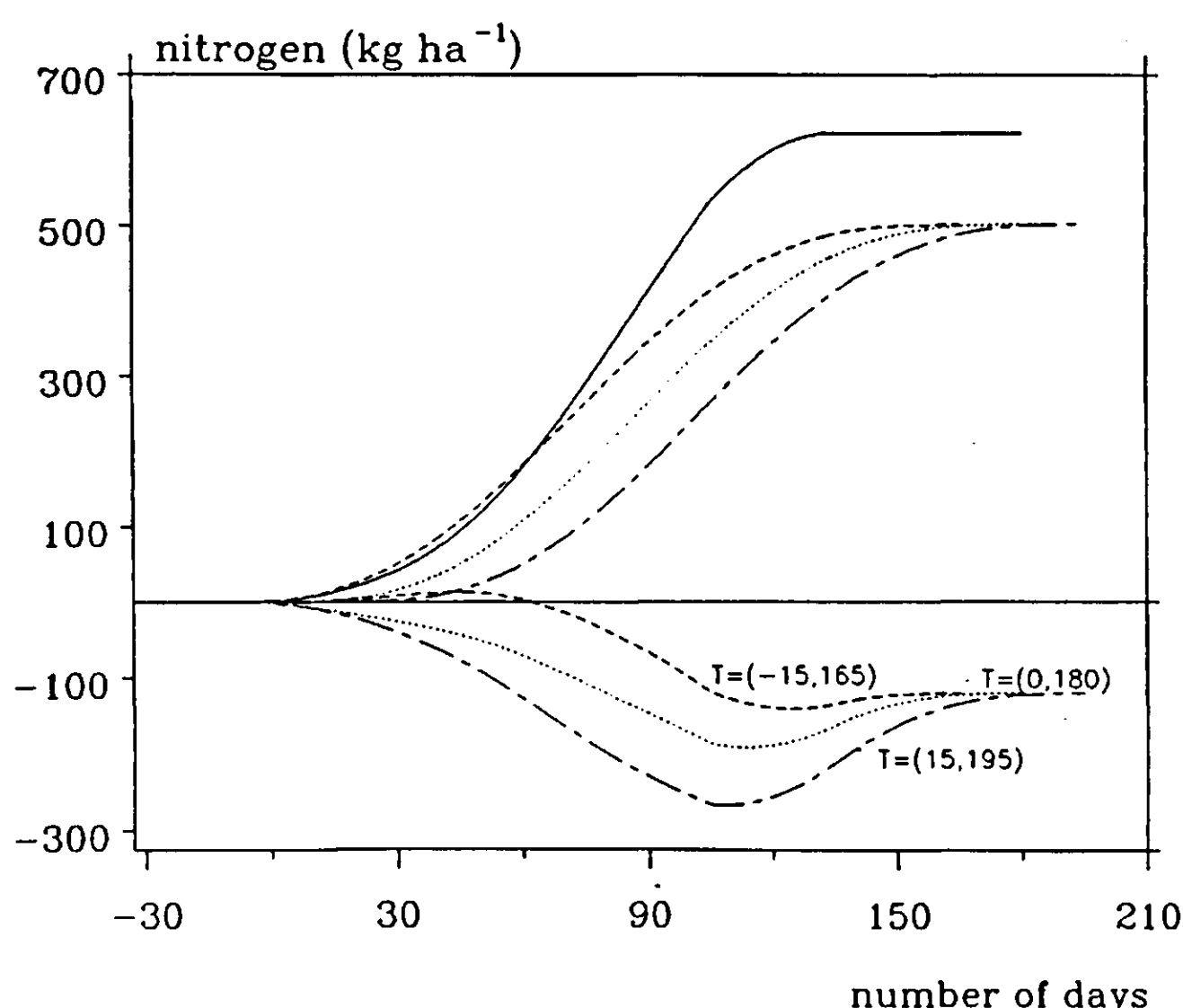


Figure 18. Accumulated uptake of nitrogen by the vegetation (solid line), accumulated nitrogen mineralization (three upper broken lines), and deficit in nitrogen supply (three lower broken lines) during the growing season when the nitrogen mineralization starts and ends at different times. For example, $T = (-15, 165)$ means that nitrogen mineralization starts 15 days ahead of the growth of the vegetation and ends on day 165 relative to the vegetation growth.

kg ha^{-1} corresponding to the fixation in stem wood at the end of the growing season. This latter deficit has to be amended by fertilization. The difference between the maximum deficit and what is accumulated in stem wood (70 kg ha^{-1}) has to be buffered by the soil system or by storage over winter in the vegetation. In other words, an amount equal to this difference has to exist as a storage at the beginning of the growing season and derives from the higher (relative to uptake) mineralization at the end of the previous growing season.

Figure 18 shows the consequences of shifts in the start of the nitrogen mineralization. A shift as small as 15 days already has drastic effects. If the nitrogen mineralization can start ahead of uptake by the vegetation, a small initial excess (less than 10 kg ha^{-1}) is created, followed by a deficit from approximately day 60 of the growing season. This deficit can reach a maximum of 140 kg ha^{-1} , which is essentially what is required to satisfy the fixation in stem wood. On the other hand, if nitrogen mineralization is delayed vis-à-vis growth, the maximum deficit increases rapidly, attaining as much as 270 kg ha^{-1} for a 15-day delay.

Figure 19 illustrates effects of changing the parameters q_o and u_o which set the initial substrate quality and base rate of decomposition, respectively. As can be seen, the temporal pattern of mineralization is changed only marginally. The maximum deficits are not changed (decreased) by more than about 20 kg ha^{-1} .

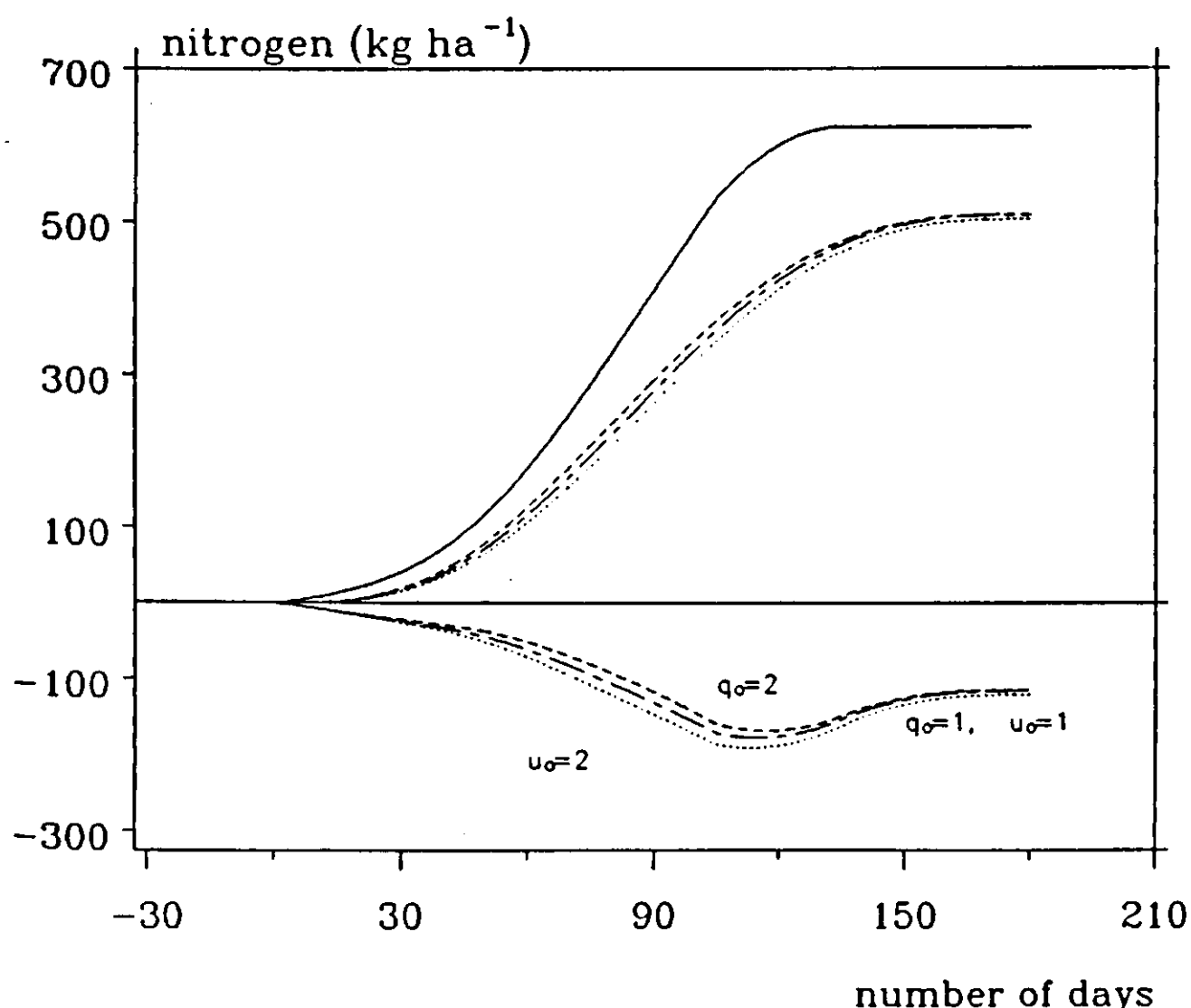


Figure 19. Accumulated uptake of nitrogen by the vegetation (solid line), accumulated nitrogen mineralization (three upper broken lines), and deficit in nitrogen supply (three lower broken lines) during the growing season for different values of q_o and u_o . The values of q_o and u_o in the figure are relative to the reference values; for absolute values refer to Tables 8 and 9.

The other parameters describing the decomposition system, β and ϵe_1 , have even less influence; with the scale used in Figure 19 they cannot be distinguished from the reference level.

7.4 Discussion

A prerequisite for the establishment of large-scale, high production energy forest is the ability to prevent nutrients being lost to surrounding ecosystems. One way of decreasing losses is by maintaining low concentrations of nutrients in the soil by managing the system in such a way that any plant-available nutrient in the soil is rapidly taken up by the plants. The potential dangers in these systems are situations where the natural mineralization continues long after the growing season has ceased, thereby building up large stores of nutrients in the soil that have to be kept over the winter and which might leach with the snow melt.

In this chapter, some of the parameters that affect how much nitrogen needs to be stored during the winter have been analysed. This analysis shows clearly that there is one factor of overriding importance – the timing of growth and mineralization. When the uptake and mineralization start and end simultaneously it is necessary to store some 70 kg ha^{-1} of inorganic nitrogen over winter. This is an amount comparable to what can be held in Swedish agricultural soils and is probably an upper limit to what is acceptable.

The effects of parameters other than those affecting the timing of growth and mineralization are rather small. Given the present objectives of the energy forestry model it is therefore justifiable to use parameters estimated for Scots pine needles rather than for *Salix* leaves and roots, and to treat leaves and roots as identical. The major importance of these parameters can be found in the time required to reach a steady state between uptake to leaves and roots and mineralization of these components as litters. With the parameter combinations in Tables 8 and 9 leading to the slowest decomposition rates, as much as 100 years would be required. However, *Salix* litter should decompose much more rapidly than Scots pine litter. This more detailed analysis suggests that using parameter values for *Salix* would show that the nitrogen cycling should be close to steady state after just over ten years, as estimated by Ingestad & Ågren (1984).

A critical point in this chapter is what sets the variation in decomposition rate over the year. I have assumed that the major source of variation is temperature, and, knowing that soil temperatures vary approximately sinusoidally, that the rate is linearly related to the soil temperature. Andrén & Paustian (1987) analysed decomposition of barley straw and found that a large improvement in the description of the decomposition curves could be obtained by restricting decomposition to periods when the soil was not frozen. Further improvements by including soil temperature and soil water content were possible, but only marginally improved the descriptions. Jansson & Berg (1985) found that mass loss of Scots pine needle litter was best explained by a temperature function

Table 8. Plant parameter values.

Para- meter	Unit	Reference value	Source
a	kg dw (kg N) $^{-1}$ d $^{-1}$	1.34	Ingestad & Ågren (1984)
b	ha (kg N) $^{-1}$ d $^{-1}$	0.00083	Ingestad & Ågren (1984)
n_{opt}	kg N (kg dw) $^{-1}$	0.04	Ingestad & Ågren (1984)
n_R	kg N (kg dw) $^{-1}$	0.04	Ingestad & Ågren (1984)
n_S	kg N (kg dw) $^{-1}$	0.006	Ingestad & Ågren (1984)
P_R	d $^{-1}$	0.016	Ingestad & Ågren (1984)
P_S	d $^{-1}$	0.052	Ingestad & Ågren (1984)

Table 9. Litter parameter values.

Para- meter	Unit	Reference value	Test values	Source
f_C	kg C (kg dw) $^{-1}$	0.5		Bosatta & Staaf (1982)
f_N	kg N (kg dw) $^{-1}$	0.04		Bosatta & Staaf (1982)
β	–	3	2 & 4	Ågren & Bosatta (1987)
$1/\varepsilon e_1$	–	6	3 & 9	Ågren & Bosatta (1987)
q_o/ε	–	1.12	2.24	Ågren & Bosatta (1987)
$u_o q_o^\beta$	d $^{-1}$	0.00052	0.00104	Ågren & Bosatta (1987)

with a Q_{10} of 1.3, although their response curve was very flat. It is possible that the low sensitivity to soil temperature found in these two studies occurs because soil temperature covaries negatively with soil water contents, such that the positive effects of high soil temperatures are counteracted by dry soils and vice versa. In high-yielding energy forest where water supply should be ample, mineralization rates should not be restricted by water availability and it is possible that a higher sensitivity to soil temperature more accurately describes the seasonal variation in mineralization rates. However, this should not qualitatively change the results obtained above. The maximum deficit in nutrient supply will occur earlier and at the same time be reduced, but it will still be the timing of growth and mineralization that is critical for the behaviour of the system.

In conclusion, it is critical that the soil biological system can be activated as early as possible in the growing season, if high-yielding energy forests are to be maintained without unacceptable losses of nutrients to surrounding environments. Management should be directed towards having a net nitrogen miner-

alization starting no later than at the beginning of the growing season and preferably even one or two weeks in advance, in order to avoid the build-up of large stocks of soil nitrogen.

7.5 List of symbols

a	= maximum nitrogen productivity, (kg kg ⁻¹ d ⁻¹)
b	= decrease in nitrogen productivity, (ha kg ⁻¹ d ⁻¹)
$C(t)$	= amount of carbon in a litter cohort, (kg ha ⁻¹)
d	= daynumber, (dimensionless)
$e(q)$	= microbial efficiency, (dimensionless)
e_0, e_1	= parameters in microbial efficiency, (dimensionless)
f_C	= carbon concentration in microbial biomass, (kg kg ⁻¹)
f_N	= nitrogen concentration, N , in microbial biomass, (kg kg ⁻¹)
n_{opt}	= optimum leaf nitrogen concentration, (kg kg ⁻¹)
L	= leaf biomass, (kg ha ⁻¹)
$N(t)$	= nitrogen amount in a litter cohort, (kg ha ⁻¹)
n_R	= optimum root nitrogen concentration, (kg kg ⁻¹)
n_S	= optimum stem nitrogen concentration, (kg kg ⁻¹)
P_R	= root growth per unit leaf biomass, (d ⁻¹)
P_S	= stem growth per unit leaf biomass, (d ⁻¹)
q	= substrate quality, (dimensionless)
q_0	= initial substrate quality, (dimensionless)
r_0	= nitrogen/carbon ratio in fresh litter, (kg kg ⁻¹)
R	= root biomass, (kg ha ⁻¹)
S	= stem biomass, (kg ha ⁻¹)
t	= time, (d)
U	= total nitrogen uptake rate by plants, (kg ha ⁻¹ d ⁻¹)
$u(q,t)$	= microbial growth rate, $u_1(q)u_2(t)$, (d ⁻¹)
u_0	= microbial growth rate on fresh litter, (d ⁻¹)
β	= parameter in quality-time function, (dimensionless)
ε	= scale factor for litter quality, (dimensionless)

7.6 References

Ågren, G.I., 1983. Nitrogen productivity of some conifers. Canadian Journal of Forest Research 13:494-500.

Ågren, G.I., 1985. Theory for growth of plants derived from the nitrogen productivity concept. Physiologia Plantarum 64:17-28.

Ågren, G.I. & Axelsson, B., 1980. Population respiration: A theoretical approach. Ecological Modelling 11:39-54.

Ågren, G.I. & Bosatta, E., 1987. Theoretical analysis of the long term dynamics of carbon and nitrogen in soils. Ecology 68:1181-1189.

Andrén, O. & Paustian, K. 1987. Barley straw decomposition in the field – a comparison of models. *Ecology* 68:1190-1200.

Bosatta, E. & Ågren, G.I., 1985. Theoretical analysis of decomposition of heterogeneous substrates. *Soil Biology and Biochemistry* 17:601-610.

Bosatta, E. & Staaf, H., 1982. The control of nitrogen turn-over in forest litter. *Oikos* 39:143-151.

Ingestad, T. & Ågren, G.I., 1984. Fertilization for long-term maximum production. In: K.L. Perttu (Ed.): *Ecology and management of forest biomass production systems*. Report 15:155-165. Swedish University of Agricultural Sciences, Department of Ecology and Environmental Research, Uppsala.

Jansson, P.-E. & Berg, B., 1985. Temporal variation of litter decomposition in relation to simulated soil climate. Long-term decomposition in a Scots pine forest. V. *Canadian Journal of Botany* 63:1008-1016.

WATER RELATIONS IN WILLOW STANDS

8 Introduction to modelling of plant water conditions

Piotr J. Kowalik and Kurth L. Perttu

8.1 Introduction

Within the soil-plant-atmosphere system the plant is linked to the water flux, which leads from a usually more or less restricted source in the soil to a sink in the ambient air. The physical site factors such as precipitation and water-holding capacity of the soil regulate the water supply, while the shortwave (solar) and longwave radiation provide the energy for the evaporation process, and the atmospheric conditions together with the canopy roughness determine the 'drying power' of the air (Mohren, 1987). In some situations when the net radiation does not meet the whole energy supply necessary for evaporation, water-demanding species like *Salix* make use of the sensible heat, and hence the air cools. If soil moisture is limited, the production of the water-demanding willow stands is primarily influenced. A decrease in the soil moisture content in the root zone results in a lower water potential, and this restricts root water uptake. As transpiration continues, the plant loses water and the bulk leaf water potential drops, with stomatal closure as the final result (Turner, 1974). This causes a reduction of the transpiration to the atmosphere, but at the same time it also limits the influx of carbon dioxide through the stomata of the leaves where the photosynthesis takes place. According to Schulze (1986a) such a shortage of soil moisture affects the shoot extension significantly and also the root to shoot ratio at the whole-plant level, and a water stress causes premature leaf senescence, finally resulting in abscission.

The importance of good plant water conditions must be related to the fact that the flux of water is about two to three orders of magnitude greater than the flux of CO₂ (Fischer & Turner, 1978), most water being lost in the process of transpiration. Only a minor proportion of the total water flux is actually used for growth (Boyer, 1985). To build up a living plant biomass, a water requirement of up to 85 g m⁻² h⁻¹ (equivalent to a precipitation of 0.085 mm h⁻¹) may be needed (Ågren, 1985) to preserve the water balance of the growing plant. Another important function of water for plants is in maintaining the heat balance, mainly by evaporative heat loss of transpired water. In some crop species the amount of water transported per day through a leaf is ten times the leaf weight (Boyer, 1985).

8.2 Material and methods

In Kowalik and Eckersten's transpiration model (Chapter 9), the driving variables consist of recorded 10-minute mean values, diurnal totals and diurnal

single values. However, research has been done to ascertain how to derive driving variables from synoptic data, and the effects of using them on this type of model (Eckersten, 1986). In the two other models (Chapter 10) and (Chapter 11), only synoptic data consisting of diurnal means and diurnal totals are necessary.

In Chapter 9, Kowalik & Eckersten discuss both the transpiration and the heat and water balance of the leaves, including the water stored in the plant. The driving variables are air temperature, relative air humidity, solar radiation, soil water potential and precipitation. The model describes the diurnal course of transpiration, stomatal behaviour, leaf water potential and leaf canopy temperature. The results indicate the importance of the evaporation of intercepted water for heat and mass exchange in the energy forest ecosystems; both amount and duration of rainfall seem to be important factors. Results from a similar soil-plant-atmosphere model developed by Norman & Campbell (1983) indicate that this type of detailed model with a time step of minutes is important for predicting canopy temperature and leaf wetness duration, which are the most important environmental factors for studies of pest development. Norman (1982) and Norman & Campbell (1983) indicate, for example, that a 3 °C increase in leaf temperature sustained for 4 days may result in twice as much damage to corn by an infestation of Banks grass mite. Simulation of leaf temperatures and of duration of wetness of leaves for pest control is only one of several possible applications of Kowalik and Eckersten's model. Other papers on transpiration and xylem water flow in willow trees (Cermak et al., 1984) and in larch and spruce trees (Schulze et al., 1985) also give indications of the need for such detailed models.

Halldin in his evaporation model (Chapter 10) applies the Penman approach to simulate willow evaporation. Two central questions arise: how to deal with time resolution of input data and how to determine the surface resistance of a willow stand. Three different diurnal distribution patterns of input data are checked. The first is a sinusoidal daytime variation, instead of a mean daily value, the second is a pulse with a duration equal to daylength, and the third is a pulse with a duration equal to 75% of daylength. This simple latter approach gives identical results with the more complex sinusoidal one, which is supposed to correspond reasonably well to real behaviour.

Many evaporation models are sensitive to the value of the surface resistance. According to Raschke (1979) and Schulze (1986b), two major control loops have been proposed for stomatal response to plant water status. The first is a feedback response via leaf water status, which leads to a stomatal closure when leaf water potential drops in the bulk leaf tissue (Turner, 1974, 1975). The second is a direct (feedforward) response to the difference in the partial pressure of water vapour between ambient air and substomatal cavities (Raschke, 1970; Lange et al., 1971; Maier-Maercker, 1983). The basic difference between Kowalik & Eckersten's model (Chapter 9) and Halldin's model (Chapter 10) is that the former follows the idea of feedback response (Cowan, 1977; Farquhar,

1978; Kowalik & Turner, 1983; Kowalik & Eckersten, 1984), whereas the latter describes, phenomenologically and using the semi-empirical Lohammar equation (Lohammar et al., 1980), the relation between ambient water vapour pressure (or vapour concentration deficit) and stomatal resistance.

The concept central to Halldin's model is to calculate evaporation, divided into transpiration and evaporation of intercepted water, and to create a simple one-layer soil water budget. The soil water is described in terms of a single compartment and thus the vertical distribution of water uptake in the soil is ignored. The soil water balance is defined as the total available soil water at field capacity minus that at the wilting point. This total is then divided into the fraction of easily available water that does not limit transpiration, and the fraction for which transpiration decreases linearly from its potential value to zero. The model has been validated by considering measured soil water contents or changes in groundwater level. Whenever the model has been applied, there has been a good agreement between measured and simulated soil water content (Grip et al., 1984; Halldin et al., 1984/85; Saugier et al., 1985; Lindroth & Halldin, 1986).

The model by Persson & Jansson (presented in Chapter 11) is a continuation of the development of earlier Swedish attempts to model soil water (Jansson & Halldin, 1979, 1980; Halldin, 1980; Jansson, 1980; Jansson & Thoms-Hjärpe, 1986), and predicts water dynamics for a variety of soils and vegetation covers. The rate of water uptake by roots from different depths depends on plant water requirements (potential demand), availability of water (actual soil water suction), and ability of the roots to take up water (related to the actual root distribution in the soil profile). The actual evapotranspiration for a one-year-old willow stand was found to be between 370 and 420 mm during the simulated period of growth (the 1983 growing season in Uppsala). The model also evaluates the effect of irrigation, and a simulation was run with and without irrigation. The decrease in transpiration without irrigation was 100 mm during the growing season. The level of this decrease was dependent on the assumed soil water suction for reduction of root water uptake (soil water availability).

8.3 Discussion

Good soil moisture conditions are important for high biomass production, because a lack of plant available water results in a decrease in the water potential close to the stomata, which then prohibits them from opening fully, thus reducing the carbon dioxide uptake. The three models discussed above can be used complementarily to determinate the various necessary variables when dealing with plant growth and water balance. Since the models are operational, they can also form the basis of further development in the field of applied science.

For a better evaluation of the influence of the water supply on willow growth, it is necessary to take into account that precipitation may vary considerably

Table 10. List of the main properties of the three models dealing with water relations in willow.

Property	Models presented in second part of book		
	Chapter 9 'Transpiration'	Chapter 10 'Evaporation'	Chapter 11 'Soil water balance'
TIME:			
Resolution	10 minutes	1 day	1 day
Step	1 minute	1 day	1 day
DRIVING VARIABLES: (time series):			
Type of meteo- rological data	biometeoro- logical data	synoptic meteorolo- gical data	synoptic meteorolo- gical data
Solar radiation	10-minute mean	daily totals	daily totals
Air temperature	10-minute mean	daily mean	daily mean
Relative humidity	10-minute mean	daily mean	daily mean
Wind speed	-	daily mean	daily mean
Rainfall	daily total	daily total	daily total
Irrigation	-	-	daily total
Surface resistance	-	-	function of daynumber
Soil water potential	daily values	-	-
CANOPY AND SOIL WATER CONCEPT:			
Geometry of:			
canopy	one compart- ment, constant in time	one compart- ment, function of day number	one compart- ment
soil profile	one compart- ment, constant in time	one compart- ment	12 compartments
Soil water	-	simulated, based on field capaci- ty, easily av- ailable water, wilting point	simulated, based on soil water retention cur- ves, unsatura- ted hydraulic conduc- tivity, wilting point, root distribution, etc.

Table 10. Continued

INTERCEPTION CONCEPT:			
Canopy storage	interception as 25% of rainfall, maximum of 4 mm water in the stand	capacity of 0.2 mm water per m ² leaf area;	capacity of 0.15 mm water, maximum of 1 mm water in the stand
Canopy drainage	takes place once per 24 hours	takes place 4 times per 24 hours	takes place once per 24 hours
TYPICAL OUTPUT VARIABLES:			
Transpiration	simulated	simulated	simulated
Evaporation of intercepted water	simulated	simulated	simulated
Root water uptake	simulated	= transpiration	= transpiration
Plant water content	simulated	-	-
Stomatal resistance	simulated	simulated	-
Surface resistance	simulated	simulated	-
Leaf water potential	simulated	-	-
Leaf temperature	simulated	implicitly	implicitly
Soil water redistribution	-	-	simulated
Soil water content	-	simulated	simulated
Soil water potential	-	implicitly	simulated
Soil water drainage	-	simulated	simulated
VALIDATION:			
	i) water balance of <i>Salix</i> in three lysimeters (weekly means) at Studsvik 1979 ii) leaf-air temperature differences for <i>Salix</i> (10-minute means) at Studsvik 1982 iii) leaf water potential in soybean (hourly) in Australia 1983	soil water storage for several forests, several seasons in Sweden and France	i) soil water potential at 4 depth in willow stand in Uppsala ii) soil water potential for several forests and agricultural crops in northern Europe

from year to year, and between different locations (Halldin et al., 1984/85). This means that the effect of water shortage can be expected to be an important cause of differences in increment rates between consecutive years, and between various sites. There is, therefore, a great need to apply these models to different time periods and sites, and to perform an analysis to determine alternatives for minimizing risks related to water deficits. Further physiological and micrometeorological studies are, therefore, needed, to arrive at a more general statement of the effects of irrigation on production. The main properties of the three models presented in this part of the book are indicated in Table 10 so that the reader can select the model most applicable to his/her problems.

8.4 References

Ågren, G.I., 1985. Limits to plant production. *Journal of Theoretical Biology* 113:89-92.

Boyer, J.S., 1985. Water transport. *Annual Review of Plant Physiology* 36:473-516.

Cermak, J., Jenik, J., Kucera, J. & Zidek, V., 1984. Xylem water flow in a crack willow tree (*Salix fragilis* L.) in relation to diurnal changes of environment. *Oecologia* 64:145-151.

Cowan, J.R., 1977. Stomatal behaviour and environment. *Advancement of Botany Research* 4:117-228.

Eckersten, H. 1986. Simulated willow growth and transpiration: the effect of high and low resolution weather data. *Agricultural and Forest Meteorology* 38:289-306.

Farquhar, G.D., 1978. Feedforward responses of stomata to humidity. *Australian Journal of Plant Physiology* 5:787-800.

Feddes, R.A., Kowalik, P.J. & Zaradny, H., 1978. Simulation of field water use and crop yield. *Simulation Monograph*. Pudoc, Wageningen, 188 pp.

Fischer, R.A. & Turner, N.C., 1978. Plant productivity in arid and semiarid zones. *Annual Review of Plant Physiology* 29:277-317.

Grip, H., Halldin, S., Lindroth, A. & Persson, G., 1984. Evapotranspiration from a willow stand on wetland. In: K.L. Perttu (Ed.): *Ecology and management of forest biomass production systems*. Report 15:47-61. Swedish University of Agricultural Sciences, Department of Ecology and Environmental Research, Uppsala.

Halldin, S., 1980. SOIL - water and heat model. I. Synthesis of physical processes. *Dissertation. Acta Universitatis Upsaliensis*, 567, 28 pp.

Halldin, S., Saugier, B. & Pontailler, J.Y., 1984/85. Evapotranspiration of a deciduous forest: Simulation using routine meteorological data. *Journal of Hydrology* 75:323-341.

Jansson, P.-E., 1980. SOIL - water and heat model. II. Field studies and applications. *Dissertation. Acta Universitatis Upsaliensis*, 568, 26 pp.

Jansson, P.-E. & Halldin, S., 1979. Model for annual water and energy flow in layered soil. In: S. Halldin (Ed.): *Comparison of forest water and energy exchange models*. Elsevier Scientific Publishing Company, pp. 145-163. Amsterdam - Oxford - New York.

Jansson, P.-E. & Halldin, S., 1980. Soil water and heat model. Technical description. Technical Report 26, 81 pp. Swedish University of Agricultural Sciences, Swedish Coniferous Forest Project, Uppsala.

Jansson, P.-E. & Thoms-Hjärpe, C., 1986. Simulated and measured soil water dynamics of unfertilized and fertilized barley. *Acta Agriculturae Scandinavica* 36:162-172.

Kowalik, P.J. & Eckersten, H., 1984. Water transfer from soil through plants to the atmosphere in willow energy forest. *Ecological Modelling*, 26:251-284.

Kowalik, P.J. & Turner, N.C., 1983. Diurnal changes in the water relations and transpiration of a soybean crop simulated during the development of water deficits. *Irrigation Science* 4:225-238.

Lange, O.L., Lösch, R., Schulze, E.-D. & Kappen, L., 1971. Response of stomata to changes in humidity. *Planta* 100:76-86.

Lindroth, A. & Halldin, S., 1986. Numerical analysis of pine forest evaporation and surface resistance. *Agricultural and Forest Meteorology* 38:59-79.

Lohammar, T., Larsson, S., Linder, S. & Falk, S.O., 1980. FAST – simulation models of gasous exchange in Scots pine. In: T. Persson (Ed.): *Structure and function of northern coniferous forest – an ecosystem study*. Ecological Bulletin (Stockholm), 32:505-523.

Maier-Maercker, U., 1983. The role of peristomal transpiration in the mechanism of stomatal movement. *Plant Cell Environment* 6:369-380.

Mohren, G.M.J., 1987. Simulation of forest growth, applied to Douglas fir stands in The Netherlands. Thesis. Pudoc, Wageningen, 184 pp.

Norman, J.M., 1982. Simulation of microclimates. In: J.L. Hatfield & I.J. Thomasson (Eds.): *Biometeorology in integrated pest management*. Academic Press, pp. 65-99, New York.

Norman, J.M. & Campbell, G., 1983. Application of a plant – environment model to problems in irrigation. In: D. Hillel (Ed.): *Advances in irrigation*. Academic Press, Volume 2, pp. 155-188, New York.

Raschke, K., 1970. Stomatal response to pressure changes and interruptions in the water supply of detached leaves of *Zea mays*. *Plant Physiology* 45:415-423.

Raschke, K., 1979. Movement of stomata. In: W. Haupt & M.E. Feinleib (Eds): *Physiology of Movements. Encyclopedia of Plant Physiology (NS)*. Springer Verlag, pp. 383-441, Berlin.

Saugier, B., Halldin, S., Pontailler, J.Y. & Nizinski, G., 1985. Bilan hydrique de forêts de chêne et de hêtre à Fontainebleau. *Revue du Palais de la Decouverte* 13:187-200.

Schulze, E.-D., 1986a. Whole-plant responses to drought. *Australian Journal of Plant Physiology* 13:127-141.

Schulze, E.-D., 1986b. Carbon dioxide and water vapour exchange in response to drought in the atmosphere and in the soil. *Annual Review of Plant Physiology* 37:247-274.

Schulze, E.-D., Cermak, J., Matyssek, R., Penka, M., Zimmermann, R., Vasicek, F., Gries, W. & Kucera, J., 1985. Canopy transpiration and water fluxes in the xylem of the trunk of *Larix* and *Picea* trees – a comparison of xylem flow, porometer and cuvette measurements. *Oecologia (Berlin)* 66:475-483.

Turner, N.C., 1974. Stomatal response to light and water under field conditions. In: R.L. Bieleski, A.R. Ferguson & M.M. Cresswell (Eds): Mechanism of regulation of plant growth. Royal Society of New Zealand, Wellington. Bulletin 12, pp. 423-432.

Turner, N.C., 1975. Concurrent comparisons of stomatal behavior, water status, and evaporation of maize in soil at high and low water potential. Plant Physiology 55:932-936.

9 Simulation of diurnal transpiration from willow stands

Piotr Kowalik and Henrik Eckersten

9.1 Introduction

In order to control irrigation and estimate field water use and the hydrological consequences of energy forestry, the transpiration of *Salix* stands must be known. Some of these factors for willow plantations have previously been studied by Grip (1981), Larsson (1981), Grip et al. (1984), Lindroth & Grip (1984), Kowalik & Eckersten (1984), Eckersten & Kowalik (1986) and Eckersten et al. (1986). In this chapter, a model of the soil-plant-atmosphere system is applied in order to simulate transpiration, evaporation of intercepted water and leaf temperature with the time step of one minute. Recent experimental data have been collected with this time resolution; such carefully designed trials can be used to test the model.

The model was originally presented by Kowalik & Turner (1983). Later Kowalik & Eckersten (1984) presented it in more detail and applied it to a willow stand. In order to simulate leaf temperature, rate of transpiration and evaporation of intercepted water, input data on the following variables and parameters are required: relative humidity, h_a , air temperature, t_a , global solar radiation, R_s , soil water potential, ψ_s , specific time, τ , the plant resistance, r_p , and aerodynamic resistance, r_a . The model simulates – even under optimum soil moisture conditions – the diurnal variation in plant water status, which is reflected by an amplitude of daily fluctuations of leaf water potential, ψ_l (Smart & Barrs, 1973; Reed & Waring, 1974; Hansen, 1975; Thompson & Hinckley, 1977; Jarvis et al., 1981).

9.2 Material and methods

9.2.1 Measurements

Data suitable to test the transpiration model were collected during two years at Studsvik, Sweden (Lat. 58.8 °N, Long. 17.4 °E, Elev. 5 m). In 1979, evapotranspiration in three lysimeters in plots of *Salix viminalis* was measured by Grip (1981). Climatic input data to the model were available for the periods: 28-29 June, 4, 7-13, 17, 21-31 July, 1-17, 29-31 August, 1-3, 6-10 September, 1979. Consequently, the comparisons were made only for these periods.

In 1982, leaf-air temperature differences were measured in a *S. viminalis* stand from 20 July to 28 September (Eckersten, 1984a). The leaf temperature was measured with thermocouples (copper/constantan). The sensor was made of a slightly elastic spring wire whose tip was applied to the lower side of the

leaf. The diameter of this tip was about 1 mm. Because of the size of the sensor and since it was mounted on the lower side of the leaf, thus sheltered from direct solar radiation, it is reasonable to assume that the measurement error caused by radiation is negligible. Eleven such sensors were distributed in the stand at levels between 150 and 250 cm above the ground and within an area of about 6 m². Air temperatures were measured at corresponding levels in the canopy.

The meteorological input variables were measured every minute (except for precipitation and soil water potential) at the reference site on an open area 100 m from the experimental field (Eckersten & Perttu, 1981; Eckersten, 1984a). The soil water potential, ψ_s , was assumed to be constant (-0.005 MPa) during the whole period, since there was a shallow groundwater level in the lysimeters, as a result of a regular irrigation.

9.2.2 *Transpiration model*

Several principal conditions determine the shape of the mathematical model of plant transpiration. The heat used for evaporation of plant water must be equal to the heat supplied. The heat balance equation of the leaf is

$$R_n = H + \lambda \cdot E + S_h \quad \text{Equation 45}$$

but the heat storage in the leaf, stem and soil, S_h , is here assumed to be zero, since during daylight S_h is usually small compared with the sum of the latent, $\lambda \cdot E$, and the sensible, H , heat flows. During early morning or late afternoon, however, S_h can be of the same order of magnitude as the net radiation, R_n (Monteith, 1981).

Ignoring any effects of, for instance, the leaf temperature, t_s , on net radiation, R_n is calculated from measurements of global radiation, R_s , using a simplified formula given by Federer (1968) and Feddes (1971)

$$R_n = 0.649 \cdot R_s - 23 \quad \text{Equation 46}$$

This equation, which largely depends on the albedo of the vegetation, was obtained from measurements on vegetables, and is a good approximation for the conditions of a willow stand (cf. Eckersten, 1986).

Assuming steady state conditions, the rate at which water vapour is removed from the evaporating surface is equal to the rate at which it is swept away by the atmosphere. Then, if the heat used to evaporate water is $\lambda \cdot E$, the evaporation from the leaf surface is (Jarvis, 1975)

$$E = \rho \cdot c_p \cdot (e_s(t_s) - e_a) / (\lambda \cdot \gamma \cdot (r_s + r_a)) \quad \text{Equation 47}$$

where ρ is the specific density of moist air, c_p the heat per unit mass of air, γ the psychrometric constant, $e_s(t_s)$ the saturated vapour pressure in the stomatal cavities, e_a the vapour pressure in the air, r_s the stomatal resistance and r_a the aerodynamic resistance. The rate at which a surface loses (or gains) sensible heat, H , can be written as

$$H = \rho \cdot c_p \cdot (t_s - t_a) / r_a \quad \text{Equation 48}$$

where t_a is the air temperature. The saturated vapour pressure, e_s , is estimated according to Feddes et al. (1978)

$$e_s = a_1 \cdot \exp((a_2 \cdot T_s - a_3) / (a_4 \cdot T_s - a_5)) \quad \text{Equation 49}$$

where $a_1 = 1.3332$, $a_2 = 1.0887$, $a_3 = 276.4884$, $a_4 = 0.0583$, $a_5 = 2.1939$, and T_s is equal to t_s expressed in kelvins. From the same expression the saturated vapour pressure of the air, e_d , is calculated using t_a instead of t_s which then gives e_d instead of e_s .

The actual vapour pressure of the ambient air, e_a , is calculated from the relative humidity of the air, h_a

$$e_a = h_a \cdot e_d(t_a) / 100 \quad \text{Equation 50}$$

Another important assumption is that there is not only a continuous supply of energy and an outward flow of vapour, but also an inward flow of water from soil to plant. The equation of van den Honert (1948) is applied, thus giving the uptake rate of water by the plant equal to

$$U = (\psi_s - \psi_l) / (r_r + r_p) \quad \text{Equation 51}$$

where ψ_s and ψ_l are the water potentials in soil and the leaves, respectively, and r_r and r_p are the resistances to flow of water in the soil and in the plant, respectively. The relation between the easily available water in the plant, V , and, ψ_l , is (Federer, 1979)

$$\psi_l = \psi_{lm} (1 - V/V_o) \quad \text{Equation 52}$$

where ψ_{lm} and V_o are parameters defining the lowest value of ψ_l and the highest value of V , respectively.

The plant water balance can then be expressed as (Kowalik and Turner, 1983)

$$V_{i+1} = V_i + \int_0^{\Delta\tau} (U - E) d\tau \quad \text{Equation 53}$$

where V_i is the initial plant water content and V_{i+1} is the plant water content after time step $\Delta\tau$. The given equations can be solved, but still the values of the resistances (r_a , r_s , r_p and r_r) are not defined.

The effect of variations in r_a on transpiration, E , is assumed to be small, which might be a good approximation for a dry canopy (Eckersten & Kowalik, 1986). Hence, r_a was taken as a constant value equal to 10 sm^{-1} .

H. von Fircks and E. Mattsson-Djos (personal communications, 1984) measured values of ψ_l and E for single leaves of a plant of *Salix viminalis* at different heights above soil surface. The root system was well supplied with water. The

plant resistance was calculated from the approximated formula (cf. Equation 51): $r_p = -\psi_l / E$. r_p is in the range of magnitude of $16 \text{ MPa s m}^2 \text{ g}^{-1}$ (Kowalik & Eckersten, 1984). Sensitivity analysis showed that when the canopy is water stressed the model is very sensitive to even small changes in values of r_p when the soil is moist whereas when the soil is dry the soil resistance becomes increasingly dominant.

According to Turner (1974) and Hansen (1975), leaf stomatal resistance, r_s , is a function of ψ_l and R_s . Two empirical relations, $r_s(R_s)$ and $r_s(\psi_l)$, have been established by fitting polynomials to the following data:

- for $r_s(R_s)$ according to Feddes et al. (1978):

$R_s (\text{W m}^{-2})$	≤ 25	100	150	200	250	≥ 275
$r_s (\text{s m}^{-1})$	1000	237	141	69	10	0

- and for $r_s(\psi_l)$ according to Kowalik & Eckersten (1984):

$\psi_l (\text{MPa})$	≤ -2.7	-2.5	-2.0	21.5	-1.3	0
$r_s (\text{s m}^{-1})$	1000	750	300	100	40	40

The actual stomatal resistance is assumed to be the larger of the values determined by leaf water potential and solar radiation. In the model the canopy is treated as if it were one 'big leaf' with the leaf area index equal to unity, making no explicit reference to the canopy structure. This large leaf achieves the radiation corresponding to that at the canopy top. Hence, the canopy stomatal resistance is taken to be equal to the leaf stomatal resistance presented above. This assumption restricts the validity of the model to stands with constant canopy structure.

The resistance at the interface between soil and root hair, r_r , is the sum of the series-linked resistances to flow of liquid water in the soil and from the soil into the hair's surface

$$r_r = b / K(\psi_s) \quad \text{Equation 54}$$

$$K(\psi_s) = a \cdot (1000 / |\psi_s|)^{-n} \quad \text{Equation 55}$$

where b and a are parameters and K is the soil hydraulic conductivity. Equations 54 and 55 mean that the root system is treated as a single unit with respect to water flow, characterized by the soil-root interface resistance $r_r(\psi_s)$.

Equation 55 was developed by Lang & Gardner (1970) for a number of fine textured soils (n between 2 and 3) and for sands (n about 5). The term a is a coefficient similar to the hydraulic conductivity of saturated soil. More examples of the application of Equation 55 have been given by Hansen (1975) and by Jansson & Halldin (1979). In Equation 54, where r_r is related to the unsaturated hydraulic conductivity $K(\psi_s)$ and to parameter b , b is the root density resistance factor which takes into account the length and geometry of the root system (Feddes, 1981)

$$b = \frac{\ln(r_2/r_1)}{2\pi \cdot L \cdot z_r} \quad \text{Equation 56}$$

where z_r is the rooting depth in the soil profile (m), L is the length of roots in the unit volume of soil (m m^{-3}), r_2 is the mean distance between roots in the soil body (m), and r_1 is the root radius (m). According to Gardner & Ehlig (1963) and Feddes & Rijtema (1972) $4 \cdot 10^{-5}$ MPa seems to be a realistic value for parameter b . According to Kowalik & Turner (1983), parameter a is $1.62 \text{ g m}^{-2} \text{ s}^{-1}$ and n is 2.1 for clay soil.

Introducing an initial value of easily exchangeable amount of water stored in the plant, V_i , enables the initial values of ψ_l (Equation 52) and $r_s(\psi_l)$ to be calculated. The corresponding value of absolute leaf temperature, T_s , was then calculated by an iterative method from the leaf heat balance

$$\min_{T_s} (|R_n - H - \lambda \cdot E|) \quad \text{Equation 57}$$

with the accuracy of 0.05 W m^{-2} (Kowalik & Eckersten, 1984). Then, the root water uptake from soil, U , was calculated using Equations 55, 54 and 51 from which a new value of exchangeable water in the plant, V_{i+1} , was achieved by several iterations. Equation 53 is solved by the Euler method of integration (forward differences) (Benyon, 1968; Goudriaan, 1982), where

$$V_{i+1} = V_i + 60 \cdot (U - E) \quad \text{Equation 58}$$

if the time step is 60 seconds. The plant water at the end of the time step is used to control U and E , and is calculated according to the procedure described by Kowalik & Eckersten (1984). The calculations are repeated, to obtain a final value of V for given time $\tau + \Delta\tau$ until the difference between two consecutive values of leaf water potentials is less than 40 kPa (taken arbitrarily). The final values of V and T_s determine the output values of r_s , ψ_l , E and U .

Evaporation of intercepted water from the wet canopy was calculated by assuming the stomatal resistance to be zero in Equation 47. Intercepted water was then taken as 25% of precipitation and irrigation but with an upper limit equal to 4 mm per day in accordance with measurements made on *Salix* by Larsson (1981). Sums of precipitation during 24-hour periods measured at 10.00 h every morning were used. Because the daily distribution of rainfall was not recorded, it was assumed that the whole amount fell within one minute at the beginning of the period concerned. Transpiration did not resume until all intercepted water had evaporated. Evaporation from the soil surface was assumed to be negligible, because only about 10% of the global radiation reached the soil surface below the closed canopy (Eckersten, 1984b).

9.3 Results

The lysimeter experiment in 1979 (Grip, 1981) gave data on accumulated evapotranspiration over ten-day periods, which were transformed into mean daily values for the period concerned. The results from simulation and from measurements for 50 days are shown in Figure 20: it can be seen that simulated values for several days approach the measured average data. Figure 20 also shows the evaporation of intercepted water.

Figure 21 gives cumulative values of measured and simulated evapotranspiration for the 50 days in 1979 at Studsvik. Simulated values are divided into evaporation of intercepted water (lower graph) and evaporation of intercepted water plus transpiration (upper graph). The cumulative values of measured evapotranspiration amounted to 126.9 mm. Simulated transpiration + evaporation from interception was 120.9 mm, of which transpiration was 96.6 mm. The difference of 6 mm during 50 days ($= 0.12 \text{ mm day}^{-1}$) can be related to the unknown distribution of the diurnal rain (only one rainfall event per day was allowed). It could also be explained by changes in leaf area index or plant height during the growing season or by the omission of the soil evaporation from the forest floor.

The models performance is exemplified by the simulation for a clear sunny day (7 August) and a cloudy and rainy day (11 August) 1979. During the clear

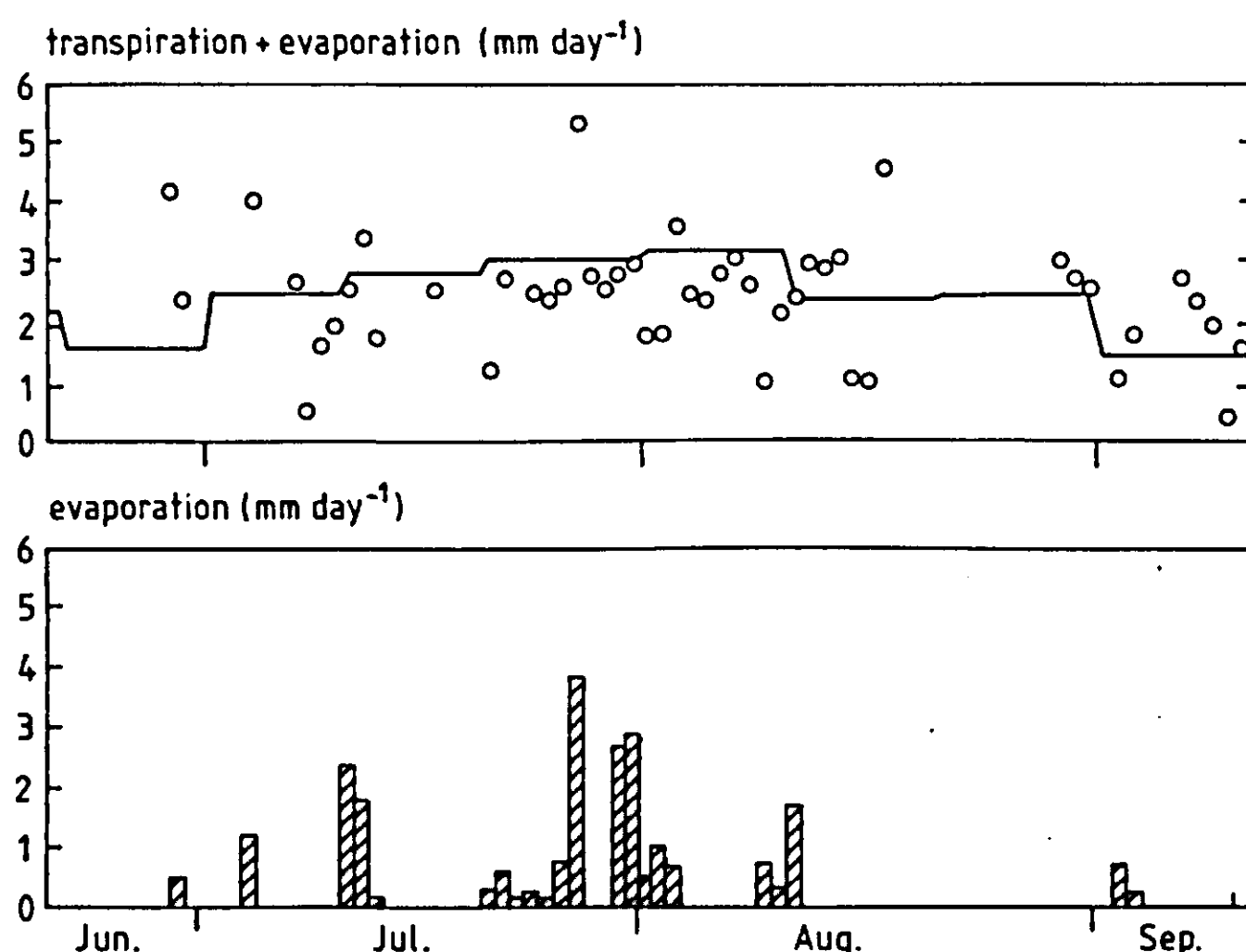


Figure 20. Daily totals of transpiration plus evaporation of intercepted water, simulated for Studsvik conditions (o) and lysimeter measurements (—) of evapotranspiration by Grip (1981) (upper graph), and simulated evaporation from intercepted water (lower graph). (After Kowalik & Eckersten, 1984).

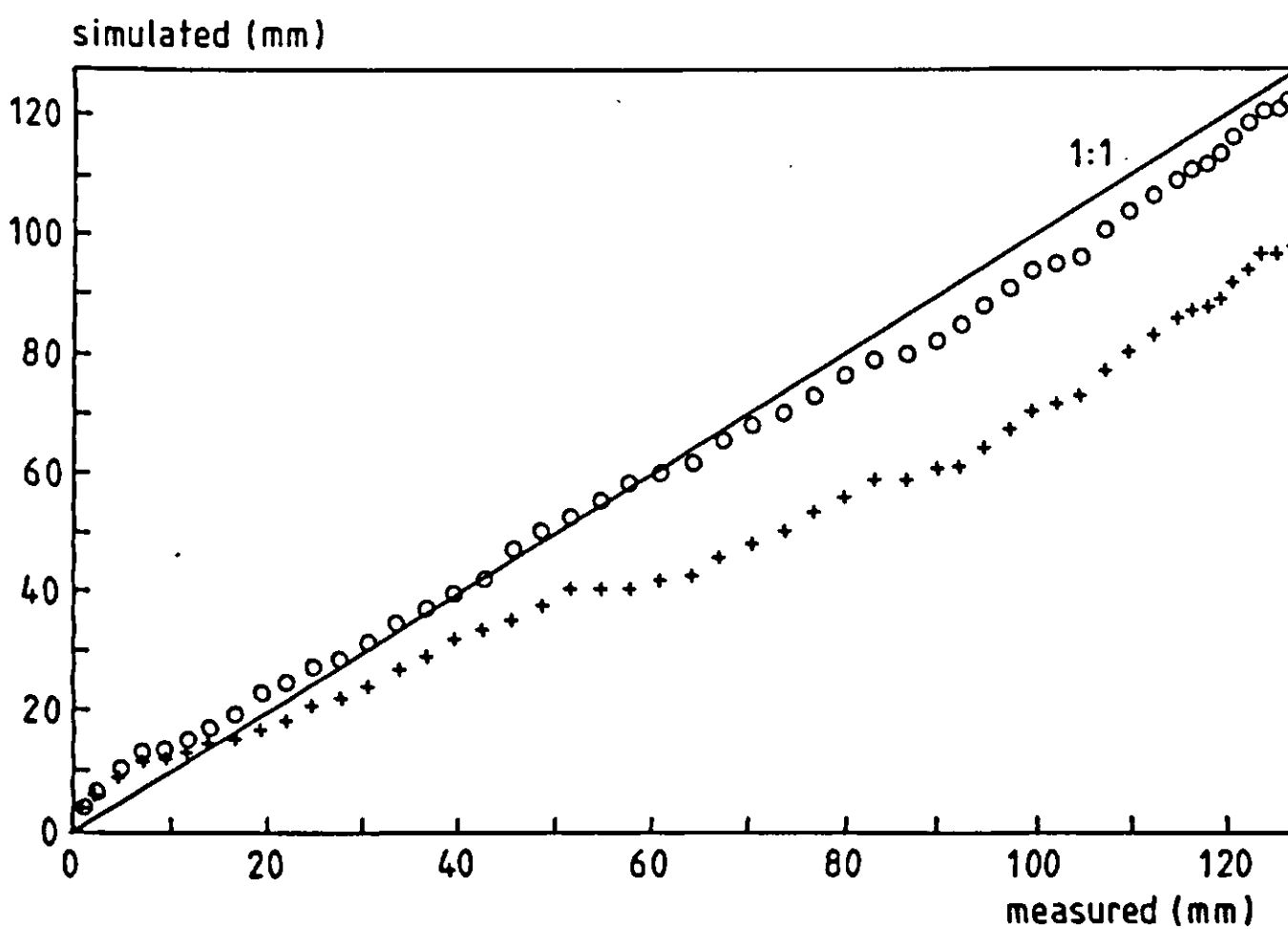


Figure 21. Relation between measured and simulated cumulative values of evapotranspiration for 50 days in summer 1979 at Studsvik. Simulated values are divided into transpiration (+) and evaporation of intercepted water plus transpiration (o). (After Kowalik & Eckersten, 1984).

day, the solar radiation, R_s , was about four times higher than on the cloudy day. The air temperature, t_a , was similar during daytime hours but the relative humidity, h_a , was much lower on 7 August, when also transpiration was high in the morning and remained high throughout the day (Figure 22). On 11 August, transpiration was low but there was much evaporation from intercepted water after 10.00 h in the morning (Figure 23). For the sunny day there was a large drop in the values of ψ_l , compared with the cloudy day. Figures 22 and 23 also show the diurnal variation of the stomatal resistance, r_s , and the influence of low radiation levels at sunrise and sunset on the opening of stomata. The stomata were open on both days, but only on the cloudy day was there an apparent variation caused by the radiation during midday. In Figure 23, values of r_s are equal to zero for the short period that intercepted water occurred on the surface of leaves. The scale of r_s makes the daytime values appear nearly constant, but there is a variation that causes the marked depression of E during midday. The leaf-air temperature differences, Δt , were less than 2 °C but varied considerably. A large cooling effect occurred during the period of evaporation of intercepted water (Figure 23). Changes in Δt are related to the simulated Bowen ratio, which is sensitive to changes in climatic driving variables.

The cumulative simulated transpiration and evaporation of intercepted water are also shown in Figures 22 and 23. The weather on the two days was different but the total daily evapotranspirations were fairly similar, being 3.07 mm day⁻¹

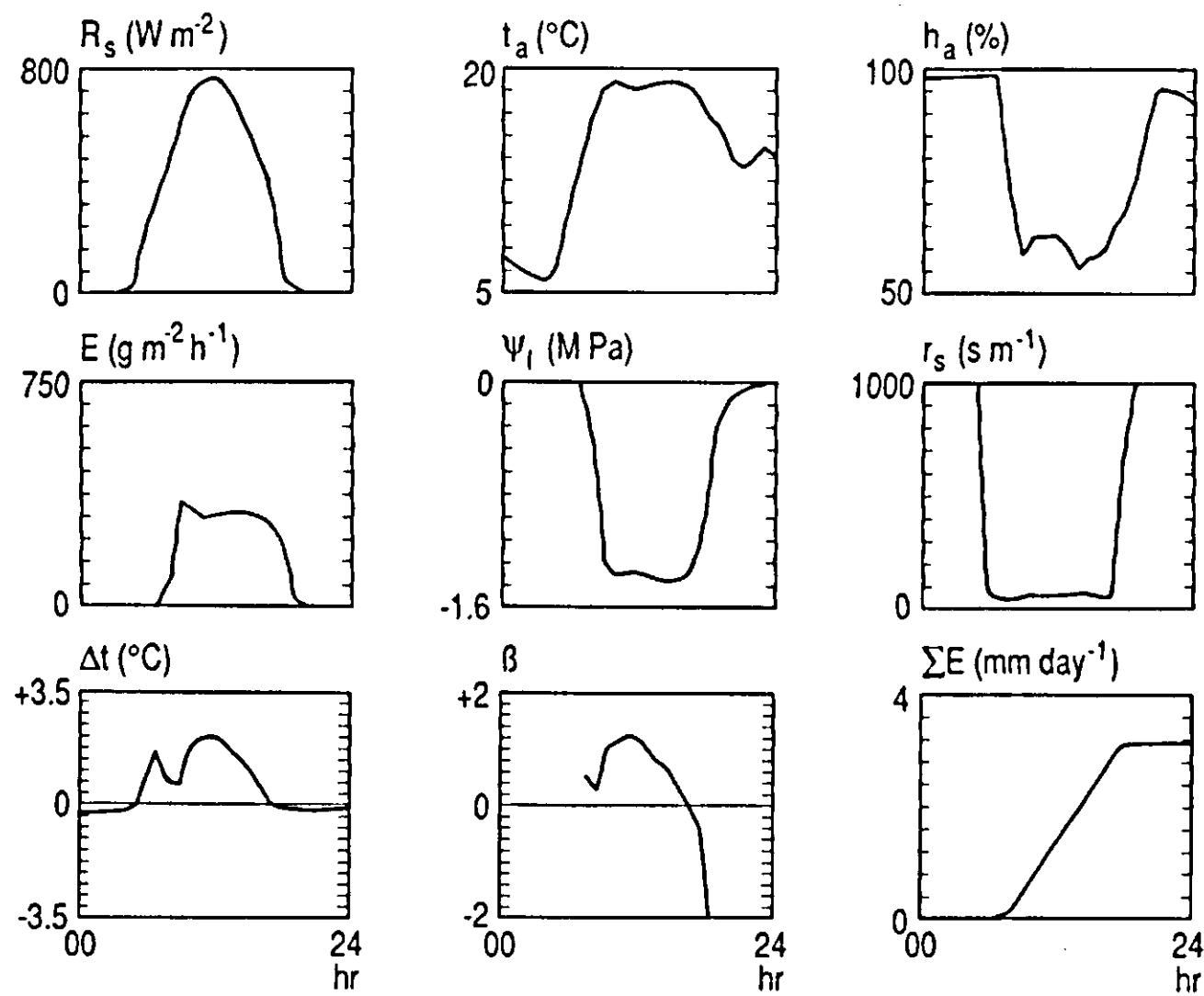


Figure 22. Example of diurnal changes of simulated variables for a clear sunny day (7 August 1979). Input driving variables are: solar radiation, R_s , air temperature, t_a , and air relative humidity, h_a . Output variables are: rate of transpiration, E , leaf water potential, ψ_l , stomatal resistance, r_s , leaf-air temperature difference, Δt , Bowen ratio, β , and cumulative transpiration, ΣE . (After Kowalik & Eckersten, 1984).

on 7 August and 2.43 mm day^{-1} on 11 August. For the clear sunny day the value was a result of intensive transpiration during the whole day, whereas for the cloudy and rainy day transpiration was very low (equal to 0.68 mm day^{-1}) and most of the water was lost during a short period of evaporation of intercepted water (equal to 1.75 mm day^{-1}). In this simulation it was found that intercepted water evaporates much faster than the dry canopy transpires.

To assess the model's performance concerning the difference between leaf and air temperature, one clear day (12 August 1982) and one semi-cloudy day (20 August 1982) were selected. For the clear day, two sensors at the level of 180 cm were the only representative ones for the comparison, and for the cloudy day only one sensor at 200 cm was accepted (Eckersten et al., 1986). The height of the stand was 225-250 cm. On the semi-cloudy day the irrigation was started at 16.00 h in the afternoon. Consequently, the evaporation of the intercepted water in the model was started at the same time.

Simulated and measured values of t_s and the difference between leaf and air temperature, Δt , are shown in Figures 24 and 25. Among the most marked effects of increasing plant water deficit during the clear and sunny day (Figure 24) was the pattern of Δt . The simulated values of t_s and Δt were similar to the

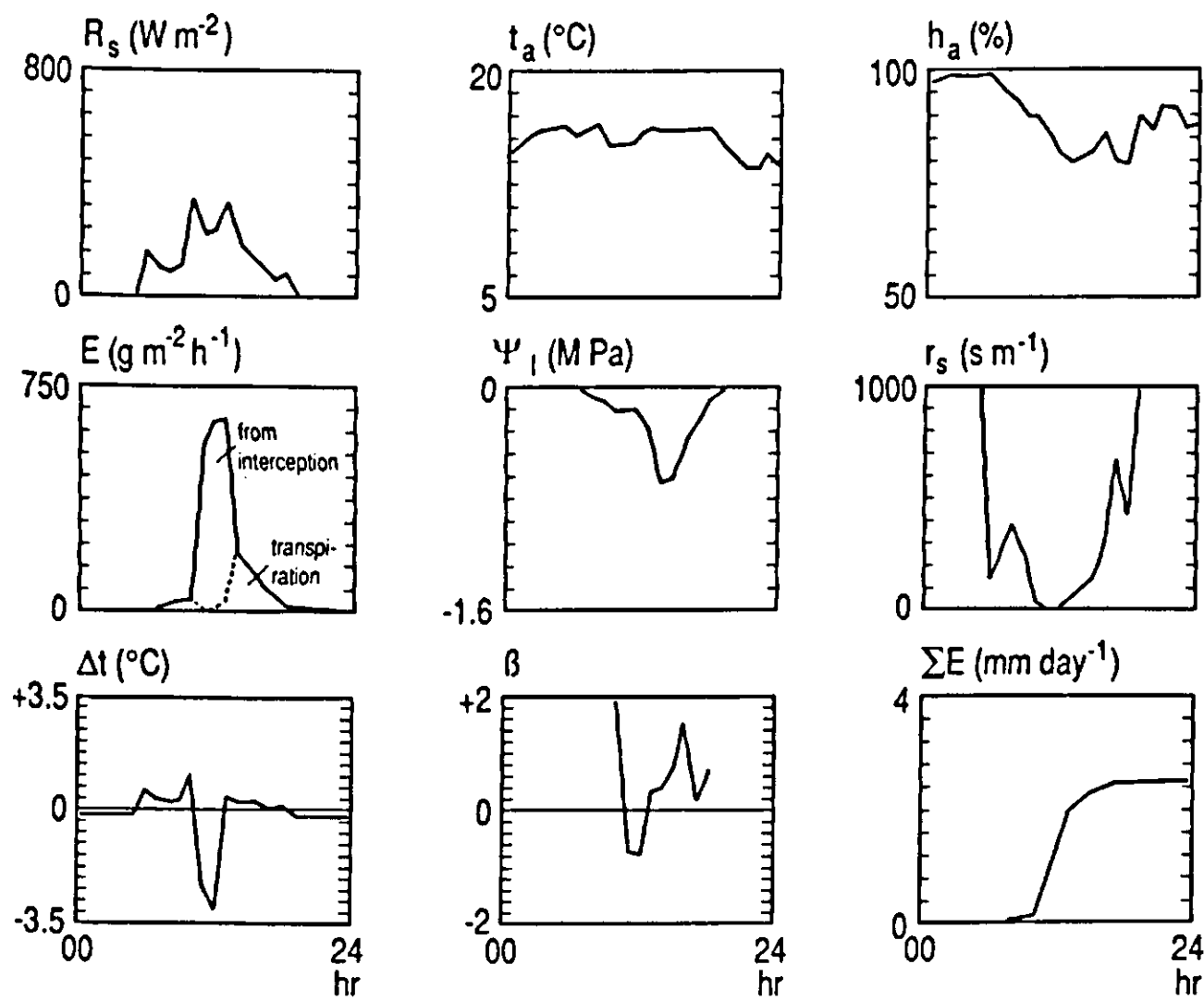


Figure 23. Example of diurnal changes of simulated variables for a cloudy day, with rain at 10.00 h (11 August 1979). For input and output driving variables refer to Figure 22, except that ΣE represents cumulative transpiration plus evaporation of intercepted water. (After Kowalik & Eckersten, 1984).

values measured in the field, except for some points. The disparity between measured and simulated Δt on 12 August 1982 in the period from 07.00 h until 10.00 h is probably caused by variations in the wind speed. In the simulation, a constant aerodynamic resistance, r_a , was assumed. However, during this particular morning there was almost no wind and r_a was thus probably under-estimated at this time.

The disparity between measured and simulated values of Δt on 20 August, 1982, from 11.00 h until 16.00 h (Figure 25), is probably caused by a small shower of rain at 11.00 h, which cooled the leaves in reality but was not accounted for in the simulation. A large cooling effect occurred during the period of evaporation of intercepted water from irrigation, beginning at 16.00 h on 20 August 1982. The rate of evaporation exceeded the rate of transpiration during the earlier parts of the day when the solar radiation was high. Δt was smaller than $+2^{\circ}\text{C}$ but varied considerably. The difference became negative in the morning of the clear day (between 06.00 h and 08.00 h) and just after irrigation on the cloudy day (between 16.00 h and 18.00 h). Evaporation of intercepted water during the cloudy day gave a much larger cooling effect than did high transpiration during the clear day.

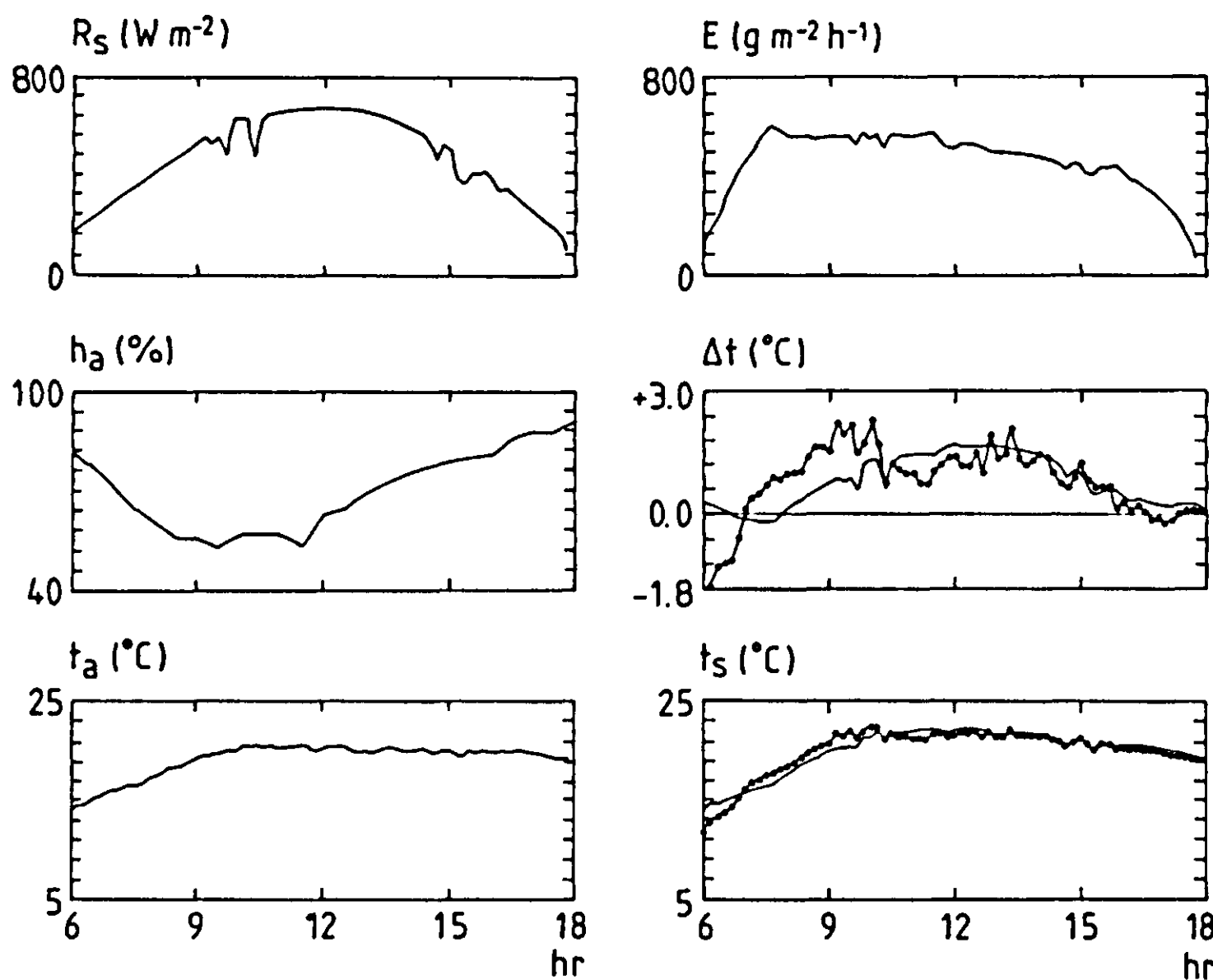


Figure 24. Example of diurnal changes of measured and simulated variables for a clear sunny day (12 August 1982). Measured input driving variables are R_s , h_a and t_a . Output variables are E , Δt and leaf temperature, t_s . For explanation of symbols see Figure 22. Comparison between simulated (solid line) and measured (points) values of Δt and t_s is shown. (After Eckersten et al., 1986).

Simulated and measured cumulative transpiration, E , when plotted against cumulative biomass production, Q , gives a line from which the water use efficiency, Q/E , might be taken. According to Ericsson (1984) the need for an adequate water supply in a willow plantation is particularly important because the water use efficiency of *Salix* is lower than for other broadleaf tree species. Von Braun (1974; 1976) found that the water consumption of *Salix alba* per unit leaf area was 60 to 80% higher than for two poplar clones.

The mean value of simulated transpiration is 1.92 mm/day (96.6 mm per 50 days) for 1979 for three lysimeters (Kowalik & Eckersten, 1984). The estimated figures for the mean shoot (stem and leaf) biomass production, Q , according to L.O. Nilsson (personal communication, 1985), for lysimeters 1, 2 and 3 are 13.0 (clone 683), 22.1 (clone 683), and $36.0 \text{ kg ha}^{-1} \text{ day}^{-1}$ (clone 666), respectively.

The water use efficiency is thus $0.7 - 1.9 \text{ g dry weight of biomass per kg of water}$. Thus, the willow plantation needs to transpire 1 mm of water to produce $7 - 19 \text{ kg}^{-1}$ of leaf and stem dry matter, which is much more than for a very

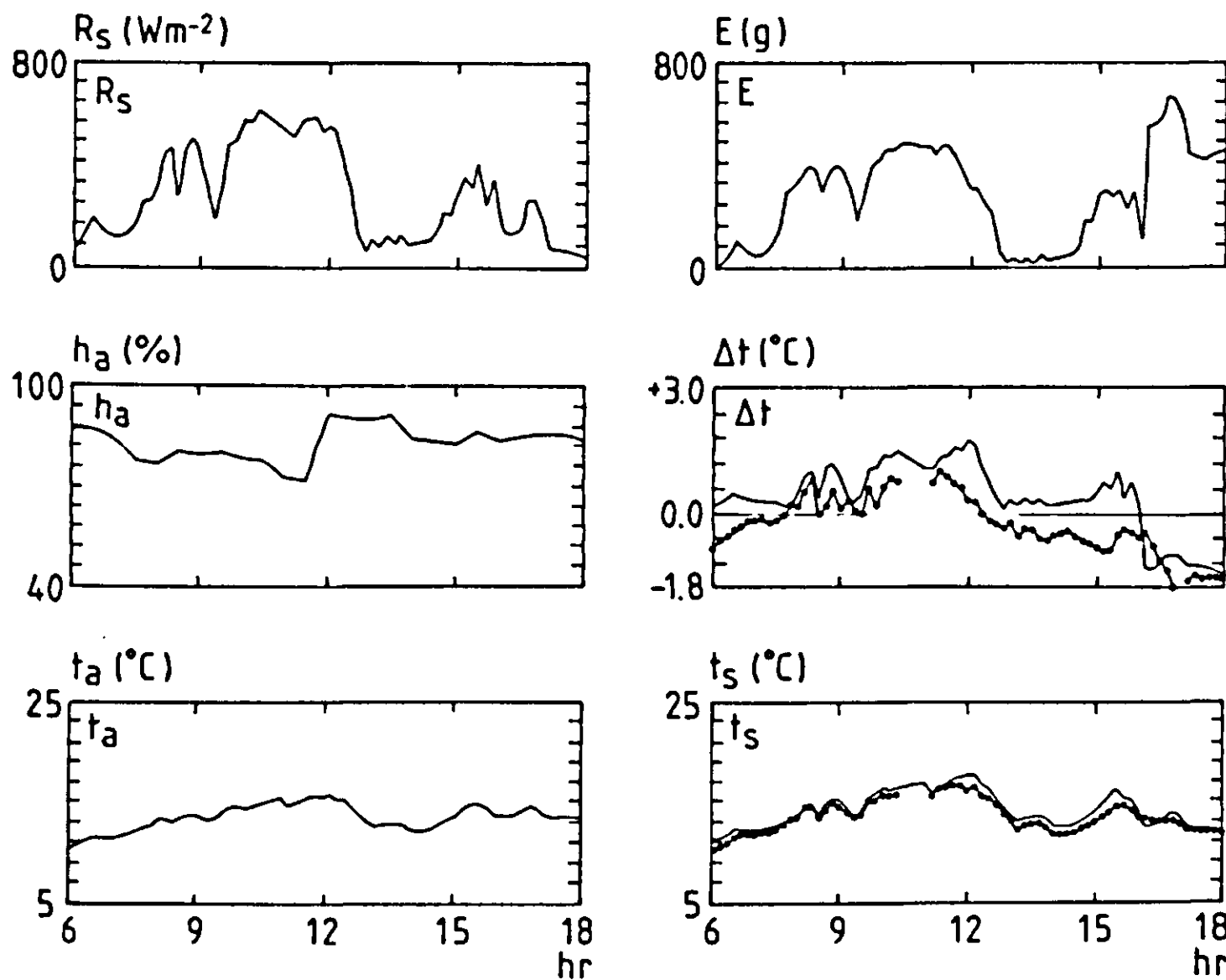


Figure 25. Example of diurnal changes of measured and simulated variables for a cloudy day with sprinkler irrigation at 16.00 h (20 August 1982). For input and output variables refer to Figures 22 and 24. Note the effect of irrigation on E , Δt and t_s . (After Eckersten et al., 1986).

efficient crop plant. Assuming this water use efficiency also valid for stands that produce more than those investigated here, the annual water deficit might be as large as 150 – 200 mm under normal weather conditions in central Sweden. Consequently, irrigation seems necessary to obtain high productivity in *Salix* stands.

9.4 Conclusions

Good agreement between estimated and measured leaf-air temperature differences and cumulative transpiration was obtained during periods when the assumptions in the model were fulfilled. Clearly, the assumptions of a constant aerodynamic resistance or soil hydraulic resistance are not satisfactory and the model should be improved on these points. The results also indicate the importance of evaporation of intercepted water for heat and mass exchange in the energy forestry ecosystem. This further implies that rainfall, both amount and duration, are important factors that must be known. Nevertheless, the results indicate that the model takes most of the important physical processes into account.

9.5 List of symbols

a	= coefficient of hydraulic conductivity of saturated soil ($\text{g m}^{-2} \text{s}^{-1}$)
a_1	= coefficient relating saturated water vapour pressure to temperature, (hPa)
a_2	= coefficient relating saturated water vapour pressure to temperature, (K)
a_3	= coefficient relating saturated water vapour pressure to temperature, (dimensionless)
a_4	= coefficient relating saturated water vapour pressure to temperature, (K)
a_5	= coefficient relating saturated water vapour pressure to temperature, (dimensionless)
b	= root density resistance factor, (MPa)
c_p	= specific heat per unit mass of air, 1004, ($\text{J kg}^{-1} \text{K}^{-1}$)
E	= rate of transpiration, or evaporation of intercepted water, related to unit surface of soil, ($\text{g m}^{-2} \text{s}^{-1}$)
$\lambda \cdot E$	= rate of latent heat flux from leaf canopy into atmosphere, (W m^{-2})
e_a	= water vapour pressure in the ambient air, (hPa)
e_d	= saturated water vapour pressure at temperature t_a , (hPa)
e_s	= saturated water vapour pressure at temperature t_s , (hPa)
H	= rate of sensible heat flux from leaves into atmosphere related to unit surface of soil, (W m^{-2})
h_a	= relative ambient air humidity, (%)
i, j	= indices
$K(\psi_s)$	= unsaturated soil hydraulic conductivity, ($\text{g m}^{-2} \text{s}^{-1}$)
L	= total length of roots per unit volume of soil, (m m^{-3})
n	= coefficient called soil pore size distribution factor, (dimensionless)
Q	= shoot biomass production, ($\text{kg ha}^{-1} \text{d}^{-1}$)
R_n	= net radiation flux in the canopy related to unit surface of soil, (W m^{-2})
R_s	= flux of incident shortwave (300-3000 nm) radiation related to unit surface of soil, (W m^{-2})
r_a	= turbulent diffusion resistance for heat and vapour flow from leaf boundary-layer into free atmosphere, (s m^{-1})
r_p	= plant resistance for liquid water transport from the roots by xylem to the mesophyll of the leaves, as root epidermis, xylem and mesophyll hydraulic resistance, ($\text{MPa s m}^2 \text{g}^{-1}$)
r_r	= soil hydraulic resistance for flow of liquid water in soil and from soil into root hair's surface, ($\text{MPa s m}^2 \text{g}^{-1}$)
r_s	= leaf stomatal resistance related to the unit surface of leaf, (s m^{-1})
r_1	= root radius, (m)
r_2	= mean distance between roots, (m)
S_h	= heat storage in the canopy related to unit soil surface, (W m^{-2})

T_s	= absolute leaf temperature, (K)
t_a	= ambient air temperature, ($^{\circ}\text{C}$)
t_s	= leaf temperature, ($^{\circ}\text{C}$)
Δt	= leaf-air temperature difference, ($^{\circ}\text{C}$)
U	= water uptake rate by whole root system, related to unit soil surface ($\text{g m}^{-2} \text{s}^{-1}$)
V	= amount of readily exchangeable water in the plant per unit area of the soil at a certain time, (g m^{-2})
V_o	= maximum exchangeable water content stored in the plant when it is not water-stressed (relative leaf water content is 100% and leaf water potential is close to zero), (g m^{-2})
V_i	= V at time equal to τ , (g m^{-2})
V_{i+1}	= V at time equal to $\tau + \Delta\tau$, (g m^{-2})
β	= Bowen ratio = $H/(\lambda \cdot E)$, (dimensionless)
γ	= psychrometric constant, 67, (Pa K^{-1})
λ	= latent heat of water vaporization, ($2459.1554 \text{ J g}^{-1}$)
ρ	= specific density of the moist air, 1.2047, (kg m^{-3})
τ	= time (s)
ψ_l	= leaf water potential of liquid water (MPa or kPa)
ψ_{lm}	= ψ_l when the exchangeable water stored is equal to zero, (MPa)
ψ_s	= soil water potential in the root zone taken in the soil layer in which the uptake of water by roots is the greatest, (MPa or kPa)

9.6 Source code

The source code of this SPAC model is written in FORTRAN 77 and makes use of the SIMP simulation modelling support programs (Lohammar, 1979; see also Chapter 14 in this volume). The code represents the model discussed above and also includes the calculation of the potential transpiration, E_p , only if $\text{WSTE10} = 1$. As of 1989, this model will also be available on an IBM-PC as a FORTRAN 77 code.

E_p is defined (according to Federer, 1979) as the transpiration that is entirely independent of the plant's internal water status (i.e. $V=V_o$). However, the program is formulated so that E_p can easily be made a function of the soil water potential, P_{sp} . This is done by cancelling: 'T0004=0 !Vp=Vo'. Explanations of the terms are found in the list of symbols and in the source code. The time step of the model is one minute.

SUBROUTINE TRANS

```

COMMI LAST PRP UPDATE 870918 11:05 PRIOR TO RUN No 105
INTEGER*2 IGO,NCOMP
COMMON/UVAL/ TIME,TIMER,IGO
DIMENSION P(38)

```

EQUIVALENCE (P,WPL10)

COMMON/UVAL/ WPL10 ,WPL11,WPR10,WPR11 ,WPR12 ,WPS10 ,WPS11
COMMON/UVAL/ WR10 ,WR11 ,WRA ,WRP ,WRR10 ,WRR11 ,WRR12
COMMON/UVAL/ WRS10 ,WRS11,WRS12 ,WRS13 ,WRS14 ,WRS15 ,WRS20
COMMON/UVAL/ WRS21 ,WRS22,WRS23 ,WRS24 ,WRS25 ,WS10 ,WS11
COMMON/UVAL/ WS20 ,WS70 ,WS71 ,WSTD10,WSTE10,WSTT10,WSTTS1
COMMON/UVAL/ WSTTS2,WTS10 ,WV10
COMMON/UVAL/PDUMMY(132)
COMMON/UVAL/ NCOMP
DIMENSION X(5)
EQUIVALENCE (X(1),X01)
COMMON/UVAL/ X01,X02,X03,X04,X05
DIMENSION T(5)
EQUIVALENCE (T,T0001)
COMMON/UVAL/ T0001,T0002,T0003,T0004,T0005
COMMON/UVAL/ G(236)
COMMON/UVAL/ D(10)

CEND1

C ***** PROGRAM SCHEDULE *****
C
C *A1* EVERY MINUTE
C *C1* FIRST STEP OF EVERY DAY
C *A2* EVERY MINUTE
C *B1* EVERY Dtau MINUTES
C LOOP1 start (pot. or act. transpiration)
C Initiation
C LOOP2 start (plant water balance)
C Leaf water potential
C Stomatal resistance
C Surface temperature
C Initiation
C LOOP3 start (canopy energy balance)
C Energy balance
C Testing surface temp. diff.
C LOOP3 stop
C Transpiration or evaporation
C Water uptake
C Water balance
C Test of leaf water potential diff.
C LOOP2 stop
C Flows

C LOOP1 stop

C Flows

C *A3* EVERY MINUTE

C *C2* LAST STEP OF EVERY DAY

C ***** DESCRIPTION OF SYMBOLS *****

C DRIVING VARIABLES

C D1-4= ha (%), ta (oC), Rs (W m⁻²), PRI (precipitation+irrigation;
C should be given at time 00:00 in the input-data file)

C STATE VARIABLES (XMM)

C X01-5= V, Evsum (Ev is evaporation of intercepted water), Esum, Vp (V
C for pot. transp.), Epsum (Ep is E for pot. transp.); (g m⁻²);
C (the notation sum means the accumulated sum during the day)

C FLOWS every Dtau minutes (TNNMM is the flow from XNN to XMM (NN=00 is
C environment)); D symbolizes a difference (delta)

C T0001-0005= DV, Ev, E, DVp, Ep; (g m⁻² (Dtau min)⁻¹)

C HELP VARIABLES (G(...)) (possible to have as output in the SIMP program)

C G100-108= Vi (g m⁻²), Evt (is E or Ev (g m⁻² s⁻¹)), U (g m⁻² s⁻¹),
C I (intercepted water (g m⁻²)), i (number of V iterations), Ev
C (kg m⁻² day⁻¹), E (ditto), Ep (ditto), E/Ep

C G110-112= Rn (W m⁻²), lambda*Evt (ditto), H (ditto)

C G120-123= Pl (leaf water potential (MPa)), Ps (soil water potential
C (MPa)), ea (hPa), es (hPa)

C G130-135= rs (s/m), rs(Rs) (s/m), rs(Pl) (s/m), rr (MPa s m² g⁻¹),
C rr+rp (ditto), rp (ditto)

C G140-143= DAYN (daynumber from 1 Jan), MINUT (minutes from 00:00),
C CODtau (counter of minutes from -Dtau to 0), SW1 (0-1) (1:st
C minute of the day? 0 --> YES, <>0 --> NO)

C G150-152= ts (oC), Dts (oC), j (number of ts iterations).

C G161= SW2 (1 or 2 <--> Ep or E)

C PRP PARAMETERS (are defined before the run in the PDAfile)

C W...=MODEL PARAMETERS

C WPL10-11= Plm (MPa), DPlmax (max difference for the water balance
C iterations (MPa))

C WPR10-12= alpha (=I/PRI (0-1)), tauI (Start of Ev (min)), Imax (max
C canopy interception of water (g m⁻² day⁻¹))

C WPS10-11= Ps (actual Ps which rather should be a driving var. (MPa)),
C Psp (Ps for the potential transpiration (MPa))

C WR10-11= a (W m⁻²) and b (-) in: Rn=a+b*Rs

C WRA= ra (s/m)

```

C WRP= rp (MPa s m2 g-1)
C WRR10-12= b (MPa), a (g m-2 s-1) and n (-) in: rr=b/a*(ABS(1000*Pl))**n
C WRS10-12= a, b and c in: rs(Rs)=1/(a+b*Rs+c*Rs**2)
C WRS13-15= rs(Rs)min (s/m), rs(Rs)max (s/m), Rsmin (Rs<Rsmin --> rs(Rs)=
C rs(Rs)max (W m-2))
C WRS20-24= a, b, c, d and e in: rs(Pl)=1/(a+b*Pl+c*Pl**2+d*Pl**3+e*Pl**4)
C ;where Pl is in units of 0.1MPa
C WRS25= rs(Pl)min (MPa)
C WTS10= DENERGYmax (max deviation in the canopy energy balance (W m-2))
C WV10= Vo(g m-2)
C
C WST...= START PARAMETERS (should be checked before every new run)
C WSTD10= DAYNo (Start dayno. in the input-data file)
C WSTE10= SW3 (Calc of Ep?; <>1 --> NO; =1 --> YES)
C WSTT10= Dtau (Integration time(min) for the calc. of water balance)
C WSTTS1-2= ts0, Dts0 ; (ts and Dts at start of iteration (oC))
C
C WS...= SENSIVITY PARAMETERS
C WS10-11= Amplitude and period in the sinusoidal variation of Ps
C WS20= Rs/Rs0
C WS70-71= rs(R)/rs0(R), rs(Pl)/rs0(Pl)
C
C HELP PARAMETERS (YW...) (are defined within the program)
C YW10-14= Ev (g m-2 (Dtau min)-1), Iremain (I not yet evaporated
C (g m-2)), I (g m-2), Pl (in units of 0.1MPa), Pli or DPl (MPa)
C YW21= Ta or Ts (K)
C YW30-33= p*cp (J K-1 m-3), gamma (mbar/K), lambda (J/g),
C a4*(Ta or Ts)-a5
C YW40-41= DENERGY (W m-2), Rs (W m-2)
C
C **** CALCULATIONS ****
C
C ****
C *A1* EVERY MINUTE ****
C Interpolation of driving variables --> minute values in the D-array
C CALL ECDCDA(TIME,D)
C IF (G(143).NE.0.0) GOTO 120 !if SW1<>0...
C
C ****
C *C1* FIRST STEP OF EVERY DAY ****
C IF (G(140).GT.0.0) GOTO 110 !if DAYN>0...
C First time step only
C G(140)=WSTD10-0.5 !DAYN=DAYNo-0.5
C

```

```

110  G(140)=G(140)+1          !DAYN=DAYN+1
      G(143)=1.0              !SWI=1
      YW12=D(4)*1000*WPR10   !I=PRI*1000*alpha
      G(103)=AMIN1(YW12,WPR12) !I=min(I,Imax)

C
C ****
C *A2* EVERY MINUTE ****
120  G(141)=(TIME-1440*(G(140)-0.5-WSTD10)) !MINUT=f(TIME,DAYN)
      T0001=0                 !DV=0
      T0002=0                 !Ev=0
      T0003=0                 !E=0
      T0004=0                 !DVp=0
      T0005=0                 !Ep=0
      G(161)=WSTE10           !SW2=SW3
      IF (G(142).LT.0.0) GOTO 350 !if CODtau<0...

C
C ****
C *B1* EVERY Dtau MINUTES ****
C
C LOOP1 start ****
C
125  IF (G(161).NE.1.0) GOTO 128      !if SW2<>1...
C Only for the potential transpiration case
      G(100)=X04                !Vi=Vp
      G(121)=WPS11               !Ps=Psp
      GOTO 130

C
C Only for the actual transpiration case
128  G(100)=X01                !Vi=V
      Ps=Pso+a*sin((DAYN-DAYNo)/b*3.14)
      G(121)=WPS10+WS10*SIN((G(140)-WSTD10)/WS11*3.14)

C
130  G(142)=-WSTT10             !CODtau=-Dtau
      D(1)=AMIN1(100.0,D(1))   !ha<=100
      YW41=D(3)*WS20
      D(3)=AMAX1(0.0,YW41)    !Rs>0
      G(104)=0                 !i=0
      G(152)=0                 !j=0
      G(130)=0                 !rs=0
140  IF (X02.LT.G(103).AND.G(141).GT.WPR11) GOTO 160!if Evt<I &
      MINUT>tauI...

C
C Only for no evaporation of intercepted water
C

```

```

C LOOP2 start ****
C
C Leaf water potential
150 G(104)=G(104)+1           !i=i+1
    G(120)=WPL10*(1-G(100)/WV10) !Pl=Plm*(1-Vi/Vo)
C
C Stomatal resistance
    G(132)=0                   !rs(Pl)=0
C
C rs(Rs)
    G(131)=1/(WRS10+WRS11*D(3)+WRS12*D(3)**2)
                                !rs(Rs)=1/(a+b*Rs+c*Rs**2)
    IF (D(3).LE.WRS15) G(131)=WRS14
    G(131)=AMIN1(WRS14,G(131)) !if Rs<=Rsmin: rs(RS)=rs(Rs)max
    G(131)=WS70*AMAX1(WRS13,G(131)) !rs(Rs)=min(rs(Rs)max,rs(Rs))
                                !rs(Rs)=max(rs(Rs)min,rs(Rs))
C
C rs(Pl)
    YW13=G(120)*10             !Pl in units of 0.1MPa
C
C rs(Pl)=1/(a+b*Pl+c*Pl**2+d*Pl**3+e*Pl**4)
    G(132)=1/(WRS20+WRS21*YW13+WRS22*YW13**2+WRS23*YW13**3+WRS24*YW13**4)
    G(132)=WS71*AMAX1(WRS25,G(132)) !rs(Pl)=max(rs(Pl)min,rs(Pl))
C
C rs
155 G(130)=AMAX1(G(131),G(132)) !rs=max(rs(Rs),rs(Pl))
C
C Surface temperature
C
C Initiation
160 G(150)=WSTTS1           !tsj=tso
    G(151)=WSTTS2           !Dtsj=Dtso
    YW30=1.2047*1004         !p*cp
    YW31=0.67                 !gamma
    YW32=2.4518E3             !lambda
    G(110)=WR10+WR11*D(3)    !Rn=a+b*Rs
    YW21=D(2)+273.2          !Ta=ta+273.2
    YW33=0.058302635*YW21-2.19386068 !a4*Ta-a5
C
C ed(Ta)=a1*exp((a2*Ta-a3)/(a4*Ta-a5))
    G(123)=1.3332*EXP((1.088719061*YW21-276.4883955)/YW33)
    G(122)=G(123)*D(1)/100   !ea=ha*ed(Ta)
C
C LOOP3 start ****
C
C Energy balance
180 G(152)=G(152)+1          !j=j+1

```

```

190   G(150)=G(150)+G(151)           !tsj=tsj+Dtsj
      YW21=G(150)+273.2           !Tsj=tsj+273.2
      YW33=0.058302635*YW21-2.19386068 !a4*Tsj-a5
C     es(Tsj)=a1*exp((a2*Tsj-a3)/(a4*Tsj-a5))
      G(123)=1.3332*EXP((1.088719061*YW21-276.4883955)/YW33)
      G(112)=YW30*(G(150)-D(2))/WRA      !H=p*cp*(tsj-ta)/ra
C     Evt*lambda=p*cp/gamma*(es(Tsj)-ea)/(ra+rs)
      G(111)=YW30/YW31*(G(123)-G(122))/(WRA+G(130))
C
C     Testing surface temp. diff.
      YW40=G(110)-(G(111)+G(112))      !DENERGY=Rn-(Evt*lambda+H)
      IF (ABS(YW40).LE.WTS10) GOTO 200   !if ABS(DE-
                                         NERGY)<=DENERGYmax...
C     Dtsj=DENERGY/ABS(DENERGY)*ABS(Dtsj)/2
      G(151)=YW40/ABS(YW40)*ABS(G(151))/2
      GOTO 180
C
C     LOOP3 stop ****
C
C     Transpiration or evaporation
200   G(101)=G(111)/YW32           !Evt=Evt*lambda/lambda
      IF (X02.LT.G(103).AND.G(141).GT.WPR11) GOTO 310!if Evt<I &
MINUT>tauI...
C
C     Water uptake (Only for no evaporation of intercepted water)
C     rr=b*(ABS(1000*Ps)**n)/a
      G(133)=WRR10*(ABS(G(121))*1000)**(WRR12)/WRR11
      G(135)=WRP                      !rp
      IF (G(121).LT.G(120)) G(135)=1000E9 !if Ps<Pl: rp=1000E9
      G(134)=G(133)+G(135)           !rr+rp
      G(102)=-(G(120)-G(121))/G(134) !U=-(Pl-Ps)/(rr+rp)
C
C     Water balance
C     integration over the Dtau minutes period
      G(100)=G(100)+(G(102)-G(101))*60*WSTT10 !V(i+1)=Vi+(U-Evt)*60*Dtau
C
C     Test of leaf water potential diff.
      YW14=G(120)                      !Pli
      G(120)=WPL10*(1-G(100)/WV10)      !Pl(i+1)=Plm*(1-V(i+1)/Vo)
      YW14=G(120)-YW14                 !DPli=Pl(i+1)-Pli
      IF (ABS(YW14).LE.WPL11) GOTO 300 !if DPli<=DPlmax...
      GOTO 150
C
C     LOOP2 stop ****
C

```

```

C   Flows
300  IF (G(161).NE.1.0) GOTO 305      !if SW2<>1...
C   Only for the potential transpiration case
T0004=(G(100)-X04)                  !DVp=V(i+1)-V
T0004=0                               !Vp=Vo
T0005=G(101)*60*WSTT10              !Ep=Evt*60*Dtau
G(161)=0                             !SW2=0
GOTO 125

C
C   LOOP1 stop ****
C
C   Flows
C   Only for the actual transpiration case
305  T0001=(G(100)-X01)                !DV=V(i+1)-V
      IF (T0001.LT.-X01) T0001=-X01   !V>=0
      T0003=G(101)*60*WSTT10        !E=Evt*60*Dtau
      GOTO 350

C
C   Only for the evaporation of intercepted water
310  YW10=G(101)*60*WSTT10          !Ev=Evt*60*Dtau
      YW11=G(103)-X02                !Iremain=I-Evtsum
      T0002=AMIN1(YW10,YW11)         !Ev=min(Ev,Iremain)

C
C   *A3* EVERY MINUTE ****
350  G(142)=G(142)+1                  !CODtau=CODtau+1
      IF (G(141).LT.1439) GOTO 400   !if MINUT<1439...

C
C   *C2* LAST STEP OF EVERY DAY ****
      G(143)=0                      !SW1=0
C   For daily outputs of Ev, E, Ep, E/Ep
      G(105)=X02/1000
      G(106)=X03/1000
      G(107)=X05/1000
      IF (X05.EQ.0.0) GOTO 390
      G(108)=X03/X05

C   Initiations
390  T0002=-X02                      !Evsum=0
      T0003=-X03                      !Esum=0
      T0005=-X05                      !Epsum=0
400  RETURN
      ENTRY INITIL
      CALL ECDCIN
      END

```

***** PDA-FILE *****

PARAMETER VALUES

WPL10 = -2.70	WRP = 16.0	WRS20 = 0.157	WS71 = 1.00
WPL11 = 4.000E-02	WRR10 = 4.000E-05	WRS21 = 2.144E-02	WSTD10 = 179.
WPR10 = 0.250	WRR11 = 1.62	WRS22 = 1.118E-03	WSTE10 = 1.00
WPR11 = 600.	WRR12 = 2.10	WRS23 = 2.617E-05	WSTT10 = 1.00
WPR12 = 4.000E+03	WRS10 = 1.384E-03	WRS24 = 2.301E-07	WSTTS1 = -10.0
WPS10 = -5.000E-03	WRS11 = -2.012E-05	WRS25 = 40.0	WSTTS2 = 25.0
WPS11 = -5.000E-03	WRS12 = 4.216E-07	WS10 = 0.000E+00	WTS10 = 0.100
WR10 = -23.0	WRS13 = 40.0	WS11 = 5.00	WV10 = 500.
WR11 = 0.649	WRS14 = 1.000E+03	WS20 = 1.00	
WRA = 10.0	WRS15 = 30.0	WS70 = 1.00	

INITIAL COMPARTMENT VALUES

X01 = 350.	X03 = 0.000E+00	X05 = 0.000E+00
X02 = 0.000E+00	X04 = 500.	

9.7 References

Benyon, P.R., 1968. A review of numerical methods for digital simulation. *Simulation* 11:219-238.

Braun, H.J. von, 1974. Growth and water economy of tree species *Alnus* and *Salix*. *Zeitschrift für Pflanzenphysiologie* 74:91-94.

Braun, H.J., von, 1976. Rhythmus und Grösse von Wachstum und Wasserverbrauch bei Holzpflanzen. *Allgemeine Forst und Jagd Zeitung* 8:163-168.

Eckersten, H., 1984a. Meteorologiska mätningar utförda inom Projekt energi skogsdling under 1982 [Meteorological measurements performed within the energy forestry project during 1982]. Internal Report 14, 57 pp. Swedish University of Agricultural Sciences, Section of Energy Forestry, Uppsala.

Eckersten, H., 1984b. Light penetration and photosynthesis in a willow stand. In: K.L. Perttu (Ed.): *Ecology and management of forest biomass production systems*. Report 15:29-45. Swedish University of Agricultural Sciences. Department of Ecology and Environmental Research, Uppsala.

Eckersten, H., 1986. Willow growth as a function of climate, water and nitrogen. Dissertation. Report 25, 38 pp. Swedish University of Agricultural Sciences, Department of Ecology and Environmental Research, Uppsala.

Eckersten, H. & Kowalik, P.J., 1986. Measured and simulated leaf-air temperature differences in a willow stand. In: H. Eckersten: Willow growth as a function of climate water and nitrogen. Report 25, 31 pp. Swedish University of Agricultural Sciences, Department of Ecology and Environmental Research, Uppsala.

Eckersten, H., Kowalik, P. & Lindroth, A., 1986. Simulation of diurnal changes of leaf temperature, transpiration and interception loss in willow energy forest. In: Institute of Water Engineering and Water Management (Ed.): Hydrological processes in the catchment. Cracow Technical University, Volume 1, p. 17-21.

Eckersten, H. & Perttu, K., 1981. Bioklimatet vid försöksstationen i Studsvik under perioden 1979-1980 [The bioclimate of the research station at Studsvik during the period 1979-1980]. Swedish University of Agricultural Sciences, Section of Energy Forestry, Uppsala. Technical Report 14, 37 pp.

Ericsson, T., 1984. Nutrient cycling in willow. IEA/FE PG 'B' – ENFOR, Canadian Forest Service, Report 1984:5, 32 pp.

Feddes, R.A., 1971. Water, heat and crop growth. Veenman, Wageningen, 184 pp.

Feddes, R.A., 1981. Water use models for assessing root zone modification. In: G.F. Arkin and H.M. Taylor (Eds): Modifying the root environment to reduce crop stress. ASAE Monograph, 4:347-390.

Feddes, R.A., Kowalik, P.J. & Zaradny, H., 1978. Simulation of field water use and crop yield. Simulation Monographs 90-220-0676-X, Pudoc, Wageningen, 188 pp.

Feddes, R.A. & Rijtema, P.E., 1972. Water withdrawal by plant roots. Journal of Hydrology 17:33-50.

Federer, C.A., 1968. Spatial variation of net radiation, albedo and surface temperature of forests. Journal of Applied Meteorology 7:789-795.

Federer, C.A., 1979. A soil-plant-atmosphere model for transpiration and availability of soil water. Water Resources Research 15:555-562.

Gardner, W.R. & Ehlig, C.F., 1963. The influence of soil water on transpiration of plants. Journal of Geophysical Research 68:5719-5724.

Goudriaan, J., 1982. Some techniques in dynamic simulation. In: F.W.T. Penning de Vries and H.H. van Laar (Eds): Simulation of plant growth and crop production. Simulation Monographs 90-220-0601-8, Pudoc, Wageningen, pp. 66-84.

Grip, H., 1981. Evapotranspiration experiments in *Salix* stands. Technical Report 15, 29 pp. Swedish University of Agricultural Sciences, Section of Energy Forestry, Uppsala.

Grip, H., Halldin, S., Lindroth, A. & Persson, G., 1984. Evapotranspiration from a willow stand on wetland. In: K.L. Perttu (Ed.): Ecology and management of forest biomass production systems. Report 15:47-61. Swedish University of Agricultural Sciences, Department of Ecology & Environmental Research, Uppsala.

Hansen, G.K., 1975. A dynamic continuous simulation model of water state and transpiration in the soil-plant-atmosphere system. I. The model and its sensitivity. Acta Agriculturae Scandinavica 25:129-149.

Honert, T.H., van den, 1948. Water transport in plants as a catenary process. Discussions of Faraday Society 3:146-153.

Jansson, P.E. & Halldin, S., 1979. Model for annual energy and water flow in a layered soil. In: S. Halldin (Ed.): Comparison of forest water and energy exchange models. Elsevier Scientific Publishing Company, pp. 145-163. Amsterdam – Oxford – New York.

Jarvis, P.G., 1975. Water transfer in plants. In: D.A. de Vries and N.H. Afgan (Eds): *Heat and mass transfer in the biosphere. I. Transfer processes in plant environment.* Halsted, pp. 369-394. Washington, DC.

Jarvis, P.G., Edwards, W.R.N. & Talbot, H., 1981. Models of plant and crop water use. In: D.A. Rose and D.A. Charles-Edwards (Eds): *Mathematics and Plant Physiology.* Academic Press, pp. 151-194. London.

Kowalik, P.J. & Eckersten, H., 1984. Water transfer from soil through plants to the atmosphere in willow energy forest. *Ecological Modelling* 26:251-284.

Kowalik, P.J. & Turner, N.C., 1983. Diurnal changes in the water relations and transpiration of a soybean crop simulated during the development of water deficits. *Irrigation Science* 4:225-238.

Lang, A.R.G. & Gardner, W.R., 1970. Limitations to water flux from soils to plants. *Agronomy Journal* 62:693-695.

Larsson, S., 1981. Influence of intercepted water on transpiration and evaporation of *Salix*. *Agricultural Meteorology* 23:331-338.

Lindroth, A. & Grip, H., 1984. Design of water balance studies in energy forest on wetland. *Vannet i Norden* 1:3-15.

Lohammar, T., 1979. SIMP - Interactive mini-computer package for simulating dynamic and static models. In: S. Halldin (Ed.): *Comparison of forest water and energy exchange models. Proceedings from an IUFRO Workshop held at Uppsala, Sweden from September 24th - 30th, 1978.* Elsevier Scientific Publishing Company, pp. 27-33. Amsterdam - Oxford - New York.

Monteith, J.L., 1981. Evaporation and surface temperature. *Quarterly Journal of the Royal Meteorological Society*, 107:1-27.

Reed, K.L., and Waring, R.H., 1974. Coupling of environment to plant response: A simulation model of transpiration. *Ecology* 55:62-72.

Smart, R.E. & Barrs, H.D., 1973. The effect on environment and irrigation interval on leaf water potential of four horticultural species. *Agricultural Meteorology* 12:337-346.

Thompson, D. R. & Hinckley, T.M., 1977. A simulation of water relations of white oak based on soil moisture and atmospheric evaporative demand. *Canadian Journal of Forest Research* 7:400-409.

Turner, N.C., 1974. Stomatal response to light and water under field conditions. In: R.L. Bieleski, A.R. Ferguson, M.M. Cresswell (Eds): *Mechanisms of Regulation of Plant Growth.* Bulletin 12, pp. 423-432. Royal Society of New Zealand, Wellington.

10 Willow stand evaporation: Simulation of diurnal distribution using synoptic weather data

Sven Halldin

10.1 Introduction

Simple models of the water balance of willow stands can be used to assess irrigation needs, possible nutrient leaching and other processes affecting water quality and water resources if energy forestry becomes widely adopted in the future. Such models meet the conflicting demands for physical realism and data availability. The evaporation process has an especially marked diurnal variation; means or one-time-of-day measurements do not represent this realistically.

This dilemma has led to the development of two distinct classes of evaporation and water balance models for various types of vegetation cover. The first type of model is that which sacrifices physical realism to meet the availability of data. This type of model (e.g., Spittlehouse & Black, 1981) is commonly based on the Penman (1948 or 1953) combination equation for evaporation in combination with a simple soil water budget model and has a time resolution of 24 hours or more. Calder et al. (1983) assessed this type of model and concluded that the inclusion of sophisticated evaporation equations does not improve prediction capacity. The second type of model (e.g., Jackson et al., 1983; Eckersten, 1985; 1986) simulates the elements of the hydrological cycle at short time intervals and depends on an algorithm to deduce the diel weather variation from data once a day. This type of more complex model may alternatively be used for a well studied area and period as a means to calibrate a simpler model (e.g., Dunin et al., 1978).

In order for a mechanistic model to be generally applicable, its parameters must be possible to obtain from measurements not related to the entity to be explained or predicted. The most important factor determining evaporation from high vegetation, especially forests, is the surface resistance. This resistance has a marked variation over the day (Gash & Stewart, 1975) as well as over the season (Lindroth, 1985a). To estimate the parameters in some functional relationship describing these variations it is necessary to perform measurements with a diel resolution. The conflict between weather data availability and necessary physical realism is, therefore, particularly important for high and aerodynamically rough vegetation like forests.

This paper presents an attempt to overcome this conflict by introducing an idealized division of the 24-hour cycle into a night-time part and a day-time part. This allows the use of instantaneous relations for various processes in the model while the demand for weather data is in accordance with the availability.

10.2 The KAUSHA model

The model presented herein, given the name KAUSHA (Swahili for 'evaporate'), was originally presented by Halldin & Grip (1979). It was first conceived for a mature pine forest in Central Sweden (see also Lindroth, 1985b) but has been used later for other forests such as oak (Halldin et al., 1984/85), beech (Saugier et al., 1985) and wetland willow (Grip et al., 1984). The model core remains the same, but certain modifications have been introduced for each specific application. The model core concerns evaporation divided into transpiration and interception evaporation, as well as a simple one-layer soil water budget.

10.2.1 *Development of the basic part of the model*

Two fundamental principles were adhered to in the conceptualization of the model. First, that the model should represent only the most basic processes of the system, such that each additional process to be included had to prove its

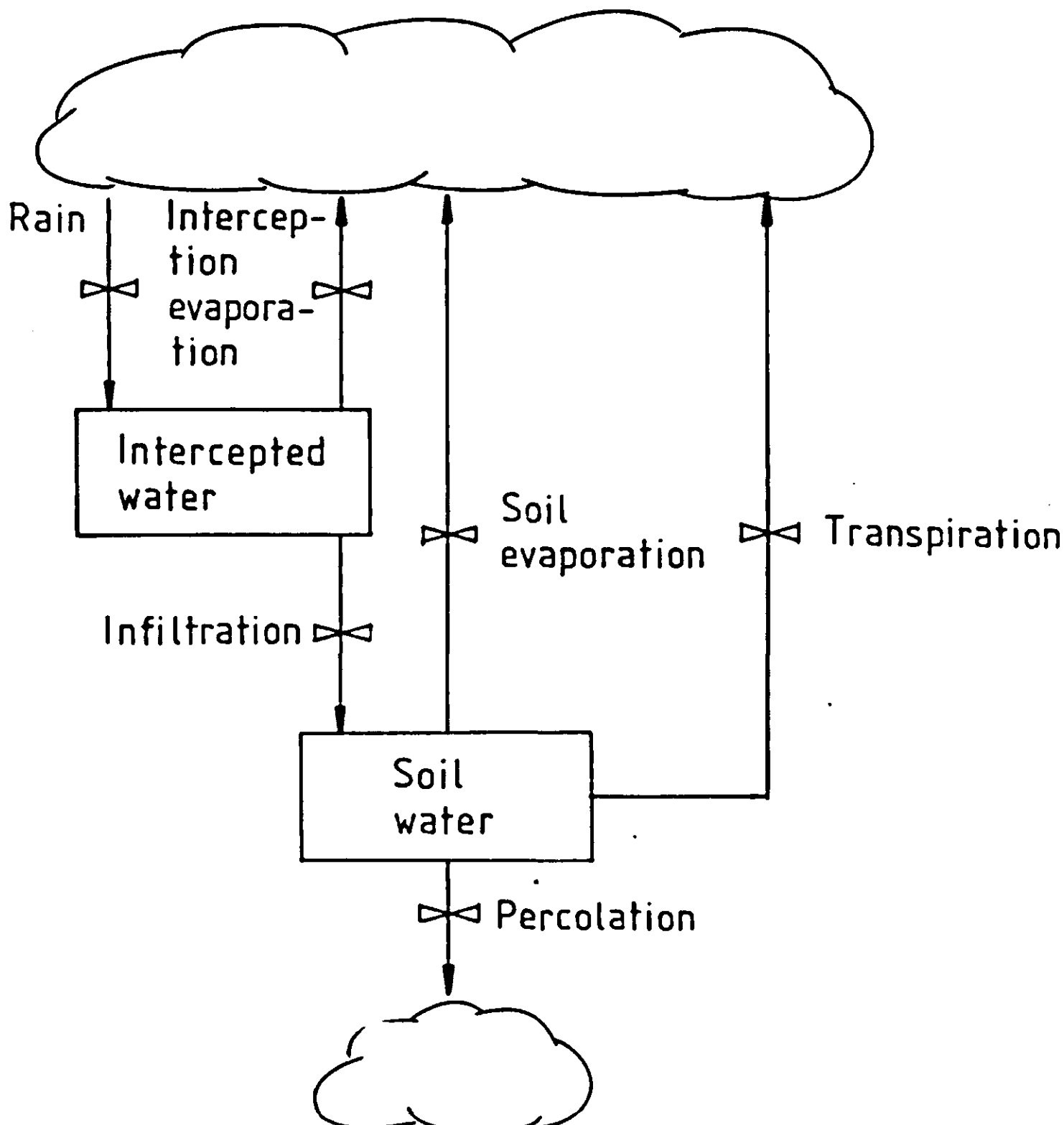


Figure 26. Structure of the KAUSHA model.

utility in a real situation. Second, that all structural parameters could be physically identified and could be measured independently of the model output.

The first principle led to the system being limited to a two-compartment system, with soil water and intercepted water as state variables (Figure 26). The interception compartment had to be included because rates of transpiration and evaporation of intercepted water are different under equal climatic circumstances (Stewart, 1977). Total evaporation, thus, depends directly on the precipitation regime. Soil/ground evaporation was disregarded in the first versions of the model, but for energy forest applications it was necessary to include this factor. The soil water was described as a single compartment. Factors such as evaporation of intercepted water during rainfall or vertical distribution of water uptake in the soil were not considered important enough to be included.

Transpiration with no soil-water stress, and the evaporation of intercepted water were calculated using the Penman (1953) equation (see list of symbols for an explanation)

$$E = \frac{\Delta (R_n - R_{ng}) + \gamma E_a}{\Delta + \gamma (1 + r_s/r_a)} \quad \text{Equation 59}$$

Evaporation from a wet vegetation cover was given with the surface resistance, r_s , zero. For a dry, unstressed vegetation cover the surface resistance was assumed equal the bulk stomatal resistance of the canopy (Lindroth & Halldin, 1986)

$$r_s = (k_s \cdot a_l)^{-1} \quad \text{Equation 60}$$

Finally, the stomatal conductance was deduced from three elementary considerations

$$\left. \begin{aligned} k_s \cdot \delta c &= k_r (\psi_s - \psi_l) \\ k_s &= k_m \cdot \frac{R_g}{R_g + R_o} + \beta \psi_l \\ \psi_s &\approx 0. \end{aligned} \right\} \quad \text{Equation 61}$$

The first condition states that transpiration equals root water uptake, i.e., steady state was assumed. In the following it was also assumed that δc , which should strictly be the difference in absolute humidity between the surface of the intercellular space and the air outside the boundary layer of the leaf/needle, could be approximated by the humidity saturation deficit of the ambient air. The second condition gives a governing equation for the stomatal functioning and the third equation means that soil water was not limiting. These equations were solved algebraically to yield the Lohammar formula (Lohammar et al., 1980)

$$k_s = \frac{R_g}{R_g + R_o} \cdot \frac{k_m}{1 + b\delta c} \quad \text{Equation 62}$$

where b is equal to β/k_r .

This equation was derived on a momentary basis and its parameters should be deduced from 'instantaneous' physiological measurements (porometers or cuvettes). In order to apply it to a model with a 24-hour time step, the 24-hour period was divided into three parts, with the daytime part positioned symmetrically around noon and surrounded by two night-time parts of equal length. Three different approaches were tested for the temporal description of the climatic input (R_g and δc) during the daytime period.

The first approach used a sinusoidal daytime variation, the second approach made use of a pulse with duration equal to daylength and the third approach used a pulse with a duration less than the astronomically determined daylength. The areas below each of these curves were the same. They equal the total 24-hour insolation and yield the measured average 24-hour vapour concentration deficit (Figure 27).

The net radiation and precipitation driving variables also had to be distributed over the 24-hour cycle. Net radiation was treated in analogy with the solar radiation, except for the rare cases when total 24-hour net radiation was negative. In this case the negative radiation was distributed as a constant value over the night-time parts and daytime net radiation was assumed to be zero. Various distributions were tested for the precipitation, and in the model presented here all precipitation is assumed to fall evenly during daytime.

The ventilation part, E_a , of Penman's formula (Equation 59) was a function of the vapour pressure deficit, δe , and the aerodynamic resistance, r_a

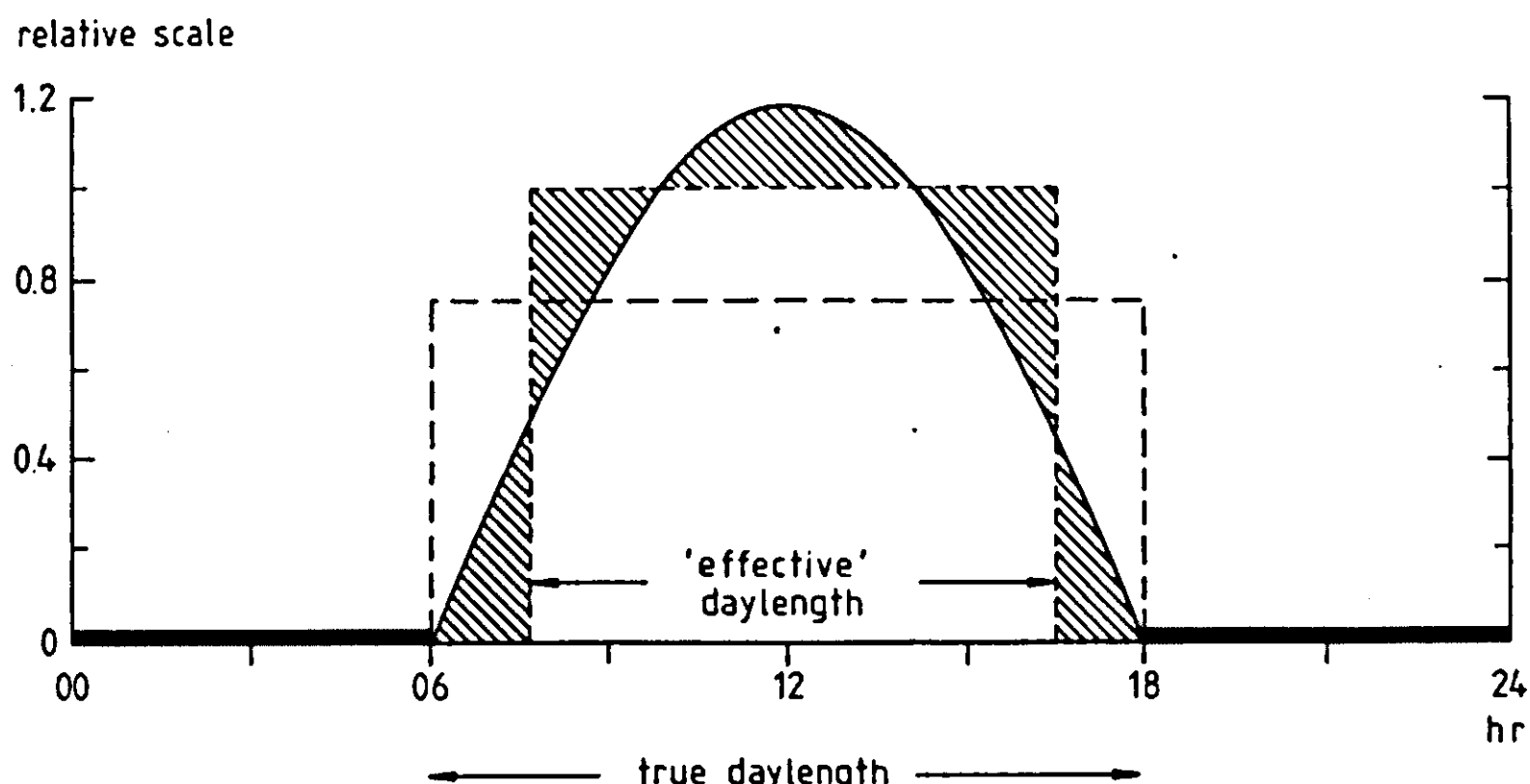


Figure 27. Three idealized diurnal distributions for net and solar radiation and vapour pressure deficit. Daylength was 'effective' when it minimized the shaded area.

$$E_a = \frac{\rho c_p}{\gamma} \cdot \frac{\delta e}{r_a} \quad \text{Equation 63}$$

The aerodynamic resistance depended on wind speed (assumed constant throughout the 24 hours) and vegetation characteristics

$$r_a = \frac{\ln^2((z-d)/z_o)}{k^2 \cdot u} \quad \text{Equation 64}$$

The displacement height, d , and the roughness length, z_o , were both assumed to be proportional to stand height.

Transpiration and interception evaporation were assumed to exclude each other. In reality there is a transition period when both occur concomitantly, but with the temporal resolution used in this model it was considered acceptable to model this period as of zero length. This way the interception evaporation persisted as long as there was water on the vegetation cover. After this time, if the daytime period had not ended, transpiration continued until sunset.

The soil water balance was modelled as a simple threshold function. The threshold was identified as the field capacity of the soil. Total available water was defined as field capacity minus capacity at the wilting point. This total was divided into the fraction of easily available water, for which transpiration was not limited, and the remaining fraction, for which transpiration was suppressed linearly between its potential value (Figure 28) and zero.

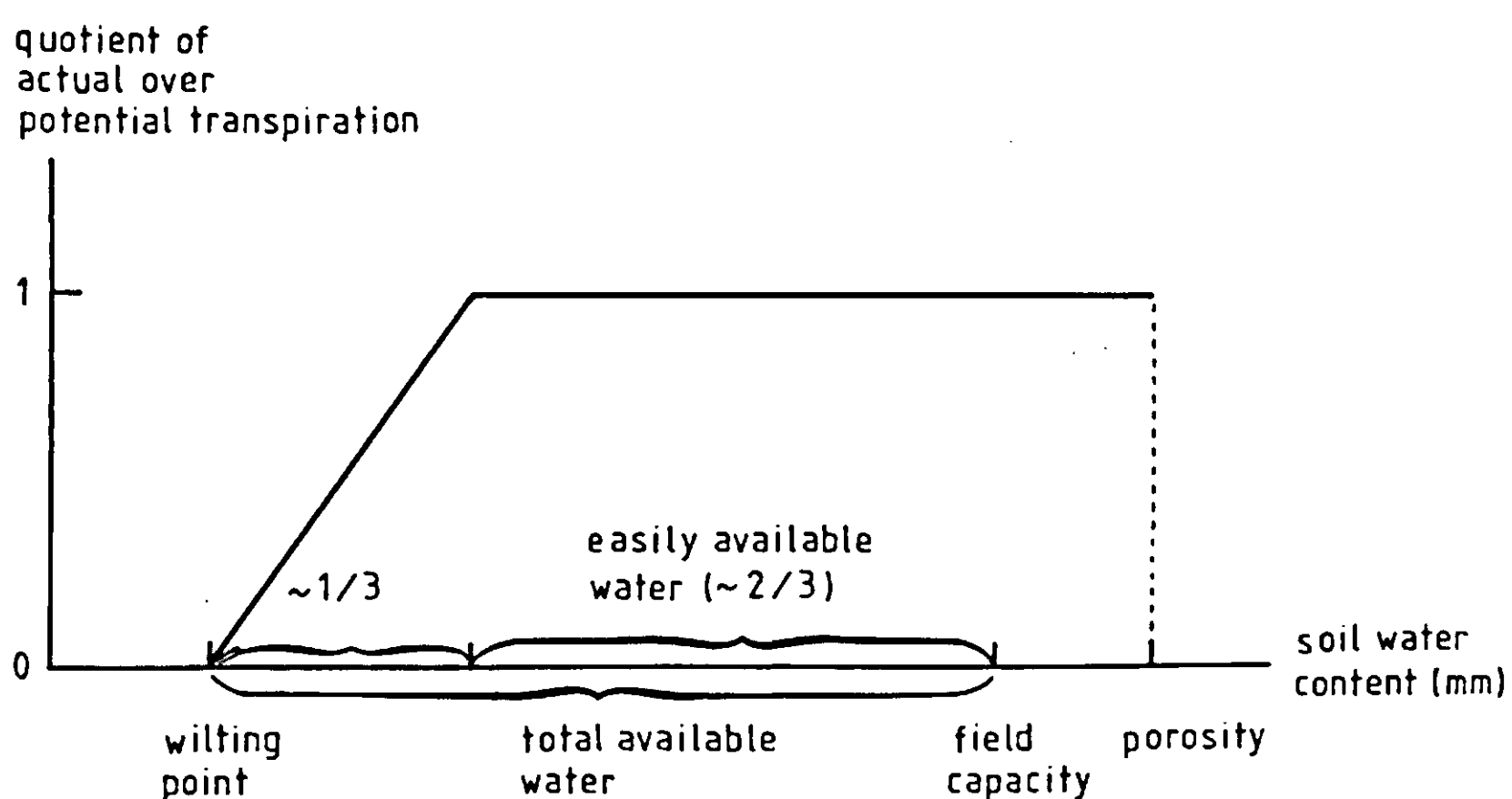


Figure 28. Soil water availability function.

10.2.2 Development of parts specific for the willow application

The source code given below relates to a specific application to willow at Studsvik, 100 km south of Stockholm. As such it contains conditions applicable for willow stands in general and also conditions specific for Studsvik.

The interception water balance was given a threshold formulation. The interception threshold, S_o , was made a function of the phenological state of the stand by simply adding the water-holding capacities of the leaf and bark surface areas

$$S_o = s_b \cdot a_b + s_l \cdot a_l \quad \text{Equation 65}$$

Contrary to other deciduous species (Halldin et al., 1984/85), willow leaves do not protect the bark surface from rain but rather direct the rain along the trunk; in this case an additive formulation was reasonable.

Evaporation from the soil was important during the year the stand was established and also during the spring, before and during leaf development. As a first approximation this evaporation was considered potential and was calculated with the Priestly-Taylor (1972) formula

$$E_g = 1.26 \frac{\Delta R_{ng}}{\Delta + \gamma} \quad \text{Equation 66}$$

where the net radiation at ground level was ascertained from the radiation above the stand, using an exponential extinction function

$$R_{ng} = R_n \exp(-\alpha \cdot (a_l + a_b/\pi)/r_{ds}) \quad \text{Equation 67}$$

The extinction parameter, α , has been discussed elsewhere, e.g., by Impens & Lemeur, 1969; r_{ds} was introduced as a compensating factor specific for the Studsvik application. Water balance was measured at Studsvik in three plots, 5m x 5m in size with a 1 m² lysimeter in the centre of each (Grip, 1981). Because of establishment problems, the stand development in the plots as a whole differed from the development of the plants in the lysimeters. This difference did not influence water balance, which was recorded specifically for each lysimeter, but the radiation balance had to be recorded for the stand as a whole. This was accomplished by introducing r_{ds} , the quotient between a_l in the lysimeter and a_l in the stand as a whole, into Equation 67.

In the Studsvik application, data on the biomass yield were also available. The model was, in this case, used to test various hypotheses concerning the water use efficiency. This was done by introducing three different yield indices. Feddes et al. (1978) propose that, although the growth-transpiration quotient is approximately constant, a better growth index would be achieved by relating growth to transpiration divided by vapour pressure deficit. For an aerodynamically rough stand, transpiration over vapour pressure deficit is approximately equal to the surface conductance of the stand. This entity was calculated by the

model and therefore it was natural to test this as an index of growth too. Since growth was given both as total above-ground growth and as stem growth, the latter being the most interesting commercially, two sets of indices were calculated.

The input of driving variables to the model was presumed always to remain of the same type, and was given in the same units. This was achieved by introducing an intermediary subroutine, KAUBAS, in which the available input data were preprocessed to fit the demands of the model. This had various repercussions for the Studsvik application; for example, net radiation had to be calculated as a linear regression on the solar radiation, and a_b was calculated as a function of the stem dry weight. On the other hand no simplified functional relation had to be used for the temporal variation of a_l and stand height in this case, because these entities were measured every week during the growing season.

10.3 Results

The evaluation of the best form of idealized distribution for driving data over 24 hours was done for a mature Scots pine forest at Jädraås, central Sweden. This forest was the main site for the large-scale interdisciplinary Swedish Coniferous Forest Project (see Persson, 1980), so synchronous micro-meteorological and physiological measurements were available. Porometer measurements of stomatal resistance allowed independent estimation of parameter values in the Lohammar equation (Figure 29). These values were used together with climatic data for the whole of 1977, in order to compare results of the various diurnal distributions for situations without precipitation. In the absence of rain, the sinusoidal distribution gives rise to a highly complex, but analytically explicit expression for daily transpiration (Lohammar et al., 1980). This expression was considered as the one which, *a priori*, best mimicked the 'true' one, and was used as a reference. Three pulses were tested. One pulse used the astronomically determined daylength as duration and a second pulse was 75% as long (cf. Figure 27). A comparison was also made with a 24-hour pulse, to see whether a model without any diurnal distribution might be as good as the other two.

From Figure 30 it can be seen that all the pulses gave reasonably coherent results but that the 24-hour pulse deviated considerably from a one-to-one relation with the sinusoidal distribution and also had the largest spread of data around the average values. The 24-hour pulse also showed an artificial, annual development when compared to the sinusoidal distribution. The pulse of day-time duration was close to linearly related to the sinusoidal distribution, but its value was 10% higher. The pulse using an effective daylength of 75% could, on the other hand, hardly be distinguished from the sinusoidal distribution in terms of resulting evaporation.

Although it was encouraging to see that the complex sinusoidal solution

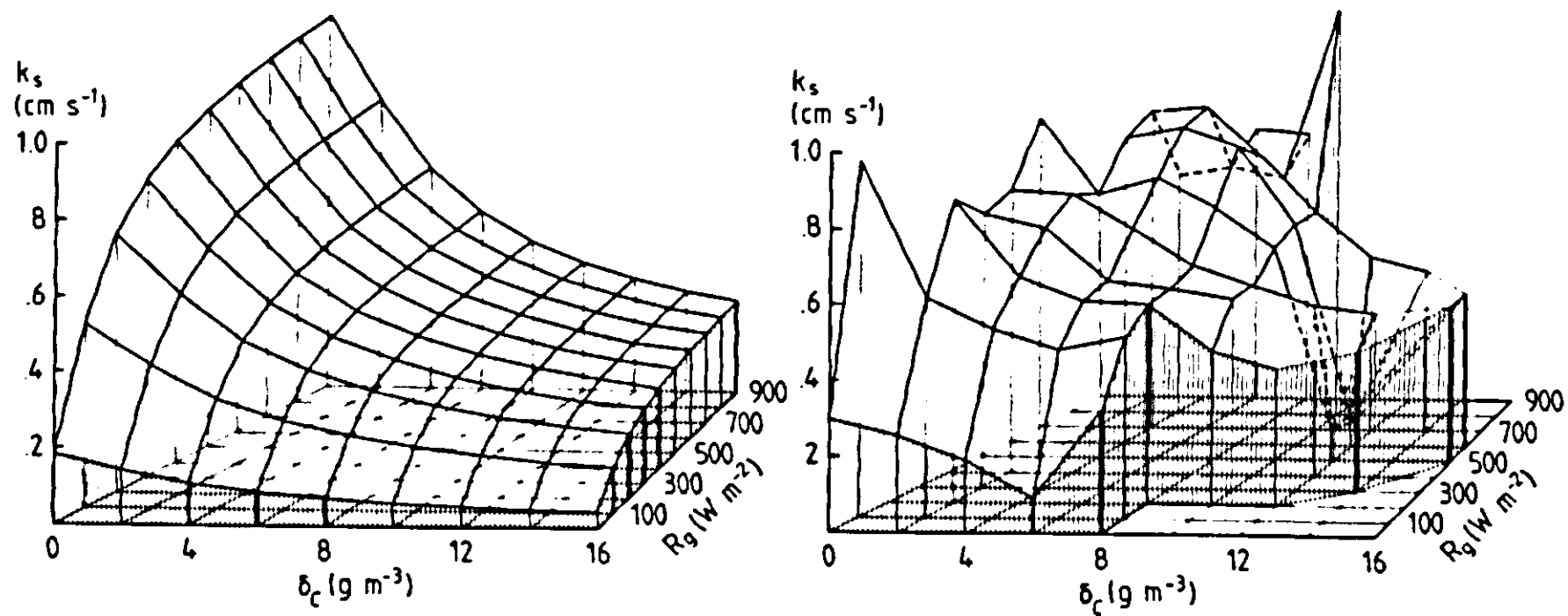


Figure 29. Functional dependence of the stomatal conductance, k_s , on solar radiation, R_g , and vapour concentration deficit, δ_c . Response surface of the Lohammar equation (left) and of measurements in a mature pine forest at Jädraås (right).

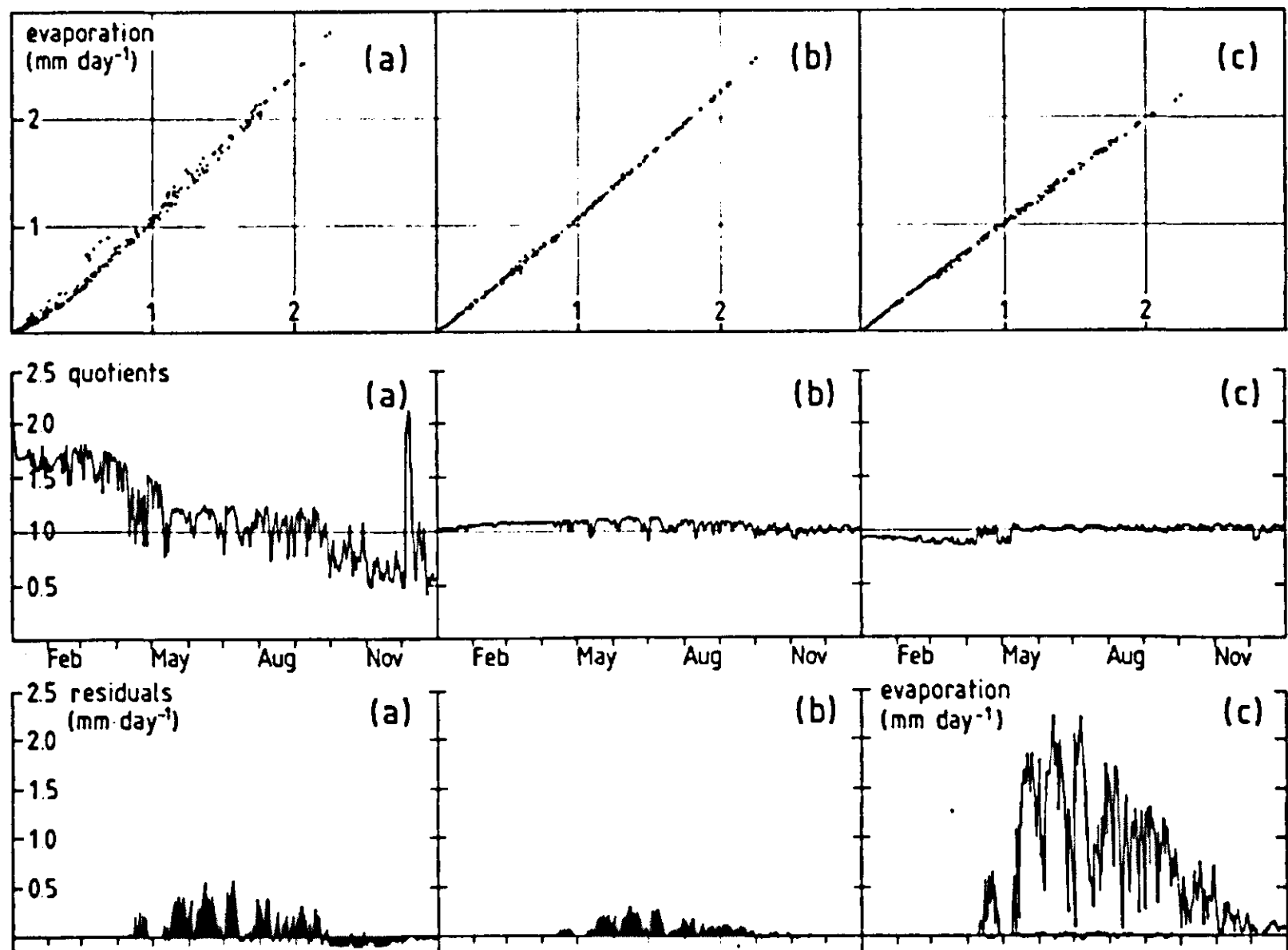


Figure 30. Accumulated 24-hour transpiration for different distributions of driving data. The reference distribution, shown in the lower right corner, is the evaporation using sinusoidally distributed input. The diagrams relate to (a) no distribution at all, i.e., a pulse lasting 24 hours, (b) a pulse with daylength duration and (c) a pulse with an 'effective' daylength of 75% of the astronomical daylength. Top row shows comparison of individual values. Abscissa is sinusoidal and ordinate is pulsed distribution. Middle row shows quotients, and bottom row differences between pulsed and sinusoidally distributed evaporation.

could be replaced by the simple '75% pulse' solution without loss of precision or accuracy, the model had to demonstrate its utility in a comparison with real measurements of evaporation. This was done using a set of hourly micro-meteorological data for evaporation in dry conditions from 9 August to 18 August 1977 (Lindroth & Norén, 1979). In this case, the model was run with an hourly resolution and actual weather data as input. The comparison between measured and simulated data showed reasonable agreement, except when measured evaporation was less than 0.02 mm h^{-1} (Figure 31a). Such low values are measured with a high degree of uncertainty. For some days, measurements were available during the whole day (Figure 31b) and it could be seen that the model produced realistic daytime variations. The simulations confirmed that the model performed well and also pointed to the sensitivity to values of a_l . Lindroth (1985a) calculated the seasonal variation of a_l for this forest. The two values shown in Figure 31b were considered to delimit the correct value of a_l for 10 August 1977.

The interception submodel was tested against data in a mature oak forest at Fontainbleau, using data from two dormant seasons and from two summers (Halldin et al., 1984/85). A constant threshold value was first used for one of the two growing seasons, but gave deviations from less reliable measurements. The measured threshold was remarkably constant over the year for this oak forest, a fact that was attributed to the high wettability of the bark surface, which is exposed only in winter and is shaded in the summer. The threshold for interception water was therefore modelled as proportional to the bark area in the winter and proportional to the leaf area in the summer and with an intermediate value depending on actual a_l over maximum a_l in the period between dormancy and full leaf development. This formulation gave good results for the first two periods tested, but results that were not fully acceptable for the two subsequent periods (Figure 32).

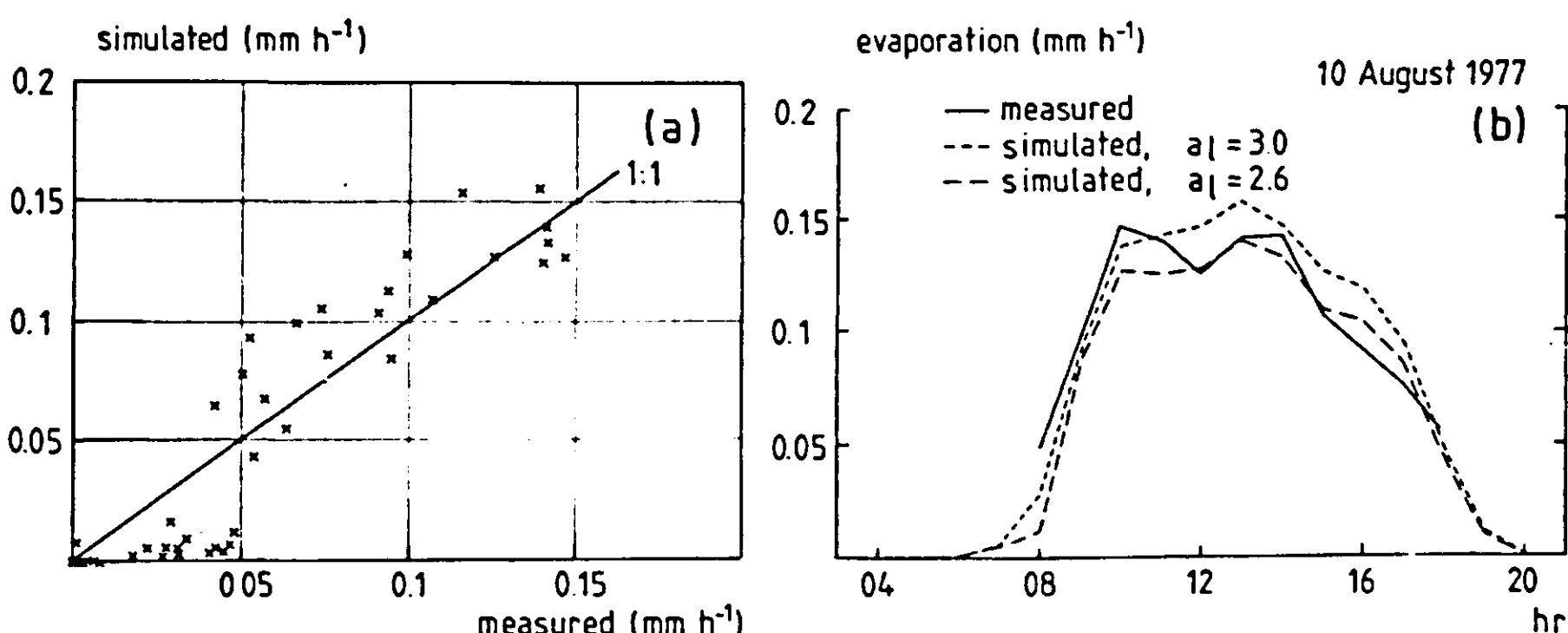


Figure 31. Evaporation, simulated and measured micro-meteorologically above a mature pine forest in Jädraås. (a) Comparison of individual hourly values and (b) daytime variation.

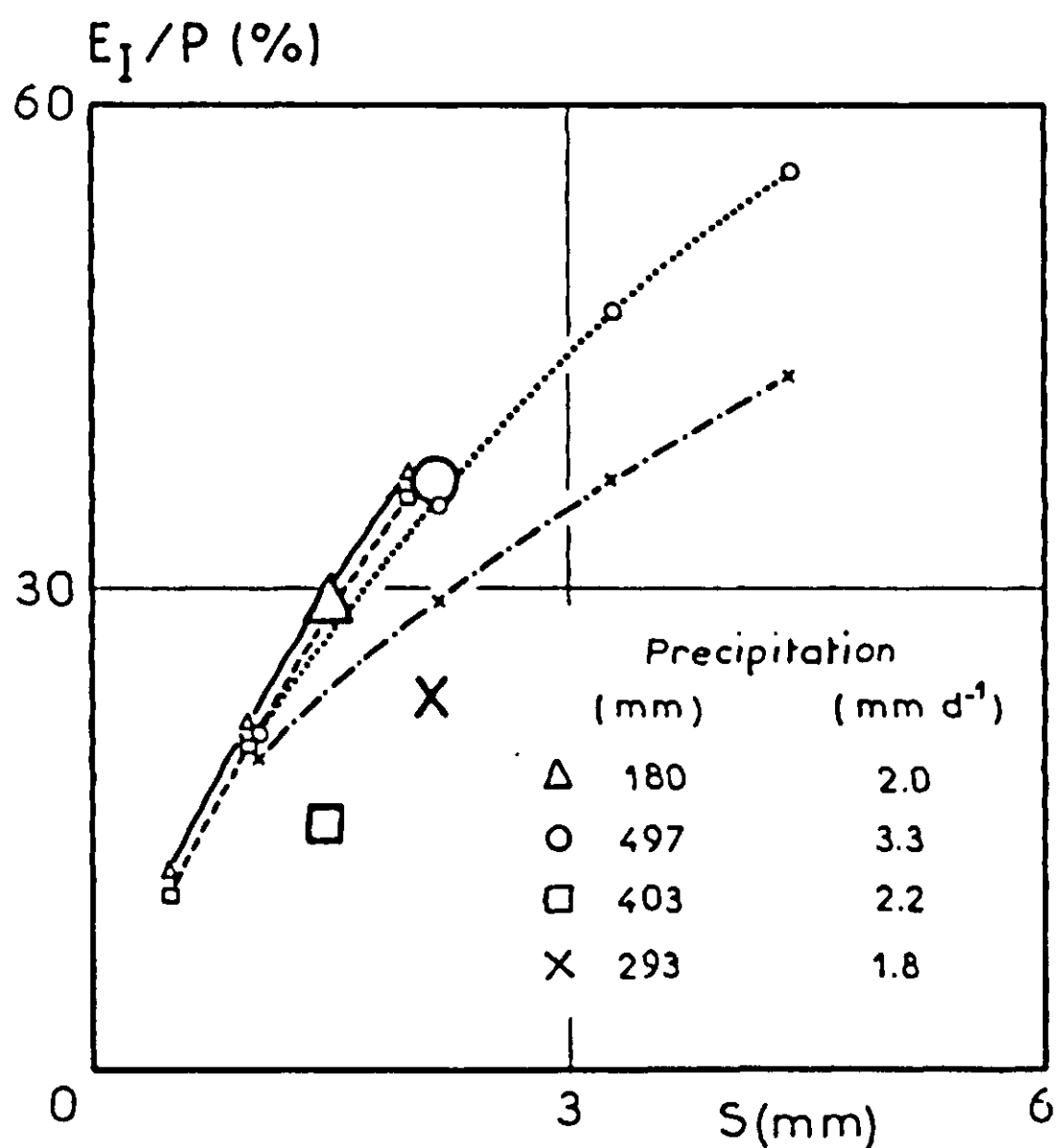


Figure 32. Simulated quotients between accumulated interception evaporation (E_I) and accumulated precipitation (P) in a Fontainbleau oak forest as a function of interception capacity (S). Large symbols represent measurements. Periods were: $\Delta = 29/1 - 23/4$ 1981; $o = 24/4 - 10/10$ 1981; $\square = 21/10$ 1981 – 20/4 1982; $x = 21/4 - 30/9$ 1982 (After Halldin et al., 1984/85).

The first application of the model to a willow stand was for a peatland plantation near the pine forest studied at Jädraås (Grip et al., 1984). Values for the parameters in the Lohammar equation were not available for this stand and the original pine stand values were utilized in combination with a rough estimate of the maximum value of the stomatal conductance. Values for the water-holding properties of the peat were taken from Finnish literature and radiation and rainfall interception properties were estimated explicitly for the stand. The first attempt to validate the model was based on gravimetrically measured soil water contents. Since this comparison of measured and simulated data showed a considerable disparity, a second analysis of soil water content was made, based on the measured groundwater level. The soil water balance measured this way agreed well with the one simulated (Figure 33). Consequently, the difference between the two measurements could be used as a measure of the groundwater leakage from the bog, previously considered negligible.

A final speculation in the paper by Grip et al. (1984) related to the concept of water use efficiency. Based on the assumption of a linear relation between transpiration and growth, growth reduction because of non-potential transpiration was estimated as 2 t dry matter ha^{-1} during the summer of 1983. In the

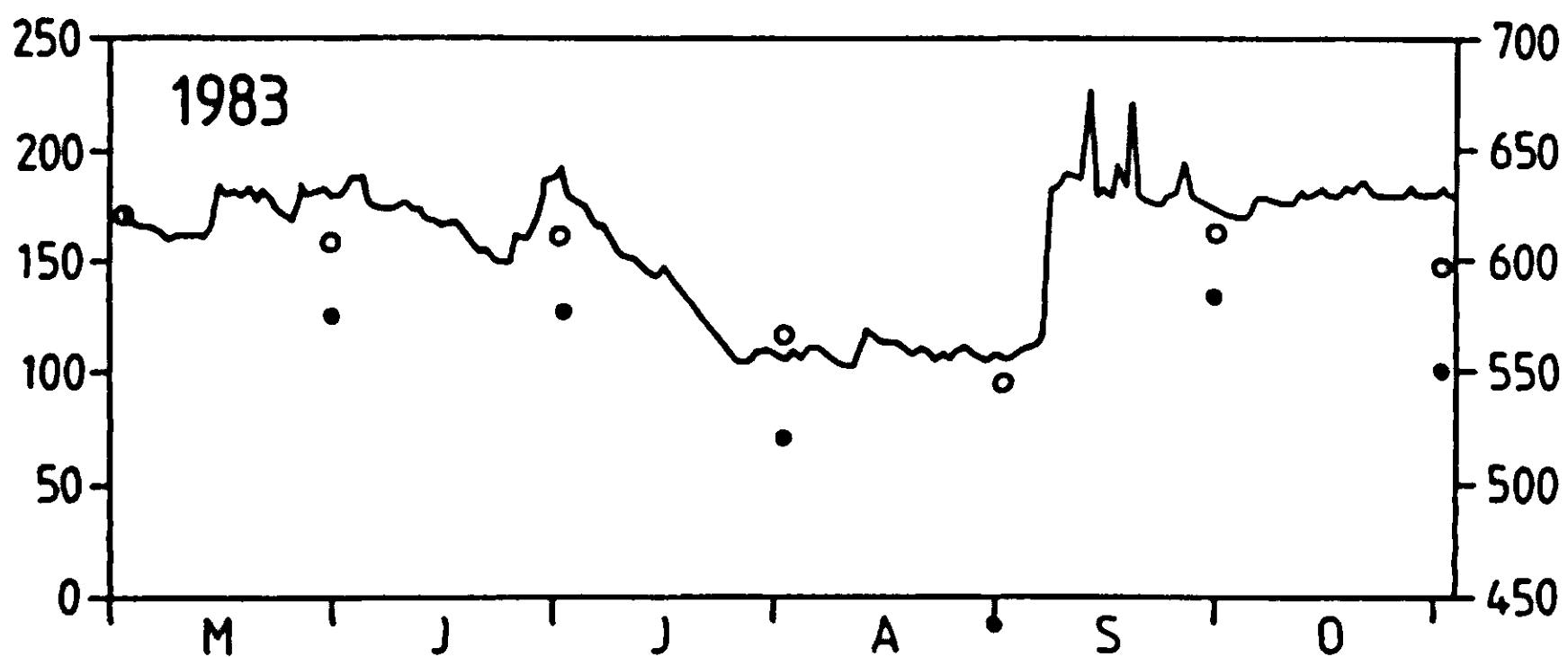


Figure 33. Water storage (mm) in a willow-planted peat soil: simulated (solid line), measured by a gravimetric method (dots) and deduced from a groundwater equilibrium relation (circles). Scales at left (simulation) and right (measurement) relate to different zero levels (After Grip et al., 1984).

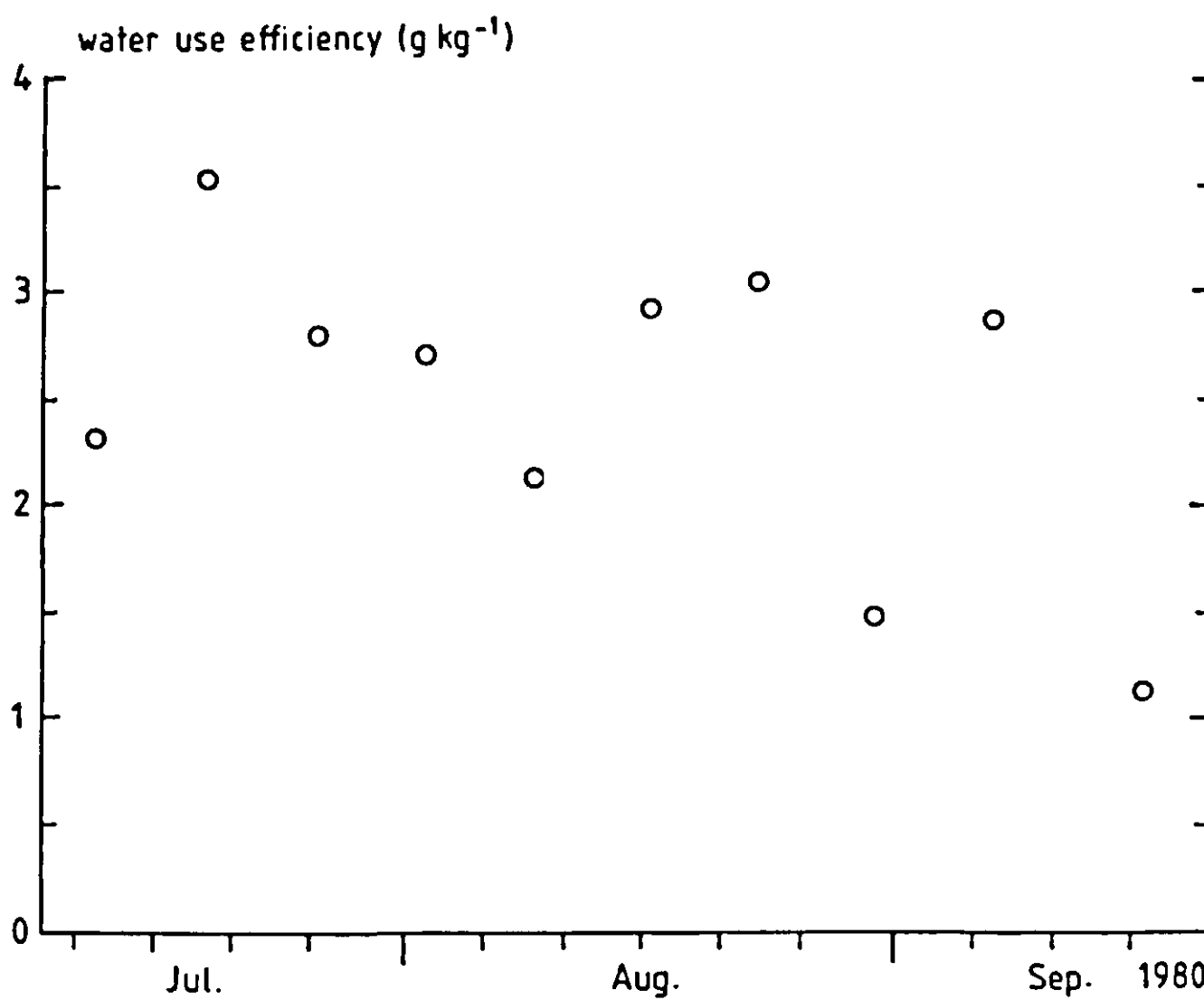


Figure 34. Water use efficiency (as defined by Grip et al., 1984) of willow in a water balance lysimeter at Studsvik.

Studsvik application, where both water balance and growth data were available, it was difficult to interpret the different growth indices calculated by the model (see example in Figure 34) because stand development in the water balance lysimeters differed from that in the surrounding area. This application highlighted the problems of size of lysimeter versus size of vegetation.

10.4 Discussion

The method proposed by the KAUSHA model to integrate momentary relationships into a model based on input data measured only once every 24 hours was shown to give results almost identical with the method using a sinusoidal variation of climatic input data measured during the daytime part of the 24 hours. Fleming (1970) compared evaporation data for all months of the year and from three locations on two continents and concluded that on clear days all daytime distributions could be described by one single distribution, if time was normalized from zero at dawn to one at sunset and if evaporation was normalized as instantaneous rate over daytime average rate. The resulting hyperbolic function lends support to the assumption that, for clear days, climatic input data are well described by a sinusoidal distribution. For cloudy days Fleming's (1970) data are less conclusive; nevertheless, he suggests that a truncated triangle gives a correct form, on average, over the normalized day. It is interesting to note that the average width of this truncated triangle is 76% of the astronomically determined daylength, i.e., is equal to the 'effective' daylength that in the KAUSHA model reproduces the more realistic 'sinusoidal' solution.

A positive practical consequence of this simplified solution is that output data are achieved both in the form of daily totals or averages and in the form of daytime average rates. As such they can easily be compared with instantaneous measurements of evaporation, percolation, interception or any of the climatic input data.

The original requirement when developing the model was that all parameter values be physically identifiable and measurable. This criterion is met by all parameters except the one relating to how much of the plant-available soil water is easily available. This quotient between easily and total available soil water is used frequently in agronomy research. For arable crops it seems to vary as a function of latitude, soil and species. For forest stands, on the other hand, most available data for this quotient seem to fall within the narrow range between 2/3 and 3/4 (see review by Rutter, 1968) and this might explain the relative success in using a 70% fraction in all reported applications of the KAUSHA model.

Of all the parameter values in the model one might suspect that those relating to the Lohammar equation would be most important in determining the output. It is, therefore, somewhat curious that all reported applications of the model have started with the original values from the Jädraås pine forest and in all cases these have given satisfactory results. There are two possible explanations for this. First, that the values from Jädraås are close to those in most of the forests found in northern and temperate climates, and that forest transpiration, which is apparently a conservative process (Roberts, 1983), is based on approximately the same stomatal response for all forests. Second, it may be postulated that the problem of determining the values in the Lohammar equation by using, for

example, gross water balance data, is poorly defined. This could, for instance, be the case if a decrease in k_m (see Equation 62) were approximately compensated for by a decrease in b . This question warrants further study, because simultaneous micro-meteorological and physiological measurements to determine the parameter values are needed both in sufficient quantity and of sufficient quality, and both of these demands seem to be difficult to meet.

The weakest point of the model may well be the formulation of the interception process. Halldin et al. (1984/85) showed that the present formulation might result in less than satisfactory results and that this was most probably the result of not accounting for the precipitation regime. Further development of this part is, however, restricted by the lack of data on the regime and on the spatial variation of precipitation, notably in summertime.

10.5 List of symbols

a_b	= bark area index (total, not projected), ($\text{m}^2 \text{ m}^{-2}$)
a_l	= single-sided leaf area index, ($\text{m}^2 \text{ m}^{-2}$)
b	= constant in Equation 62, ($\text{m}^3 \text{ kg}^{-1}$)
c_p	= specific heat of air at constant pressure, 1005, ($\text{J kg}^{-1} \text{ K}^{-1}$)
d	= zero displacement height, normally $0.75 \cdot h$, (m)
E	= canopy evaporation, (W m^{-2})
E_a	= ventilation component of Penman's formula, (W m^{-2})
E_g	= ground evaporation, (W m^{-2})
h	= stand height, (m)
k	= von Kármán's constant, 0.4, (dimensionless)
k_m	= maximum stomatal conductance in Equations 61 and 62, (m s^{-1})
k_r	= conductance of liquid pathway from soil to evaporating surface in the leaf intercellular space, (s m^{-1})
k_s	= stomatal conductance (per unit single-sided leaf area), (m s^{-1})
R_o	= constant in Equations 61 and 62, (W m^{-2})
R_g	= global shortwave radiation, (W m^{-2})
R_n	= net radiation above stand, (W m^{-2})
R_{ng}	= net radiation below canopy, (W m^{-2})
r_a	= aerodynamic resistance at height z , (s m^{-1})
r_{ds}	= quotient between a_l in lysimeter and surrounding stand (Studsvik application)
r_s	= surface resistance of stand, (s m^{-1})
S_o	= water-holding capacity of stand surface area, (mm)
s_b	= water-holding capacity per unit bark area, a_b , (kg m^{-2})
s_l	= water-holding capacity per unit leaf area, a_l , (kg m^{-2})
u	= wind speed at height z , (m s^{-1})
z	= reference height for measurements above stand, (m)
z_o	= roughness length, normally $0.1 \cdot h$, (m)
α	= net radiation decay parameter in Equation 67, 0.5 (dimensionless)

β	= constant in Equation 61, (m s ⁻¹ Pa ⁻¹)
γ	= psychrometric 'constant', 66, (Pa K ⁻¹)
Δ	= temperature derivative of saturated vapour pressure function, $\partial e_s / \partial t$, (Pa K ⁻¹)
δc	= vapour concentration deficit, (kg m ⁻³)
δe	= vapour pressure deficit at height z , (Pa)
ρ	= density of dry air, 1.2, (kg m ⁻³)
ψ_l	= leaf water potential, (Pa)
ψ_s	= soil water potential, (Pa)

10.6 Source code for the KAUSHA model

The source code for the KAUSHA model is written in FORTRAN 77 and makes use of the SIMP simulation modelling support programs. Please refer to the discussion of this software in the Appendix. The model consists of the main program, followed by the input data preprocessing subroutine KAUBAS, the subroutine ASTRO used to calculate the astronomically determined day-length, given the latitude and, finally, a small function sub-program calculating the saturated vapour pressure, given the air temperature. The model, as presented here, is in the form used for an application based on water balance and biomass data from an experimental willow plantation at Studsvik in 1980 (see Grip, 1981)

SUBROUTINE TRANS

COMMI LAST PRP UPDATE 860325 16:35 PRIOR TO RUN No 20

INTEGER*2 IGO,NCOMP

COMMON/UVAL/ TIME,TIMER,IGO

DIMENSION P(22)

EQUIVALENCE (P,ALPHAR)

COMMON/UVAL/ ALPHAR,ALT ,B ,C1 ,C2 ,C3 ,CORAIN

COMMON/UVAL/ DH ,FWEA,K0 ,LATDEG,LATMIN,LYSNO,OPTSTD

COMMON/UVAL/ RG1 ,RG2 ,RIS0 ,SB ,SL ,VMAX ,VMIN

COMMON/UVAL/ Z0H

COMMON/UVAL/ PDUMMY(148)

REAL K0 ,LATDEG,LATMIN,LYSNO

COMMON/UVAL/ NCOMP

DIMENSION X(2)

EQUIVALENCE (X(1),X01)

COMMON/UVAL/ X01,X02

DIMENSION T(4)

EQUIVALENCE (T,T0001)

COMMON/UVAL/ T0001,T0100,T0102,T0200

COMMON/UVAL/ G(240)

COMMON/UVAL/ D(10)

CEND1

```
INTEGER*2 IDUM
COMMON/MCON/ IDUM,TSTART,TEND
  REAL LV,LV0,NL,LAI,LAT(2),LP,LDW,LDWOLD,MTB,MTE
  REAL INFIL1,INFILD,INFIL2,INFILT,INTERD,KS
  REAL SUM(3),YAG(3),YS(3)
  SAVE IERR
  INTEGER ID(5)
  DATA ID/5,6,7,8,9/
```

C

C ****

C***** MNEMONIC AND SIMP EQUIVALENCES *****

C ****

C

FOR STATE VARIABLES

C

EQUIVALENCE

I (WINT ,X01),(WSOIL ,X02)

C

FOR FLOWS

C

EQUIVALENCE

I (PRECS ,T0001),(EVAP ,T0100),(INFILT,T0102),(WLOSS ,T0200)

C

FOR AUXILIARY VARIABLES (GROUP 1)

C

EQUIVALENCE

I (ET ,G(1)),(PERCOL,G(2)),(RA ,G(3)),(RAT ,G(4))

2,(RS ,G(5)),(SPEPD ,G(6)),(SR ,G(7)),(SWR ,G(8))

3,(TRANSP,G(9))

C

FOR AUXILIARY VARIABLES (GROUP 2)

C

EQUIVALENCE

I (CET ,G(10)) ,(CETM ,G(11)) ,(CONDN ,G(12)) ,(DED ,G(13))

2,(EAD ,G(14)) ,(ERR ,G(15)) ,(ETM ,G(16)) ,(ETS ,G(17))

3,(EVAPD ,G(18)) ,(INFIL1, G(19)) ,(INFIL2 ,G(20)) ,(INFILD ,G(21))

4,(INTERD ,G(22)) ,(LDW ,G(23)) ,(LP ,G(24)) ,(MTB ,G(25))

5,(MTE ,G(26)) ,(PEVAPD ,G(27)) ,(PRECD ,G(28)) ,(RISD ,G(29))

6,(RNTB ,G(30)) ,(RNTD ,G(31)) ,(RNTN ,G(32)) ,(S0 ,G(33))

7,(SBAI ,G(34)) ,(SDW ,G(35)) ,(SLAI ,G(36)) ,(SP ,G(37))

8,(STR ,G(38)) ,(TRANSD ,G(39)) ,(USTRAN ,G(40)) ,(VCDD ,G(41))

9,(WINT1 ,G(42)) ,(WINTD ,G(43)) ,(YS ,G(44)) ,(YAG ,G(47))

C

C FOR AUXILIARY VARIABLES (GROUP 3)

C

EQUIVALENCE

1 (CE ,G(50)) ,(CETMOL ,G(51)) ,(CETOLD ,G(52)) ,(DE ,G(53))
2,(DELTA ,G(54)) ,(DIM ,G(55)) ,(DL ,G(56)) ,(EAP ,G(57))
3,(ES ,G(58)) ,(ETP ,G(59)) ,(GAMMA ,G(60)) ,(KS ,G(61))
4,(LDWOLD,G(62)) ,(LV ,G(63)) ,(NL ,G(64)) ,(PA ,G(65))
5,(PL ,G(66)) ,(PRA ,G(67)) ,(PRECN1 ,G(68)) ,(PRECN2 ,G(69))
6,(RDS ,G(70)) ,(SDWOLD ,G(71)) ,(TK ,G(72)) ,(TIMOLD ,G(73))
7,(VCD ,G(74)) ,(VCS ,G(77)) ,(SUM ,G(76)) ,(Z0 ,G(79))

C

C FOR DRIVING VARIABLES

C

EQUIVALENCE

1 (HR ,D(1)) ,(TA ,D(2)) ,(RIS ,D(3)) ,(RNT ,D(4))
2,(U ,D(5)) ,(PRI ,D(6)) ,(H ,D(7)) ,(LAI ,D(8))
3,(BAI ,D(9))

C

C FOR PARAMETERS

C

EQUIVALENCE

1 (LAT(1),LATDEG),(LAT(2),LATMIN)

C

C***** PHYSICAL CONSTANTS *****

C

DATA	GAMMA0/64.6/
	PSYCHROMETRIC CONSTANT <PA/K>
DATA	LV0/2.501E6/
	HEAT OF VAPOURIZATION <J/KG>
DATA	PA0/101300./
	MEAN AIR PRESSURE AT SEA LEVEL <PA>
DATA	PI/3.14159262/
	HALF CIRCUMFERENCE OF UNIT CIRCLE <RAD>
DATA	RM/461.51/
	GAS CONSTANT FOR WATER VAPOUR <J/KG*K>
DATA	TC/86400./
	TIME CONVERSION <SEC/DAY>

C

C***** READ INPUT DATA *****

C INPUT DATA SHOULD BE: RELATIVE HUMIDITY (%)
C AIR TEMPERATURE (DEG. CELSIUS)
C SHORTWAVE RADIATION (W/M²)
C NET RADIATION (W/M²)
C WIND SPEED (M/S)
C PRECIPITATION AND IRRIGATION (MM/24 H)
C STAND HEIGHT (M)
C PROJECTED LEAF AREA INDEX (M²/M²)
C TOTAL BARK AREA INDEX (M²/M²)
C BIOMASS MEASUREMENT INDICATOR (-)
C

CALL KAUBAS(CETM,MTB,MTE,SDW,LDW,CORAIN,RG1,RG2,LYSNO)

C *****
C *****
C ***** DAYLENGTH AND OTHER BASIC ENTITIES *****
C *****
C

CALL ASTRO(TIME,LAT,RISP,DL)
DL=DL/24.
PL=C3*DL
NL=(1.-PL)/2.
DELTA=SVP(TA+0.5)-SVP(TA-0.5)
PA=PA0-11.2*ALT
GAMMA=GAMMA0*PA/PA0*(1.+0.001*TA)
LV=LV0*(1.-0.000952*TA)
TK=TA+273.16
DIM=LV/(RM*TK)

C *****
C *****
C ***** INPUT DATA TO MODEL *****
C *****
C

ES=SVP(TA)
VCS=ES/(RM*TK)
DE=ES*(1.-HR/100.)/C1
VCD=VCS*(1.-HR/100.)/C2
RNTD=AMAX1(0.,RNT/PL)
RNTN=0. C
RNTN=AMIN1(0.,RNT/NL)
RISD=RIS/PL
RDS=AMAX1(0.,AMIN1(1.,1.073-0.00207*MOD(TIME,365.)))
RAT=EXP(-ALPHAR*(LAI+BAI/PI)/RDS)
RNTB=RAT*RNTD

```

IF(NINT(OPTSTD).GE.1) THEN
    LAI=OPTSTD*LAI/RDS
    BAI=OPTSTD*BAI/RDS
ENDIF
DED=DE/PL
VCDD=VCD/PL
PRECD=PRI
PRECN1=0.
PRECN2=0.
PRECS=PRECD+PRECN1+PRECN2
Z0=AMAX1(0.01,Z0H*H)
PRA=(ALOG((H+2.-DH*H)/Z0)/0.4)**2
C
C
C***** END OF DATA INPUT SECTION *****
C
C
C***** RESISTANCES *****
C
C
C
RA=PRA/U
KS=RISD/(RISD+RIS0)*K0/(1.+B*VCDD)
RS=0.
IF(KS*LAI.GT.0.) RS=1./(LAI*KS)
C
C
C***** POTENTIAL TRANSPERSION *****
C
C
C
EAD=DIM*DED/RA
USTRAN=0.
IF(LAI.LE.0.) GO TO 20
USTRAN=(DELTA*(RNTD-RNTB)+GAMMA*EAD)/(DELTA+GAMMA*
(1.+RS/RA))
USTRAN=USTRAN*TC/LV
C
C
C***** COMBINATION EQUATION *****
C
C
20 PEVAPD=(DELTA*(RNTD-RNTB)+GAMMA*EAD)/(DELTA+GAMMA)
CONDN=DELTA*RNTN/(DELTA+GAMMA)

```

```

PEVAPD=PEVAPD*TC/LV
CONDN=CONDN*TC/LV
PEVAPD=AMAX1(0.,PEVAPD)
CONDN=-AMINI(0.,CONDN)

C
C
C***** SOIL EVAPORATION *****
C
C
SPEPD=1.26*DELTA*RNTB/(DELTA+GAMMA)
SPEPD=SPEPD*TC/LV
SPEPD=AMAX1(0.,SPEPD*PL)

C
C
C***** INTERCEPTION WATER BALANCE *****
C
C
SLAI=SL*LAI
SBAI=SB*BAI
S0=SLAI+SBAI
INFIL1=AMAX1(0.,WINT+PRECN1+NL*CONDN-S0)
WINT1=WINT+PRECN1+NL*CONDN-INFIL1

C
C**** FROM MIDNIGHT TO SUNRISE
C
INFILD=AMAX1(0.,WINT1+PRECD-S0)
INTERD=WINT1+PRECD-INFILD
EVAPD=AMINI(INTERD,PL*PEVAPD)
WINTD=INTERD-EVAPD

C
C**** DURING DAYLIGHT
C
INFIL2=AMAX1(0.,WINTD+PRECN2+NL*CONDN-S0)

C
C**** FROM SUNSET TO MIDNIGHT
C
INFILT=INFIL1+INFILD+INFIL2
EVAP=EVAPD-2.*NL*CONDN
EVAPD=EVAPD/PL

C
SR=0.
IF(PEVAPD.GT.0.) SR=1.-AMINI(1.,INTERD/(PL*PEVAPD))
STR=0.
IF(EVAPD.GT.0.AND.USTRAN.GT.0.) STR=PEVAPD/USTRAN

```

```

C
C
C***** SOIL WATER BALANCE *****
C
C
C
SWR=AMIN1(I.,AMAX1(0.,(WSOIL-VMIN)/((I.-FWEA)*(VMAX-VMIN))))
TRANSD=SR*SWR*USTRAN
TRANSP=PL*TRANSD
PERCOL=AMAX1(0.,WSOIL-TRANSP-SPEPD-VMAX)
WLOSS=TRANSP+PERCOL+SPEPD
C
C
C***** EVAPOTRANSPIRATION *****
C
C
C
ET=EVAP+TRANSP+SPEPD
C
C
C***** PENMAN EVAPORATION *****
C
C
C
EAP=0.00263*(1.+0.526*U)*DE
ETP=(DELTA*RNT*TC/LV+GAMMA*EAP)/(DELTA+GAMMA)
C
C
C***** YIELD CALCULATIONS *****
C
C
C
SUM(1)=SUM(1)+TRANSP
IF(DE.GT.0.) SUM(2)=SUM(2)+TRANSP/DE
F(RS.GT.0.) SUM(3)=SUM(3)+SR*SWR/RS
IF(TIME.EQ.TSTART) GO TO 15
IF(TIME.EQ.TEND) GO TO 5
IF(NINT(MTB).EQ.0) GO TO 30
5 SP=SDW-SDWOLD
LP=LDW-LDWOLD
SUM(1)=SUM(1)-TRANSP
IF(DE.GT.0.)
SUM(2)=SUM(2)-TRANSP/DE
IF(RS.GT.0.) SUM(3)=SUM(3)-SR*SWR/RS
DO 10 I=1,3
YS(I)=0.
IF(SUM(I).GT.0.) S(I)=SP/SUM(I)
YAG(I)=0.

```

```

10  IF(SUM(I).GT.0.) YAG(I)=(SP+LP)/SUM(I)
15  SDWOLD=SDW
  LDWOLD=LDW
  SUM(1)=TRANSP
  SUM(2)=0.
  IF(DE.GT.0.) SUM(2)=TRANSP/DE
  SUM(3)=0.
  IF(RS.GT.0.) SUM(3)=SR*SWR/RS
C
C
C***** VALIDATION CALCULATIONS *****
C***** *****
C
30  IF(TIME.EQ.TSTART) CE=CETM
  CET=CE
  CE=CE+ET
  IF(TIME.EQ.TSTART) GO TO 35
  IF(TIME.EQ.TEND) GO TO 25
  IF(NINT(MTE).EQ.0) RETURN
25  ETM=(CETM-CETMOL)/(TIME-TIMOLD)
  ETS=(CET-CETOLD)/(TIME-TIMOLD)
  ERR=ERR+(CET-CETM)**2
  IERR=IERR+1
35  CETMOL=CETM
  CETOLD=CET
  TIMOLD=TIME
  RETURN
C
C
C***** INITIAL CALCULATIONS *****
C***** *****
C
C
  ENTRY INITL
  CALL ECDCID(5,ID)
  IERR=0.
  ERR=0.
  RETURN
C
C
C***** FINAL CALCULATIONS *****
C***** *****

```

```
ENTRY TERMIN
ERR=SQRT(ERR)/IERR
RETURN
END
```

```
SUBROUTINE
KAUBAS(CETM,MTB,MTE,SDW,LDW,CORAIN,RG1,RG2,LYSNO)
```

C

```
REAL A(24),LAI,MT,LDW,LYSNO
```

```
INTEGER*2 IDUM1,IDUM2
```

```
COMMON/UVAL/ TIME,DUM1,IDUM1,DUM2(170),IDUM2,DUM3(246),D(10)
```

C

```
EQUIVALENCE
```

```
1 (HR ,D(1)) ,(TA ,D(2)) ,(RIS ,D(3)) ,(RNT ,D(4))
2,(U ,D(5)) ,(PRI ,D(6)) ,(H ,D(7)) ,(LAI ,D(8))
3,(BAI ,D(9))
```

C

C UNITS FOR INPUT DATA: RELATIVE HUMIDITY (%)

C AIR TEMPERATURE (DEG. CELSIUS)

C GLOBAL RADIATION (W/ M2)

C WIND SPEED (M/S)

C BIOMASS MEASUREMENT INDICATOR (-)

C EVAPORATION DATA INDICATOR (-)

C (FOR EACH LYSIMETER) PRECIPITATION + IRRIGATION (MM/24 H)

C (FOR EACH LYSIMETER) STAND HEIGHT (CM)

C (FOR EACH LYSIMETER) ONESIDED LEAF AREA INDEX (M2/M2)

C (FOR EACH LYSIMETER) STEM DRY WEIGHT (TON/HA)

C (FOR EACH LYSIMETER) LEAF DRY WEIGHT (TON/HA)

C (FOR EACH LYSIMETER) EVAPOTRANSPIRATION (MEASURED) (MM/24 H)

C

```
LNO=NINT(LYSNO)
```

```
CALL ECDCDA(TIME+0.5,A)
```

```
CALL ECDCDD(TIME,1.,5,MTB)
```

```
CALL ECDCDD(TIME,1.,6,MTE)
```

```
CALL ECDCDD(TIME,1.,7,A(7))
```

```
CALL ECDCDD(TIME,1.,8,A(8))
```

```
CALL ECDCDD(TIME,1.,9,A(9))
```

C

```
HR=AMIN1(100.,A(1))
```

```
TA=A(2)
```

```
RIS=AMAX1(0.,A(3))
```

```
RNT=RG1+RG2*RIS
```

```
U=AMAX1(A(4),.001)
PRI=A(6+LNO)*CORA1N
H=A(9+LNO)/100.
LAI=A(12+LNO)
SDW=A(15+LNO)
BAI=-0.1349+0.47937*SDW**0.43315
IF(SDW.LT.0.66) BAI=0.4023*SDW
LDW=A(18+LNO)
CETM=A(21+LNO)
```

C

```
RETURN
END
```

SUBROUTINE ASTRO(TIME,LAT,RISET,DL)

```
C
C This is a FORTRAN realization by Sven Halldin,
C 3 March 1985, of a set of equations proposed by:
C Z.J. Svehlik, 1979, Approximating equations for space-time
C estimates of the extraterrestrial radiation and evaporation.
C Extended abstract of a paper presented at the Sixth Annual
C EGS Meeting, Vienna, 11-14 September 1979.
```

C

C Symbol definitions:

=====

C

```
C DELTA = Sun's declination <degrees>
C DL = Possible sunshine duration <hours>
C LAT(1) = Latitude <whole degrees>
C LAT(2) = Latitude <minutes fraction>
C OMEGA = Hour angle at zero sun's altitude <degrees>
C PSI = Latitude <degrees, decimal fraction>
C RISET = Extraterrestrial radiation <MJ/m2*day>
C RO = Radius vector of the earth <A.U.>
C DAYNR = Daynumber after 1 January
```

C

```
REAL LAT(2)
DATA PI/3.141593/
C Half circumference of unit circle
DATA C/37.22/
C Numeric parameter in equation for RISET
```

C

```
DAYNR=INT(MOD(TIME,365.))
IF(DAYNR.LT.94.) A=PI*(DAYNR+266.8)/180.
```

```

IF(DAYNR.GE.94..AND.DAYNR.LE.278.) A=PI*(DAYNR-93.2)/185.
IF(DAYNR.GT.278) A=PI*(DAYNR-98.3)/180.
RO=1.+0.01675*SIN(A)
IF(DAYNR.LT.80.) B=PI*(DAYNR+278.)/178.6
IF(DAYNR.GE.80..AND.DAYNR.LE.266.) B=PI*(DAYNR-80.)/186.
IF(DAYNR.GT.266.) B=PI*(DAYNR-87.)/180.
DELTA=PI*(23.45*SIN(B))/180.
PSI=PI*(LAT(1)+LAT(2)/60.)/180.
X=-TAN(PSI)*TAN(DELTA)
IF(X.GT.1.) OMEGA=0.
IF(X.LT.-1.) OMEGA=PI
IF(ABS(X).LE.1.) OMEGA=ACOS(X)
DL=24./PI*OMEGA
RISET=C/RO**2*(OMEGA*SIN(PSI)*SIN(DELTA)+  

ISIN(OMEGA)*COS(PSI)*COS(DELTA))

```

C

RETURN

END

FUNCTION SVP(T)

C THIS FUNCTION COMPUTES THE SATURATION VAPOUR PRESSURE
C DEPENDING ON TEMPERATURE.

K1=2.

C IF K1=2., THE PRESSURE WILL BE IN PASCAL, IF K1=0. THE PRESSURE
C WILL BE IN MBAR.

IF(T) 1,2,2

1 SVP=10.**(K1+10.5553-2667./(273.16+T))

RETURN

2 SVP=10.**(K1+9.4051-2353./(273.16+T))

RETURN

END

10.7 Acknowledgements

The author is grateful to Mr. T. Lohammar for his initial cooperation in developing the equation bearing his name, to Dr. L-O. Nilsson for supplying biomass data in the Studsvik application and to Dr. H. Grip and Dr. A. Lindroth for valuable comments during the work. Figure 32 and Figure 33 are reproduced by kind permission of Elsevier Science Publishers and the Swedish University of Agricultural Sciences, respectively.

10.8 References

Calder, I.R., Harding, R.J. & Rosier, P.T.W., 1983. An objective assessment of soil-moisture deficit models. Journal of Hydrology 60:329-355.

Dunin, F.X., Aston, A.R. & Reyenga, W., 1978. Evaporation from a Themeda grassland. II. Resistance model of plant evaporation. *Journal of Applied Ecology* 15:847-858.

Eckersten, H., 1985. Transpiration of *Salix* simulated with low and high time resolution weather data. In: *Research Reports, Biotechnical Faculty, University E.K. of Ljubljana, Supplement 10*, pp. 49-55.

Eckersten, H., 1986. Simulated willow growth and transpiration: The effect of high and low resolution weather data. *Agricultural and Forest Meteorology* 38:289-306.

Feddes, R.A., Kowalik, P.J. & Zaradny, H., 1978. *Simulation of Field Water Use and Crop Yield. Simulation Monographs*. Pudoc, Wageningen, 189 pp.

Fleming, P.M., 1970. A diurnal distribution function for daily evaporation. *Water Resources Research* 6:937-942.

Gash, J.H.C. & Stewart, J.B., 1975. The average surface resistance of a pine forest derived from Bowen ratio measurements. *Boundary-Layer Meteorology* 8:453-464.

Grip, H., 1981. *Evapotranspiration Experiments in Salix Stands. Report 15*, 29 pp. Swedish University of Agricultural Sciences, Section of Energy Forestry, Uppsala.

Grip, H., Halldin, S., Lindroth, A. & Persson, G., 1984. Evapotranspiration from a willow stand on wetland. In: K.L. Perttu, (Ed.): *Ecology and management of forest biomass production systems. Report 15*, pp. 47-61. Swedish University of Agricultural Sciences, Department of Ecology and Environmental Research, Uppsala.

Halldin, S. & Grip, H., 1979. Actual forest transpiration by a simple model. Abstract. *EOS (Transactions, American Geophysical Union)* 60(32):580.

Halldin, S., Saugier, B. & Pontailler, J.Y., 1984/85. Evapotranspiration of a deciduous forest. Simulation using routine meteorological data. *Journal of Hydrology* 75:323-341.

Impens, I. & Lemeur, R., 1969. Extinction of net radiation in different crop canopies. *Archiv für Meteorologie, Geophysik und Bioklimatologie, Serie B*, 17:403-412.

Jackson, R.D., Hatfield, J.L., Reginato, R.J., Idso, S.B. & Pinter, Jr., P.J., 1983. Estimation of daily evapotranspiration from one-time-of-day measurements. *Agricultural Water Management* 7:351-362.

Lindroth, A., 1985a. Canopy conductance of coniferous forests related to climate. *Water Resources Research* 21:297-304.

Lindroth, A., 1985b. Effects of within and between seasonal variations of needle area on pine forest evapotranspiration. In: *Research Reports, Biotechnical Faculty University E.K. of Ljubljana, Supplement 10*, pp. 29-38.

Lindroth, A. & Halldin, S., 1986. Numerical analysis of pine forest evaporation and surface resistance. *Agricultural and Forest Meteorology* 38:59-79.

Lindroth, A. & Norén, B., 1979. Evapotranspiration measurements in Jädraås. Instrumentation, data gathering and processing. In: S. Halldin, (Ed.): *Comparison of Forest Water and Energy Exchange Models*. Elsevier Scientific Publishing Company, Amsterdam - Oxford - New York, pp. 15-26.

Lohammar, T., Larsson, S., Linder, S. & Falk, S., 1980. FAST - Simulation models of gaseous exchange in Scots pine. In: T. Persson, (Ed.): *Structure and function of*

northern coniferous forests – An ecosystem study. *Ecological Bulletins* (Stockholm) 32:505-523.

Penman, H.L., 1948. Natural evaporation from open water, bare soil and grass. Royal Society of London, *Proceedings Series A* 193:120-145.

Penman, H.L., 1953. The physical basis of irrigation control. In: P.M. Synge, (Ed.): *Report of the Thirteenth International Horticultural Congress 1952, Volume Two*. London, The Royal Horticultural Society, pp. 913-924.

Persson, T. (Ed.), 1980. Structure and function of northern coniferous forests – An ecosystem study. *Ecological Bulletins* (Stockholm) 32, 609 pp.

Priestly, C.H.B. & Taylor, R.J., 1972. On the assessment of surface heat flux and evaporation using large-scale parameters. *Monthly Weather Review* 100:81-92.

Roberts, J., 1983. Forest transpiration. A conservative hydrological process? *Journal of Hydrology* 66:133-141.

Rutter, A.J., 1968. Water consumption by forests. In: T.T. Kozlowski (Ed.): *Water Deficit and Plant Growth, Volume II. Plant Water Consumption and Response*. New York, Academic Press, pp. 23-84.

Saugier, B., Halldin, S., Pontailler, J.Y. & Nizinski, G., 1985. Bilan hydrique de forêts de chêne et de hêtre à Fontainebleau. *Revue du Palais de la Decouverte* 13:187-200.

Spittlehouse, D.L. & Black, T.A., 1981. A growing season water balance model applied to two Douglas fir stands. *Water Resources Research* 17:1651-1656.

Stewart, J.B., 1977. Evaporation from the wet canopy of pine forest. *Water Resources Research* 13:915-921.

11 Simulated water balance of a willow stand on clay soil

Gunn Persson and Per-Erik Jansson

11.1 Introduction

Quantitative knowledge of the water balance components of willow stands is necessary when developing farming practices aiming at high biomass production. Few hydrological studies have been done on willow stands. Evapotranspiration from a stand on a raised bog was calculated by the water balance method and by a model (Grip et al., 1984). Small lysimeters (1 m^2) within a willow stand were used by Grip (1981) when calculating evapotranspiration by the water balance method. Most highly productive willow stands are limited to small plots, which means that the traditional hydrological 'watershed' methods are not applicable. Estimations of the water balance of small plots thus require detailed information on the soil moisture storage.

The present chapter, which deals with water balance estimates from a clay soil, is based on a soil moisture study. The measurements are evaluated using a physically based soil water model (Jansson & Halldin, 1979) giving the flow components, such as evapotranspiration and percolation, as output. This model is now also available on IBM-compatible PC. The authors can be contacted for further information. Uncertainties in parameter values for soil and plant properties, such as soil description, root distribution, and surface resistance are evaluated. Evapotranspiration is estimated, and possible errors in the estimate caused by uncertainty in soil and plant properties are discussed.

11.2 Site and measurements

The field site was located at Ultuna ($59^{\circ}49'N$, $17^{\circ}40'E$, alt. 5 m) about 5 km south of Uppsala (Figure 35). The stand included different willow clones, mainly *Salix viminalis*. The field, 0.6 ha, was planted with 2 cuttings m^{-2} in the spring of 1981 and the shoots were cut back in the winter of 1981-82. At the beginning of the 1983 growing season the shoots in the studied area of the field were one year old (Figure 35).

The soil is a clay sediment with an upper layer of about 70 cm of postglacial material, underlain by a glacial material down to about 3 m. The postglacial material is described as a heavy clay with a clay content of 30-45% (Olsson & Samils, 1984). The area has been used as arable land for a long time. The soil allows good root penetration and growth. Earthworm burrows and root channels allow favourable soil aeration and drainage (Johansson, 1983).

Thirty-two tensiometers with mercury manometers (Soil Moisture Equipment, St. Barbara, USA) were installed in four lines at 15, 30, 45 and 60 cm

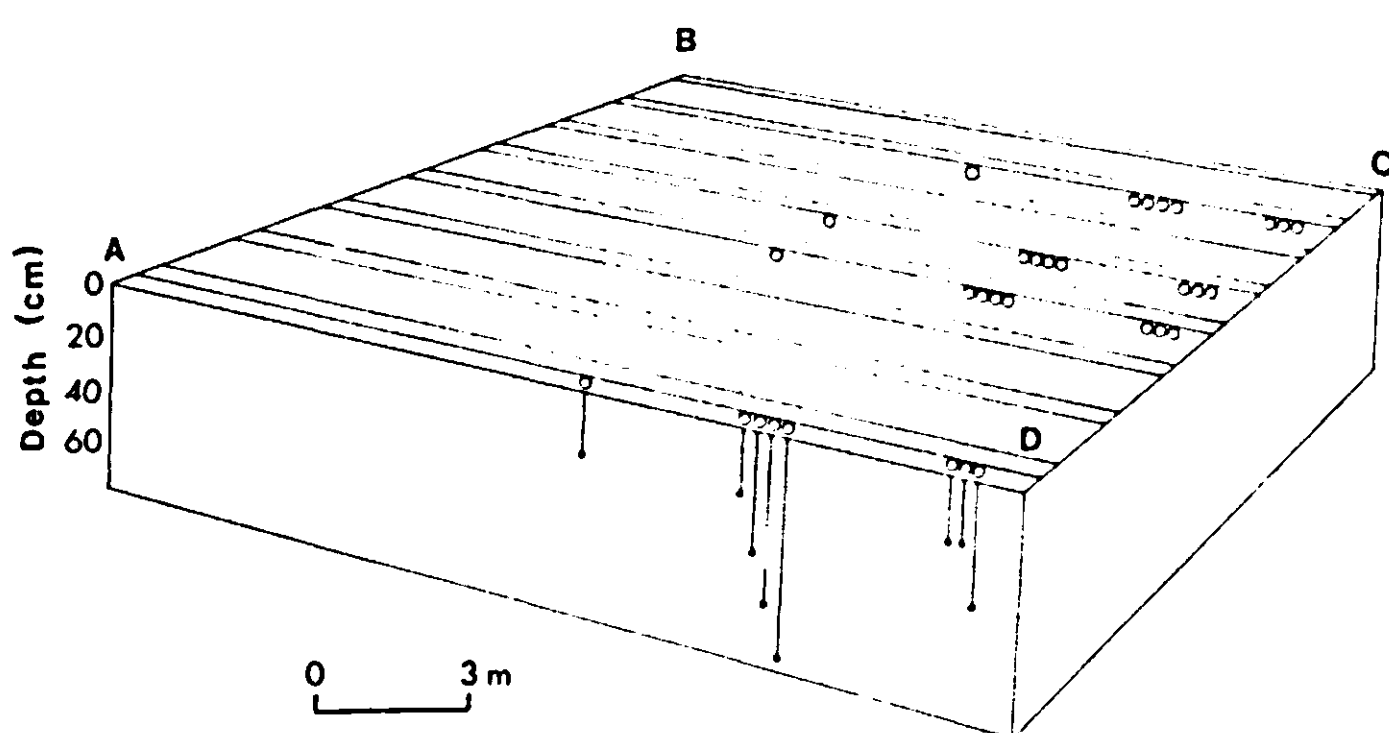
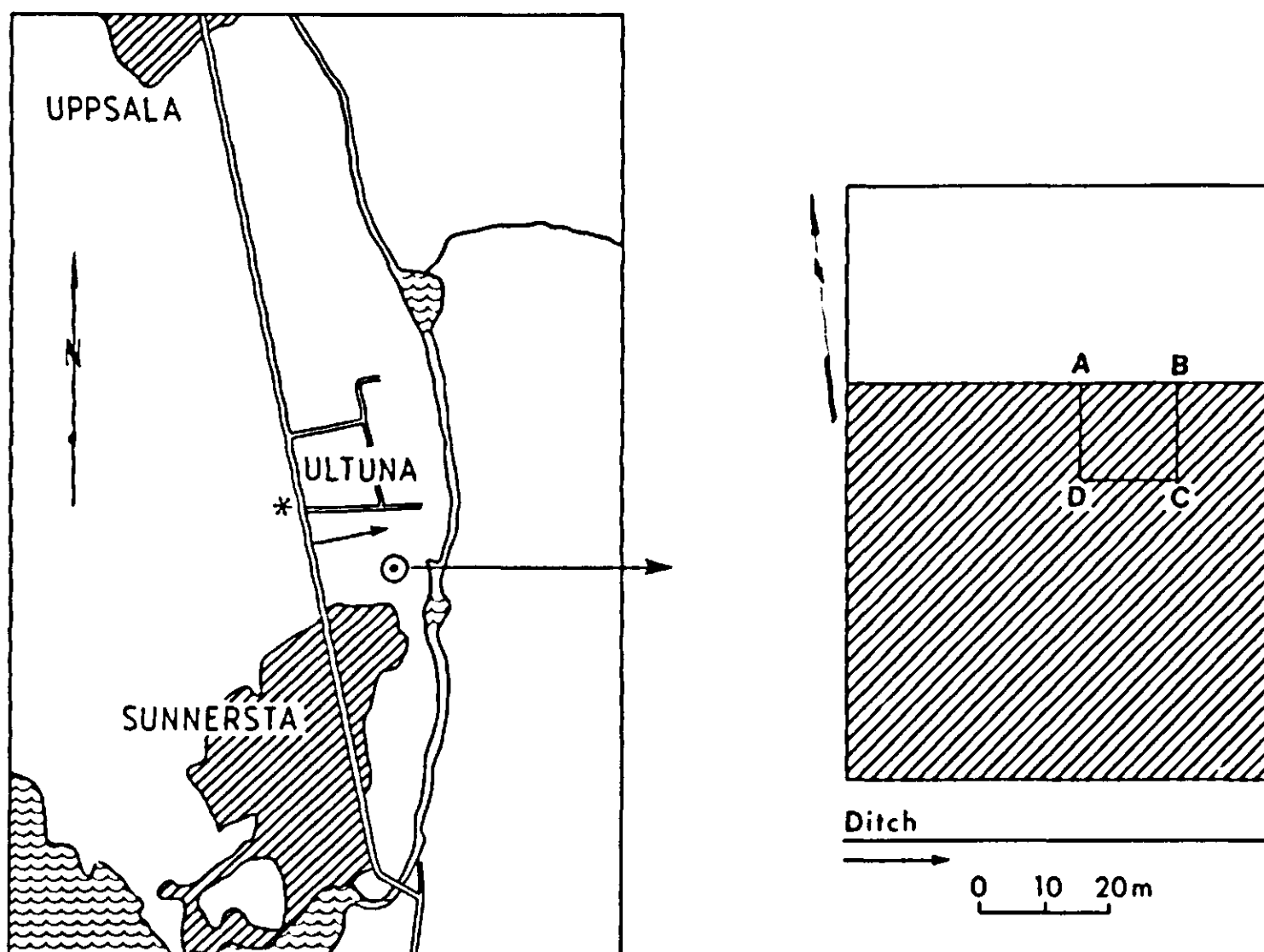


Figure 35. The map shows the location of the experimental area at the Compres of the Agricultural University (asterisk marks the meteorological station and the open circle the tensiometer plot). The enlargement of the plot (middle diagram) shows the energy forest stand and the area (marked A, B, C, D) where the tensiometers were installed. Further enlargement of this area (right) shows the positions and depths of the tensiometers.

depth (Figure 35). Most tensiometers were situated at shallow depths. The tensiometers were sited to characterize a flat area of $15 \times 15 \text{ m}^2$ in which willows were equally spaced and were of uniform height. The willow shoots were tied together loosely, to prevent them from interfering with the tensiometers. Groundwater tubes were installed in the field in July to a depth of 2.7 m.

11.3 Description of model

The model, named SOIL, was originally designed to predict annual soil climate in forest ecosystems (Jansson, 1980). A detailed technical description of the model is given by Jansson & Halldin (1980). The model is general enough to predict water and heat dynamics for a variety of soils and vegetation covers. Jansson & Thoms-Hjärpe (1986) presented a modified version of the model applicable to annual crops and clayey soils. That version of the model was also used in the present application.

The SOIL model is based on an extension of Richards's equation (Richards, 1931; Ogata et al., 1960)

$$\frac{\delta\Theta}{\delta t} = - \frac{\delta}{\delta z} \left(K \cdot \left(\frac{\delta\psi}{\delta z} + 1 \right) \right) - S(t) \quad \text{Equation 68}$$

where Θ = soil water content, ψ = water tension, K = unsaturated conductivity, S = sink term, accounting for water uptake by roots. The form of the model presented here consists of 12 layers (Figure 36).

In this clay soil with a structure of macropores, an air-filled volume was considered below the so-called air entry pressure (ψ_e) in the expression of Brooks & Corey (1964)

$$S_e = (\psi/\psi_e)^{-\lambda} = \frac{\Theta - \Theta_r}{\Theta_s - \Theta_r} \quad \text{Equation 69}$$

where ψ is the water tension (a positive tension corresponds to a negative water potential), λ is the pore size distribution index, S_e is the effective saturation, Θ_s is the porosity and Θ_r is the residual water content. Equation 69 was used when the air-filled porosity exceeded 4% by volume and the tension was below an equivalent pF of 3. A simple linear relation between the tension and the water content was used between the tension corresponding to an air-filled porosity of 4% by volume according to Equation 69 and the null tension corresponding to saturation. At tensions between an equivalent pF of 3 and the wilting point a log-linear relation is used. The unsaturated conductivity is calculated using the equation given by Mualem (1976)

$$K = K_s \cdot S_e^{\eta+2+2/\lambda} \quad \text{Equation 70}$$

where K_s is the conductivity at saturation and η is a parameter accounting for the tortuosity of flow path. The saturated conductivity in this equation did not account for rapid flows in macropores, which may be important in clayey soils. To account for this, an additional contribution to the conductivity was added when the air-filled porosity was below 4% by volume. The importance of the influence of macropores on the conductivity function has previously been analysed by Bouma & Andersson (1973).

PRECIPITATION EVAPORATION TRANSPIRATION

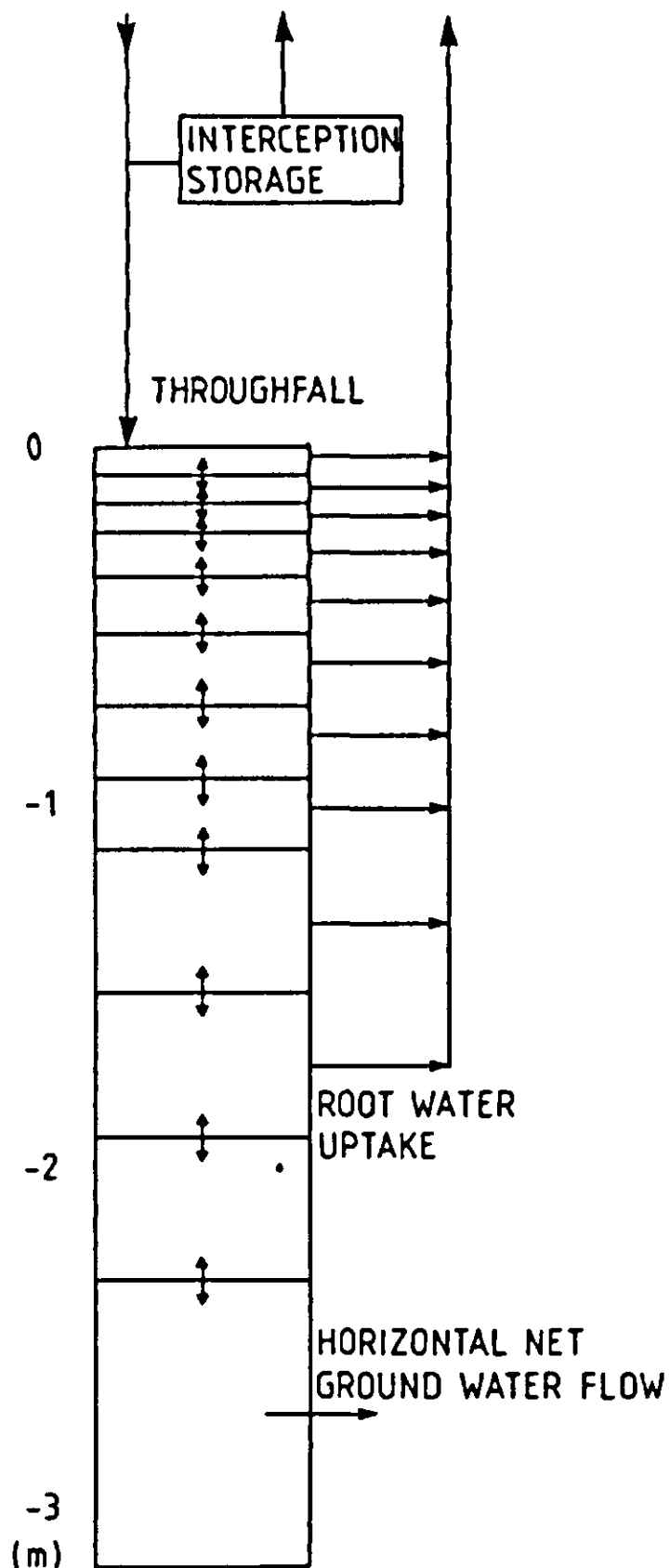


Figure 36. Structure of the model.

The bottom boundary condition was such that a water table was present. Drainage rates, q_d , from the saturated zone of the soil profile were calculated as a function of the groundwater level, z_{sat}

$$q_d = q_1 \max(0, (z_1 - z_{sat})/z_1) + q_2 \max(0, (z_2 - z_{sat})/z_2) \quad \text{Equation 71}$$

The parameters q_1 and z_1 represent a 'peak flow', whereas q_2 and z_2 represent the contribution from a 'base flow'.

The precipitation intercepted by vegetation was treated as a single storage given by a simple threshold formulation. The interception storage was described by a function accounting for the development of the crop: Evaporation from water intercepted by the crop was calculated with the Penman combination equation as given by Monteith (1965). The surface resistance when intercepted water occurs was assumed to be 5 s m^{-1} .

Water uptake by roots from different depths and evaporation from the soil surface were calculated as a function of potential demand, a depth distribution of root activity, and actual tensions in the soil. The potential demand, E_p , was given from the combination equation with a surface resistance which varied seasonally. When evaporation of intercepted water occurred, the demand from the soil profile was assumed to fall. The remaining demand from the soil, E_{pot} , was then calculated as

$$E_{pot} = (1 - \frac{E_{aint}}{E_{pint}}) \cdot E_p \quad \text{Equation 72}$$

where E_{pint} is the potential demand of intercepted water and E_{aint} is the actual amount of water evaporated from the interception storage. Water uptake from the soil profile was calculated as

$$S(t) = \sum_{i=1}^n f_i \cdot R\psi(z) \cdot E_{pot} \quad \text{Equation 73}$$

where n is number of soil layers and f_i the actual root distribution.

The reduction, $R\psi$, was calculated as

$$R\psi(z) = (\psi_c / \psi(z))^{aE_p + b} \quad \text{Equation 74}$$

(a, b = empirical constants) when the tension exceeded a critical value, ψ_c . Below this critical tension no reduction was made; $R\psi = 1$. When the tension exceeded the wilting point $R\psi$ was equalled to zero.

11.4 Adaptation of the model

11.4.1 Meteorological data

Daily totals of precipitation, irrigation, global radiation and averages of air temperature, vapour pressure and wind speed were used as driving variables for the model. They were taken from the meteorological station at the Swedish University of Agricultural Sciences, Ultuna, Sweden. Irrigation data were supplied by the Energy Forestry Project, which also is responsible for the plantation.

11.4.2 Soil properties

Water retention curves for a 1 m deep soil profile (Figure 37) were obtained from a field about 50 m from the site (Johansson, 1983). Two estimation procedures were used to evaluate the uncertainty of the coefficients in Equation 69. One estimate made use of the least squares technique for all the measured points (fit A), the other estimate was concentrated on the agreement with

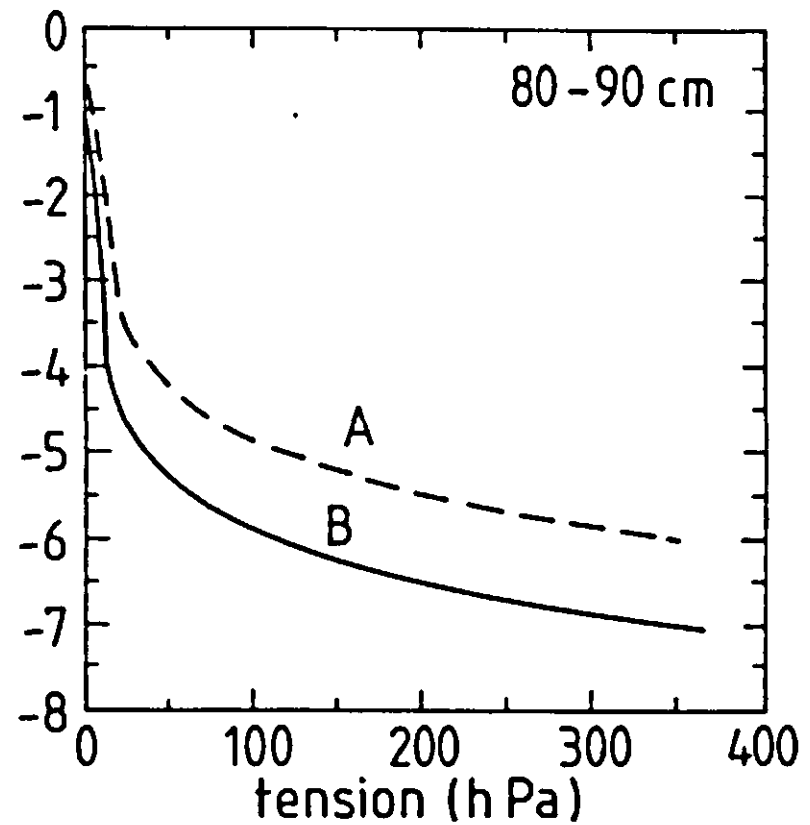
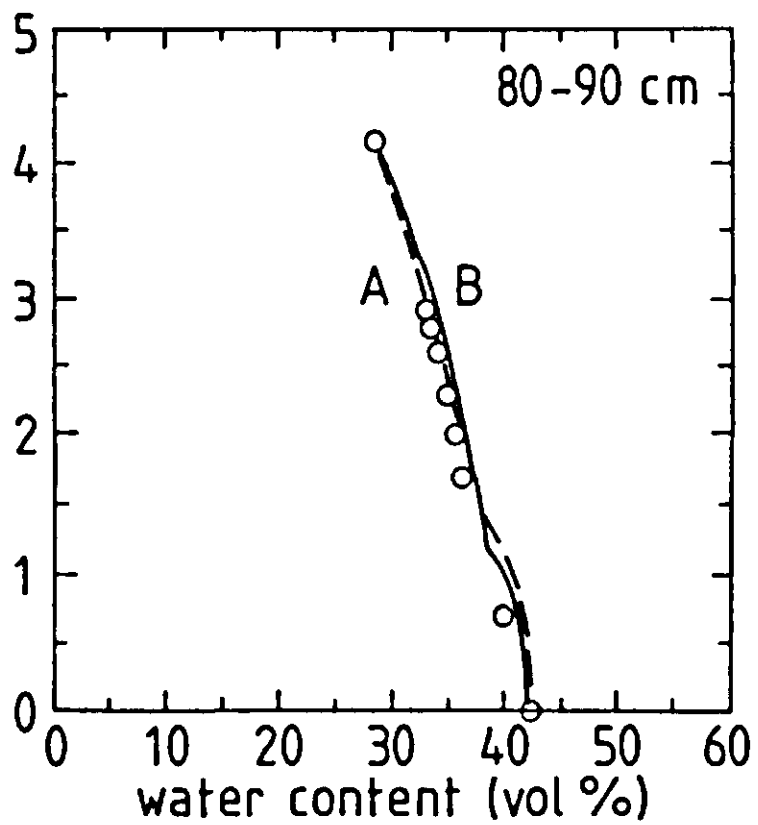
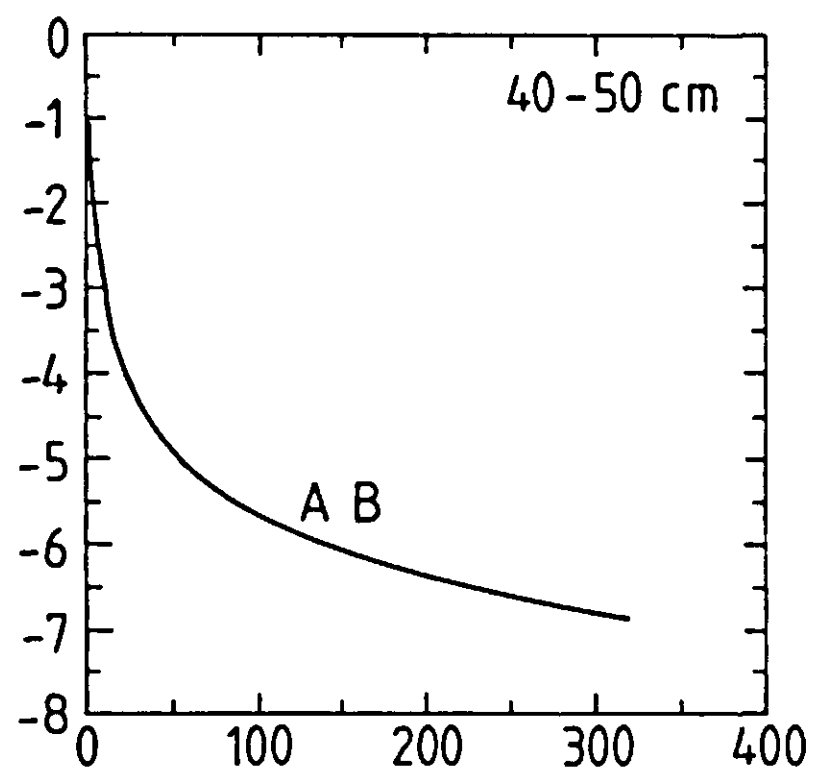
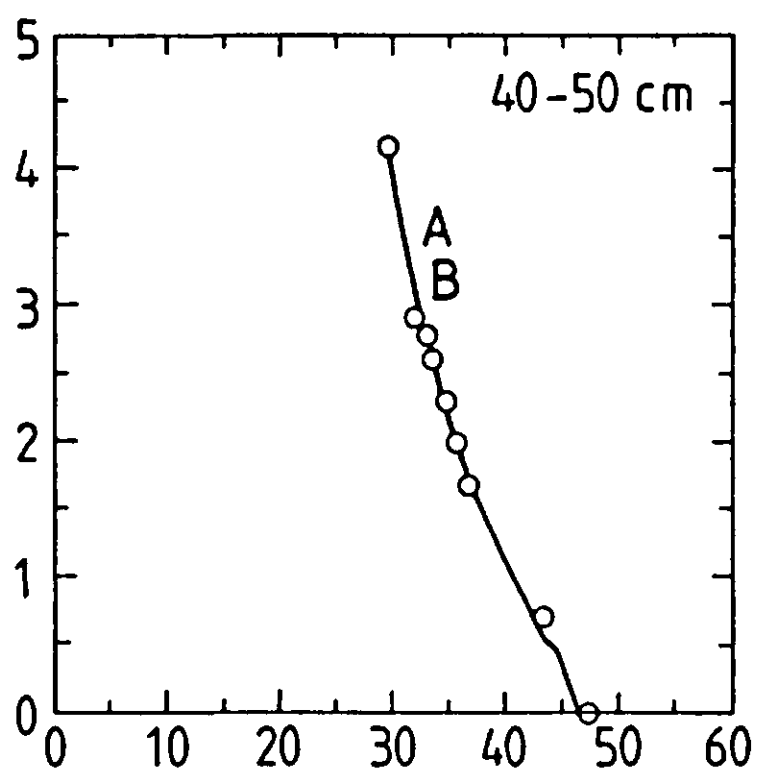
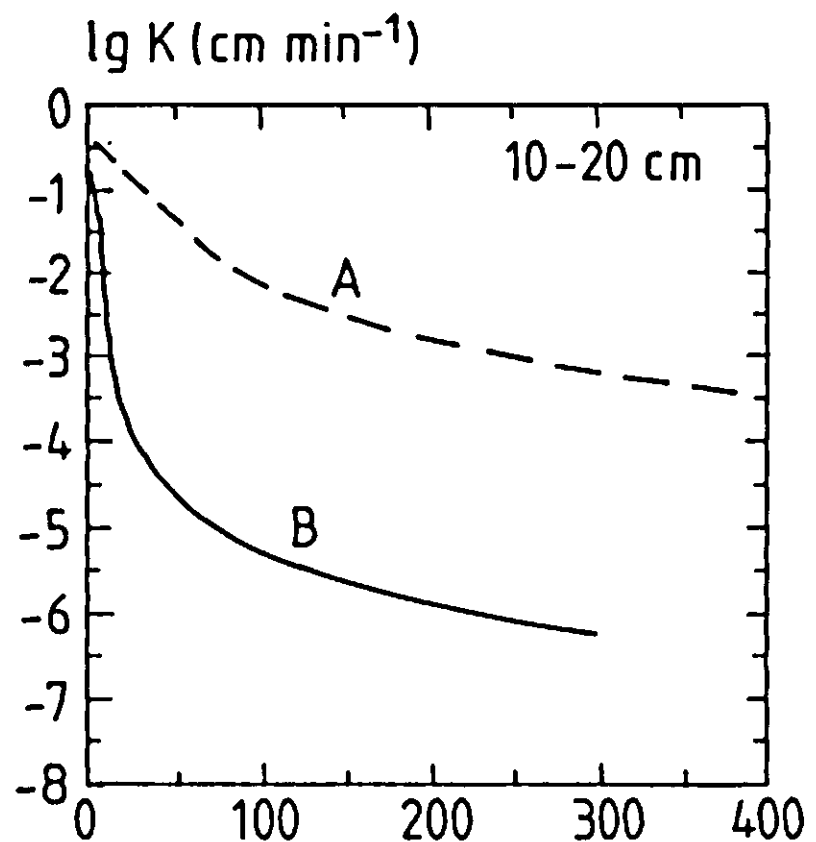
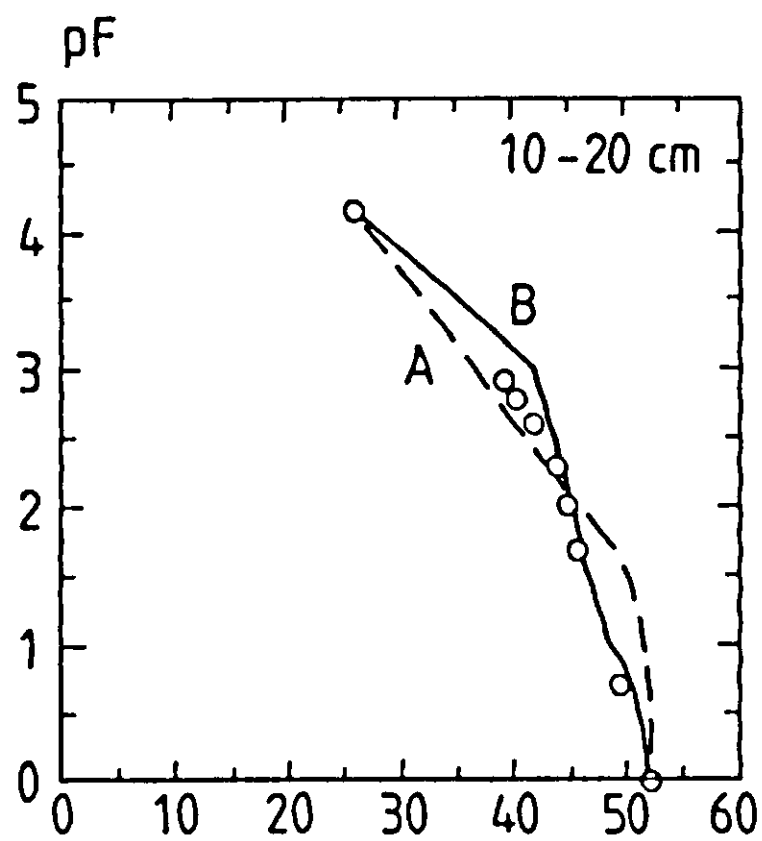


Figure 37. Soil water retention curves and unsaturated conductivity, K , (cm min^{-1}) for soil fits A and B. The circles represent measured values.

measured points in the range from 50 to 800 cm water (fit B), (Figure 37). Disparities between the two estimates occurred mainly for the two uppermost layers. The layers between 30 and 70 cm were thus given coefficients according to common estimates. The saturated conductivities measured in the laboratory were assumed to represent the maximum conductivity, taking the macropores into account. Unsaturated conductivity was not measured independently. The saturated conductivity in Equation 70, excluding macropores, was estimated as 0.10 cm min^{-1} within the layer 0-10 cm, 0.13 cm min^{-1} within 10-60 cm and 0.07 cm min^{-1} between 60 and 100 cm. These were more or less 'guesstimates' based on experiences about a 'field capacity' at a certain tension. The tortuosity factor, n , in Equation 70 was assumed equal to 1.0 for all layers.

No direct observations of drainage from the field were made and only a few observations of groundwater depth were available. To handle this uncertainty about the lower boundary condition for the soil profile, two different assumptions were tested by introducing either a shallow or a deeper water table.

The maximum drainage flow was kept constant in both assumptions ($q_1 = 10 \text{ mm day}^{-1}$ and $q_2 = 6 \text{ mm day}^{-1}$, Equation 71) but in order to obtain a shallow water table the levels where the respective continuous flow ceased were changed from 2 to 0.5 m for z_1 and from 5 to 1 m for z_2 .

11.4.3 Stand properties

The interception storage was estimated to be a maximum of 1.0 mm at the end of August on the basis of an interception storage capacity of 150 g m^{-2} leaf area (Larsson, 1980) and a maximum leaf area index of 6.7 measured in a dense stand with first-year shoots (Eckersten et al., 1983). The surface resistance for evaporation from the interception storage was estimated as 5 s m^{-1} , accounting also for the differences in exposure of the various parts of the canopy. The aerodynamic resistance was calculated from the logarithmic wind profile, assuming that the roughness length corresponded to 10% of stand height: this resulted in a variation from 10 cm in early June to 30 cm in late August (Figure 38).

The surface resistance (Figure 38), including both the soil surface resistance and the sum of all stomatal resistances, was assumed to decrease with increase of leaf area. Only semi-quantitative information on the maximum root depth and the vertical distribution of roots was available for the stand (Samils & Strandberg Arveby, 1987). To evaluate the importance of the distribution of vertical water uptake in the model, three alternative assumptions were tested (Figure 39): (a) and (b) had a common maximum depth of 0.9 m, but (c) had a maximum depth close to 2 m. The two extremes were chosen to include all possible situations whereas the intermediate was most similar to the observations from the field. The critical tension (ψ_c) for reduction of water uptake (Equation 74) was assumed to be 400 hPa.

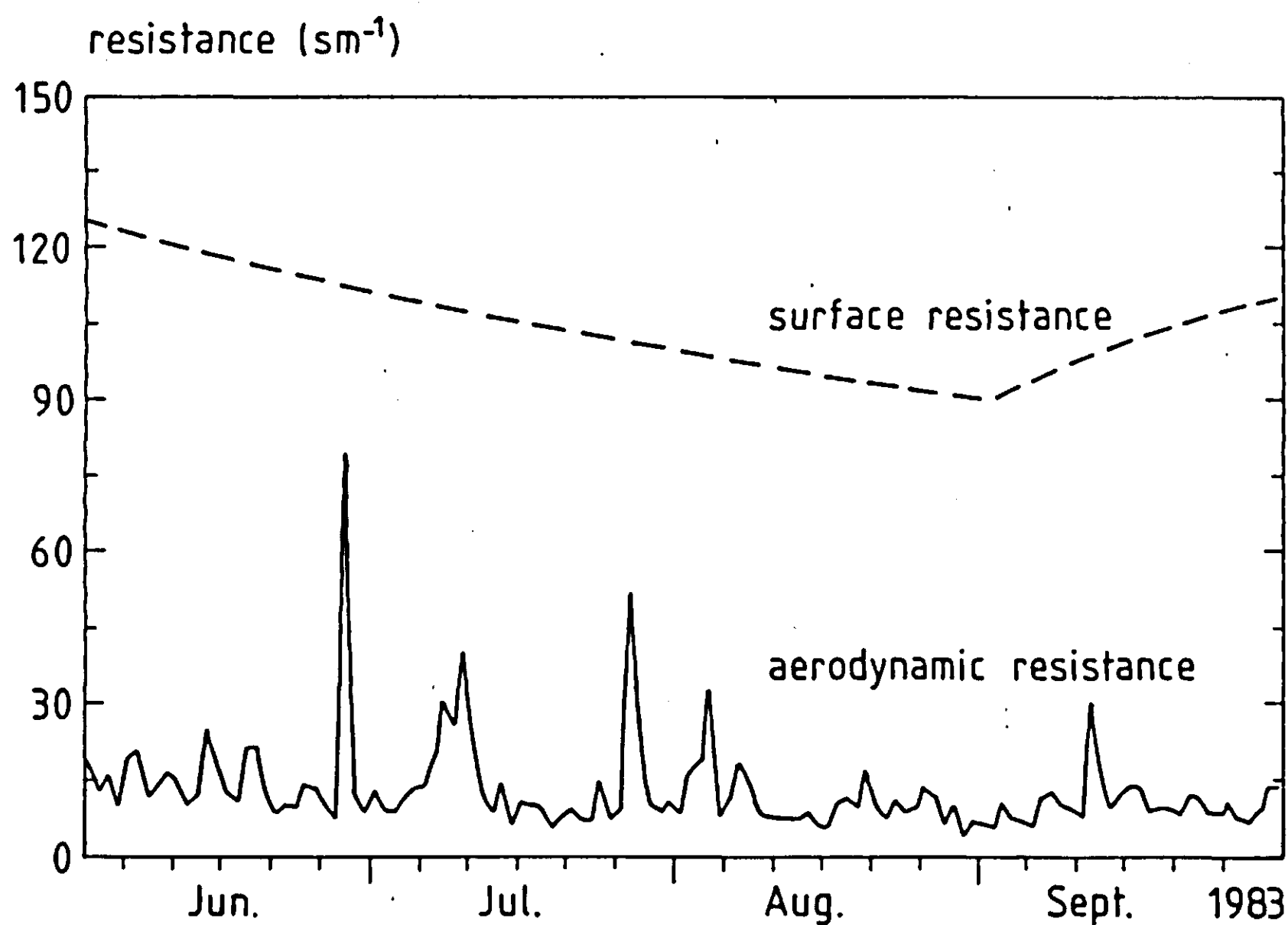


Figure 38. Daily means of the aerodynamic resistance as calculated from wind speed and roughness together with an assumed course of the surface resistance.

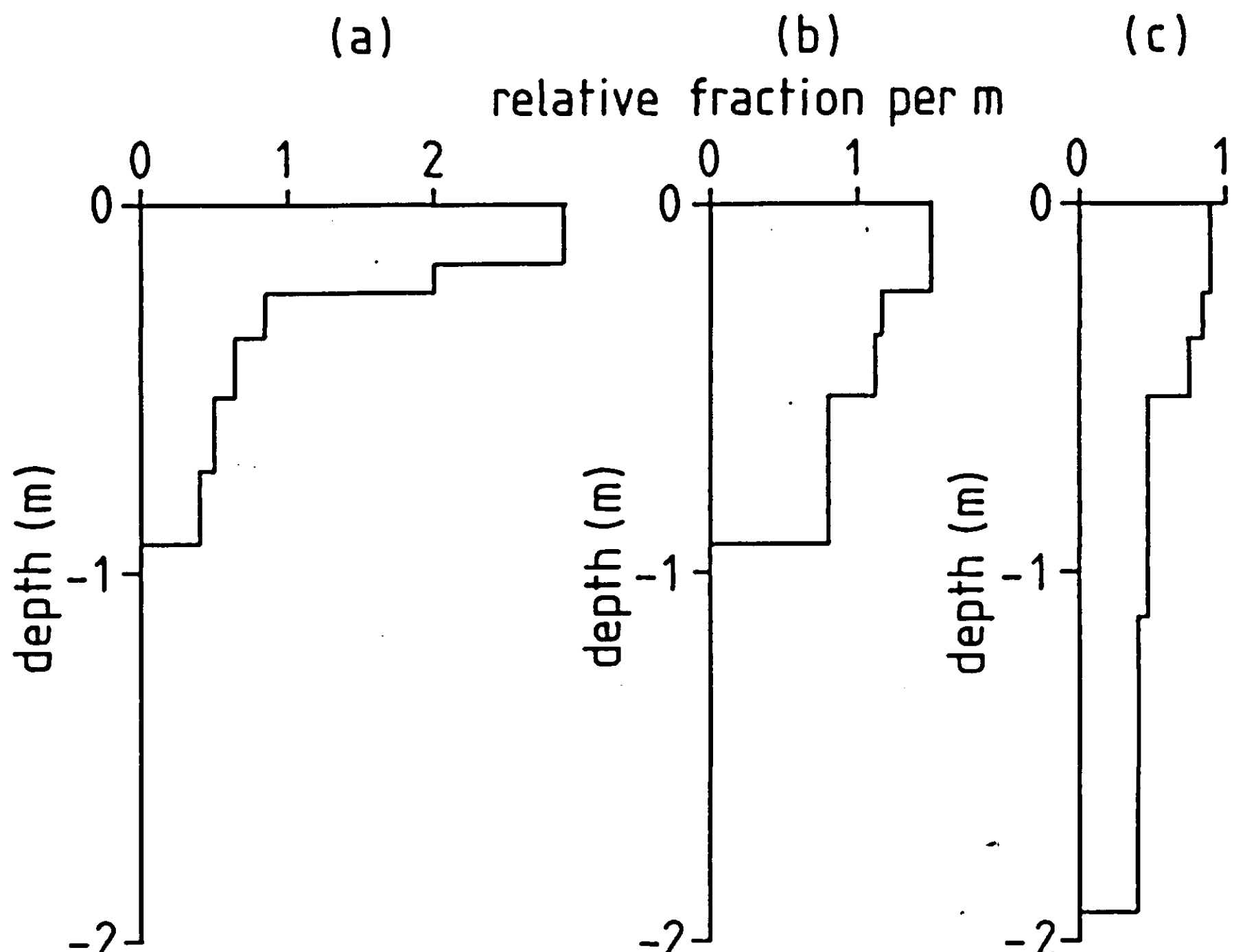


Figure 39. The relative root distributions (a, b and c) used in the simulations.

11.4.4 Initial conditions

The simulation period started in the spring after the snow-melt period. This enabled reasonable initial conditions to be estimated. Initial water storages above the groundwater level were given from a tension in equilibrium with the initial groundwater level but with a maximum tension of 60 cm water.

11.5 Results and discussion

The 1983 growing season was unusually dry, except for rainy periods in early and late June and in September (Table 11). Because of the irrigation applied in July and August the drought spells were interrupted; this prevented the soil water tension from exceeding 800 cm water (Figure 40).

When different combinations of soil and plant properties were used in the model, more or less good agreement was obtained between simulated and measured tensions. Because of uncertainties in parameter values for these properties a number of simulations were made to evaluate the model's sensitivity, especially to the seasonal estimate of evapotranspiration. For all these simulations the magnitude of the surface resistance for potential transpiration was adjusted until a reasonable agreement was obtained between measured and simulated tensions. With the exception of the surface resistance, alternative parameter sets were defined for groundwater conditions, soil properties and vertical root distributions. Some combinations of these alternative parameter sets could be excluded because of their lack of ability to produce a reasonable agreement between simulated and measured tensions.

A shallow root distribution could only be used in combination with the soil properties according to fit A. The reason was that fit A implied that more water in the range between pF2 and pF2.7 was available in the topsoil than in the underlying layers (see Figure 37). When comparing the best simulation with soil properties using fit A with the corresponding best simulation using fit B and a more evenly vertical root distribution (b), substantial differences occurred for

Table 11. Climate at Ultuna during 1983. Normal values (1931-60) supplied by the Swedish Meteorological and Hydrological Institute.

Variable	June	July	August	September
Normal temperature, (°C)	14.5	17.3	15.9	11.4
Temperature, (°C)	14.5	17.8	17.0	12.0
Normal precipitation, (mm)	48	66	76	58
Precipitation, (mm)	97	49	19	137
Irrigation, (mm)	-	58	81	-

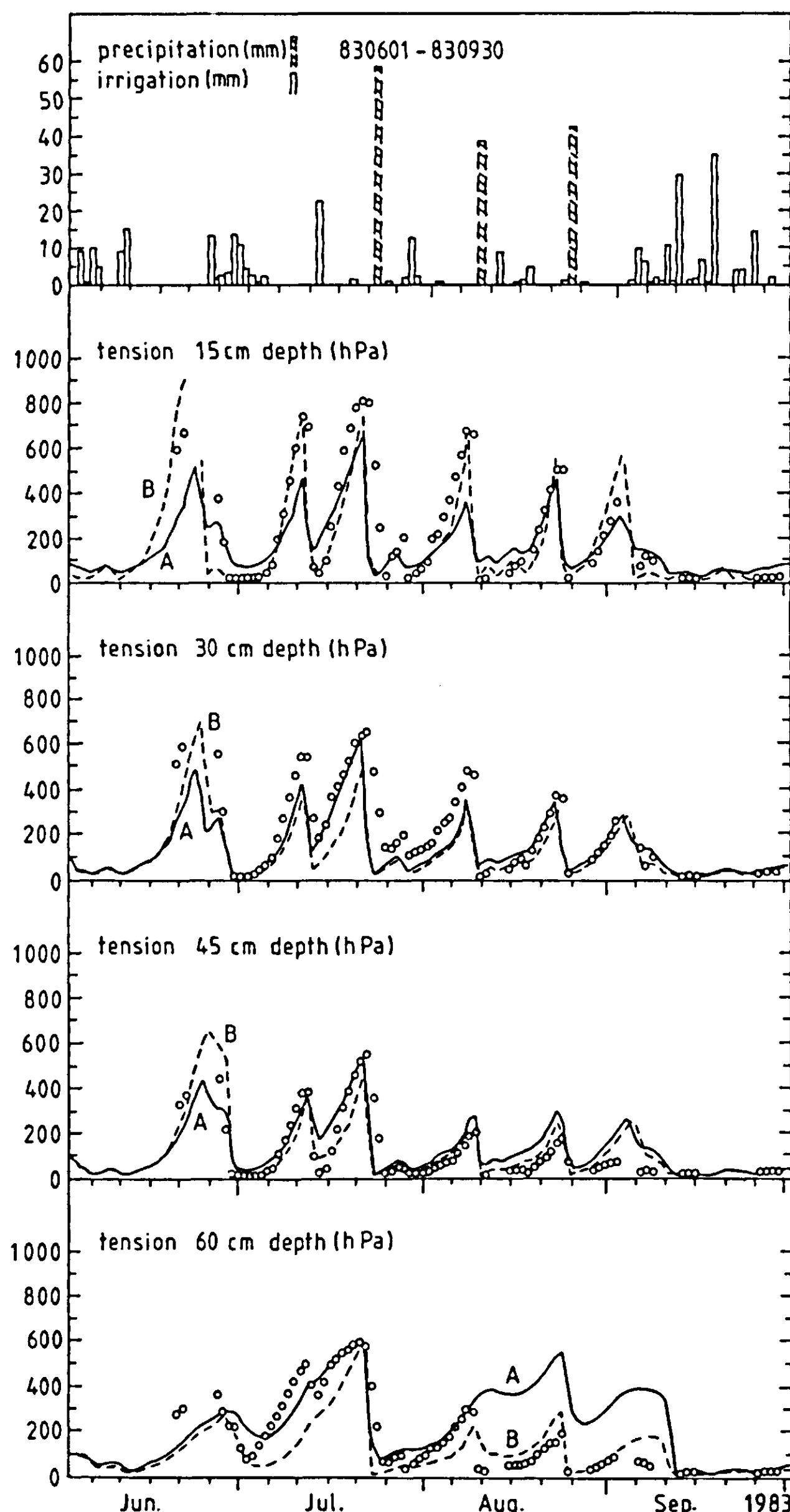


Figure 40. Daily precipitation/irrigation, together with the simulated and measured tensions at 15, 30, 45 and 60 cm depth during 1/6-30/9 1983. Solid lines represent simulation using soil fit A and broken lines represent simulation using soil fit B (cf. Table 12). The circles represent the measured tensions.

Table 12. Effect of different boundary conditions and soil-plant properties on the water balance.

Treatment	Drain- age effi- cien- cy	Soil fit (cf. Fig. 37)	Root descr. (cf. Fig. 39)	Surface resist. (s m ⁻¹)	Transpi- ration (mm)	Evapo- ration (mm)	Evapo- transpi- ration (mm)	Run- off (mm)
Irrigated	Good	B	(b)	90-160	335	41	376	113
Irrigated	Poor	B	(b)	90-160	336	41	377	8
Irrigated	Good	A	(a)	90-160	342	41	383	138
Irrigated	Good	B	(c)	60-130	367	41	408	96
Irrigated	Poor	B	(c)	50-120	393	41	434	0
Unirrigated	Good	B	(b)	90-160	230	38	268	98

the deeper layers (Figure 40). Using fit A it was not possible to simulate the rapid drops of tensions at 60 cm depth in connection with infiltration events in July and August. This, and the fact that measured points on the pF curve corresponded better to fit B, was taken as indicating that fit B was the most valid for the field conditions simulated. This also implies that root distributions according to (a) could be dismissed as not being good approximations of our field conditions.

If the above conclusions are accepted, uncertainties still remain with respect to the influence of groundwater conditions and the occurrence of roots deeper than assumed with (b). However, when poor drainage of the subsoil was introduced, neither the agreement with measured tensions nor the simulated evapotranspiration, was affected when the intermediate root distribution was used (Table 12). The differences obtained were that the runoff decreased when the groundwater was kept at a shallower level of about 2 m throughout the season and that tensions became somewhat different below 60 cm depth (Figure 41). When good drainage efficiency was used, the groundwater level fell from 2 m to about 4.5 m at the end of the growing season (Figure 41).

To obtain an influence of the groundwater conditions it was necessary to introduce the deep root distribution (Figure 39). In that case the simulated tension in the uppermost metre could be kept similar to the other simulations by adjusting the surface resistance to lower values (Table 12). The simulated evapotranspiration increased by 8% and 15%, depending on which assumption was used for the groundwater conditions. According to the sparse observations of groundwater, an intermediate groundwater situation could be expected; thus the uncertainty in the simulated evapotranspiration because of efficient deep roots could be estimated as being about 14%. However, this was considered to

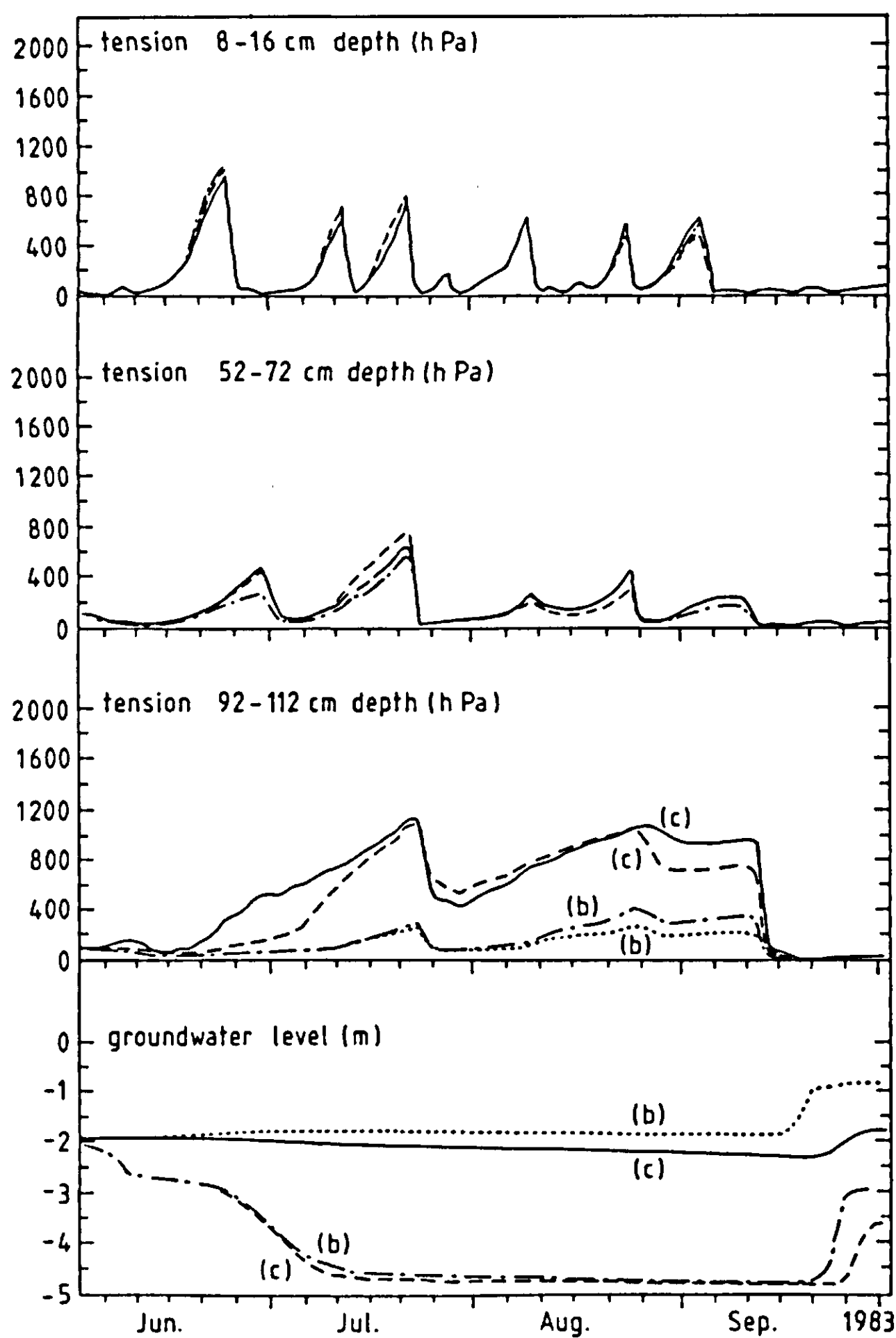


Figure 41. Simulated tensions for the layers 8-16, 52-72 and 92-112 cm depth using root distributions (b) and (c) (cf. Figure 39) together with the simulated groundwater level (cf. Table 12).

be the maximum uncertainty, because the tensions simulated at 1 m depth (see Figure 41) appreciably were higher than the observations at 60 cm depth (see Figure 40).

To evaluate the effect of irrigation, a simulation without irrigation was also made (Table 12). The most likely parameter set, namely intermediate root distribution and soil properties of fit (B), was used. The decrease in transpiration was 100 mm. The decrease could have been even larger if the actual irrigation had been better scheduled (Figure 42). However, the level of the

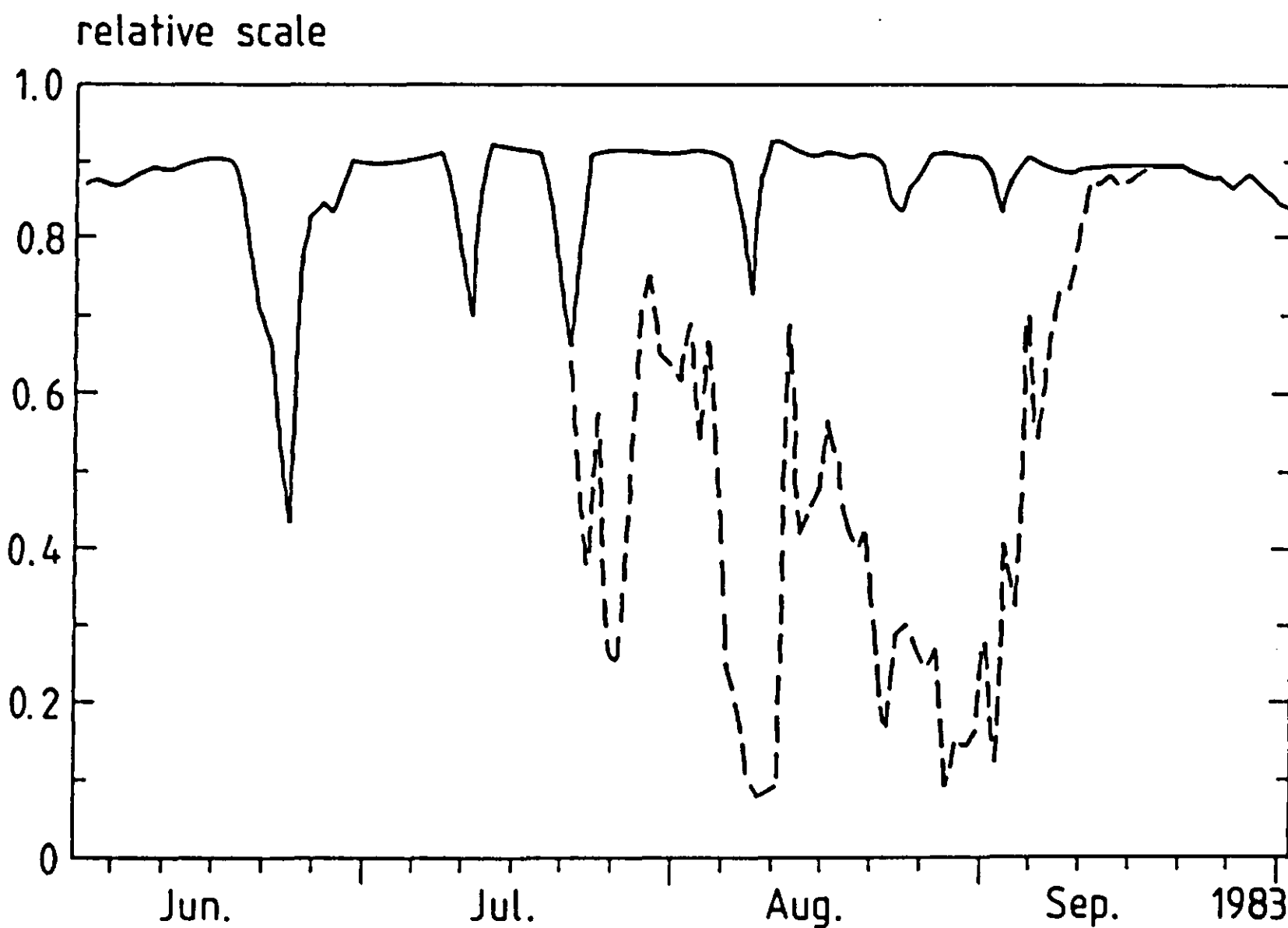


Figure 42. Ratio between actual and potential water uptake from soil. Solid line represents simulation with irrigation and broken line that without irrigation.

decrease was not very certain, because it greatly depended on the assumed tension for reduction of water uptake (Equation 74). Unfortunately, no plant physiological or micro-meteorological data were available for more accurately estimating if transpiration declined during the season.

11.6. Conclusions

The good agreement between simulated and measured soil water tensions made it reasonable to believe that the simulated evapotranspiration was also close to the actual level. The uncertainty of most importance for the simulated evapotranspiration was the occurrence and efficiency of deep roots, especially if the deep roots were combined with a poor drainage efficiency. A reasonable range for the actual evapotranspiration during the simulated period would be between 370 and 420 mm.

The estimated range for actual evapotranspiration exceeds the potential evapotranspiration ($= 335 \text{ mm}$) as calculated by the Penman formula. Grip (1981) also found higher evapotranspiration than calculated by Penman. He reported high values, especially in the late summer and early autumn (5-40% higher than Penman). The two independent investigations now available for Swedish conditions both indicate the crucial role of an efficient water supply for the successful cultivation of willow plantations.

For further studies of evapotranspiration from this stand it would be preferable if more properties could be determined from independent measurements. This would allow the uncertainty about the simulated evapotranspiration to be narrowed and would permit a more confident generalization to new climatic situations or to new sites.

11.7 List of symbols

a, b	= coefficients in the reduction function (dimensionless)
E_{aint}	= actual evaporation rate of intercepted water, (mm d^{-1})
E_p	= potential evaporative demand from the soil profile given by the Penman-Monteith combination equation, (mm d^{-1}); Monteith (1965)
E_{pint}	= potential evaporation rate of intercepted water, (nm d^{-1})
E_{pot}	= potential evaporative demand from the soil profile when evaporation of intercepted water occurs, (mm d^{-1})
f_i	= actual root distribution in the layers $i = 1 \dots n$, (dimensionless)
K	= unsaturated conductivity, (cm h^{-1})
K_s	= saturated conductivity excluding any contribution from macropores, (cm h^{-1})
n	= number of soil layers, (dimensionless)
q_d	= actual drainage rate from the soil profile, (mm d^{-1})
q_1	= maximum rate of 'peak' groundwater flow, (mm d^{-1})
q_2	= maximum rate of 'base' groundwater flow, (mm d^{-1})
R_ψ	= reduction of water uptake caused by low water content, (dimensionless)
S	= water uptake from the soil profile, (mm d^{-1})
S_e	= effective saturation in the Brooks & Corey (1964) expression, (dimensionless)
t	= time, (h, d)
z_1	= depth where 'peak' flow ceases, positive downwards, (m)
z_2	= depth where 'base' flow ceases, positive downwards, (m)
z_{sat}	= ground water level, positive downwards, (m)
η	= parameter accounting for the tortuosity of flow path in the Mualem (1976) expression, (dimensionless)
Θ	= soil water content by volume, (%)
Θ_r	= residual water content in the Brooks & Corey (1964) expression, by volume, (%)
Θ_s	= porosity by volume, (%)
λ	= pore size distribution index in the Brooks & Corey (1964) expression, (dimensionless)
ψ	= water tension, (hPa)
ψ_c	= critical tension for reduction of potential water uptake, (hPa)
ψ_e	= air entry pressure in the Brooks & Corey (1964) expression, (hPa)

11.8 Acknowledgement

The authors are jointly responsible for this chapter. Ms. Gunn Persson was largely responsible for tensiometer measurements in the field and she also ran the model on the computer. Mr. Jerzy Melaniuk assisted during field work. Valuable comments on the manuscript were given by Dr. Harald Grip, Dr. Sven Halldin, Dr. Piotr Kowalik and Dr. Anders Lindroth. The project was sponsored by the Swedish National Environmental Protection Board.

11.9 References

Bouma, J. & Andersson, J.L., 1973. Relationships between soil structure characteristics and hydraulic conductivity. In: *Field soil water regime*. SSSA Special publication series, 5:77-105.

Brooks, R.H. & Corey, A.T., 1964. Hydraulic properties of porous media. *Hydrology Paper No. 3*, 27 pp. Colorado State University, Fort Collins, Colorado.

Eckersten, H., Kowalik, P., Nilsson, L-O. & Perttu, K., 1983. Simulation of total willow production. Report 32, 45 pp. Swedish University of Agricultural Sciences, Section of Energy Forestry, Uppsala.

Grip, H., 1981. Evapotranspiration experiments in *Salix* stands. Report 15, 29 pp. Swedish University of Agricultural Sciences, Section of Energy Forestry, Uppsala.

Grip, H., Halldin, S., Lindroth, A. & Persson, G., 1984. Evapotranspiration from a willow stand on wetland. In: K.L. Perttu (Ed.): *Ecology and management of forest biomass production systems*. Report 15:47-61. Swedish University of Agricultural Sciences, Department of Ecology and Environmental Research, Uppsala.

Jansson, P-E., 1980. Soil water and heat model. II. Field studies and applications. Dissertation. *Acta Universitatis Upsaliensis*, 568, 26 pp.

Jansson, P-E. & Halldin, S., 1979. Model for annual energy and water flow in a layered soil. In: S. Halldin (Ed.): *Comparison of forest water and energy exchange models*. Elsevier Scientific Publishing Company, pp. 145-163. Amsterdam – Oxford – New York.

Jansson, P-E. & Halldin, S., 1980. Soil water and heat model. Technical description. Technical report 26, 81 pp. Swedish University of Agricultural Sciences, Swedish Coniferous Forest Project, Uppsala.

Jansson, P-E. & Thoms-Hjärpe, C., 1986. Simulated and measured soil water dynamics of unfertilized and fertilized barley. *Acta Agriculturae Scandinavica* 36:162-172.

Johansson, W., 1983. Marken som rotens fysikaliska miljö [Soil as the physical environment of the roots]. In: *Roten och rotens miljö II*. Allmänt No. 47, 5-12. Swedish University of Agricultural Sciences, Konsulentavdelningen, Uppsala.

Larsson, S.O., 1980. Inverkan av interceptionsvatten på transpirationen hos *Salix* [Influence of intercepted water on the transpiration rate of *Salix*]. Report 9, 14 pp. Swedish University of Agricultural Sciences, Section of Energy Forestry, Uppsala.

Monteith, J.L., 1965. Evaporation and environment. In: G.E. Fogg (Ed.): *The state and movement of water in living organisms*. 19th Symposium of the Society for Experi-

mental Biology, Volume 19, pp. 205-234. Cambridge: The Company of Biologists.

Mualem, Y., 1976. A new model form predicting the hydraulic conductivity of unsaturated porous media. *Water Resources Research* 12:513-522.

Ogata, G., Richards, L.A. & Garduer, W.R., 1960. Transpiration of alfalfa determined from soil water content changes. *Soil Science* 89:179-182.

Olsson, M.T. & Samils, B., 1984. Site characterization at energy forest production. Report 48:27-35. Swedish University of Agricultural Sciences, Department of Forest Soils, Uppsala.

Richards, L.A., 1931. Capillary conduction of liquids in porous mediums. *Physics* 1:318-333.

Samils, B. & Strandberg Arveby, A., 1987. Rotutveckling och rotodynamik [Root development and dynamics]. In: K.L. Perttu (Ed.): *Projekt energiskog. Slutrapport för perioden 1984-04-01 – 1987-03-31* [Project energy forestry. Final report for the period April 1, 1984 – March 31, 1987]. Swedish University of Agricultural Sciences, Section of Energy Forestry, Uppsala, pp. 139-150.

ENERGY FORESTRY: ITS ECONOMICS AND PROSPECTS

12 Economic potential of intensively cultivated energy forests in Sweden

Göran Lönnér and Matti Parikka

12.1 Introduction

Much biological research has been done on intensively cultivated energy forestry (Sirén, 1983) but there is a dearth of estimates of the economic potential of energy forestry. According to Anderson & Zsuffa (1980) the Mitre Corporation in the United States concluded that the production of silvicultural biomass under intensively managed short rotation was not an energy-intensive operation and would not be precluded on the basis of an unfavourable energy budget (Inman & Salo, 1977). It has been suggested that annual productivities of at least 12 t ha^{-1} are necessary for energy plantation to be considered as a realistic alternative to many land uses in the United States (Fege et al., 1979). The economics of intensively cultivated energy forestry in Sweden may be different to that ascertained by Fege et al. There are still very few truly commercial plantations of energy forests in Sweden, but there are four large-scale research plantations and some smaller, private managed ones. The large surplus production of agricultural crops makes it important for many farmers to find alternative products. Intensively cultivated energy forests could be one such alternative. In 1986 a number of small-scale privately managed plantations were established in southern Sweden (about 500 ha in total). A number of farmers were chosen for this project and given a government subsidy to start such plantations.

The purpose of this analysis is to illustrate the economic potential of intensively cultivated energy forestry in Sweden in comparison with alternative domestic fuels and land uses.

The economic calculations represent a time horizon of about five years. Consequently, only well-known cultivation techniques are considered. The following soil types are distinguished in the calculations (Lönnér et al., 1985): good agricultural land, peat land, forest land. The experts have also estimated the possible production level for different cultivation intensities.

12.2 Material and methods

12.2.1 *Definition of soil types*

Good agricultural land can be cultivated immediately. The land rent for this type of soil, which also includes investment and operation costs, is generally $1000 \text{ SEK ha}^{-1} \text{ yr}^{-1}$ in southern Sweden (Kasberg, 1986). Peat land consists of all kinds of wetlands, including marshlands. Forest land includes soils deve-

loped on glacial and post-glacial sediments, which can be used for cultivation of energy forest. The costs of renting peat and forest land are set at zero in the calculations.

12.2.2 *Cultivation programme*

Two different cultivation programmes are defined for good agricultural land: namely, small- and large-scale cultivations (Lönner et al., 1985). For peat and forest land, calculations are only made for large-scale programmes.

As a basic alternative a 'normal' case for each soil type is presented. The cultivation programme for 'good agricultural land' is shown as an example (Table 13).

Table 13. Cultivation programme for 'good agricultural land, normal and small-scale'. Net production 12 oven-dry tonnes (ODt) $ha^{-1} yr^{-1}$, 3-year harvesting and 22-year rotation period. (After Lönner et al., 1985).

Year	Operation	Code	Cost (SEK yr^{-1})	Oper. code
1	planning	a	1400	0
	fertilizing	q1	890	0
	rotary cultivation	k2	400	0
	planting	o2	9330	0
	weed control	p	760	0
	land rent	-	1000	0
2,5,8	weed control	p	760	0
11,14	fertilizing	q1	890	0
17,20	land rent	-	1000	0
3,6,9	fertilizing	q1	860	0
12,15	land rent	-	1000	0
18,21				
4,7,10	fertilizing	q1	890	0
13,16	harvest	t2	47	11
19,22	storage	u	5	11
	chipping	v2	135	11
	transport	x2	55	11
	land rent	-	1000	0

12.2.3 *Technical systems*

The economic calculations are based on systems that the experts consider to represent the best techniques currently available. This means that these systems may be typical for the next five-year period. The techniques used in small-scale cultivations involve a combination of farming and forestry machines; large-scale cultivations require more sophisticated equipment and better performance (Lönner et al., 1985).

The development of a harvester for energy forestry has been slower than expected. However, two prototypes are now available. The harvester for small-scale cultivations generally operates well, and has now been tested under field conditions. The harvester for large-scale cultivations is still at an early phase of development. The technical development potential is estimated to be very large.

12.3 **Results**

12.3.1 *Initial costs*

The initial costs of establishing energy forests are high and there are large differences between soil types and cultivation programmes (Table 14). The price level is given in constant 1985 SEK.

12.3.2 *Alternative land use*

One way to compare the profitability of energy forests with alternative land use is to include a cost for land rent. If it is possible to pay, for example, 1000 SEK ha^{-1} for land use and retain profitability, the energy forest can compete with other crops that give an annual yield of 1000 SEK ha^{-1} or less.

12.3.3 *Production levels*

The results are shown in unitary diagram form, where the total cost for the fuel chips delivered at a district heating plant in SEK per megawatt hour (SEK

Table 14. Initial costs on different types of land. (After Lönner et al., 1985). Price level constant 1985 SEK.

Soil type	Costs (SEK ha^{-1})
Good agricultural land	13000 - 15000
Peat land	28000 - 36000
Forest land	28000 - 36000

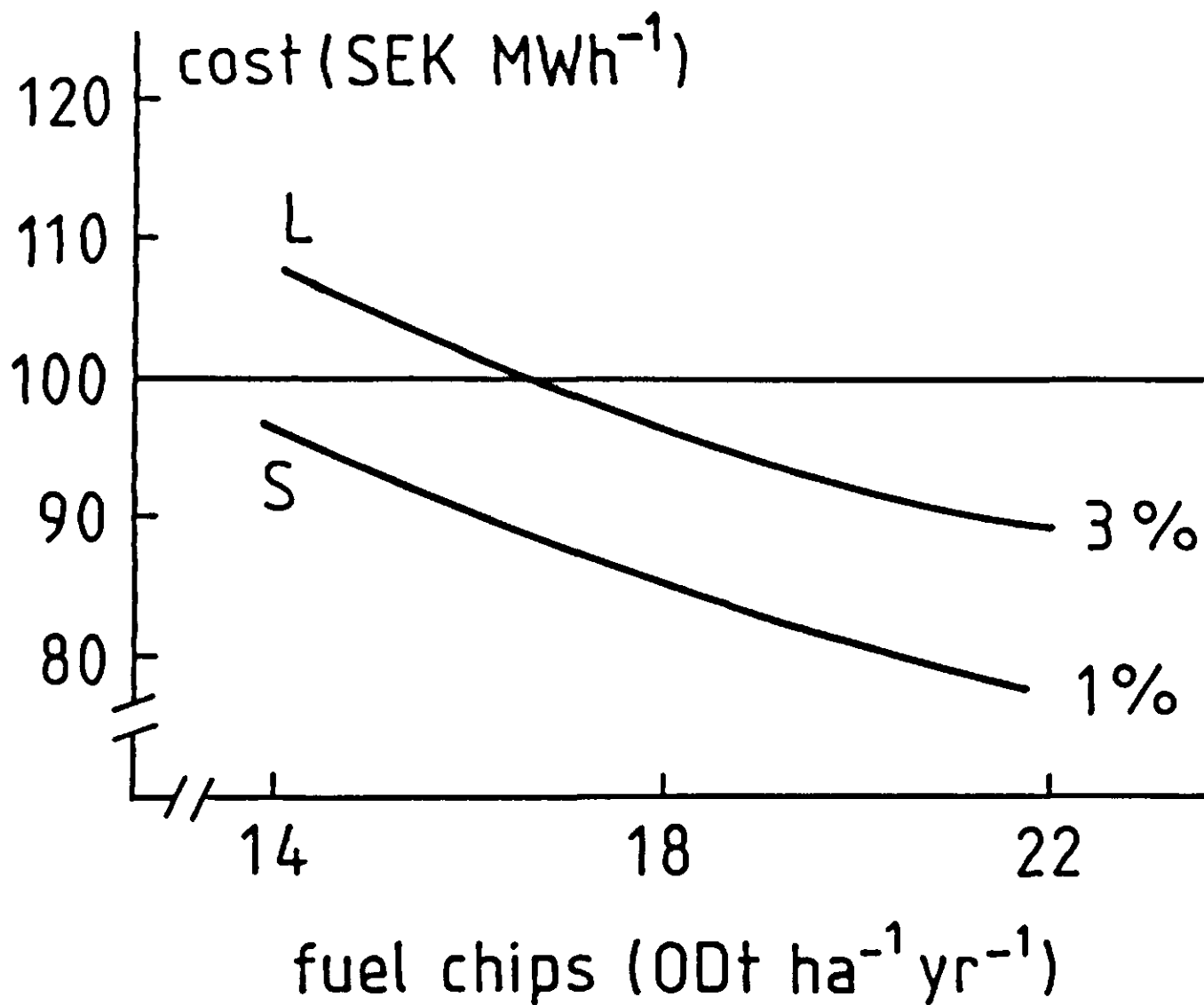


Figure 43. Production costs (SEK MWh⁻¹) for fuel chips (ODt ha⁻¹ yr⁻¹) produced on good agricultural land with a land rent of 1000 SEK ha⁻¹ yr⁻¹. L = large-scale and S = small-scale cultivations with a real interest of 3% and 1%, respectively.

(MWh)⁻¹) is shown as a function of net production of stem biomass in oven-dry tonnes (ODt) ha⁻¹ yr⁻¹, including losses at harvest, chipping and transport. A line has been drawn at the level of 100 SEK per MWh. This is the average price for forest fuels in Sweden in 1985 (Lönnér & Parikka, 1985b). If the curve lies below the line, the alternative is profitable at present interest rates and production level (Figure 43).

The results show that small-scale cultivations can be profitable at a production level of 10-12 ODt ha⁻¹ yr⁻¹ for good agricultural land. Large-scale cultivation requires a much higher production and the corresponding level is 14-19 ODt ha⁻¹ yr⁻¹ (Figures 44-49).

It is evident that break-even levels are lower in small-scale cultivations than in large-scale ones (Table 15). The difference may be 5-7 ODt ha⁻¹ yr⁻¹. This can be explained by the assumptions regarding the different organization forms, such as: 15% versus 5% management costs, 3% versus 1% real interest, 50 km versus 35 km transport distance.

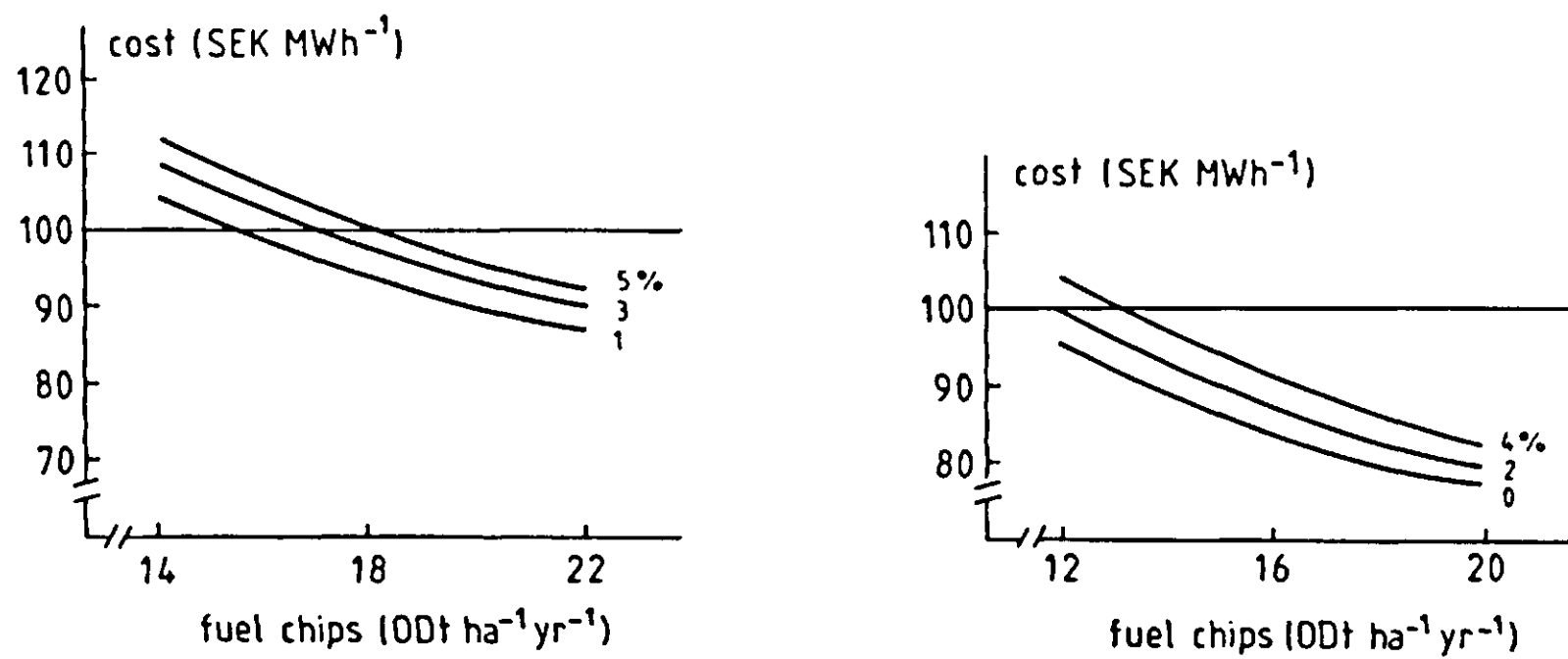


Figure 44. Effects of different real interest rates (%) on the production costs (SEK MWh⁻¹) for fuel chips (ODt ha⁻¹ yr⁻¹) on 'good agricultural land / normal' in large-scale (left) and small-scale (right) cultivations.

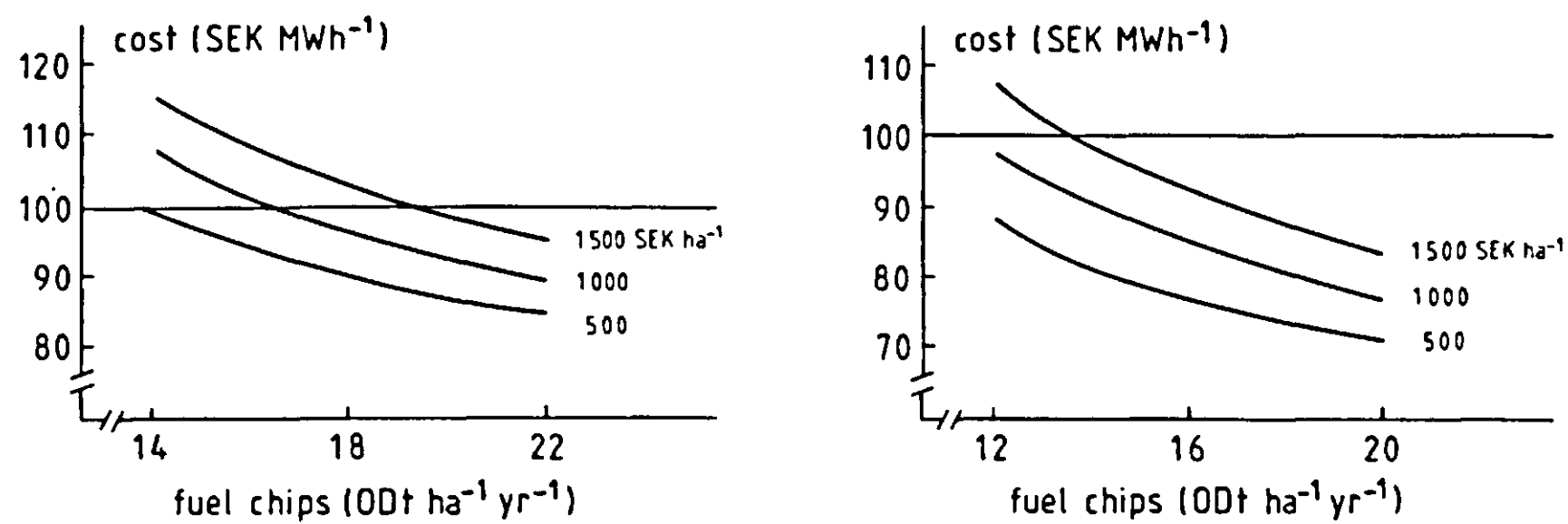


Figure 45. Effects of different land rents (SEK ha⁻¹) on the production costs (SEK MWh⁻¹) for fuel chips (ODt ha⁻¹ yr⁻¹) on 'good agricultural land / normal' in large-scale (left) and small-scale (right) cultivations.

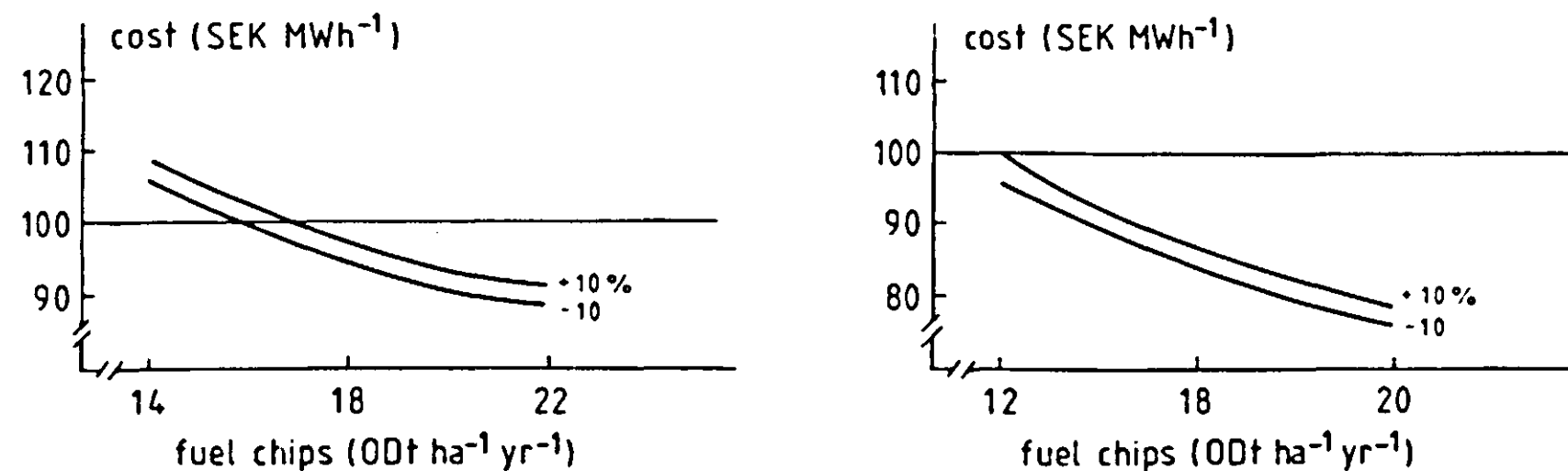


Figure 46. Effects of different investment costs ($\pm 10\%$) on the production costs (SEK MWh⁻¹) for fuel chips (ODt ha⁻¹ yr⁻¹) on 'good agricultural land / normal' in large-scale (left) and small-scale (right) cultivations.

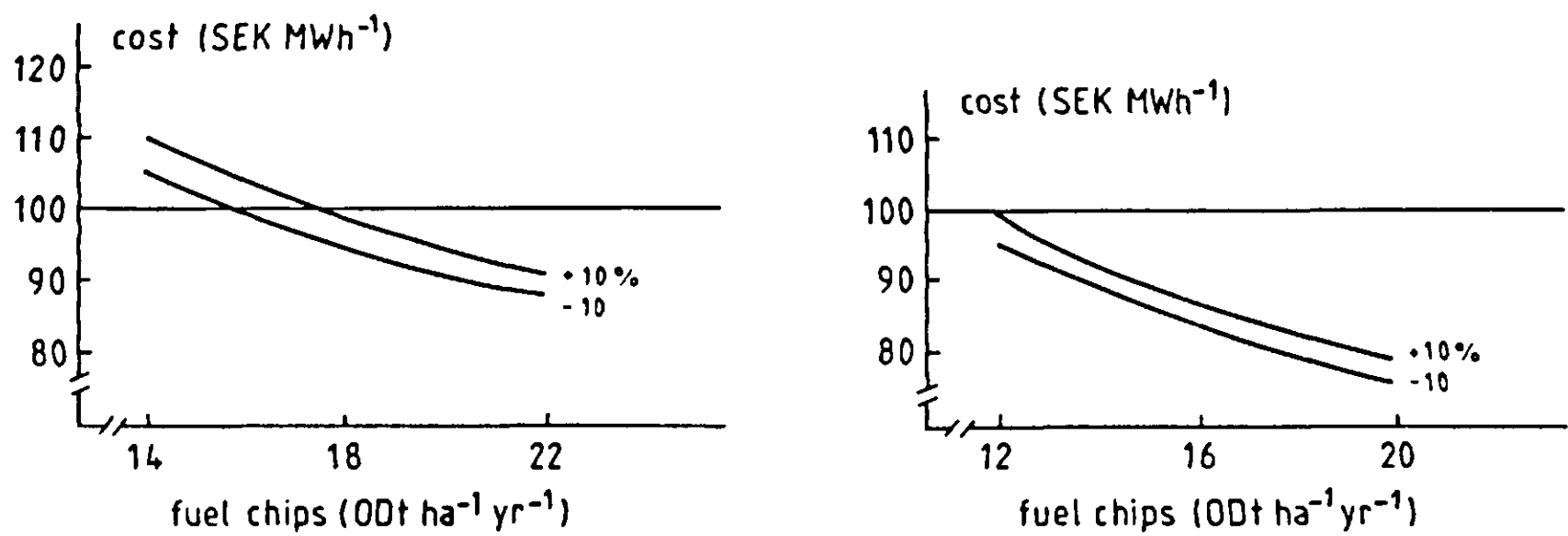


Figure 47. Effects of different maintenance costs ($\pm 10\%$) on the production costs (SEK MWh $^{-1}$) for fuel chips (ODt ha $^{-1}$ yr $^{-1}$) on 'good agricultural land / normal' in large-scale (left) and small-scale (right) cultivations.

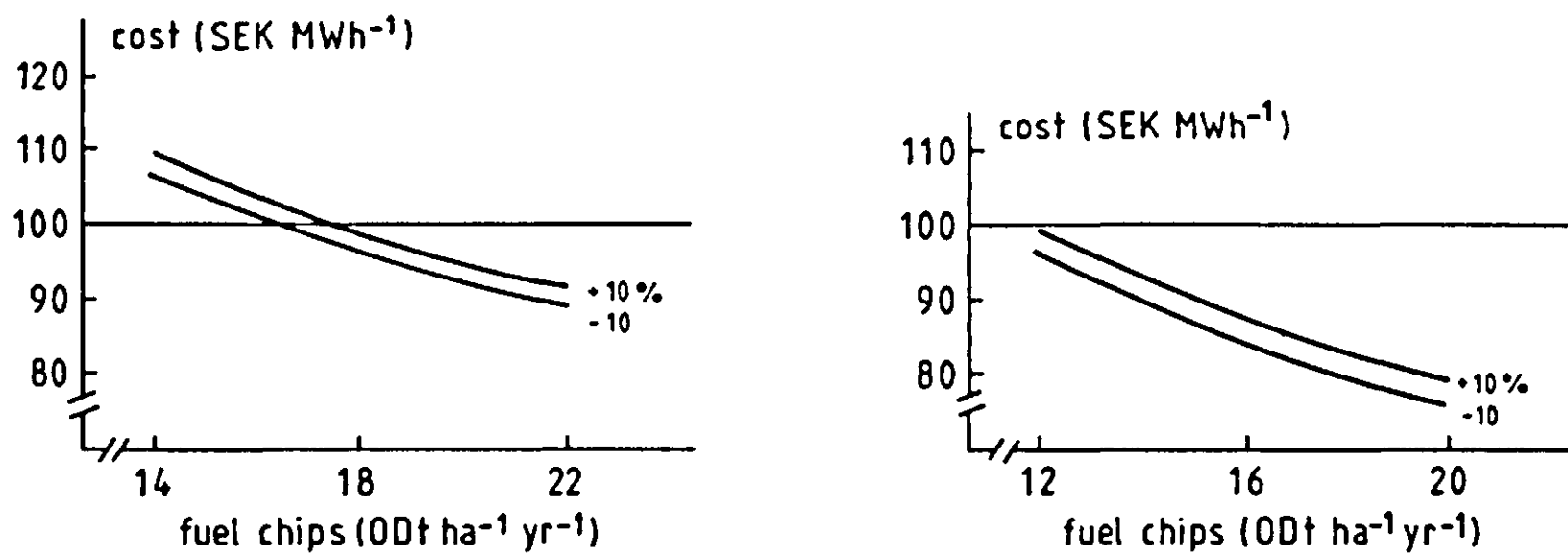


Figure 48. Effects of different harvesting costs ($\pm 10\%$) on the production costs (SEK MWh $^{-1}$) for fuel chips (ODt ha $^{-1}$ yr $^{-1}$) on 'good agricultural land / normal' in large-scale (left) and small-scale (right) cultivations.

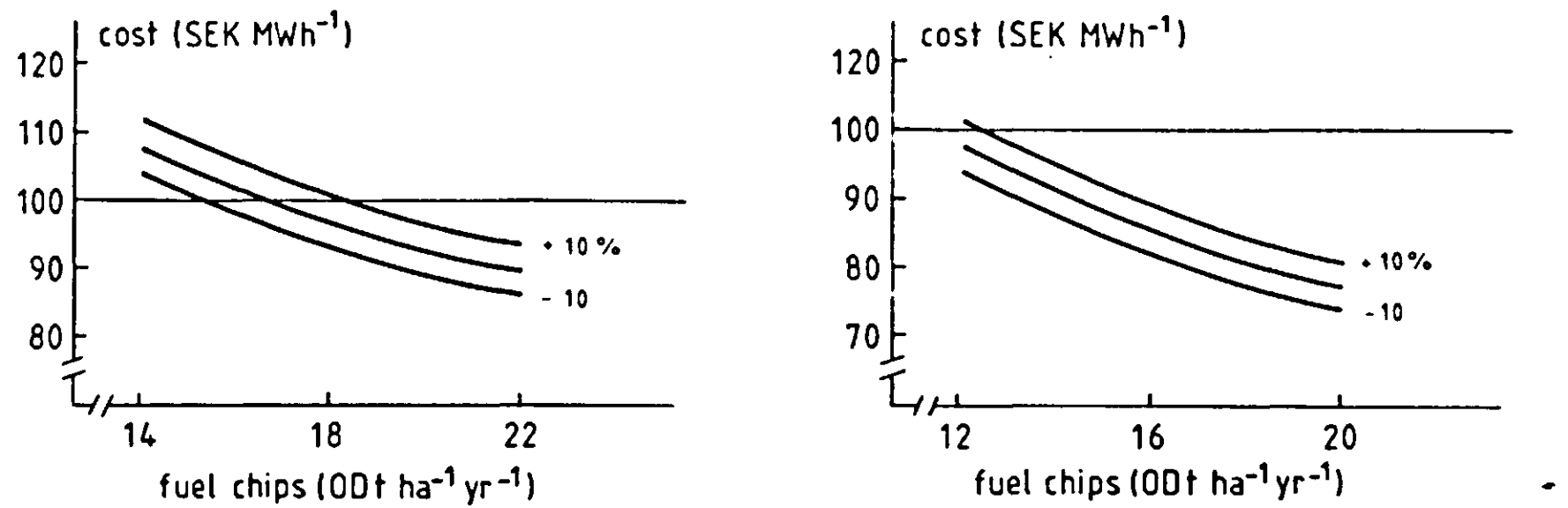


Figure 49. Effects of different transport costs ($\pm 10\%$) on the production costs (SEK MWh $^{-1}$) for fuel chips (ODt ha $^{-1}$ yr $^{-1}$) on 'good agricultural land / normal' in large-scale (left) and small-scale (right) cultivations.

Table 15. Break-even levels in oven dry tonnes (ODt) $ha^{-1} yr^{-1}$ for small- and large-scale cultivations.

Soil type	Small	Large
Good agricultural land	11-12	17
Peat land	-	19
Forest land	-	19

12.4 Sensitivity analysis

12.4.1 General

The sensitivity analysis was performed in order to show how different costs change in various situations. However, it is only shown for the 'normal' cases. The following costs and conditions were varied (Table 16): interest rate, land rent, maintenance cost, harvesting cost, chipping cost, and transport distance.

In general, costs associated with investments are more sensitive than the annual costs, which are more stable. The effects of changing initial costs are dependent on the soil type. Forest land and peat land are more sensitive to the same kind of changes and show greater variation than agricultural land. Variations in interest rate have a larger effect on the total cost for peat and forest land. Otherwise they have little or moderate effect.

Table 16. Results of the sensitivity analysis for the 'normal' cases on three different soil types (1: good agricultural land, 2: peat land, 3: forest land).

Condition	Costs (SEK (MWh) $^{-1}$) on different soil types			Figure No.*
	1	2	3	
Interest rate	3-4	6-10	-	44
Land rent	5-9	-	-	45
Initial cost	1-2	3-4	3-4	46
Maintenance	2-3	2-3	2-3	47
Harvest	1-2	1-2	1-2	48
Chipping	3	3	3	-
Transport distance	3-4	3-4	3-4	49

* The figures are presented only for 'good agricultural land' in large-scale and small-scale cultivations.

The cost of land rent has a large effect on good agricultural land, but generally the sensitivity is low or moderate for changes in these costs and conditions.

12.4.2 Special cases

Three special cases were chosen for study, namely: marginal costs for small-scale cultivations, investment subsidies, and extensively cultivated energy forest (*Alnus*, *Betula*, *Populus*).

When considering the marginal costs for small-scale cultivations, the machine and labour costs are regarded as fixed costs. This is applicable only for machines owned by the farmers and for the farmers' own work. The effects of a 50% reduction of both cost items can vary from 10 to 15 SEK per MWh in the case of good agricultural land.

The government may encourage development during an introduction period, by giving investment grants to the farmers. The effect of a 50% investment grant is 5 SEK per MWh for agricultural land.

Cultivation of *Salix* spp. has some limitations in regions with cold climate. A large proportion of potential energy forest land is located in northern Sweden (Perttu, 1986). One way of utilizing these areas is to use indigenous, relatively fast-growing alders, birches, and poplars. Preliminary calculations have shown that the break-even levels of yield in such extensively cultivated energy forest systems lie between 2-3 ODt $ha^{-1} yr^{-1}$. This level can be reached with the techniques and plant material currently available (Lönnér & Parikka, 1985a).

12.5 Conclusions

Small-scale intensively cultivated energy forestry can be an interesting alternative to farmers. According to the analyses presented, break-even levels of yield can be reached with today's techniques and price levels. For good agricultural land, the minimum levels are within 10-12 ODt $ha^{-1} yr^{-1}$. Small-scale, extensively cultivated birch in northern Sweden seems to be an interesting alternative. The existing plantations are, however, too young to allow correct conclusions to be drawn now.

Large-scale cultivations are more capital-dependent than small-scale ones. Costlier machinery, higher profitability requirements, higher administration costs, and longer transport distances influence the production level, which in this case must be higher than in small-scale cultivations. For good agricultural land this limit lies at a level of 17 ODt $ha^{-1} yr^{-1}$. Large- and small-scale cultivations on peat and forest land are not profitable today because investment costs are too high.

The main problem concerning the calculations is that machinery for planting and harvesting is still in an early phase of development and no machines have yet been developed for applying fertilizers in full-grown stands. Aircraft operations seem to be more costly than distribution with methods similar to those

used in agriculture. There is also a lack of knowledge about the production losses caused by disease and insects.

Shortage of suitable, high-producing planting material gives rise to some uncertainties, as does the surplus production of domestic fuels (wood wastes) in some regions. However, most of these areas are not especially interesting for energy forestry at present.

12.6 Source code for the economic model with explanations and examples

12.6.1 *Introduction*

This program is based on FORTRAN 77. It may be necessary to modify the program if computers other than VAX-8530 are used. The program is constructed for the economic simulation of intensively cultivated energy forests. Note the following limitations:

- the economic simulation is made from the farmer's point of view
- the rotation period (time-span between two consecutive plantings) is 21-33 years. This means 7-11 harvesting occasions, since the interval between two consecutive harvests is chosen to be 3 years, except for the first harvest, which is made after 4 years
- all the costs are total costs including: capital, labour, social security costs, maintenance, and material
- operations after year 1 (investment start) are followed continuously to the end of the rotation period
- the program disregards losses on combustion.

12.6.2 *Input data*

The data input procedure is divided into two blocks: infile routines and interactive routines. The infile routines facilitate the in-data file to be created by the editor, supported by the operating system. This file contains all the costs for the cultivation system, but the costs must be grouped by year. Costs depending on production or harvesting have to be separated and tagged with the number 11. Other costs are tagged with zero (0). The income after each harvest is defined by the production and the price of fuel chips at the heating plant. It is, therefore, not necessary to put the income explicitly into the file. An example of the cultivation program is given in Table 13. It is also the content of the datafile (note, however, that the name of the operation and the code are not present in the model's data library). The values presented are used in the simulation example given below. Input of costs by year is only needed for the first year, because the order of the operations is defined and the program is constructed to distribute the costs in the right order.

The interactive routines define all other conditions needed. Input or changes

can be made during execution of the program. The variables that can easily be changed are:

- expected production in ODt $ha^{-1} yr^{-1}$
- price of fuel chips at the heating plant per ODt
- real interest rate in %
- expected number of harvests during the rotation period.

12.6.3 Calculations

The annual costs and revenues are discounted and a net present value, annuity of net present value and the break-even price are calculated. The results are generated on a file called 'OUTDAT.LIS'. They are divided into four blocks: variable conditions; cashflow (year, revenue, cost and contribution); present value for revenues and costs, and net present value; annuity for net present value and break-even price for the fuel chips.

12.6.4 Use of the program

It is possible to make a sensitivity analysis by varying the conditions; for example, for different production levels, interest rates, and chip prices. A new output file is automatically created and it is called 'OUTDAT.LIS;X', where X is the version number from 1 to 100. If it is necessary to change the costs for different operations, this has to be done by using the editor, supported by the operating system.

12.6.5 Example of output

The economic simulation of energy forest cultivation gives the following types of results:

- expected production	=	12.00	oven dry t (ODt) yr^{-1}
- expected harvest	=	36.00	ODt total
- real interest rate	=	1.00	%
- price of fuel	=	500.00	SEK per ODt
- rotation period	=	22	Years
- first harvest after	=	4	Years
- next harvest after	=	3	Years
- number of harvests	=	7	

The following cash flow (SEK) can be achieved:

Year	Revenue	Cost	Accumulated contribution
1	0.00	13780.00	−13780.00
2	0.00	2650.00	−16430.00
3	0.00	1890.00	−18320.00
4	18000.00	10638.00	−10958.00
5	0.00	2650.00	−13608.00
6	0.00	1890.00	−15498.00
7	18000.00	10638.00	− 8136.00
8	0.00	2650.00	−10786.00
9	0.00	1890.00	−12676.00
10	18000.00	10638.00	− 5314.00
11	0.00	2650.00	− 7964.00
12	0.00	1890.00	− 9854.00
13	18000.00	10638.00	− 2492.00
14	0.00	2650.00	− 5142.00
15	0.00	1890.00	− 7032.00
16	18000.00	10638.00	330.00
17	0.00	2650.00	− 2320.00
18	0.00	1890.00	− 4210.00
19	18000.00	10638.00	3152.00
20	0.00	2650.00	502.00
21	0.00	1890.00	− 1388.00
22	18000.00	10638.00	5974.00
Present value	110908.90	107609.07	
Net present value			3299.83SEK ha ⁻¹
Annuity of net present value			167.84 SEK ha ⁻¹ yr ⁻¹
Break-even price			485.12 SEK (ODt) ⁻¹

12.6.6 Source code

```
*****
C      MATTI PARIKKA, SLU-SIMS, UPPSALA, 1986-10-05
C      PROGRAM ESO ECONOMIC SIMULATION
C      VARIABLES
REAL MAT(1:31,1:2),TWOCOST,THREECOST,FOURCOST,NETPROFIT
REAL FACTOR,PRVALBEN,PRVALCOST,ANNU,ANNPROF,BREPRIC
REAL PROD,PRICE,INTER,PRESUM,ANNTOT,FFOURCO,ONECOST
INTEGER IN,OUT,WR,SC,YEAR,COST,P,HARV,ROTPER,FIRST,NEXT
INTEGER ANS,EOF
```

```

CHARACTER*8 INFILE
IN=3                      !INPUT OUTPUT UNITS
OUT=4
SC=5
WR=6
*****
C
C  DEFINE DATA
C *****
100  WRITE(WR,*)"NAME OF THE DATAFILE ?"
READ(SC,*)INFILE
*****
C
C  OPEN FILE FOR INPUT
C *****
101  ONECOST=0
TWOCOST=0                  !ZERO
THREECOST=0
FOURCOST=0
FFOURCO=0
PRVALBEN=0
PRVALCOST=0
PRESUM=0
EOF=0
OPEN (UNIT=IN,NAME=INFILE,STATUS='OLD',READONLY) !OPEN FILE
DO WHILE (EOF.EQ.0)
  READ(IN,*,IOSTAT=EOF)YEAR,COST,P      !READ INDATA
  IF (EOF.EQ.0) THEN
    IF (YEAR .EQ. 1) THEN      !DEFINE ANNUAL TOTAL COSTS
      ONECOST=ONECOST+COST
    ELSEIF (YEAR .EQ. 2) THEN
      TWOCOST=TWOCOST+COST
    ELSEIF (YEAR .EQ. 3) THEN
      THREECOST=THREECOST+COST.
    ELSEIF (YEAR .EQ. 4 .AND. P .LT. 11) THEN
      FOURCOST=FOURCOST+COST
    ELSEIF (YEAR .EQ. 4 .AND. P .EQ. 11) THEN
      FFOURCO=FFOURCO+COST
    ENDIF
  ENDIF
ENDDO
CLOSE(UNIT=IN)                !CLOSE UNIT
*****
C
C  CONTINUE INTERACTIVE ROUTINE
C *****

```

```

110  WRITE(WR,*)"EXPECTED PRODUCTION IN ODT/YEAR/HA"
    READ(SC,*)PROD
        IF (PROD .LT. 3 .OR. PROD .GT. 30) THEN
            GOTO 110
        ENDIF
120  WRITE(WR,*)"PRICE OF FUEL AT HEATING PLANT CHIPPED IN /ODT"
    READ(SC,*)PRICE
        IF (PRICE .LT. 0 .OR. PRICE .GT.1500) THEN
            GOTO 120
        ENDIF
130  WRITE(WR,*)"REAL INTEREST RATE IN % (0-15)"
    READ(SC,*)INTER
        IF (INTER .GT. 15 .OR. INTER .LT. 0) THEN
            GOTO 130
        ENDIF
140  WRITE(WR,*)"EXPECTED NUMBER OF HARVESTS (7-10)?"
    READ(SC,*)HARV
        IF (HARV .GT. 10 .OR. HARV .LT. 7) THEN
            GOTO 140
        ENDIF
C   ****
        ROTPER=((HARV*3)+1)          !ROTATION PERIOD
        DO 15 I=1,ROTPER             !ZERO MATRIX
            DO 10 J=1,2
                MAT(I,J)=0
            CONTINUE
15      CONTINUE
            MAT(I,I)=ONECOST          !MATRIX
            DO 30 I=2,ROTPER-2,3
                MAT(I,I)=TWOCOST
            CONTINUE
30      DO 40 I=3,ROTPER-1,3
            MAT(I,I)=THREECOST
            CONTINUE
40      DO 50 I=4,ROTPER,3
            MAT(I,I)=FOURCOST+FFOURCO*3.0*PROD
            MAT(I,2)=PRICE*PROD*3.0
            CONTINUE
50      DO 55 I=1,ROTPER
            IF (MAT(I,2) .GT. 0) THEN
                FIRST=I
                NEXT=I-1
                GOTO 56
            ENDIF

```

```

55      CONTINUE
*****
C      OPEN FILE OUTPUT.LIS;X
*****
C      *****
56      OPEN(UNIT=OUT,NAME='OUTDAT.LIS',STATUS='NEW')
      WRITE(OUT,*)'*****'
      WRITE(OUT,*)'***** RESULT *****'
      WRITE(OUT,*)'*****'
      WRITE(OUT,*)'*****'
      WRITE(OUT,*)'*** ECONOMIC SIMULATION OF ENERGY FOREST ***'
      WRITE(OUT,*)'*****'
      WRITE(OUT,1030)'- EXPECTED PRODUCTION =',PROD,
      1 'TONNES OF DRY MATTER PER YEAR AND HECTARE'
      WRITE(OUT,*)'*****'
      WRITE(OUT,1030)'- EXPECTED HARVEST =',PROD*3.0,
      1 'TONNES OF DRY MATTER PER HECTARE IN TOTAL'
      WRITE(OUT,*)'*****'
      WRITE(OUT,1030)'- REAL INTEREST RATE =',INTER,'%'
      WRITE(OUT,*)'*****'
      WRITE(OUT,1030)'- PRICE OF FUEL =',PRICE,
      1 'SEK PER TONNE OF DRY MATTER'
      WRITE(OUT,*)'*****'
      WRITE(OUT,1040)'- ROTATION PERIOD =',ROTPER,'YEARS'
      WRITE(OUT,*)'*****'
      WRITE(OUT,1040)'- FIRST HARVEST AFTER =',FIRST,'YEARS'
      WRITE(OUT,*)'*****'
      WRITE(OUT,1040)'- NEXT HARVEST AFTER =',NEXT,'YEARS'
      WRITE(OUT,*)'*****'
      WRITE(OUT,1040)'- NUMBER OF HARVESTS =',HARV
      WRITE(OUT,*)'*****'
      WRITE(OUT,*)'CASH-FLOW'
      WRITE(OUT,*)'*****'                                ACCUMULATED'
      WRITE(OUT,*)'YEAR      REVENUE      COSTS      CONTRIBUTION'
      WRITE(OUT,*)'*****'
      DO 60 I=1,ROTPER                                !SUM
      NETPROFIT=NETPROFIT+(MAT(I,2)-MAT(I,1))          !NETPROFIT
      WRITE(OUT,1000)I,MAT(I,2),MAT(I,1),NETPROFIT
      CONTINUE
      WRITE(OUT,*)('*',I=1,50)
      WRITE(OUT,*)'*****'
      FAKTOR=(1.0+INTER/100.0)                          !DISCOUNT
      DO 65 I=4,ROTPER,3
      PRESUM=PRESUM+FACTOR**(-I)                      !SUM OF DISCOUNT
      CONTINUE
      DO 70 I=1,ROTPER                                !PRESENT VALUE

```

```

    PRVALBEN=PRVALBEN+MAT(I,2)*FACTOR**(-I)
    PRVALCOST=PRVALCOST+MAT(I,1)*FACTOR**(-I)
70  CONTINUE
C ****
C ANNUITY
C ****
    ANNU=((INTER/100.0)*FACTOR**(ROTPER))/(FAKTOR**(ROTPER)-1.0)
    ANNPROF=(PRVALBEN-PRVALCOST)*ANNU      !ANNUAL PROFIT
    BREPRIC=PRVALCOST/(PROD*3.0*PRESUM)    !BREAKEVEN
    ANNTOT=PRVALBEN-PRVALCOST              !TOTAL NETPROFIT
    WRITE(OUT,1010)'PRESENT VALUE =',PRVALBEN,PRVALCOST
    WRITE(OUT,*)'
    WRITE(OUT,*)'
    WRITE(OUT,1020)'NET PRESENT VALUE                      =',ANNTOT,
    1 'SEK PER HECTARE'
    WRITE(OUT,1020)'ANNUITY OF NET PRESENT VALUE=',ANNPROF,
    1 'SEK PER YEAR AND HECTARE'
    WRITE(OUT,1020)'BREAKEVEN PRICE                      =',BREPRIC,
    1 'SEK PER OVEN DRY TONNE'
    WRITE(OUT,*)'
    WRITE(OUT,*)'RESULTS - OUTDAT.LIS'
    WRITE(OUT,*)'
    WRITE(OUT,*)'END'
    WRITE(OUT,*)('*',I=1,50)
    CLOSE (UNIT=OUT)                      !CLOSE OUTPUT
C ****
    NETPROFIT=0                           !ZERO
    PRESUM=0
    PRVALBEN=0
    PRVALCOST=0
C ****
80  WRITE(WR,*)"CHANGE      PARAMETERS,NEW      FILE      OR      CAN-
    CELL'                                !DISPLAY
    WRITE(WR,*)'
    WRITE(WR,*)"YOUR CHOICE!!!!"
    WRITE(WR,*)'
    WRITE(WR,*)"** CHANGE PRODUCTION = 1"
    WRITE(WR,*)"** PRICE OF FUEL = 2"
    WRITE(WR,*)"** INTERESTRATE = 3"
    WRITE(WR,*)"** ROTATION PERIOD = 4"
    WRITE(WR,*)"** NEW DATAFILE = 5"
    WRITE(WR,*)"** END = 6"
    READ(SC,*)ANS
    IF (ANS .LT. 1 .AND. ANS .GT. 6) THEN

```

```

GOTO 80
ENDIF
GOTO (110,120,130,140,100,2000) ANS
GOTO 80
C ****
C      FORMAT
C ****
1000  FORMAT('',I3,TR7,F9.2,TR4,F9.2,TR4,F9.2)
1010  FORMAT('',A,TR3,F9.2,TR3,F9.2)
1020  FORMAT('',A,TR3,F9.2,TR3,A)
1030  FORMAT('',A,TR3,F8.2,TR3,A)
1040  FORMAT('',A,TR3,I8,TR3,A)
2000  STOP
3000  END

```

12.7 References

Anderson, H.W. & Zsuffa, L., 1980. Hybrid poplar plantation biomass – a potential source of energy in Ontario, Canada. In: Proceedings of the International Poplar Commission, 16th session, November 4-8, 1980, 13 pp. Izmir, Turkey.

Fege, A.S., Inman, R.E. & Salo, D.J., 1979. Energy farms for the future. *Journal of Forestry* 77:358-361.

Inman, R.E. & Salo, D.J., 1977. Silvicultural energy farms. *Proceedings from symposium on Fuels from biomass*, University of Illinois, Urbana-Champaign, pp. 29-36.

Kasberg, N-E. (Ed.), 1986. *Databok för driftsplanering* [Databook for operational planning in agriculture]. Swedish University of Agricultural Sciences, Research Information Centre, Uppsala. 405 pp.

Lönnér, G. & Parikka, M., 1985a. *Ekonomisk analys av energiskogsödning* [Economic analysis of energy forestry]. Report 8, 16 pp. Swedish University of Agricultural Sciences, SIMS, Uppsala.

Lönnér, G. & Parikka, M., 1985b. *Trädbränslen* [Forest fuels in Sweden]. Report 10, 16 pp. Swedish University of Agricultural Sciences, SIMS, Uppsala.

Lönnér, G., Parikka, M. & Söderberg, L., 1985. *Ekonomisk analys av energiskogsodling* [Economic analysis of energy forestry]. In: *Energiskog*, Statens energiverk 1985:9:433-464. Norstedts Tryckeri, Stockholm.

Perttu, K., 1986. Energieholzversuche in Europa – bisherige Ergebnisse und Zukunftsaussichten. In: E. Scheiber (Ed.): *Energie aus Biomasse*. 16. Internationales Symposium vom 13. bis 15. Oktober 1986, Gmunden, Oberösterreich. Österreichische Gesellschaft für Land- und Forstwirtschaftspolitik, Österreich, pp. 82-97.

Sirén, G., 1983. *Energiskogsodling* [Cultivation of energy forests]. No. 1983:11, 255 pp. Nämnden for energiproduktionsforskning, Stockholm.

13 Short-rotation forestry: an alternative energy resource?

Kurth Perttu

13.1 Introduction

Both biomass and fossil fuels originate from solar energy. The latter have accumulated during millions of years, whereas biomass is the result of a few seasons of stored energy. The energy density of fossil fuels is high compared with biomass; oil, for instance, contains about 12 MWh t^{-1} whereas wood only contains 4.5 MWh t^{-1} at 50% dry matter content (Anonymous, 1984). On the other hand, gases and particles that have been bound into fossil fuels during millions of years are rapidly released during combustion. This places a very serious strain on the environment by increasing the carbon dioxide (CO_2) content of the atmosphere, acidifying lakes and soils, etc. The environment's capacity to cope with pollution from the combustion of fossil fuels is limited; this is obvious from all the reports on different types of damage. In many countries the use of fossil fuels has already created very serious ecological problems. Biomass is, therefore, an attractive alternative to such fuels, because its harmful effects on the environment are considerably less than those from fossil fuel. For example, the amount of CO_2 released at combustion during winter time is bound into biomass during the growing season, with no net increase as a result.

The prerequisites for energy forestry in Sweden are good. The climate permits relatively high yields to be obtained in central and southern parts and along the eastern coast to the north of Stockholm (Perttu, 1980; Perttu & Lindroth, 1986). Within these areas the growing period normally lasts between 160 – 230 days and the heat sums lie between 1100 – 1700 day-degrees (Odin et al., 1983; Perttu, 1983; Perttu, 1985a). During the growing season, an average incoming solar radiation of $14 \text{ MJ m}^{-2} \text{ day}^{-1}$ is estimated for the area concerned. The value is about the same both in the north and in the south of Sweden. About 1% of the incoming solar radiation is converted into wood biomass by net photosynthesis.

In Sweden, energy forests are intensively cultivated short-rotation shrub or tree-shaped stands, mostly of *Salix* and *Alnus* spp. (Sirén et al., 1984). They have been found very suitable for energy wood production because of their high yield response to intensive management. *Salix* can be planted as cuttings and *Alnus* as rooted plants, the latter being inoculated to facilitate nitrogen fixation. Sometimes they can be grown together in a combined cultivation system, thus using the nitrogen-fixing capacity of *Alnus* as a nutrient source for the whole stand (Granhall, 1982, Granhall et al., 1983).

13.2 Considerations

Wood quality is a major factor when producing biomass. There are large differences in wood density between *Salix* clones, and also between shoots of different ages from the same clone (Sirén et al., 1987). This is, therefore, one of the main criteria when testing different clones and also when finding the optimal age for harvesting in terms of production and of economics. The heat value and energy content of wood from the best clones is comparable with that of wood from coniferous trees (Anonymous, 1985).

The water use efficiency of *Salix* is rather unfavourable, because it is a water-demanding species. In Chapter 10, Halldin showed that the above-ground production is about 25 kg of oven-dry biomass per mm of water. In Chapter 6, Eckersten & Ericsson showed that the leaf biomass constitutes about 35% of the above-ground biomass. The average amount of oven-dry stem biomass in central and southern Sweden for a three-year cycle is about $11 \text{ t ha}^{-1} \text{ yr}^{-1}$ (see Chapter 5). These figures show that an annual production of $11 \text{ t stem wood ha}^{-1}$ requires 680 mm of water.

The nitrogen content of *Salix* leaves is typically 3.5% on a dry matter basis (see Chapter 5). If the production is 11 t oven-dry stem wood, then the leaf biomass is about 6 t, containing about 200 kg of nitrogen. When the stand has reached a balance in the nutrient circulation, only the amount removed by harvesting of the stem biomass needs to be applied. For instance, the nitrogen content in willow wood is about 0.7-1.0%, which indicates that in this case $80-110 \text{ kg ha}^{-1} \text{ yr}^{-1}$ have to be applied. It is very important to apply the fertilizers in time, so that uptake is not delayed, otherwise the growth decreases drastically (see Chapter 7).

13.3 Discussion and conclusions

In Sweden, energy forestry is related more to agriculture than to conventional forestry (Perttu, 1985b). The interval between two consecutive harvests is 3-5 years and the rotation period (the time between two planting occasions) is about 25 years. In traditional coniferous forestry the harvesting cycle and the rotation period are the same, 70-120 years, depending on site and climate. Simulated willow production has reached levels of $10-12 \text{ t oven-dry stem biomass ha}^{-1} \text{ yr}^{-1}$, about 6 t leaves and 5-6 t roots (cf. above). The variation is caused by climate, soil, nutrients, etc. Annual production of 10-15 t has been obtained in full-scale plantations at several locations in Sweden (Ohlsson, 1986). Under good conditions, very intensively managed *Salix* plantations have given even higher yields (Sirén et al., 1984). The expectations are $15 \text{ t stem wood ha}^{-1} \text{ yr}^{-1}$ in commercial cultivations within the next ten years when farmers have acquired knowledge and experience about the cultivation techniques and when the plant material has been developed further (Anonymous, 1985). Applying average climate data in the growth model developed by Perttu et al. (1984), the

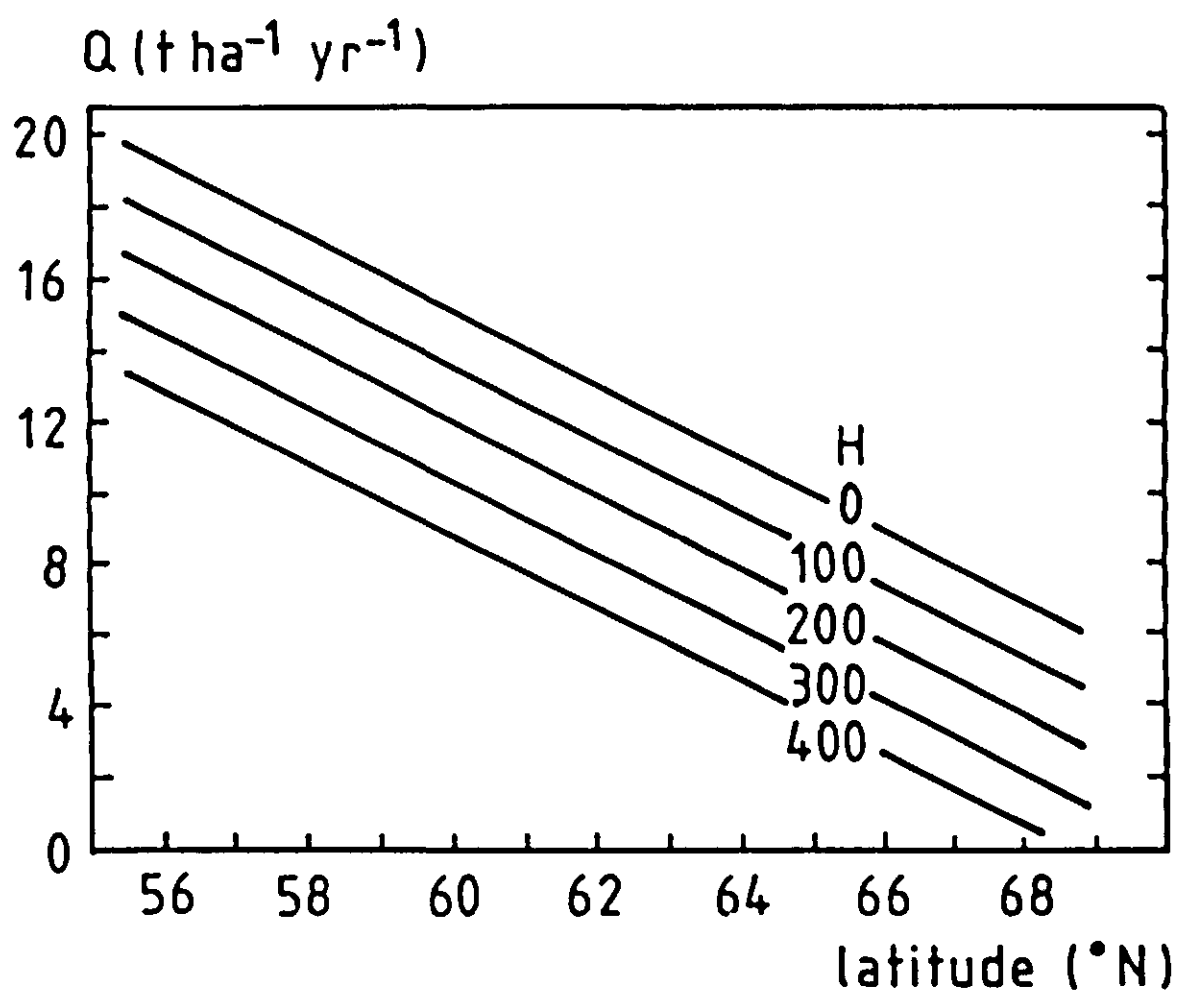


Figure 50. Average willow stem production (Q) at different latitudes and heights above sea-level (H) in Sweden calculated by means of growth models and available climatic data. (After Perttu & Lindroth, 1986).

potential stemwood production of willow at different latitudes and elevations can be estimated as 10-20 t oven-dry stem wood $\text{ha}^{-1} \text{yr}^{-1}$ in central and southern Sweden (Figure 50).

In Chapter 12, the break-even level was found to be 10-12 oven-dry t stem wood $\text{ha}^{-1} \text{yr}^{-1}$. Other economic calculations have shown that in the 1990s energy from intensively cultivated short-rotation forests on agricultural land will be more profitable than energy from oil, coal, electricity, peat, and waste from conventional forests (Table 17). The costs of extracting 1 kWh in the form of hot water from a district heating plant ($> 1 \text{ MW}$), from a small industrial plant (0.2-1 MW), and from a house furnace ($< 200 \text{ kW}$) are estimated as SEK 160, 190, and 260, respectively (Gunnarson, 1985).

During the winter of 1984/85, the Swedish National Energy Administration conducted an evaluation of energy forestry in Sweden (Anonymous, 1985). The results of this evaluation can be summarized as follows:

- practical experience has been obtained, especially on agricultural land
- no negative environmental consequences have been observed
- for combustion purposes, energy forest wood and conventional forest wood are of the same quality
- the best economic situation for energy forestry is with small-scale farmers and good agricultural land
- the costs of energy forest wood are 90 – 110 SEK per MWh (1987), delivered to a district heating plant

Table 17. Comparison of energy costs in SEK from different types of fuel after combustion, estimated for the 1990s. (After Gunnarson, 1985).

Energy source	Power plant (> 1 MW)	Small industry (0.2-1 MW)	House (< 200 kW)
Energy forest*	160	190	260
Oil, heavy (2-5)	240	-	-
Oil, light (1)	-	320	350
Coal	180	-	-
Electricity	-	-	280
Peat	150	-	-
Waste wood	150	180	270
Heat pump	-	-	250-320

* Estimated net production 13.5 oven-dry t stemwood $ha^{-1} yr^{-1}$. The costs include soil preparation, planting, weed control, fertilization, irrigation, harvesting, transport, chipping and combustion.

- energy forest wood can economically compete with coal, peat and conventional forest wood
- there will probably be a market for energy forest fuel in the 1990, and around the year 2000; the annual contribution from such fuel is estimated to be 7-8 TWh, using an area of about 100 000 ha.

The different evaluations of Swedish energy forestry have shown that it should be attempted on a practical scale. According to simulations and experiments, the production of woody biomass can be assumed to reach levels where it is economically profitable in plantations on agricultural land. The Federation of Swedish Farmers decided to start energy forest plantations on a large scale, aiming at 200 000 ha by the year 2000.

The public sector also benefits from energy forestry. The most important benefit is not only measurable in financial terms, but in other aspects, such as less dependence on imported energy, and less strain on the environment. A significant number of new jobs will be created, in the order of two persons per 100-150 ha of energy forest. Additional jobs will be created in the engineering industry for producing machinery for planting, management, and harvesting (Sirén et al., 1984; Perttu, 1986).

13.4 References

Anonymous, 1984. Energiläget 1984. Information om energianvändningen i Sverige och utvecklingen på de internationella energimarknaderna [The energy situation 1984. Information on the energy use in Sweden and the international development]. Statens energiverk, Stockholm. 16 pp.

Anonymous, 1985. Energiskog. Resultat, slutsatser och förslag från det svenska energiskogsprogrammet [Energy forestry. Results, conclusions and proposals from the Swedish energy forestry programme]. Statens energiverk, Norstedts Tryckeri, Stockholm. 533 pp.

Granhall, U., 1982. The use of *Alnus* in energy forestry. Proceedings from 2nd National Symposium on Nitrogen Fixation, June 1982. Helsinki. Nitrogen project 1. The Finnish National Fund for Research and Development, pp. 273-285.

Granhall, U., Ericsson, T. & Clarholm, M., 1983. Dinitrogen fixation and nodulation by *Frankia* in *Alnus incana* as affected by inorganic nitrogen in pot experiments with peat. Canadian Journal of Botany 61:2956-2963.

Gunnarson, S., 1985. Energiskogens ekonomiska konkurrensförmåga [The economic competitive power of energy forests]. Skogsfakta. Inventering och ekonomi 7/1985, 4 pp. Swedish University of Agricultural Sciences, Uppsala.

Odin, H., Eriksson, B. & Perttu, K., 1983. Temperaturklimatkartor för svenska skogsbruk [Temperature climate maps for Swedish forestry]. Report 45, 57 pp. Swedish University of Agricultural Sciences, Department of Forest Soils, Uppsala.

Ohlsson, T., 1986. Produktionsresultat i svenska odlingar av energiskog [Production results from Swedish energy forest plantations]. Swedish University of Agricultural Sciences, Section of Energy Forestry, Uppsala, 76 pp.

Perttu, K., 1980. Abiotic premises for growing energy forests. In: K. Perttu (Ed.): Proceedings from a symposium arranged by the international energy agency (IEA) planning group on growth and production, September 24, 1979, Bogesund, Stockholm. Report 8:25-34. Swedish University of Agricultural Sciences, Section of Energy Forestry, Uppsala.

Perttu, K.L., 1983. Temperature restraints on energy forestry in Sweden. International Journal of Biometeorology, Volume 27(3):189-196.

Perttu, K., 1985a. Role of meteorology in Swedish conventional and short-rotation forestry. Report 40, 29 pp. Swedish University of Agricultural Sciences, Section of Energy Forestry, Uppsala.

Perttu, K., 1985b. Projekt Energiskog lägger om kursen [Project energy forestry changes its policy]. Biomassa & Energi 2/85:2. Swedish University of Agricultural Sciences, Department of Operational Efficiency, Garpenberg.

Perttu, K., 1986. Energieholzversuche in Europa – bisherige Ergebnisse und Zukunftsaussichten. In: E. Scheiber (Ed.): Energie aus Biomasse. 16. Internationales Symposium vom 13. bis 15. Oktober 1986, Gmunden, Ober österreich. Österreichische Gesellschaft für Land- und Forstwirtschaftspolitik, Österreich, pp. 82-97.

Perttu, K., Eckersten, H., Kowalik, P.J. & Nilsson, L-O., 1984. Modelling potential energy forest production. In: K. Perttu (Ed.): *Ecology and management of forest biomass production systems*. Report 15:467-480. Swedish University of Agricultural Sciences, Department of Ecology and Environmental Research, Uppsala.

Perttu, K. & Lindroth, A., 1986. Climatic influences on energy forest growth in Sweden. *Proceedings from 18th IUFRO World Congress, 7-21 September 1986, Ljubljana, Yugoslavia. Division 1, Volume 1:84-96.*

Sirén, G., Perttu, K., Sennerby-Forsse, L., Christersson, L., Ledin, S. & Granhall, U., 1984. *Energy forestry. Information on research and experiments at the Swedish University of Agricultural Sciences, Section of Energy Forestry, Uppsala.* 16. pp.

Sirén, G., Sennerby-Forsse, L. & Ledin, S., 1987. Energy plantations – Short rotation forestry in Sweden. In: D.O. Hall & R.P. Overend (Eds): *Biomass, regenerable energy*. John Wiley & Sons, Chichester, New York, Brisbane, Toronto, Singapore, pp. 119-143.

APPENDIX

14 Computer use in modelling energy forestry in Sweden

Sven Halldin

14.1 Introduction

The large-scale, interdisciplinary Swedish Energy Forestry (SEF) Project (now the Section of Energy Forestry, Swedish University of Agricultural Sciences) has continued and strengthened the tradition, started in the 1970s, of relying on the digital computer as a vital research tool. With much of its research staff trained in the Swedish Coniferous Forest (SWECON) Project (see Halldin, 1979 and Persson, 1980), it was natural to continue the utilization and development of the software from this project. This appendix presents the software, so that readers can understand the simulation programs presented in earlier chapters (cf. Chapter 2). The future implications of using this software are also touched upon.

14.2 Computer environment

At Swedish Universities, notably at Uppsala, three trends have prevailed when it comes to computer environment. The first relates to the dominant position of Digital Equipment Corporation (DEC) in university computing. As such, the SEF Project, and earlier the SWECON Project, have used PDP/RSX and VAX/VMS computers. The second trend relates to rapid development in networking. Besides the world-wide EARN and the nation-wide SUNET, the university computer installations in Uppsala are linked by UPNET, a terminal network with limited capacity for file transfer but no electronic mail facilities. Parallel to UPNET and SUNET there is a DECNET, which allows efficient file transfer and has electronic mail but which can only be used by DEC computers. For these reasons an unfortunate bias towards DEC-based software is to be found in the SEF research, which commonly makes use of idiosyncrasies in the VMS FORTRAN dialect and is also structured along the lines of the VMS operating system. Most of the programs are, therefore, not directly portable to any other installation. This is the more regrettable, since the third, very strong, trend relates to the use of personal computers in applications where larger machines used to dominate.

14.3 Supporting software

Two major needs for supporting software were expressed at the beginning of the SEF Project. The first concerned simplified development and use of simulation models and the second concerned a system for acquiring, retrieving,

correcting and presenting data. In both cases the software, SIMP and ECO-DATA (Engelbrecht et al., 1980), was inherited from the SWECON Project. Because of the age of these packages, development was requested for both. At the time of writing, the ECODATA package (see also Svensson, 1979) has been replaced by the considerably modernized PGRA system (Jansson & Christoferson, 1985). The SIMP simulation support package (see also Lohammar, 1979), on the other hand, has not yet been replaced by the more modern system developed by the present author.

14.3.1 Data acquisition, retrieval, correction and presentation

In general terms, a large number of different types of data are collected and analysed in the SEF research. Those of relevance here are the time-series data on biomass, hydrology and meteorology. The biomass and hydrological data are normally collected and put into the PGRA database system manually. The meteorological data are collected through micro-loggers (Campbell 21X and CR10) and automatically fed into the PGRA database system, as conceived by Perttu (1985). The main reason for using the PGRA/ECODATA system instead of a more widely known database/graphical support package is the special emphasis by PGRA on time-series data and on simplicity of learning and using. These features are handled less well by the more general type of systems. For data other than time-series data, SAS (SAS Institute Inc., 1985) is frequently used.

14.3.2 Simulation support package

It is still common for researchers to put much effort into programming problems such as input/output operations, numerical integration schemes, multiple simulation, fitting of parameters, changing input data, graphical presentation of results, etc. In order to use computer capacity efficiently it would be better if the researcher could concentrate on the subject area in which he/she is a specialist. The SIMP package (Lohammar, 1979) was conceived to relieve the user of all the technical problems mentioned above. Since several of the models presented in the previous chapters of this volume use SIMP, its major properties are presented below.

When using SIMP, a first-order differential equation type of model is coded in FORTRAN 77 as a subroutine to the governing program, named LOOP (Figure 51). Only the model processes in a strict sense have to be coded and certain conventions must be obeyed. Five types of entities are used: X for state variables, T for transfer variables, G for auxiliary variables, D for external variables, and P for parameters (constants).

The model system is conceived in box-and-flow visualization and only the flow equations are coded. With the simple model in Figure 52, two FORTRAN statements are needed: T0001 and T0100. The corresponding equation

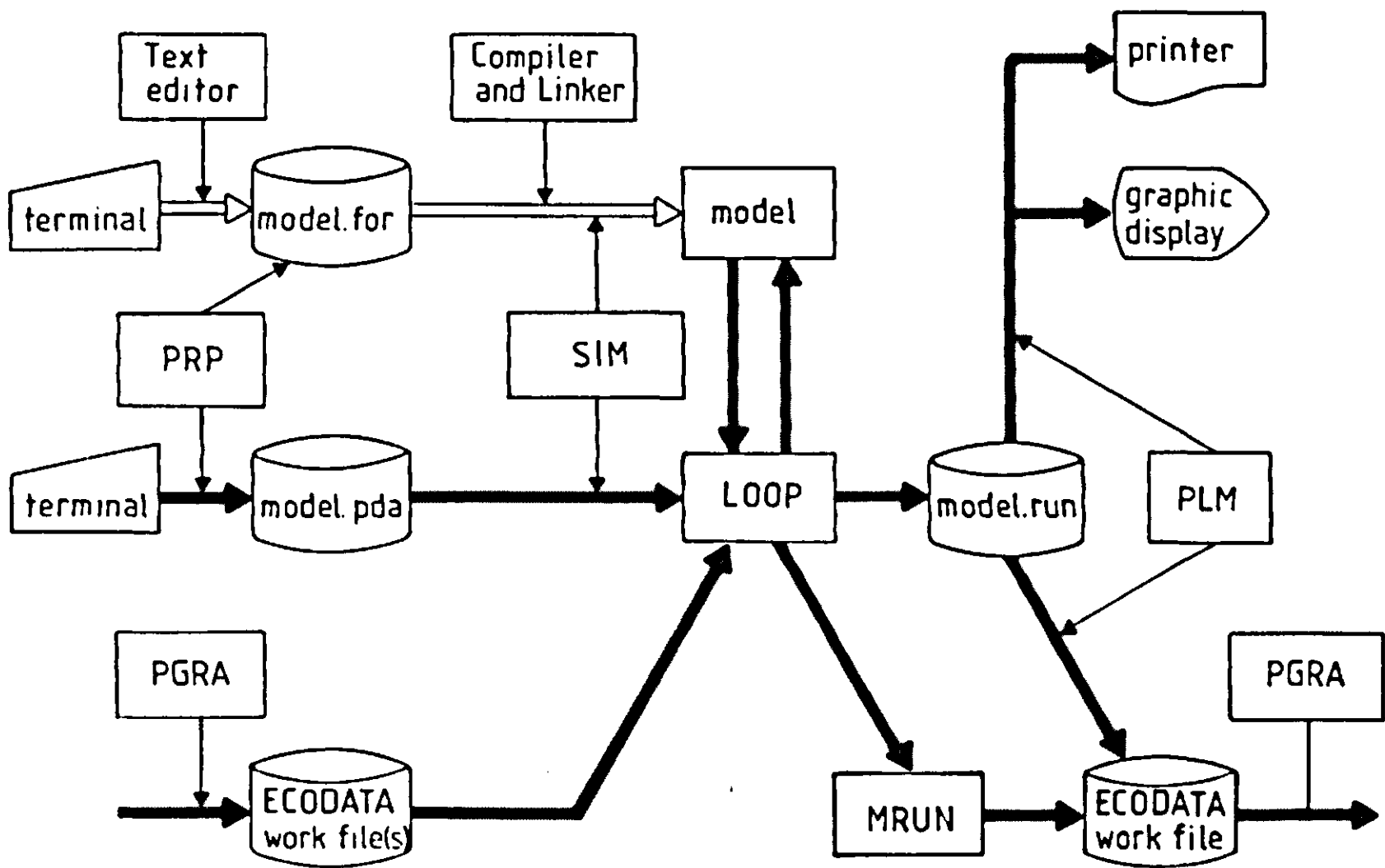


Figure 51. Structure of the SIMP simulation support package.

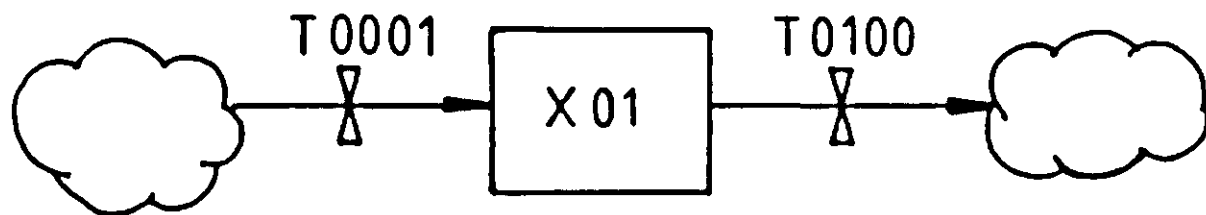


Figure 52. Box-and-flow visualization of a simple first order differential equation.

$$dX01/dt = T0001 - T0100$$

Equation 75

is solved automatically by SIMP, which also accounts for the conservation laws of the system. SIMP uses only explicit forward differencing integration (Euler method) based on a user-defined default time step. The lack of more sophisticated integration routines can partly be compensated for by the ability to change the time step as a function of model performance during the simulation.

Certain other information is necessary before a simulation can be carried out. Names and values of parameters in the FORTRAN code must be specified. Initial values for the state variables and the flow structure of the system are also needed. These data are fed into a special file through the preparatory program PRP (Figure 51). This can also account for a number of other items of information that are not strictly necessary to perform a simulation. Such examples are time unit, integration time step, and number of variables to be stored in the resulting output file.

Once the FORTRAN source code and structural information have been specified, SIMP automatically edits a new source code which contains a section that assures communication between the executing program LOOP and the

model. This new source code must be compiled and linked by the user, like any other FORTRAN program (Figure 51).

When the executable model is ready, the simulation is carried out by the SIM program. If the default values in the PRP file are sufficient, the simulation can be started directly by SIM. If, on the other hand, the user wants to change the default values of, e.g., the simulation time span, the initial state variables, or parameters, this can be done interactively before commencing the run.

SIMP is connected to the ECODATA database system in both directions. This increases the utility of both programs considerably. Time-series data can be read into the model by specifying three subroutine calls in the source code:

- CALL ECDCIN initializes the connection between SIMP and ECODATA
- CALL ECDCDA transmits continuous time-series data (e.g. temperature)
- CALL ECDCDD transmits discrete time-series data (e.g. precipitation).

In this way, any type of data stored in an ECODATA or PGRA (these two programs can be seen as equivalent in this context) file can be used as driving data in a model. All problems connected to time unit, interpolation of data to fit the model, time step etc. are handled by SIMP.

Data resulting from simulations can also be directed to an ECODATA or PGRA database for subsequent processing. This is done by the PLM program-module which accounts for all output from SIMP. Three main options are offered to the user. The whole or any fraction of the simulation result can be listed on a printer or a file, displayed graphically by a self-sustained graphical program, or it can be directed to a time-series database. SIMP always produces a standard result summary output file.

In addition to these major facets of SIMP, the package also offers routines for comparing measured and simulated data and a multiple simulation mode. A sample SIMP program is given below to show how some of these options are carried out in a model source code.

14.4 Discussion

Development in the computer industry is extremely rapid and even basic concepts of soft-, hard- or firmware may change or lose their meaning more or less overnight. This makes it difficult to speculate about the possible utility of the SEF software in the future. The only certainty is that the programs presented in this paper will be useless in the future unless they are continuously upgraded and maintained.

When it comes to the software described in this paper, ECODATA, PGRA, and SIMP, a number of problems must be addressed. All of these programs are, to begin with, written in the local VAX/VMS FORTRAN dialect and make use of its non-standard features as well as of specific features of the VMS operating system. This problem of non-portability has recently been solved for the PGRA system, which is continuously maintained and for which a version for the PC market has recently become available (Chapter 11). Secondly, both SIMP and

ECODATA were conceptualized before the arrival of FORTRAN 77 and suffer from the 'spaghetti structure' commonly found in old FORTRAN programs.

Maintenance and development of the SIMP system has not been active, but there is a renewed version of SIMP written by the present author, with portability and improved user interface as its prime objectives. This version, however, will not be released for public use until the tedious work of documentation and production of a User's Manual has been finished. Another objective, which is not met by any current SIMP version, is the distinction between the needs of the model user and the model creator. SIMP has been biased towards the needs of the model creator and developer. In this case, the simplicity of the user interface is not the most important facet. For user-oriented simulation support software, on the other hand, this interface must be the prime objective.

The relation between the older ECODATA system and its successor PGRA is not clear either. A few options in the ECODATA system are still not available in PGRA, such as smooth correction of some time specification errors or the ability to calculate new entities from old data using complex analytical forms. At present, no direct connection between PGRA and SIMP exists and it is probable that this coupling will only be seen between a new 'SIMP' and a further developed PGRA.

14.5 Sample source code for a SIMP model

This source code for the SAMPLE model is written in FORTRAN 77 (excepting the comments after exclamation marks and the INTEGER*2 declaration in the first, non-user written, section) and makes use of the SIMP simulation modelling support programs. The SAMPLE model is not supposed to be a functioning model but only a framework for demonstrating of various features of SIMP.

SUBROUTINE TRANS

COMM1	LAST PRP UPDATE 860915 12:03	PRIOR TO RUN No 1
INTEGER*2	IGO,NCOMP	
COMMON/UVAL/	TIME,TIMER,IGO	! This section of the program,
DIMENSION	P(2)	! limited by COMM1 and CEND1, is
EQUIVALENCE	(P,KAPPA)	! inserted by SIMP. It accounts
COMMON/UVAL/	KAPPA ,VDVERS	! for the communication between
COMMON/UVAL/	PDUMMY(168)	! the model and SIMP. Certain array
REAL	KAPPA	! and variable names (TIME,TIMER,
COMMON/UVAL/	NCOMP	!IGO,P,PDUMMY, NCOM,P,X,T,G and D)
DIMENSION	X(1)	! are reserved by SIMP and must not
EQUIVALENCE	(X(1),X01)	! be used with another meaning in
COMMON/UVAL/	X01	! the model source code. Default
DIMENSION	T(2)	! INTEGER names in the parameter
EQUIVALENCE	(T,T0001)	! list are automatically declared

COMMON/UVAL/ T0001,T0100 ! REAL by SIMP.
 COMMON/UVAL/ G(243)
 COMMON/UVAL/ D(10)

***** DATA INPUT *****

CALL ECDCDA(TIME,D) ! The first call accounts for continuous input data, read into the
 CALL ECDCDD(TIME,TIMLEN,2,D(2)) ! D-array at simulation time TIME,
 ! from an ECODATA file, whose
 ! version number can be specified
 ! either by default or prior to each run.

! The second call asks for discrete treatment of the
 ! second input variable read into D(2). Its value will be zero
 ! unless there is a non-zero value in the file for a time in the
 ! interval TIME to TIME+TIMLEN.

***** ACTUAL MODEL CODE *****

G(1)=FUNCT(D(1))*KAPPA ! This is the model code proper. The
 T0001=D(2) ! first three lines show only an example of how one could use the re-
 T0100=G(1)*SIN(X(1)) ! served SIMP names to express
 CALL ECDCVD(1,T0100,IFIX(VDVERS)) ! the model equation. The call
 RETURN ! to ECDCVD shows the ability
 ! to calculate, at simulation
 ! time TIME, a difference between simulated
 ! (here one variable, i.e., T0100) and validation data,
 ! measured at any time. The comparison data are stored in an ECO-
 ! DATA file with the version number VDVERS. Subroutine ECDCVD cal-
 ! culates the mean square difference, ECDCVM the average and
 ! ECDCVA the absolute value difference.

***** INITIAL CALCULATIONS *****

ENTRY INITIL ! The INITIL entry point allows
 CALL ECDCID(1,2) ! calculations that do not require
 RETURN ! to be repeated during the simulation to
 ! be made. In this case it was necessary to ini-
 ! tiate the connection between SIMP and ECODATA by

```

C ! the ECDCID subroutine call. This call announces that one
C ! variable, the second, should be treated as discrete. With no
C ! discrete input data, one could instead have used the ECDCIN
C ! subroutine, which, without argument, tells SIMP that the model
C ! uses a connection between ECODATA and SIMP.

C ****
C **** FINAL CALCULATIONS ****
C ****

C ! The TERMIN entry point enables
C ! calculations to be made after the
C ! end of the simulation. In this case the
C ! ECDCVT subroutine was called to calculate,
C ! for one simulated variable, the root-mean-square
C ! error ERROR for the whole simulation period, based on the
C ! squared differences calculated previously for each simulation
C ! time step.

C
C END

```

14.6 Acknowledgements

The author is grateful to Dr. P-E. Jansson, Dr. L-C. Lundin and Mr. T. Lohammar for their comments on the manuscript.

14.7 References

Engelbrecht, B., Lohammar, T., Pettersson, I., Sundström, K-B. & Svensson, J., 1980. Data handling and simulation technique used in the Swedish Coniferous Forest Project. In: T. Persson, (Ed.): Structure and function of northern coniferous forests – An ecosystem study. Ecological Bulletins (Stockholm) 32:65-71.

Halldin, S. (Ed.), 1979. Comparison of forest water and energy exchange models. Proceedings from an IUFRO Workshop September 24th – 30th, 1978, Uppsala, Sweden. Elsevier Scientific Publishing Company, 258 pp. Amsterdam – Oxford – New York.

Jansson, P-E. and Christofferson, L., 1985. PGRA User's Manual, 77 pp. Swedish University of Agricultural Sciences, Department of Soil Sciences, Uppsala.

Lohammar, T., 1979. SIMP – Interactive mini-computer package for simulating dynamic and static models. In: S. Halldin (Ed.): Comparison of forest water and energy exchange models. Elsevier Scientific Publishing Company, pp. 35-43. Amsterdam – Oxford – New York.

Persson, T. (Ed.), 1980. Structure and function of northern coniferous forests – An ecosystem study. Swedish Natural Science Research Council, Stockholm. Ecological Bulletins 32, 609 pp.

Perttu, K., 1985. Data for forest environmental measurements in Sweden. In: B.A. Hutchison and B. B. Hicks (Eds): The forest-atmosphere interaction. D. Reidel Publishing Company, pp. 105-115. Dordrecht, Holland.

SAS Institute Inc., 1985. SAS User's Guide: Basics, Version 5 Edition, 1290 pp. Cary, North Carolina.

Svensson, J., 1979. Storage, retrieval and analysis of continuously recorded ecosystem data. In: S. Halldin (Ed.): Comparison of forest water and energy exchange models. Elsevier Scientific Publishing Company, pp. 27-33. Amsterdam - Oxford - New York.

Index

- aerodynamic resistance 125, 153
- allocation pattern 21, 22
- allometric function 71
- areal leaf weight 69, 70
- assimilate 33, 36
- Beer's law 35
- biomass
 - production 41, 42, 44, 47
 - use 9, 181
- Blackman limiting response 26, 29
- break-even level 171, 183
- breeding 7
- carbon allocation 21, 22
- carbon dioxide 25, 89
- climate 4, 5
- computer source code 14, 51, 109, 134, 175, 193
- conductivity
 - hydraulic 100
 - saturated 149
 - unsaturated 149
- cost
 - energy 184
 - harvesting 170
 - initial 167
 - investment 169
 - maintenance 170
 - transport 170
- cultivation programme 166
- cutting cycle 41
- damage 9
- economic
 - model 165
 - potential 165
- edaphic conditions 5
- energy
 - consumption 3
 - density 181
 - forestry 3, 5, 9, 13
- establishment 8
- Euler integration method 101
- evaporation 5, 98, 101, 123, 129
- evaporation model 122
- evapotranspiration 101, 159
- fossil fuel 181
- fuel wood 9, 10
- gross assimilation 21
- growing period 9, 37, 181
- growth
 - data 38
 - foliage 37
 - model 33
 - rate 35
 - respiration 35
 - start 33
- harvesting 9
- heat
 - balance 89, 90, 98, 101
 - value 9, 182
- input data 38, 97, 173, 194
- interception 101
 - storage 150, 153
 - threshold 126
- interest rate 169
- land rent 167, 169
- leaf
 - fall 37

heat balance 101
litter 37
nitrogen concentration 43, 46, 47
shade-, sun- 26, 29
leaf-shoot ratio 37
leaf-stem partitioning 67, 69
light
compensation point 29
extinction 35, 36, 38
response curve 21, 26
saturated rate 26
Lohammar equation 123, 128
management 3, 7, 8
mathematical modelling 13
Michaelis-Menten equation 35
microbial growth rate 78
model
economic 165
evaporation 122
growth 33
sensitivity 40, 171
source code 14, 51, 109, 134, 175, 193
soil water 147
transpiration 98
verification 38, 40, 93

nitrogen
application 8
concentration 43, 46, 47
content 182
fixation 3, 181
mineralization 78
productivity 77
uptake 80, 81
nutrition 28, 31

parameter values 30, 48, 61, 83, 117
Penman equation 123
photon flux density 25
photosynthesis
canopy 36
net 25, 181

nitrogen dependence 35
potential 36, 69
photosynthetic
active radiation 5, 21, 37
capacity 26
light response 25
rate 21, 28, 30
plant material 7, 9
Priestley-Taylor equation 126
radiation 98, 124
resistance
aerodynamic 125
plant 100
soil-root interface 100
stomatal 100, 123
surface 90, 150, 153
respiration 21, 26, 35
root-shoot partitioning 66, 67
rotation period 182
sensible heat 98
short rotation forestry 13
simulation model 19
soil
nutrient status 6, 8
type 6, 165
water 6, 91, 92, 125, 131, 149
solar constant 37
sprouting 33
stomatal conductance 123
substrate quality 78
sun declination 38
sunshine duration 38
surface resistance 90, 150, 153
symbols 31, 48, 74, 84, 108, 133, 160

temperature
air 4, 5, 21, 104
leaf 5, 97, 104
soil 79, 82
sum 3, 4
time resolution 92
transpiration 102, 123

transpiration model 98

tortuosity factor 153

vapour pressure 99

variable

driving 90, 92

input 38, 98

output 93, 174

water

flux 89

tension 149

uptake 149, 151

water use efficiency 126, 131, 182

wilting point 149

wood density 182